

© Copyright 2021

Christopher R. L. Large

**FROM LAB TO LAGER: AN INVESTIGATION OF ADAPTATION, ADMIXTURE,
AND ALE BREWING YEASTS**

Christopher R. L. Large

A dissertation

submitted in partial fulfillment of the
requirements for the degree of

Doctor of Philosophy

University of Washington

2021

Reading Committee:

Maitreya J. Dunham, Chair

Harmit S. Malik

Benjamin Kerr

Program Authorized to Offer Degree:

Molecular and Cellular Biology

University of Washington

Abstract

From lab to lager: An investigation of adaptation, admixture, and ale brewing yeasts

Christopher R. L. Large

Chair of the Supervisory Committee:

Maitreya J. Dunham, Professor

Department of Genome Sciences

Creating a predictive model of evolution is a central goal of biology and necessitates understanding the genetic basis of adaptation. Using experimental evolution, adaptation can be explored in real time and connected to genetic variation through sampling and sequencing a population over several generations. I use a general paradigm of evolving and resequencing to explore the genetic basis of adaptation from the laboratory to the brewery. First, I explore population sequencing data from a set of over a hundred evolution experiments conducted in continuous culture devices under glucose-, phosphate- and sulfur-limitation and find a high level of reproducibility of evolutionary outcomes. Specifically, by correlating the frequencies of mutational outcomes with datasets indicating the frequency and relative fitness of the mutations, I find that genome context likely influences the outcomes of adaptive evolution. Next, I explore the effect of environment, specifically temperature on the adaptation and evolution of a proto-

lager hybrid that resembles the ancient hybridization between *S. cerevisiae* and *S. eubayanus*. Through experimental evolution in conditions favoring either of the two parental species, I find that, at certain loci, the parental genome is retained in conditions favorable to that species, indicating that environment has an effect on hybrid genome evolution. Finally, I explore the evolution of beer brewing yeasts within the natural niche of the brewery through partnerships with breweries across North America. By sequencing serially reused populations of beer yeast and phenotyping clonal isolates from the populations, I find that structural variation in the form of mitotic recombination and aneuploidy likely contribute to the adaptation and domestication of the beer brewing yeasts. Overall, findings across all three systems support the notion that the results of adaptive evolution are highly reproducible and that non-stereotypical forms of variation such as mitotic recombination and copy number variation play a vital role in evolution.

TABLE OF CONTENTS

List of Figures	v
List of Tables	vii
Acknowledgements.....	ix
Author Contributions	x
Chapter 1. Introduction	1
1.1. Yeast as a “change agent” throughout history	1
1.2. Overview of the <i>Saccharomyces</i> genus	2
1.3. Ancestral origins of the <i>S. cerevisiae</i> species	4
1.4. Differences between ale and lager yeasts	5
1.5. Focus on ale yeasts: genomic and phenotypic diversity	8
1.6. The Beer 1 ale yeast cluster arose by admixture	10
1.7. How can new technologies help innovation in the brewing industry?	11
1.8. Genetic engineering of beer strains	12
1.9. Linking genetics to performance in the brewery	13
1.10. Yeasts in the laboratory	16
1.11. Using yeasts in the understanding of evolutionary biology.....	17
1.12. Specific Aims.....	17
1.12.1. Reproducibility and contingency in experimental evolution.....	18
1.12.2. Effect of environment on hybrid genome evolution.....	18
1.12.3. Domestication and adaptation of beer brewing yeast in the brewery	19

Chapter 2. Highly parallel chemostat experimental evolution reveals importance of genome context in routes to adaptation	21
2.1. Introduction.....	22
2.2. Results.....	25
2.2.1. Evolutionary outcomes in the chemostat are highly reproducible.....	25
2.2.2. Proximity to a Pol III-transcribed gene likely influences the rate of gene disruption by Ty element during adaptive evolution	30
2.2.3. Chromosomal amplifications potentially dependent on genome context.....	31
2.3. Discussion.....	33
2.4. Materials and Methods.....	38
Chapter 3. Temperature preference can bias parental genome retention during hybrid evolution	42
3.1. Introduction.....	43
3.2. Results.....	47
3.2.1. Laboratory evolution of hybrids and their parents at cold temperatures	47
3.2.2. Loss of <i>S. cerevisiae</i> alleles in cold evolved hybrids	47
3.2.3. Environment-dependent loss of heterozygosity aids in temperature adaptation in hybrids	54
3.2.4. Pleiotropic fitness costs resulting from loss of heterozygosity.....	55
3.2.5. Mutations in <i>TPK2</i> are likely responsible for flocculation phenotype	61
3.3. Discussion.....	63
3.4. Materials and Methods.....	66

Chapter 4. Genomic stability and adaptation of beer brewing yeasts during serial repitching in the brewery.....	71
4.1. Introduction.....	71
4.2. Results.....	77
4.2.1. Recurrent whole-chromosome copy number increase indicates adaptive evolution	80
4.2.2. Recurrent <i>de novo</i> changes in heterozygosity on chromosome VIII suggests an adaptive benefit	82
4.2.3. Loss of <i>BATI^{A234D}</i> as a candidate for a driver of an adaptive benefit.....	84
4.2.4. Long-read sequencing analysis reveals heterozygous genomic rearrangements at the end of chromosome VIII.....	86
4.2.5. Increase in yeast settling behavior correlated with an increase in Lg- <i>FLO1</i> copy number	88
4.2.6. No observable change in growth rate of clones bearing the chromosome VIII mitotic recombination in simulated brewing conditions	89
4.2.7. Potential shifts in sensory profile of final timepoint yeast clones	90
4.3. Discussion.....	91
4.4. Materials and Methods.....	98
4.5. Acknowledgments	107
Chapter 5. Conclusions and Future Directions	108
5.1. Contingency and stochasticity in evolution.....	109
5.1.1. The influence of genome context on <i>SUL1</i> CNV	109
5.1.2. Probing influence of Ty element mobilization bias on evolutionary outcomes	110

5.1.3. Epistasis in adaptive evolution	111
5.2. Further relevance of structural variation in brewing	112
5.3. Mapping functional variation in brewing yeast	114
5.4. What are the consequences of life history trait shifts?	116
Bibliography	118
Appendix.....	153
VITA.....	209
Publications.....	210

LIST OF FIGURES

Figure 1.1. Species and major interspecific hybrids of the <i>Saccharomyces</i> genus.....	7
Figure 1.2. Whole-genome phylogeny of yeast strains isolated from a variety of environments and geographies	10
Figure 2.1. Comparisons to all known chemostat experimental evolution sequencing reveals common targets and newly discovered mutation targets	27
Figure 2.2. Recurrent targets of mutation impacted by bias in mutational preference	29
Figure 2.3. Recurrent amplification of the primary sulfate transporter potentially impacted by local sequence context	32
Figure 2.4. Local sequence context of <i>PHO84</i> provides no additional benefit or detriment to a chromosomal amplification	33
Figure 3.1. Loss of heterozygosity directionality results from selection on different species’ alleles at different temperatures	53
Figure 3.2. Fitness assays exhibit that loss of heterozygosity can result in antagonistic pleiotropy	57
Figure 3.3. Fitness assays.....	60
Figure 4.1. Research strategy to investigate a natural evolution experiment occurring in the brewery	77
Figure 4.2. Copy number variation of chromosome V occurs multiple times between breweries and within the same brewery	82
Figure 4.3. Mitotic recombination events spanning the same region recurrently mutated across multiple populations.....	86

Figure 4.4. Flocculation rate increases correlated with mitotic recombination on chromosome VIII.....	89
Figure B.1. Copy number plots of cold-evolved hybrids populations	172
Figure B.2. Amplification of <i>S. cerevisiae</i> <i>SUL1</i> in hybrids evolved at 15°C and 30°C	173
Figure B.3. Copy number plots of cold-evolved <i>S. cerevisiae</i> diploid populations.	174
Figure B.4. Copy number plots of cold-evolved, flocculent <i>S. cerevisiae</i> diploid populations .	175
Figure B.5. Loss of heterozygosity plots of cold-evolved <i>S. cerevisiae</i> diploid populations	176
Figure B.6. Loss of heterozygosity plots of cold-evolved, flocculent <i>S. cerevisiae</i> diploid populations	177
Figure B.7. Copy number plots of cold-evolved <i>S. uvarum</i> diploid populations	178
Figure B.8. Protein alignment of <i>PHO84</i>	179
Figure B.9. Predicted protein structure of <i>PHO84</i>	180
Figure B.10. Flocculation assay of several flocculent clones isolated from <i>S. cerevisiae</i> cold-evolved populations	181
Figure C.1. A maximum-likelihood phylogeny of the American brewing strains reveals several large clades.....	192
Figure C.2. Allele frequency of the Postdoc Brewing Co. replicate 1 population and a clone isolated from that population showing the number and pattern of haplotypes on chromosome V	193
Figure C.3. Allele frequency of chromosome V for every brewery population.....	193
Figure C.4. Allele frequency of chromosome VIII for clones isolated from the first Postdoc Brewing Co. replicate	194
Figure C.5. Allele frequency of chromosome XII and XV for every brewery population.....	195

Figure C.6. Copy number of chromosome I for every brewery population showing an increase at the left terminal end for every population that experienced a mitotic recombination event.....	195
Figure C.7. Growth rate measurements of brewery isolates from the first Postdoc Brewing replicate indicating no change in growth patterns	196

LIST OF TABLES

Table 2.1. Contingency table of the number of Ty element insertions near predictors of mobilization	31
Table 3.1. Mutations in cold-evolved hybrid populations	48
Table 4.1. Record of strains from brewery collaborations.....	78
Table 4.2. Sensory analysis of beers brewed with clones from the first Postdoc Brewing replicate.....	91
Table A.1. All mutations observed during the chemostat evolution experiments	153
Table B.1. Mutations in cold-evolved <i>S. cerevisiae</i> diploid populations.....	182
Table B.2. Mutations in cold-evolved <i>S. uvarum</i> diploid populations.....	183
Table B.3. Comparison of single nucleotide variants called in 15°C and 30°C experimental evolution	183
Table B.4. Strain list.....	184
Table B.5. Competitive fitness of evolved hybrid strains	185
Table B.6. Filters used in variant calling	186
Table C.1. Record of repitching populations from Postdoc Brewing Co.	196
Table C.2. Record of repitching populations from Elysian Brewing Co.....	197

Table C.3. Record of samples used in Figure C.1.....	198
Table C.4. The frequencies of recurrent mutation during Postdoc Brewing replicate 1.....	199
Table C.5. Mutations in populations and clones.....	200
Table C.6. Recurrent mutations across all brewery evolution experiments.....	207
Table C.7. Results of a sensory panel sampling beer produced by clones isolated from the Postdoc Brewing Replicate 1 populations	207
Table C.8. Filters used in variant calling	208

ACKNOWLEDGMENTS

None of the work presented herein would have been possible without the guiding hand of numerous mentors, colleagues, and friends. Thank you to my first research mentor, Professor Leslie Saucedo opened my eyes to the true world of science and taught me that academia is not just full of stiffs. Thank you to Dr. Harmit Malik, who inspired me to pursue evolutionary biology as a research topic and, being one of the kindest people I have ever met, has been a perpetual source of drive, energy, and guidance throughout my career. Thank you for the mentorship provided by Dr. Aida de La Cruz and for connecting me with Professor Nitin Phadnis who opened his home to me during personal strife, guided me to graduate school. I would also like to thank my graduate committee for their thoughtful discussion, insight, and perpetual challenge to become the best scientist they knew I could be. I must also thank my dear colleague and friend, Dr. Caiti Smukowski Heil for the countless hours of discussion, debate, and caring advice. Most notably, I want to thank Professor Maitreya Dunham for her perpetual support, mentorship, and kindness. Additionally, thank you to the Dunham lab for your support, assistance, and friendship. Thank you to the many academic colleagues, who have allowed me to explore numerous exciting topics outside of my main project including Bonny Brewer, M. K. Raghuraman, Bryce Taylor, and Michelle Walker. During my time in graduate school, I also had an amazing support network of friends, not limited to, but including Stephan Raiders, Meghan Garrett, Dylan Harvey, and Taiga Harimoto. I must also humbly thank my mother, father, and grandparents for their endless support and love. Thank you to my brother, Dr. Timothy Livingston Large for guiding my path forward, and always being there when needed. And finally, my deepest gratitude to my partner, Kendra Ann Cruickshank for her tireless love and support.

AUTHOR CONTRIBUTIONS

Chapter 1

The writing presented in **Chapter 1** is derived from an upcoming book chapter sponsored by the Master Brewers Association of the Americas and was written collaboratively by Christopher R. L. Large, Barbara Dunn, and Maitreya J. Dunham. Sections 1.1-1.4 were written primarily by Barbara Dunn while sections 1.5-1.12 were written primarily by Christopher R. L. Large. All authors edited the works and Christopher Large refined some of the language for a more academic audience.

Chapter 2

The work presented in **Chapter 2** was written by Christopher R. L. Large and edited by Maitreya J. Dunham. The laboratory experiments including the evolution experiments and sequencing were conducted by Aaron W. Miller, Bryony Lynch, Annie Young, and Mei Huang. All sequencing analysis was conducted by Christopher R. L. Large.

Chapter 3

The work described in **Chapter 3** is derived from Smukowski Heil CS, Large CRL, Patterson K, Hickey ASM, Yeh CLC, Dunham MJ. 2019. Temperature preference can bias parental genome retention during hybrid evolution. *PLoS Genet* **15**:e1008383. doi:10.1371/journal.pgen.1008383. Caiti S. Smukowski Heil and Christopher R. L. Large conducted the evolution experiments. Caiti S. Smukowski Heil, Christopher R. L. Large, Kira Patterson, Angela S. M. Hickey, Chiaan-Ling C. Yeh conducted follow-up experiments. Caiti S. Smukowski Heil and Christopher R. L. Large conducted sequencing analysis. Caiti S. Smukowski Heil wrote the original manuscript and Christopher R. L. Large, and Maitreya J. Dunham contributed to writing and editing. The project was conceptualized by Caiti S. Smukowski Heil and Maitreya J. Dunham.

Chapter 4

The work presented in **Chapter 4** was written by Christopher R. L. Large. Samples were collected and transported by Tom Schmidlin, Daniela A. Moreno-Habel, Hal McConnellogue, Richard Preiss. Samples were processed and Illumina sequenced by Noah Hanson and Christopher R. L. Large. Oxford nanopore sequencing was conducted by Andreas Tsouris and Omar Abou Saada. Sequencing analysis, visualization, and follow-up experiments were conducted by Christopher R. L. Large. Editing was provided by all contributors and Jirasin Koonthongkaew, Yoichi Toyokawa, Hiroshi Takagi, Joseph Schacherer, and Maitreya J. Dunham. Conceptualization was conducted by Maitreya J. Dunham and Christopher R. L. Large.

Chapter 5

Chapter 5 was written by Christopher R. L. Large.

CHAPTER 1 INTRODUCTION

The writing herein is derived from an upcoming book chapter written collaboratively by Christopher R. L. Large with Barbara Dunn and Maitreya J. Dunham and sponsored by the Master Brewers Association of the Americas. Full details of author contributions are available above.

1.1 *Yeast as a “change agent” throughout history*

The deliberate production of alcoholic beverages by humans has been performed and perfected over many millennia, possibly starting ~13,000 or more years ago (Hornsey, 2003; McGovern, 2009). Alcoholic beverages have served important roles in human civilization, not only socially and economically (Hockings and Dunbar, 2019), but also for human health and medicine (McGovern, 2019a). The quest to create alcoholic beverages has often served as an impetus for scientific progress, especially in the areas of chemistry, biochemistry and microbiology (McGovern, 2019b); the brewing industry has even been cited as the foundation for the field of biotechnology (Bud, 1994).

During the frothy era of the European “scientific revolution”, from the late 17th through the late 18th centuries, many scientists were intrigued by the transformation of mashed grain into beer, which was thought to occur when a yeast paste was added. At the time, yeast was considered by most to be an inanimate substance that catalyzed the conversion of sugar to alcohol and carbon dioxide. In 1680, using well-crafted versions of earlier microscopes, Antonie van Leeuwenhoek was the first to visualize yeast cells, reporting 2- to 6-lobed globules; however, he still did not think they were living organisms (Chapman, 1931). The realization that yeast were living creatures did not occur until the 1830’s when three independent investigators (Charles Cagniard-Latour in France, and Theodor Schwann and Friedrich Kiitzing in Germany), using microscopy to observe active fermentations, described yeast cells as living and dividing organisms (Schlenk, 1985). Cagniard-Latour reported that yeasts were responsible for alcoholic

fermentation and that in fact yeast paste was comprised of living cells that actively divided. He observed them microscopically across a time course of the brewing process and noted that the number of globules increased over time, including observations of small buds growing off the larger ones. Noting that the yeast globules did not move on their own, he classified them as “plants”.

Another giant leap forward in fermentation sciences occurred in 1883 when Emil Hansen at the Carlsberg brewery in Denmark used serial dilutions to isolate single yeast cells from beer and then grew the single cells into large amounts of “pure cultures” derived from that single cell. He was able to show that pure cultures isolated from either bottom- or top-fermenting brews reproduced their fermentation style (Hansen, 1883), and that pure cultures from better-performing fermentations retained the beneficial characteristics. This innovation led to the development of pure yeast cultures that could be selected for best brewing performance and at the same time were free of contaminants, greatly aiding the brewing industry in the reproducibility of their beers.

1.2 *Overview of the Saccharomyces genus*

The yeasts responsible for producing almost all alcoholic beverages, including beer, wine, sake and distilled spirits, are “budding yeasts”, small single-celled fungi that belong to the genus *Saccharomyces* (Latin for “sugar fungus”). During fermentations, *Saccharomyces* yeasts earn their Latin name by consuming the simple sugars present in the starting material and converting them into ethanol and carbon dioxide. The sugars available to the yeast depends on the industry, with mostly fructose and glucose being present in grapes in the case of wine and mostly maltose, glucose, and maltotriose in wort in the case of beer. In addition, yeasts will convert some more

complex molecules present in grapes or wort into novel flavor and aroma molecules (Carrau et al., 2015; Larroque et al., 2021; Van Wyk et al., 2019). After fermentation, the yeasts will form cellular aggregates and fall out of solution, allowing for the easy separation of yeast from beer in a process called flocculation. Within the *Saccharomyces* genus, there are at least eight closely related, naturally occurring species, as described in detail in a recent review (Alsammar and Delneri, 2020). The two species most relevant to brewing yeasts are *S. cerevisiae* and *S. eubayanus*, both of which will be discussed in further detail below.

All yeasts within the *Saccharomyces* genus are similar on the sequence level, both having the same number and orientation of chromosomes and with most genes and synteny shared among all species except for a small number of reciprocal translocations. Likewise, all *Saccharomyces* species share the same basic life cycle and mating systems. Haploid cells can exist briefly within the sexual mating cycle, derived by sporulation of the diploid cell, or can exist indefinitely as free-living cells if they are unable to mate successfully. Cells of all ploidy levels expand their numbers via asexual mitotic cell division when there are sufficient nutrients available. However, when nutrients, especially nitrogen, become limiting, a diploid cell can progress through meiosis and produce 4 haploid spores: two spores each of two of the different mating types, called “a” and “alpha”. When the two haploid cells mate (fuse together) they create a new diploid cell that combines the nuclear genomes of each parent, receiving one set of chromosomes from each parent. Likely given the negative effects of remaining in the haploid state long-term, yeast cells can spontaneously switch their mating type and thus generate a new mating partner.

Interestingly—and importantly for industrial applications—all eight *Saccharomyces* species are able to mate and form interspecific hybrids with each other; this occurs both in the

wild and in human-related environments (reviewed by (Morales and Dujon, 2012)). These interspecific hybrids cannot efficiently proceed through sexual division (meiosis) but are able to indefinitely reproduce in the mitotic asexual (clonal) manner. Other mechanisms, such as multiple rounds of spontaneous genome duplication, or aberrant mating between diploids, can lead to polyploidy within a species. Similar aberrant mating of higher ploidy cells between different species can give rise to interspecific hybrids of varying ploidy levels (Borneman and Pretorius, 2015; Hittinger, 2013). Finally, if a yeast cell has 2 or more copies of the haploid set of chromosomes (i.e. if it is diploid or polyploid), it can often tolerate the loss or gain of a single chromosome, or even several chromosomes, leading to a state called “aneuploidy” (Barrio et al., 2006; Storchova, 2014). For brewing yeasts, these concepts of ploidy and aneuploidy, as well as interspecific hybridization, are very important, as discussed in detail further below.

1.3 *Ancestral origins of the S. cerevisiae species*

Where did brewing yeasts originally come from? It turns out that *Saccharomyces* yeasts are not only found in industrial facilities such as breweries, wineries or bioethanol refineries, but are also found in nature, often in association with trees (mostly oaks in the Northern hemisphere and southern beeches in the Southern hemisphere), as well as rotting fruits and insect guts (reviewed in Alsammar and Delneri, 2020). Of the various species in the *Saccharomyces* genus, a concerted effort to collect isolates from around the world and to characterize genomic variation has been most exhaustively performed for *S. cerevisiae* because of its industrial/economic importance and because of its history as a premier laboratory model organism (Liti and Schacherer, 2011). The breadth and depth of these studies has allowed a population genomics approach to be taken, resulting in the ability to define the geographic origins of *S. cerevisiae*.

The location of *S. cerevisiae* species origination has been shown to be in Asia, specifically within China (Duan et al., 2018; Peter et al., 2018), where it arose as a distinct species. The details of exactly how *S. cerevisiae* has subsequently come to inhabit every continent in the world are still unknown, but distribution by animals, insects—and especially humans—have all undoubtedly contributed to its global dissemination.

The many different environments in which *S. cerevisiae* is found worldwide—varying widely in available nutrients as well as in environmental parameters such as temperature—has led to evolutionary adaptations to the specific environments, resulting in both genomic and phenotypic diversity across this species (Peter et al., 2018). For example, wine yeasts as a group are quite similar to each other on the genome and phenotype level (e.g., for sugar utilization and temperature optimum) compared to “wild” strains that grow near oak trees, which themselves form a similar group. Because brewing yeasts have been exposed to a relatively unchanging environmental milieu (i.e., boiled grains and hops) over the millennia that they have been utilized by humans, one might think that brewing yeast strains could be very similar to each other. However, there is a very wide variation in genomes and phenotypes across brewing yeasts, as discussed in detail below.

1.4 *Differences between ale and lager yeasts*

The most basic difference among brewing yeast strains is one that distinguishes ale yeasts and lager yeasts. Ale yeasts belong to the *S. cerevisiae* species, while lager yeasts are interspecific hybrids formed by the mating of *S. cerevisiae* with *S. eubayanus* (Figure 1.1; (Libkind et al., 2011)). However, the fact that lager yeasts are hybrids (and thus not a “pure” species) was not clear when they were first studied; instead, they were thought to represent unique species and

were given species names such as *S. pastorianus* and/or *S. carlsbergensis*; for convenience they are still often referred to by these names. Similarly, *S. bayanus* is the name originally given to what is now known to be a collection of similar interspecific hybrid strains, most involving *S. uvarum*, *S. cerevisiae* and *S. eubayanus* as the component genomes; these hybrids have been found in wine, cider and other fermentations (see (Nguyen et al., 2011; Pérez-Través et al., 2014) for detailed descriptions of the complex genomes and history of *S. bayanus* yeasts). It is important to note that *S. uvarum* and *S. eubayanus* are both cold-tolerant species, preferring to grow at ~5 - 15 °C, while *S. cerevisiae* prefers much higher growth temperatures of ~23 – 33 °C (Hebly et al., 2015). For both the “*S. pastorianus*” and the “*S. bayanus*” hybrids, it appears that the driving forces of adaptation were to allow effective ethanol production at lower temperatures, such as for lager, cider and cold-climate wines: when *S. cerevisiae* is combined in an interspecific hybrid with either *S. eubayanus* or *S. uvarum*, the hybrid now can grow well at cold temperatures, yet retains the strong fermentation characteristics of *S. cerevisiae*.

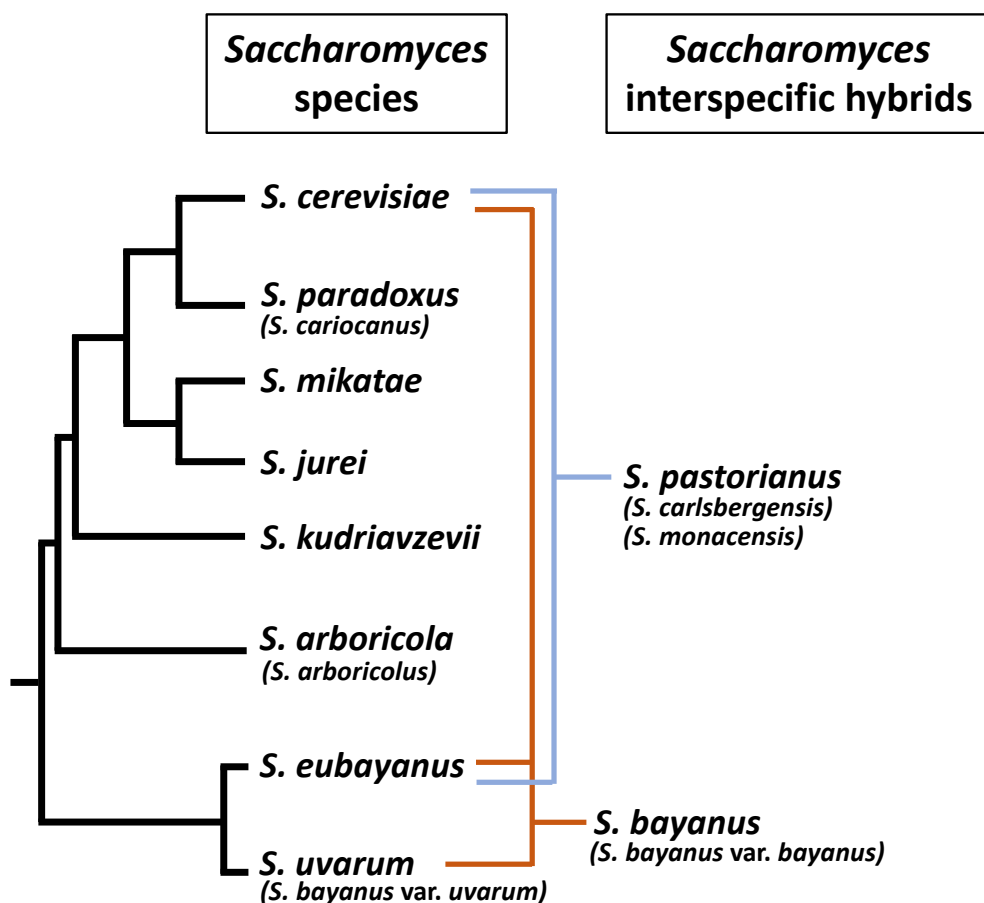


Figure 1.1. Species and major interspecific hybrids of the *Saccharomyces* genus; commonly-used synonyms are shown in parentheses. This figure is a redrawing from work presented in (Alsammar and Delneri, 2020).

Among the lager hybrids, many strains' genomes have been investigated, showing that ploidy levels and aneuploidy also vary from strain to strain (Barros Lopes et al., 2002; Dunn and Sherlock, 2008; Gibson and Liti, 2015; Hewitt et al., 2014; Liti et al., 2005; Monerawela et al., 2015; Monerawela and Bond, 2017; Okuno et al., 2016; Rainieri et al., 2006; van den Broek et al., 2015; Wendland, 2014). It is possible that the widespread occurrence of aneuploidy and higher ploidies seen among brewing yeasts reflect selective events that give advantage to these cells in the brewing environment; indeed, polyploidy and aneuploidy have been observed to be adaptive in laboratory yeasts under some growth environments (Dunham et al., 2002; Selmecki

et al., 2015; Storchova, 2014; Sunshine et al., 2015). These altered ploidy levels can presumably be tolerated, and even selected for, because brewing yeasts are not required to pass through a sexual phase as part of their lifestyle, instead being propagated asexually in perpetuity during the brewing process.

1.5 Focus on ale yeasts: genomic and phenotypic diversity

The first expansive description of the diversity of ale yeast brewing strains using whole-genome next-generation sequencing came from Kevin Verstrepen's group at K.U. Leuven in Belgium in 2016 (Gallone et al., 2016). The observations made in this publication were quickly followed up by another group led by José Paulo Sampaio from Universidade Nova de Lisboa, in Caparica, Portugal (Gonçalves et al., 2016). In both these publications, they sequenced a large number of industrial strains from beer and wine environments and performed evolutionary and functional genomics on the sequenced yeasts to identify evidence of historical yeast domestication. Using a phylogenetic approach which reconstructs the familial relationships between different yeasts using their genetic sequence, they observed that there was one primary group containing the majority of European beer yeast strains, herein called Beer 1 (See **Figure 1.2** for a reanalysis of the data to produce an updated tree). The Beer 1 strains are further separated into a number of sub-groups, including the wheat beer yeast, and strains from the United States, German/Belgian and the United Kingdom. Additionally, the Verstrepen group identified another group herein called the Beer 2 group of strains, which are more closely related to wine yeast and contain mostly strains from Belgium, the United Kingdom, the United States, Germany, and Eastern Europe. A minority of the European beer strains, primarily used to bottle referment (carbonate using yeast) strong Belgian beers fall within another group containing bread yeasts. Furthermore,

the Verstrepen group was also able to show that the yeasts most closely associated with American brewing yeasts share a recent common ancestor with the British brewing strains, meaning that the United States' yeasts are likely descended from early British colonizers in the Americas in the 17th century.

More recently, yeast used in Norwegian farmhouse brewing styles, colloquially known as the Kveik yeasts, have been isolated, sequenced, and placed on a phylogenetic tree near the wheat beer strains (Preiss et al., 2018). These strains have garnered particular attention in recent years for their ability to ferment efficiently at warmer temperatures, their ethanol tolerance and ability to produce a range of fruity esters. While there are a number of questions still remaining about the origins of the kveik strains in reference to their domestication outside of industrial settings, in the upcoming years, there will likely be more traditional farmhouse strains from other regions outside of Norway that will be discovered and added to the catalog of yeast strains.

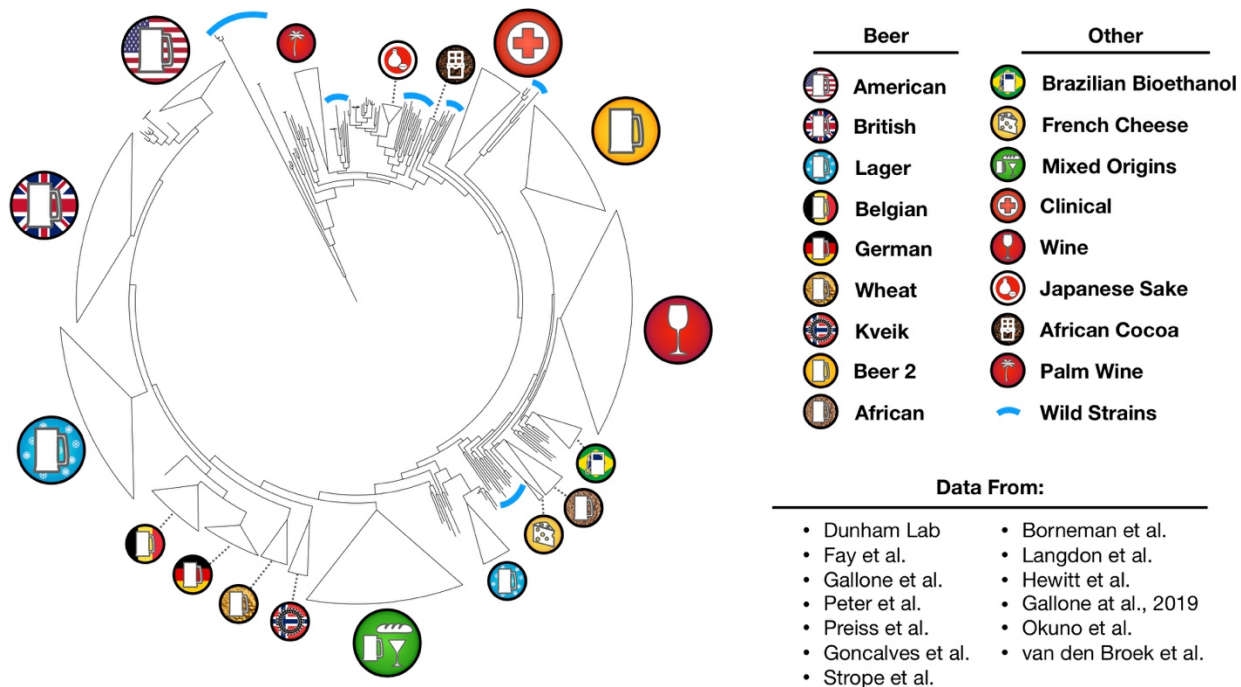


Figure 1.2. Whole-genome phylogeny of yeast strains isolated from a variety of environments and geographies. The genome data used in the generation of this figure comes from work presented in this thesis as well as: (Borneman et al., 2016; Fay et al., 2019; Gallone et al., 2019, 2016; Gonçalves et al., 2016; Hewitt et al., 2014; Langdon et al., 2019; Okuno et al., 2016; Peter et al., 2018; Preiss et al., 2018; Strope et al., 2015; van den Broek et al., 2015). The figure was generated using the phylogenetic tree software, IQ-Tree2.0 with the following parameters: GTR4+ γ . A complete record of the methods is available in **Chapter 4**.

1.6 *The Beer 1 ale yeast cluster arose by admixture*

The yeasts in the Beer 1 group have four copies of their genome (referred to as a “tetraploid” genome), unlike the typical two copies (“diploid”) seen in wine, sake, and wild strains. In addition, most of the Beer 1 strains that have been sequenced have at least one deviation from a perfect set of four chromosomes, i.e., “aneuploidy” - an occurrence that would cause either death or severe consequences in humans. Yet, these yeasts tolerate, and potentially gain benefit from these alterations. One strong question that arose as a result of these previously described works was how these yeasts were formed. In a recent publication by Justin Fay and colleagues, more light was shed on this observation (Fay et al., 2019), where the authors suggested that the origin of the beer brewing yeasts came from a combination of strains from and Asian and European

wine strains along with a no-longer extant lineage of beer strains. The admixture is thought to have resulted in a lineage of yeast with increased genetic diversity.

1.7 *How can new technologies help innovation in the brewing industry?*

In hand with the collection and categorization of virtually all modern brewing strains used in industrial beer fermentation, the question gets raised: what is next? Will brewers continue to find novel strain characteristics through generation of new “house strains”? Or is there a natural limit to the diversity of novel characteristics that can be generated? With the invention of yeast propagation companies, the majority of brewers do not reuse their yeast strains in perpetuity (also known as repitching), meaning that there is less opportunity for new strain innovation. This naturally leads to the reduced number of new strains being introduced to the community. So where will tomorrow’s new strain come from?

One exciting possibility is to look to nature for novelty. So called ‘bioprospecting’ of non-conventional yeasts utilizes the wild capture of yeasts (both *S. cerevisiae* and other *Saccarocymces* species such as *S. eubayanus*) from sources such as nature and non-traditional fermentations (reviewed in (Cubillos et al., 2019)). Often these strains have the capability to produce characteristics not seen in modern brewing strains, such as new and interesting flavors and the ability to ferment efficiently at lower or higher temperatures (Steensels et al., 2014b). In particular, significant genetic and characteristic diversity exists in other *Saccharomyces* species that could be leveraged to make truly novel strains. However, as many of these strains have not been reared for generations in industrial brewing conditions, they often do not efficiently produce ethanol at the same rate as industrial strains. Finding inspiration in the lager yeasts, several groups have started utilizing interspecies hybridization to combine the positive brewing

characteristics of a traditional brewing strain with the low temperature tolerance and increased flavor metabolite production of an unconventional, non-cerevisiae strain (reviewed in (Gibson et al., 2017; Krogerus et al., 2017, 2015)).

Whether novel strains are generated through bioprospecting or hybridization, they are often not well adapted to the brewing environment, meaning that they will be unstable and experience rapid evolutionary change if introduced into the brewery. This could potentially result in a changing product over the course of several repitches, or inconsistent batches from a propagation company due to genetic evolution in the yeast grow-up process. A common strategy to improve the stability of a strain is to serially reuse the strain in simulated brewing conditions for several hundred generations, such that a more adapted strain arises and can be isolated from the population (reviewed in (Gibson et al., 2020)). Through experimental evolution, or repitching in the brewery, a more stable form can be achieved and allow for a more consistent product.

1.8 Genetic engineering of beer strains

One of the most remarkable and innovative recent introductions to the brewing industry involves the use of a laboratory technique called CRISPR/Cas9. Using proteins and DNA originally found in bacteria, scientists can introduce exogenous genetic changes to beer brewing strains in an efficient manner. After the modifications are completed and the genetic changes are introduced, the bacterial DNA and protein can be removed from the cells, making the strain safe for consumption. The most striking example of these modern genetic techniques was the modification of an American brewing yeast strain to have the ability to stably produce hoppy flavor monoterpenes (Denby et al., 2018). While CRISPR/Cas9 has enabled the rapid and efficient production of novel strains, it has been possible for several years, albeit in a less

efficient manner (reviewed in (Steensels et al., 2014a)). Notably, the sale of beer made by yeast with these sorts of genetic modifications are possible in the United States due to our food and beverage regulatory market. With the proper care and precision, I believe that these genetic modifications are completely safe and provide a valuable and interesting new angle to the fermentation industry.

1.9 Linking genetics to performance in the brewery

Beyond an expansion in the diversity of available technologies to generate novel brewing strains, in the future, we will see a further expansion of our collective knowledge around what genes are responsible for the diversity of behaviors, flavors, and characteristics within brewing yeasts.

Herein, I will discuss four prominent established connections between the gene sequence of the yeasts and the way they perform in the brewery: (1) the production of certain metabolites that contribute to flavor, (2) the strength and speed of flocculation, (3) the processing of starch, and (4) the catabolism of maltose and maltotriose.

There are several examples of specific genes, which when mutated can dramatically change the flavor profile of the beer. The first example, commonly referred to as the phenolic off flavor (POF), involves the decarboxylation of ferulic acid into 4-vinylguaiacol (4-VG) by *PADI* and *FDCI* genes, resulting in a clove or smoke-like flavor (Chen et al., 2015; Mukai et al., 2014). Through a systematic analysis of the genomes of ale brewing yeasts, it has been found that there is an inactivation of these two genes through mutation in the majority of the ale brewing yeasts, but that function is retained in the wheat and Belgian brewing strains, where the flavor is desired (Gallone et al., 2016; Gonçalves et al., 2016). The second example involves genes responsible for the production of diacetyl, a common buttery flavor that can be regarded as

a positive or negative depending on the beer style. Diacetyl itself is derived from a metabolic intermediate known as α -acetolactate, which is produced from pyruvate by the action of an enzyme encoded by *ILV2*. With the knowledge of the direct connection between the enzymes that are involved in the production of diacetyl, many groups have engineered variants in the *ILV2* gene in order to reduce the total amount of α -acetolactate, and thus diacetyl produced (reviewed in (Krogerus and Gibson, 2013)). In the future, there will likely be more specific connections between variation in flavor metabolite production and variation in genome sequence.

Flocculation is one of the most variable traits among the brewing yeasts and can lead to undesired outcomes such as under fermented wort if not properly predicted. Yeast flocculation is most commonly caused by the interaction of a set of extracellular proteins known as flocculins with the mannoproteins present on the exterior of neighboring yeast cells. The flocculin proteins themselves are encoded by a family of genes known as the *FLO* genes, which can vary between strains in both presence as well as copy number. The mechanism of flocculation has been previously divided into two main categories, *FLO1*-like and NewFlo-like (reviewed in (Verstrepen et al., 2003)). The defining difference between these mechanisms of flocculation is whether the flocculins themselves are inhibited through their preferential binding to mannose, as is the case with *FLO1*-like, or additional sugars that are present in wort such as glucose, maltose, and sucrose, as in the case with NewFlo. The NewFlo mechanism was associated in lager yeast with a gene fusion event between *YAL065c* and *FLO5* leading to a new gene, called Lg-*FLO1* (Kobayashi et al., 1998; Ogata et al., 2008). Previously, Lg-*FLO1* was thought to have originated in the lager yeast, however a recent analysis found its presence within ale yeast, indicating that Lg-*FLO1* originated in *S. cerevisiae* ancestor of the ale and lager yeast (Ogata et al., 2020; Van Mulders et al., 2010). While much of the genetic basis of flocculation as been determined, there

is still difficult in using the genome sequence of a yeast to predict how it will perform in the brewery due to technical limitations of the sequencing technology. However, new forms of sequencing that rely on different technology could resolve this issue and allow for future researchers to create a more predictive model of flocculation.

The most notorious of phenotypes of the brewing yeasts involves the spoilage organism traditionally known as *S. diastaticus*. These strains, while now understood to be members of the Beer 2 group, produce a novel glucoamylase enzyme, STA1, that allows them to break down and ferment starches and other oligosaccharides, which can lead to the super-attenuation of wort, and eventually to exploding bottles. *STAI* itself, similar to Lg-*FLO1* originates from a gene fusion event between *FLO11* and *SGAI* (Krogerus and Gibson, 2020). Recently, it has been discovered that the presence of *STAI* in the yeast genome does not necessarily guarantee its ability to digest starch and that, for several strains in the Beer 2 clade, there is a genetic deletion outside of the gene coding region that leads to the lack of proper production of the glucoamylase enzyme (Krogerus et al., 2019). Through molecular techniques, the presence of the complete *STAI* or the deleted version can be determined, allowing for the accurate delineation of strains that are capable of digesting starch and the avoidance of these strains when desired.

One of the most important functions of any brewing strain is the efficient breakdown and fermentation of the sugars present in wort. Within the brewing strains, there are a set of genes known as the *MAL* genes that handle the uptake and breakdown of maltose and maltotriose. These functions are split into clusters of proteins encoded by three genes in the yeast genome. The first, *MALx1* encodes for a transporter that allows for importation of the maltose and other sugars into the yeast cell. There is extensive variation in the *MALx1* gene ‘versions’ that causes a differential ability to uptake maltose, maltotriose, and other sugars in both ale and lager strains

(Han et al., 1995). *MALx2* encodes for an enzyme that breaks maltose and maltotriose into its component glucose molecules. Finally, *MALx3* allows for the proper genetic control of *MALx1* and *MALx2* in the presence of the appropriate sugars. Between yeast strains there is variation in the presence or absence of these *MAL* gene clusters, with a total of five of these sets having been identified (*MAL1*, *MAL2*, *MAL3*, *MAL4*, and *MAL6*; (Naumov et al., 1994)). Similar to the *FLO* genes, there is also variation in the copy number of the various *MAL* clusters that can differ between even closely related strains (Gallone et al., 2016; Gonçalves et al., 2016; Steenwyk and Rokas, 2017). Future work will likely work towards a more direct link between performance and the brewery and the number of functional copies of the *MAL* gene clusters.

1.10 *Yeasts in the laboratory*

In addition to yeasts' role as the premier fermentation organism, it has also served as one of the core eukaryotic genetic model systems (Botstein and Fink, 2011). With its fast growth rate, amenability to genetic screens, and ease of genetic manipulation, *S. cerevisiae* has yielded insight into a vast array of topics such as the genetic basis of cell cycle control (Hartwell et al., 1970), autophagy (Takeshige et al., 1992), and telomere maintenance (Shampay et al., 1984). In the modern era, *S. cerevisiae* has continued its legacy with a cast of new functional genomics tools such as strain libraries consisting of deletions (Giaever et al., 2002), amplifications (Ho et al., 2009), and fluorogenic tags (Huh et al., 2003) of nearly every protein coding gene in the yeast genome. Given the scale of community provided data ranging from genome-scale genetic interaction maps (Costanzo et al., 2010), to the availability and whole genome sequencing of 1,011 yeast strains (Peter et al., 2018), and to the creation of a 100% synthetically generated

organism (Richardson et al., 2017), yeast is an ideal organism for the continued study of genetics, genomics, and evolutionary biology.

1.11 Using yeasts in the understanding of evolutionary biology

Saccharomyces yeast have been extensively utilized as a model system for eukaryotic experimental evolution given their genetic tractability, controllable life stages, and genome size. Through variation in the environmental conditions, genetic background, and passaging regime, numerous questions have been asked about the influence of fundamental processes on evolution, including sex (McDonald et al., 2016), ploidy (Selmecki et al., 2015) and mutation rate (Raynes et al., 2018). Evolution in the laboratory is commonly conducted in one of two main experimental setups, batch culture and continuous culture. Batch culture relies on the continual back dilution of a culture to allow for population expansion. Conversely, continuous culture devices utilize either a nutrient limitation, as in the case of the chemostat or mechanical means to maintain a constant selective pressure and growth rate. Within this thesis, I will describe research that utilizes both continuous culture (in **Chapter 2** and **3**), and batch culture (**Chapter 4**) and will provide a more extensive review of these techniques and their impacts within the respective chapters.

1.12 Specific Aims

The work presented here focuses on the use of *Saccharomyces* yeasts to study the mechanisms and sources of evolutionary adaptation in both the laboratory and the brewery. Within, I use a generalizable paradigm of evolve and resequence, wherein an isogenic starting yeast population is exposed to and allowed to adapt a stressful environment for hundreds of generations.

Afterwards, the mechanisms of adaptation are explored through genomic resequencing of the population. The experiments range from the use of highly controlled chemostat experimental evolution to evolution occurring within the modern yeast niche of the brewery. Overall, the aim of this thesis is to garner a greater understanding of the influences of genomic context and environment on adaptation.

1.12.1 Reproducibility and contingency in experimental evolution

The use of the chemostat for experimental evolution has previously been stymied by the lack of ability to produce a large number of replicates due to technical limitations. Specifically, questions relating to the reproducibility of evolutionary outcomes, the rates by which certain outcomes occur, and the influence of epistasis in evolution have been difficult to determine.

Herein I describe the use of a multiplexed and miniaturized version of chemostat to conduct 95 separate evolution experiments in glucose-, sulfur-, and phosphate-limited media conditions.

Overall, I discovered new targets of mutation, numerous *de novo* transposable element mobilizations, and over forty chromosomal amplifications with unique breakpoints. I subsequently made comparisons between existing datasets and the neutral biases in yeast transposable element mobilization rates to discover the importance of genome context in evolutionary outcomes.

1.12.2 Effect of environment on hybrid genome evolution

Within extant strains of the natural interspecific hybrid, *S. pastorianus* there is a reduction in the genomic contribution from the original parental species, *S. cerevisiae* and *S. eubayanus* through mitotic recombination, gene conversion, and aneuploidy. Given the time since the original

hybridization, it is difficult to determine the events post hybridization that could lead to the favoring of one genome over another across the genome from extant *S. pastorianus* sequences. Previous work performed by Dr. Caiti Smukowski Heil and colleagues discovered that when a proto-lager hybrid between *S. cerevisiae* and *S. uvarum* was experimentally evolved at conditions favorable to *S. cerevisiae*, that the *S. cerevisiae* portion of the genome was repeatably amplified over the *S. uvarum* contribution at certain loci (Smukowski Heil et al., 2017). However, it was unclear from those experiments whether the *S. cerevisiae* sequence at these loci would have been globally favored in any condition, or whether the environment influenced the direction of hybrid genome retention. Together, Dr. Smukowski Heil and I evolved the same proto-lager hybrids in conditions favoring *S. uvarum* to explore this question. Through subsequent whole-genome sequencing, we discovered that environment does influence hybrid genome evolution.

1.12.3 Domestication and adaptation of beer brewing yeast in the brewery

As mentioned previously, *Saccharomyces* yeasts have been utilized for hundreds of years for the production of fermented beverages and food. Analysis of the extant genome sequences of ale brewing yeasts has revealed multiple signatures of domestication, indicating their adaptation to the brewing environment during this time (Gallone et al., 2016; Gonçalves et al., 2016). The ale yeast themselves are thought to originate from a within species admixture event that led to a high degree of within strain genetic variation (Fay et al., 2019). Since the original hybridization, some of the intragenomic variation has been reduced through aneuploidy and mitotic recombination, however it is unclear whether these events produced adaptive outcomes. Furthermore, it is unclear whether ale brewing yeasts are still undergoing domestication. To explore these

questions, I partnered with multiple breweries across North America who conducted evolution experiments using similar strains of American yeast. Through analysis of population sequences over time in the brewery, I discovered that ale brewing yeast are still undergoing domestication and that structural variation in the form of mitotic recombination and aneuploidy are driving these new adaptations.

CHAPTER 2 HIGHLY PARALLEL CHEMOSTAT EXPERIMENTAL EVOLUTION REVEALS IMPORTANCE OF GENOME CONTEXT IN ROUTES TO ADAPTATION

Experimental evolution provides a reproducible testing ground for the study of adaptive evolution where the numerous degrees of freedom impacting the trajectory of evolution can be limited to their most controlled form. Evolution in a continuous culture device known as the chemostat further constrains the variables that introduce stochasticity by maintaining constant selective pressure and environmental conditions. Using a multiplexed miniature chemostat setup, we generated the largest set of sequenced chemostat evolution experiments in glucose-, phosphate-, and sulfur-limited media conditions with a total of nearly a hundred replicates. Through analysis of the adaptive variation that occurs within the evolution experiments we discover a high level of recurrence of gene mutations between experiments in the same condition and the targeting of multiple members of the SAGA complex, sirtuin gene family, and MAPK signaling pathway. We additionally find over one hundred new transposable element mobilizations, indicating their importance in adaptive evolution. Comparing the frequency of genes impacted by a single nucleotide polymorphism, insertion, deletion, transposable element mobilization, or copy number variation, we find that a gene's location in the genome likely impacts its adaptive potential. Finally, we find additional evidence that the fitness consequences of copy number variation rely on the collective fitness effects of multiple loci. Overall, through high replication of chemostat evolution experiments, we have been able to identify how the biases in mutational frequency and the effect of gene sequence context impact the direction of evolution.

2.1 Introduction

One of the central goals of evolutionary biology is to create a predictive model of evolution. However, there are numerous complicating factors that impede the study of the evolutionary process in nature. Through experimental evolution in the laboratory, we can limit or modulate some of the expansive number of degrees of freedom that generate stochasticity in the evolutionary process such as shifts in the environment, variation in population size, and changes in selective pressures. By repeating an evolution experiment we can achieve what is rarely possible in nature and observe the same conditions being played out in real time, allowing for the application of statistical methods to determine the source of variation in evolutionary outcomes. Historically, experimental evolution has yielded insights into the influence of a vast array of factors such as ploidy (Selmecki et al., 2015), mutation rate (Raynes et al., 2018), sex (McDonald et al., 2016), genome composition (Gorter De Vries et al., 2019; Smukowski Heil et al., 2019, 2017), pleiotropy (Jerison and Desai, 2015), clonal interference (Kao and Sherlock, 2008; Lang et al., 2013), and epistasis (Kryazhimskiy et al., 2014; Kvitek and Sherlock, 2011). Similar to the variety of questions that can be asked during experimental evolution, there is considerable variation in the practiced methodologies for culturing an organism for hundreds of generations.

One of the more controlled forms of evolution in the laboratory is growth in a type of continuous culture device known as chemostat in which the population size, selective pressure, and environmental conditions can be precisely monitored and controlled (reviewed in (Gresham and Dunham, 2014)). Commonly, the growth rate of the culture inside of a chemostat is limited by the constant low concentration of one necessary nutrient such as carbon, nitrogen, phosphorus, or sulfur (Ziv et al., 2013). This is in sharp contrast to batch culture experimental evolution in which the concentration of nutrients, and thus selective pressures vary over course

of the experiment (Li et al., 2018). While chemostats were first introduced in the 1950's, their utility for the understanding of the evolutionary process at the molecular level has become newly possible with the introduction of genome analysis technologies (Monod, 1950; Novick and Szilard, 1950). The combination of evolution in the chemostat and subsequent genotyping of clones or populations isolated from the chemostat has yielded numerous insights into the genetic targets of adaptation and the mutational mechanisms by which they occur. First, copy number variation (CNV) was shown to be an adaptive form of mutation through observation of the recurrent copy number amplification of the primary glucose, amino acid, and sulfate transporters (HXT6/7, GAP1, and SUL1, respectively) in yeast grown in limited media conditions (Brown et al., 1998; Gresham et al., 2010, 2008). Second, a model describing a novel type of gene amplification known as Origin-Dependent Inverted-Repeat Amplification (ODIRA) was developed based on observations made from sequencing of clones derived from sulfate-limited chemostats bearing *SUL1* amplifications (Brewer et al., 2015, 2011; Payen et al., 2014). The ODIRA model specifically describes a replication fork error, originating at a set of inverted repeats that leads to an extrachromosomal replication intermediate mediated by the presence of an autonomous replicating sequence (ARS), which can subsequently reintegrate into the genome and create a region of amplification. More recently, a separate group identified multiple examples of amplifications of *DUR3* and *GAP1* matching the requirements of ODIRA in nitrogen limited chemostats (Lauer et al., 2018). Finally, from clones derived from experiments described herein, chemostat evolution experiments were found to favor the evolution of cellular aggregation, likely to avoid being diluted from the chemostat vessels. From a bulk segregant analysis performed on clones isolated from the cellular aggregates, Hope et al. were able to identify one of the primary genetic mechanisms to be from the insertion of a yeast transposable

element (Ty element) upstream of a flocculin gene, *FLO1*, indicating transposable elements as a potential source of adaptive variation during evolution (Hope et al., 2017).

However, the utility of the chemostat for the study of evolution has been limited by inherent challenges to use the device such as their difficulty to multiplex. When the metric by which a particular mutation is viewed as important or adaptive is the degree of recurrence between experiments, the number of replicates becomes crucial. Several strategies to resolve these challenges have been generated, including our generation of the ‘ministat’, which constitutes a cheap and multiplexed alternative to traditional hand-blown glass, or expensive industrially produced chemostats (Miller et al., 2013).

Despite the reduction in cost and difficulty in conducting evolution experiments in nutrient-limited chemostats with accompanying whole genome sequencing data, the total number of population replicates conducted in any given condition remains low, with the most replication conducted in glucose limitation with a total of 25 sequenced populations across all available studies. Given the paucity of replication for nutrient limited chemostat evolution experiments we sought to both codify and quantify the observations of previous evolution experiments as well as attempt to discover phenomena that are only observable in high replication. Using highly multiplexed miniature chemostat setups, we were able to generate a large dataset of nearly a hundred evolution experiments from three separate nutrient limitations that were sequenced to high coverage (median of 113.6x) using short-read sequencing. As this constitutes the largest set of sequenced chemostat evolution experiments, we sought to explore the emergent patterns of mutation and selection that influence the direction and predictability of evolution. To this end, we explored the routes to adaptation through recurrence of mutations in certain pathways, the

influence of mutational bias on evolution, and influence of genome context in segmental chromosomal amplification.

2.2 Results

2.2.1 *Evolutionary outcomes in the chemostat are highly reproducible*

The design of these experiments focuses on the use of a large sample size to make inferences about evolutionary dynamics using repeatability of mutational targets as an output. Overall, we cultured 95 independent populations of isogenic, haploid yeast in sulfur- (31 replicates), phosphate- (32 replicates), and glucose- (32 replicates) limited conditions for over 200 generations. Within all populations, we discovered a total of 367 SNPs/InDels with a between population specific mutation count of 134 in glucose-limited, 124 in phosphate-limited, and 109 in sulfate-limited mediums. Additionally, through employment of the transposable element detection software, McClintock (Nelson et al., 2017), and manually curating the resulting calls, we discovered 141 new transposable element mobilizations (Glucose-limited, Ty:34; Phosphate-limited Ty:24; Sulfate-limited Ty: 83). Combining the *de novo* mutation and mobilization calls, we revealed a strong pattern of recurrence between populations from the same condition, with nearly half of all new mutations occurring in the same or similar location as another mutation (Recurrent mutations: 237; Total mutations: 508). Additionally, we identified one lineage in a glucose-limited population that contained a mutation in the DNA damage repair enzyme, *MSH2*, which could account for an increase in the number of mutations in the population from an average of 2.49 to 17 in the *MSH2* population.

Given that recurrence is the metric by which a mutation is considered impactful within this study, we sought to find a null hypothesis for the rate by which recurrence happens by

chance. To simplify comparisons between experiments, any mutation that has reached a detectable frequency in the population is considered regardless of its frequency. Conducting a simple simulation using the estimated number of mutations within the experiments and an assumption of equal mutational probability across all genes, we found that for every set of 32 populations, there should be one instance of a recurrently targeted gene by chance and a diminishingly small probability that a gene will be affected three times. Given these rates, for subsequent analysis we decided to use a cutoff of two mutations per gene to maximize discovery while limiting the noise of hitchhiker mutations (See methods for more details).

Categorizing these recurrent mutations based on the genes they impacted, we generated both a measure of frequency of recurrence to mutations that were previously observed as well as new targets of mutation (**Figure 2.1**). Similar to previous findings, both of the primary nutrient transporters for sulfate and phosphate, *SUL1* and *PHO84* respectively, were some of the most recurrently impacted genes. We suspect that the mutations impacting these genes are likely gain of function mutations given that they led to substitutions in two amino acid positions in *SUL1* and one in *PHO84* without generating any new stop codons. Several genes that have been previously identified in other chemostat evolution experiments as being mutated were similarly found here, such as *GSH1*, *WHI2*, *SGF73*, and *SIR1* (**Figure 2.2A-C**). Not surprisingly, these targets were among the most recurrently targeted within our experiments, providing additional evidence of their adaptive benefit within their given condition.

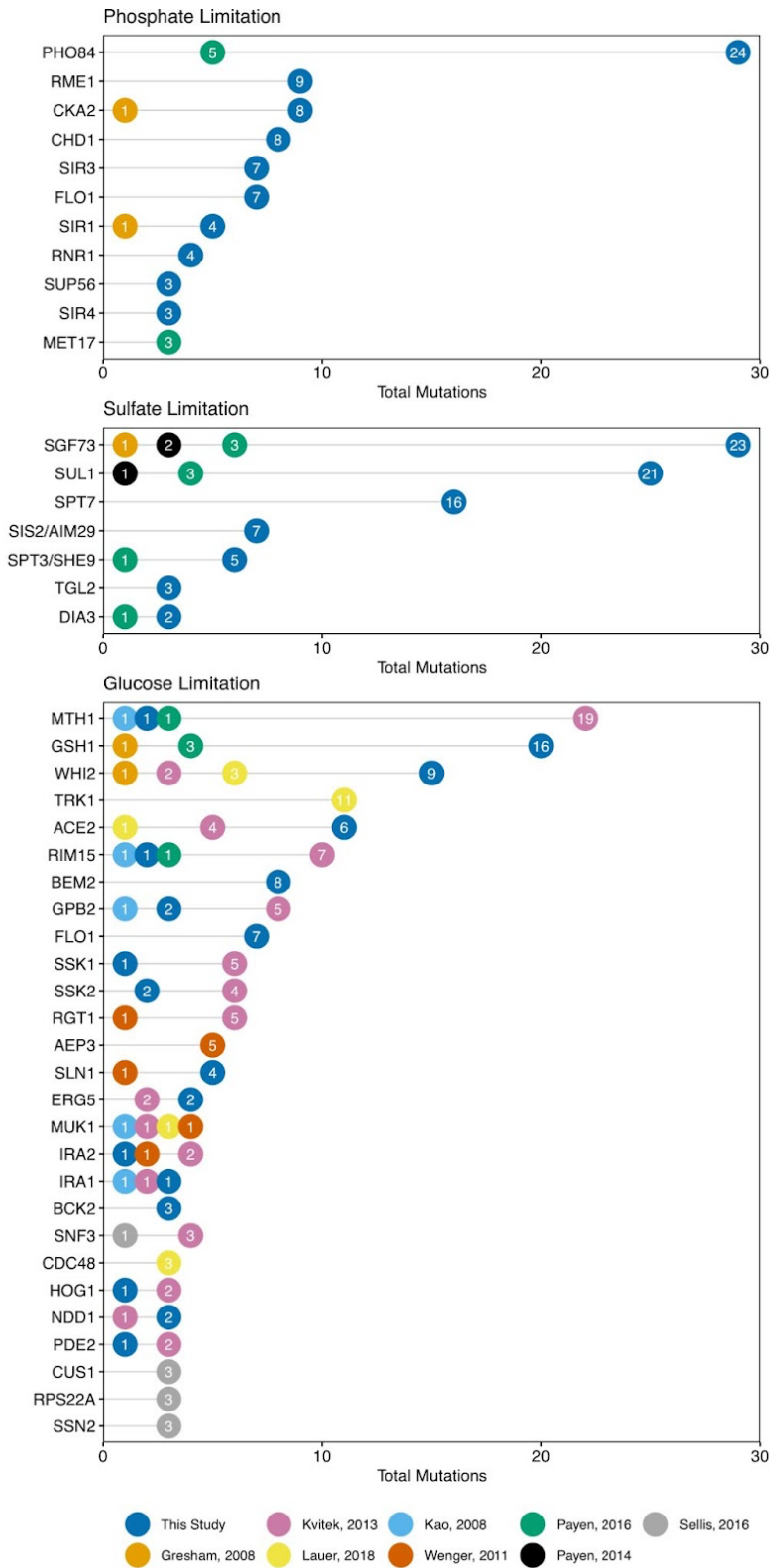


Figure 2.1. Comparisons to all known chemostat experimental evolution sequencing reveals common targets and newly discovered mutation targets. The values contained within the bubble show the number of occurrences within that study while the horizontal position denotes the cumulative number across all studies.

Looking for commonalities between the recurrently targeted genes within their condition, we found specific examples of multiple members of complexes and pathways being recurrently targeted (Figure 2.2). In sulfate-limited media specifically, we discovered that four separate members of a large, multi-protein complex known as the SAGA complex were recurrently targeted (p-value from bonferroni corrected GO-term analysis: 3.312×10^{-6}). While it was previously known that *SGF73* was a common target in sulfur-limited media, *SPT7*, *SPT3*, and *HFII* were newly found to be important due to increased replicate number. Similarly, in phosphate-limited media, we found four separate members of the sirtuin family, *SIR1*, *SIR2*, *SIR3*, and *SIR4*, recurrently targeted (p-value from bonferroni corrected GO-term analysis: 5.563×10^{-6}). Finally, within glucose-limited populations, we found both the recurrent targeting of the MAPK signaling pathway through *SLNI* and *SSK2* (p-value from bonferroni corrected GO-term analysis: 2.587×10^{-2}) as well as an association with the biological process of response to oxygen-containing compound through *GSH1*, *WHI2*, *FLO1*, *GPB2*, and *GPA2* (p-value from bonferroni corrected GO-term analysis: 1.652×10^{-3}).

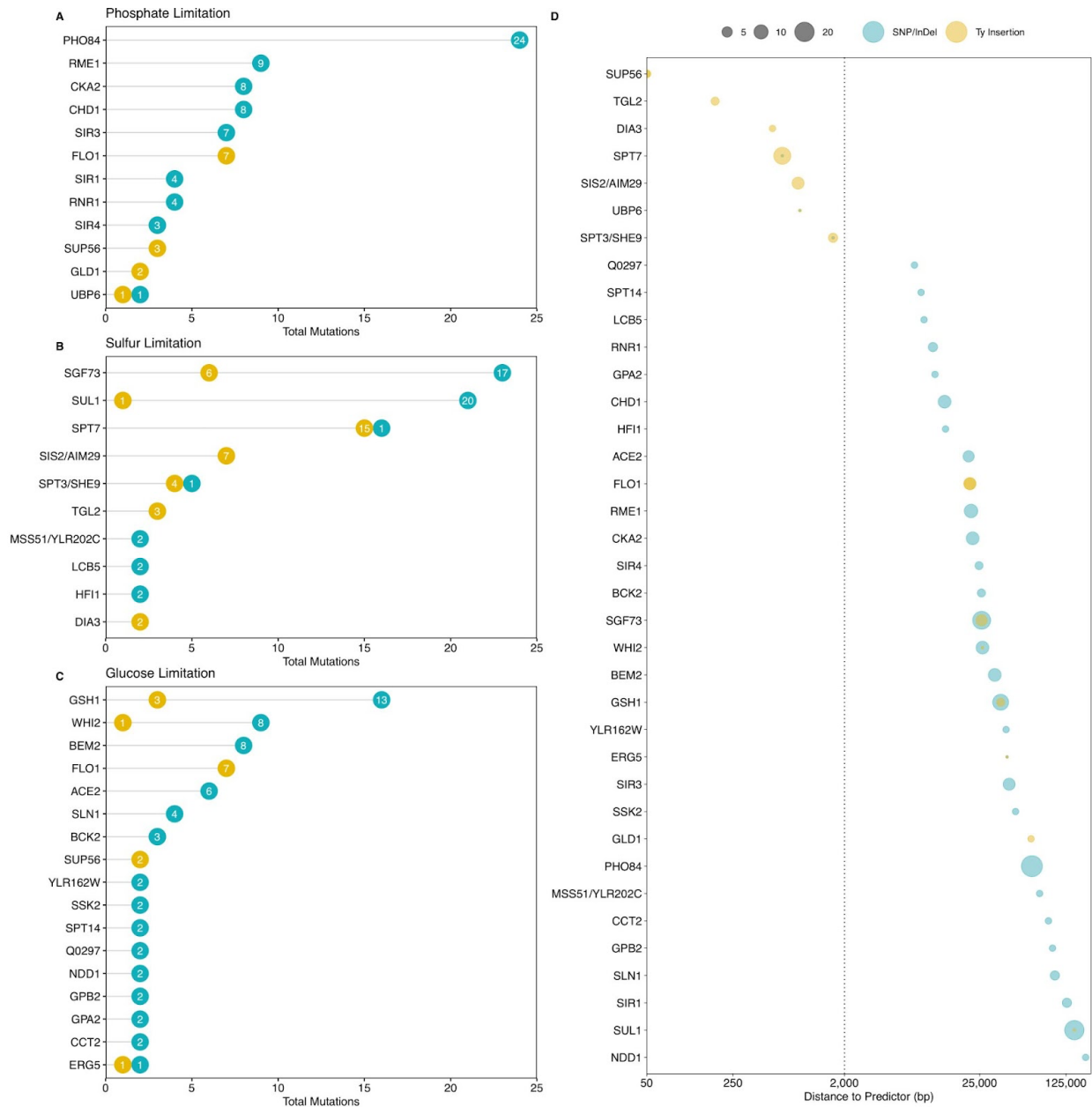


Figure 2.2. Recurrent targets of mutation impacted by bias in mutational preference. (A-C) Summaries of mutations generated by Ty element mobilizations (Orange), and SNPs/InDels (Blue) in 32 phosphate, 31 sulfur, and 32 glucose limited chemostat evolution experiments show the recurrent nature of adaptive evolution. The values contained within the bubble show the number of occurrences of that type of mutation while the horizontal position denotes the cumulative number across both Ty elements and SNP/InDels. (D) The distance between the recurrently targeted genes and a predictor of Ty element mobilization shows the neutral patterns of mutational bias still holds in adaptive conditions.

2.2.2 Proximity to a Pol III-transcribed gene likely influences the rate of gene disruption by Ty element during adaptive evolution

In addition to certain pathways and loci being recurrently affected in the same condition, we similarly observed certain loci being recurrently affected by Ty element mobilization. The known patterns of Ty element mobilization indicate that under neutral conditions, new mobilizations should preferentially occur within two kilobases upstream of genes transcribed by RNA Polymerase III (Baller et al., 2012; Bridier-Nahmias et al., 2015; Mularoni et al., 2012). Given the number of new mobilizations observed within these experiments, we explored whether the neutral patterns of mutation would be evident when challenged by the pressures of natural selection. Within sulfur-limited conditions, we observed that *SPT7* was targeted 15 times by Ty element mobilization and only once by an interrupting SNP. Conversely, *SGF73*, which is a member of the same complex, was targeted 6 times by Ty element mobilization, but 17 times by interrupting SNPs and InDels. An obvious difference that could explain the preference by which either gene was interrupted was its proximity to a Pol III-transcribed gene. Formalizing this observation, we analyzed across the whole dataset the distance of every gene observed to be mutated to a Pol III-transcribed gene (**Figure 2.2D**). For all of the mobilizations within the dataset, 70 of the 141 mobilizations fell within 2 kb of a Pol III-transcribed gene, which is significantly more than if there was no mobilization preference (expectation of 6.57 mobilizations within 2 kb of a predictor under a model with no mobilization preference). Of the 66 mobilizations that fell near recurrently targeted genes, 37 were within 2 kb of a Pol III-transcribed gene, indicating that selection did not dramatically reduce the neutral mobilization biases. To test whether a gene's proximity to a predictor correlated with whether it was preferentially disrupted by a Ty element mobilization or SNP/InDel, we conducted a chi-square

test of significance on the data displayed in **Table 2.1** (p-value < 2.2e-16). These results indicate a strong correlation between the proximity of a Pol III-transcribed gene and the preferential interruption of a gene sequence by a Ty element versus an interrupting SNP or InDel.

Table 2.1. Contingency table of the number of Ty element insertions near predictors of mobilization

Recurrent insertions		Near Predictor	
		Yes	No
Ty Element Insertion	Yes	32	28
	No	3	169

2.2.3 Chromosomal amplifications potentially dependent on genome context

Investigating the role of copy number variations in the three sets of nutrient-limited chemostat evolution experiments, we found partial chromosomal amplifications in all three conditions. Strikingly, in sulfur-limited populations, we discovered that every single population experienced a partial chromosomal amplification impacting the primary sulfur transporter, *SUL1* (**Figure 2.3**). Additionally, we found that multiple amplification events had occurred simultaneously in the populations, leading to competing lineages within an experiment and a total of 42 separate amplifications among the 31 populations. Between the 42 amplifications, no single pair of breakpoints on either side of the amplification was shared, indicating that each amplification was unique. Mapping the sequencing coverage of the populations from sulfate limitation and juxtaposing them alongside previously generated measurements of the impact of individual amplifications (Payen et al., 2016), we found that the span of the amplifications preferentially included regions that provided a positive fitness benefit, while regions that were deleterious were

not included. In particular, we discovered that 28 of the 42 amplifications included the *SNF5* gene, which was previously shown to provide a 14.4% positive fitness benefit when amplified in sulfate limited media. Also, only 5 of the 42 amplifications included the *DUG2* and *MRLP27* genes, which have both been shown to respectively have a 20.1% and 5.1% negative effect on relative fitness when amplified in sulfur limited media conditions.

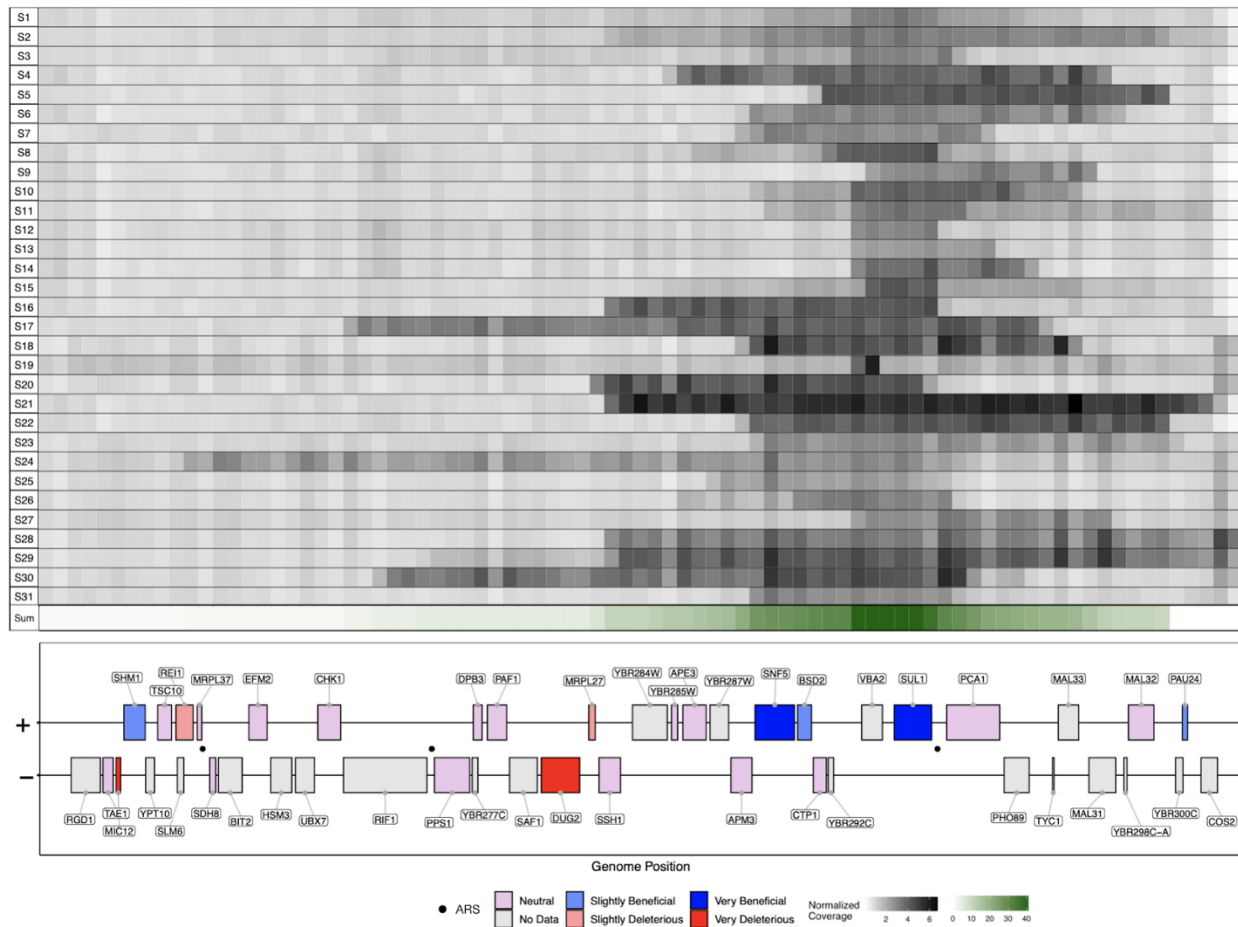


Figure 2.3. Recurrent amplification of the primary sulfate transporter potentially impacted by local sequence context. The normalized copy number of all 31 populations evolved in sulfate limited chemostats shows the recurrent amplification of *SUL1* in 42 separate amplifications. A summary of the span of all of these amplifications was generated through visual inspection of the coverage breakpoints using split and discordant sequencing reads. The span of the amplifications were compared with the ORFs (below) contained in the amplifications and their predicted impact when amplified at low-copy numbers (Payen et al., 2016). The span of the amplifications suggest that *SNF5* and *BSD2* was preferentially included while *DUG2* and *MRPL27* were avoided.

When analyzing the potential adaptive benefit of a *PHO84* amplification, we found that eight populations showed evidence of an increase in copy number (Data not shown).

Interestingly, when analyzing the adaptive consequences of an amplification of *PHO84* in the context of its chromosomal location, we discovered that there were no potential adverse fitness consequences to an amplification of the neighboring region to a low copy number (**Figure 2.4**).

Additionally, we observed that two populations, grown in glucose-limited media, experienced an increase in copy number of *HXT6/7* (Data not shown), their primary glucose transporters, which has been previously observed (Kvitek and Sherlock, 2011).

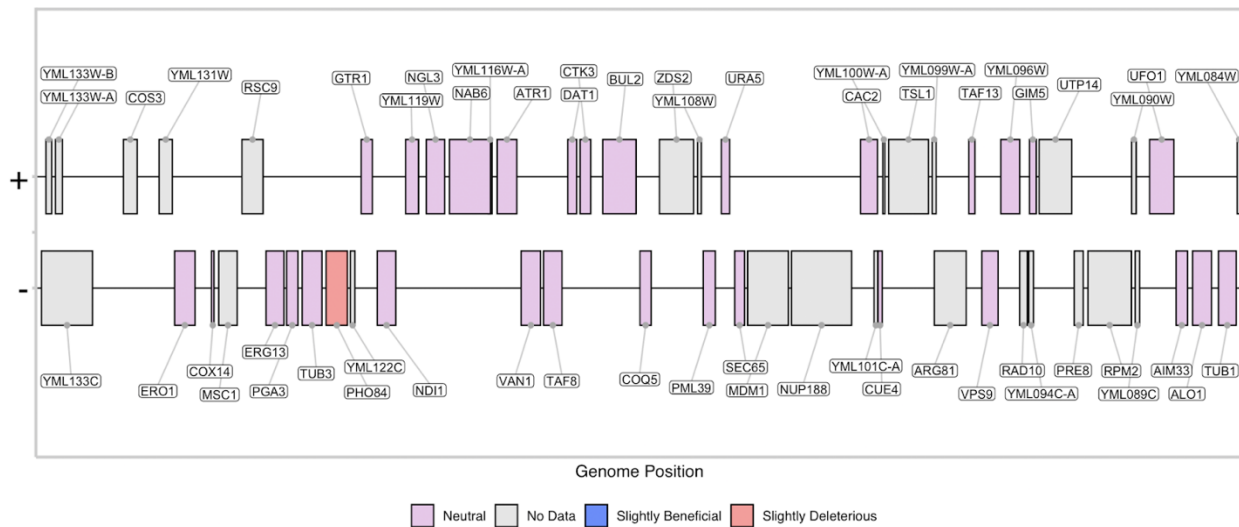


Figure 2.4. Local sequence context of *PHO84* provides no additional benefit or detriment to a chromosomal amplification. The ORFs neighboring *PHO84* are displayed with their associated predicted impact when amplified at low-copy numbers (Payen et al., 2016).

2.3 Discussion

2.3.1 Level of recurrence among parallel evolution experiments

Across the 95 evolution experiments conducted here, we discovered a more complete spectrum of the adaptive targets of evolution, including 52 copy number amplifications, 367 SNPs and InDels, and 141 Ty element transpositions. This includes both additional evidence for the

adaptive benefit of genes with minimal evidence in previous experiments as well as novel targets only identified here. Within the glucose-limited chemostats, having the most replication across other studies, there is a sizable disagreement between the most recurrently mutated genes with Kvitek et al. finding *MTH1* as the most recurrently mutated, this study with *GSH1* and *WHI2*, and Lauer et al. with *TRK1*. The most striking difference between these studies is the use of a different dilution rate for media entering the chemostats (Kvitek et al., 0.2 hr⁻¹, this study, 0.17 hr⁻¹ and Lauer et al., 0.12 hr⁻¹). A difference in dilution rate could generate differences in the population density, availability of glucose, and whether fermentation or respiration is favored. Similarly, Sellis et al. and Wenger et al. utilized a diploid strain of yeast and had a different spectrum of mutations, likely due to the recessive nature of some of the mutations. Therefore, despite using highly similar conditions, even subtle differences between culturing conditions can produce a distinct spectrum of mutations.

Within sulfur-limited conditions, the most recurrently targeted gene is the primary sulfate transporter, *SUL1*, which experienced 21 SNP's, 1 transposable element insertion into its promoter, and 42 separate amplifications. Additionally, multiple members of a large, multiprotein transcriptional complex known as the SAGA-complex were newly discovered to be recurrent targets in sulfate limited conditions (*SGF73*, *SPT3*, *SPT7* and *HF11*). Considering the low number of replicates of sulfate limited chemostat evolution experiments prior to these experiments, there had only been six observations of *SGF73* mutations and only one observation of a *SPT3* mutation. Given that we now know that there are recurrent mutations in multiple members of the SAGA-complex that are each a part of separate domains within the complex, the presumed benefit of these mutations likely depends on a shared effect of all of them (reviewed in (Cheon et al., 2020; Donczew et al., 2020)). However, given that the SAGA-complex is

responsible for a large fraction of the total transcription within the cell, an individual benefit to these mutations has not been determined to date.

Finally, within phosphate limited conditions, matching with previous findings, *PHO84* was recurrently mutated 24 times in two amino acid positions as well as amplified in at least 8 populations (Payen et al., 2016). Additionally, we discovered all four of the sirtuin genes with SNPs or InDels, commonly leading to an early stop codon. Previously, the one mutation found in *SIR1* in Gresham et al. was presumed to be a neutral hitchhiker given its performance in a competition assay, however given its recurrence here along with the other members of the sirtuin family, it is likely an adaptive mutation. Furthermore, we newly found four instances of nonsynonymous mutation in a member of the dNTP synthesis complex, *RNRI*. Previously, in a large screen using the yeast deletion collection, the disruption of *RNRI* was found to lead to a 23.4% competitive fitness defect in phosphate limitation, indicating that the recurrent nonsynonymous mutations in *RNRI* likely led to a gain of function phenotype.

2.3.2 Transposition bias likely shifts adaptive outcomes

Given the capacity of transposable element mobilization to result in a diversity of fitness consequences in many Eukaryotic organisms (Schrader and Schmitz, 2019), and our ability to detect these new mobilizations using whole genome sequencing data (Chen and Zhang, 2021; Nelson et al., 2017), we sought to determine the interplay between Ty element mobilization and evolutionary outcomes during adaptive evolution. Comparing the position of new Ty element mobilizations with the known predictors of mobilization (location of targets of Pol III), we found evidence that even under adaptive scenarios, the neutral biases are maintained at a strong predictive rate. There were several notable exceptions to this trend including *SGF73*, *GSH1* and

FLO1. Given that *SGF73* and *GSH1* are the most recurrently mutated genes in sulfur and glucose limited conditions respectively, we suspect that despite the lower predicted mobilization rate in these regions, there is a much higher selective pressure for these mobilizations events than other background locations, which allows them to be observed in our experiments. *FLO1* was likely so recurrently observed because it was one of the rare instances where a new Ty element mobilization led to a gain of function through increasing transcription of *FLO1*, leading to a cellular aggregation phenotype (Hope et al., 2017).

Additionally, we found that a majority of the transposition events landed in regions that generated loss of function mutations through interruption of the reading frame. Given that a majority of the transposition events generated a loss of function effect, which was similarly achieved through a SNP or InDel leading to an early stop codon, we sought to determine whether there was a preference for a gene to be impacted by a Ty mobilization event or SNP/InDel when it was either near or a Pol III-transcribed gene or not. We found that there was a large preference for genes near Pol III-transcribed genes to be impacted by transposition events. These results indicate that the presence of a Pol III-transcribed gene in the local sequence neighborhood of a gene could significantly impact its long term evolutionary outcome.

2.3.3. Dependence of copy number variation on local sequence

Chromosomal amplifications are an important form of mutation that increase the relative dosage of genes encompassed by the amplification, which can provide either a fitness benefit or detriment depending on the genes amplified. Given that amplifications typically span multiple gene segments, the collective adaptive benefit of these amplifications typically depends on their total span and which genes are encompassed. During the early stages of adaptation, a large

quantity of possible amplifications are explored, with the population typically narrowing to just a few prominent lineages after 250 generations (Lauer et al., 2018). Which lineages become dominant by the later timepoints likely depends on the adaptive benefit of the amplification and additional mutations that occur in their genetic background. Previous experiments using a collection of strains with synthetically generated chromosomal amplifications that extended to the telomere (the TAMP collection) showed that the selective benefit of an amplification depends on a few specific genes instead of the accumulative small effects of a large number of genes (Sunshine et al., 2015). Additionally, the same group, using a targeted collection of strains with amplifications on the right arm of chromosome II were able to specifically show that in sulfate-limited conditions the adaptive benefit of amplifications within that region not only depend on the primary adaptive driver, *SUL1*, but also, a segment of DNA just upstream, containing *SNF5* and *BSD2*. From 42 separate amplifications containing the *SUL1* in sulfate limited conditions, we were able to replicate these observations with naturally generated strains from experimental evolution. We also observed that the amplifications on the right arm of chromosome II preferentially terminated before the inclusion of two genes, *DUG2* and *MRPL27*, which both provide a deleterious effect when individually amplified at low copy number (Payen et al., 2016). This would indicate that the adaptive benefit of an amplification depends both on the presence of genes that provide a benefit when amplified within the local neighborhood and the lack of genes that are deleterious when amplified. Alternatively, the amplifications could preferentially end before *DUG2* and *MRPL27* due to mechanistic constraints on their length, which would be based on the type of amplification. However, the average length of amplifications containing *GAPI* from experiments done in nitrogen limited conditions was 105 kilobases, which is more than twice the distance between the telomere of chromosome II and

DUG2, indicating the lack of a mechanistic constraint that would lead to a preferential end of amplifications before *DUG2* (Lauer et al., 2018). Together, these data indicate that the landscape of possible adaptive amplifications depends on both the benefit of an individual gene amplification as well as the local sequence neighborhood.

2.4 Materials and Methods

Strains and chemostat experimental setup

Wild-type FY *MATa* prototrophic yeast was used for all experiments in this study. For each experiment, a single colony was inoculated into glucose-, phosphate-, or sulfate-limited media and grown as overnight cultures with rotation. From the overnight cultures, 100 μ L was sterically inoculated into 20 mL of nutrient-limited media in the miniature chemostats. After 30 hours of growth inside of the miniature chemostats, the peristaltic pumps that controlled flow of media to the chambers were turned on and used to maintain a constant dilution rate of $0.17 \pm 0.01 \text{ hr}^{-1}$. After an estimated 200 generations of growth, 10 mL of culture were sampled from the miniature chemostats for subsequent genome sequencing. The glucose-, phosphate-, or sulfate-limited media were prepared as previously described and the recipes are readily available (<https://dunham.gs.washington.edu/protocols.shtml>).

Whole genome sequencing

DNA was extracted using the YeaStar Genomic DNA extraction kit (Zymo Research Inc.). Genomic DNA libraries were prepared for sequencing using the Nextera sample preparation kit per manufacturer's instructions (Illumina Inc.). Sequencing libraries were quantified on a Qubit Fluorometer (Invitrogen Inc.) and pooled by molarity. The libraries were then sequenced on an Illumina NextSeq 550 per manufacturer's instructions for 150 basepair paired-end sequencing

reads. The sequencing reads were demultiplexed using the bcl2fastq software with standard parameters.

Whole genome alignments, SNP and InDel variant calling

Whole genome sequencing reads were aligned to the SacCer3 reference genome (R64-1, SGD) using BWA/0.7.15 mem and were sorted and indexed using SAMtools/1.9. Subsequently, the reads were deduplicated with PicardTools/2.23.3 and realigned around indels using GATK/3.7. Variants were then called using bcftools/1.9, freebayes/1.0.2-6-g3ce827d and lofreq/2.12. The outputs of these three software tools were filtered with the parameters listed in Table 1. Afterwards, every variant was checked in the Integrative Genomics Viewer (IGV) versus the ancestral sequencing for veracity, similar to as described (Robinson et al., 2017). The filtered variant calls were then annotated for their position relative to the R64-1 gene features file with a previously described script (Pashkova et al., 2013).

Transposable element mobilization calling

De novo Ty element mobilizations were called versus the ancestral FY4 strain using the McClintock software package with a few modifications (Nelson et al., 2017). As an input to the software package, reads from multiple sequencing runs were concatenated using unix commands to provide a single, high coverage input. Given the high level of false-positives detected in the resulting calls, the Ty element mobilization calls were first filtered by their proximity to miss-calls in the FY4 output. Subsequently, the mobilizations were visually inspected for veracity, tabulating the number of split and discordant reads supporting each individual mobilization, and checking for the precise position of insertion. A Ty element call was only considered if there were at least 6 reads supporting the call. The proximity of a Ty element mobilization to gene

features in the yeast genome was added to each call using a script written in the python coding language.

Simulations for recurrent mutation threshold

The threshold for when the degree of recurrence of a gene is not likely to be by chance was generated through a simplistic simulation script written in the R programming language. The mean number of mutations per population within a coding ORF from our previous variant and Ty element mobilization calling was randomly distributed among the 6694 possible genes in the yeast genome. This process was repeated 32 times to simulate the number of populations in the study. Afterwards, the number of recurrently targeted genes among those 32 populations was calculated. The simulation of the 32 populations was then repeated 10,000 times. Afterwards, the total number of recurrences was plotted and averaged among the 10,000 simulations to find the number of recurrences that are expected among 32 populations by chance.

Genome coverage and copy number

Detection of copy number variants and summaries of relative copy number were generated from the previously mentioned sequencing alignments for all of the evolved populations. First, the mean coverage across 1000-bp sliding windows was generated using IGVtools. The coverage of the sliding windows was then normalized by the total coverage across the genome excluding the mitochondrial DNA through GATK DepthOfCoverage. For samples with likely amplifications of either *SUL1* or *PHO84*, the total coverage mean excluded their corresponding chromosomes. The span of each of the amplifications from populations derived from sulfate-limited media was estimated using a combination of the normalized 1000-bp coverage files and split and discordant

reads. The split and discordant reads were generated from alignments to the SacCer3 reference genome using the samblaster/0.1.24 software.

CHAPTER 3 TEMPERATURE PREFERENCE CAN BIAS PARENTAL GENOME RETENTION DURING HYBRID EVOLUTION

The work described here is derived from: Smukowski Heil CS, Large CRL, Patterson K, Hickey ASM, Yeh CLC, Dunham MJ. 2019. Temperature preference can bias parental genome retention during hybrid evolution. *PLoS Genet* **15**:e1008383. doi:10.1371/journal.pgen.1008383. Full details of author contributions are available above.

Interspecific hybridization can introduce genetic variation that aids in adaptation to new or changing environments. Here, we investigate how hybrid adaptation to temperature and nutrient limitation may alter parental genome representation over time. We evolved *Saccharomyces cerevisiae* x *Saccharomyces uvarum* hybrids in nutrient-limited continuous culture at 15°C for 200 generations. In comparison to previous evolution experiments at 30°C, we identified a number of responses only observed in the colder temperature regime, including the loss of the *S. cerevisiae* allele in favor of the cryotolerant *S. uvarum* allele for several portions of the hybrid genome. In particular, we discovered a genotype by environment interaction in the form of a loss of heterozygosity event on chromosome XIII; which species haplotype is lost or maintained is dependent on the parental species temperature preference and the temperature at which the hybrid was evolved. We show that a large contribution to this directionality is due to a temperature dependent fitness benefit at a single locus, the high affinity phosphate transporter gene *PHO84*. This work helps shape our understanding of what forces impact genome evolution after hybridization, and how environmental conditions may promote or disfavor the persistence of hybrids over time.

3.1 Introduction

Comparative genomics of thousands of plants, animals, and fungi has revealed that portions of genomes from many species are derived from interspecific hybridization, indicating that hybridization occurs frequently in nature. However, the influence of processes such as selection, drift, and/or the presence or absence of backcrossing to a parental population on hybrid genome composition in incipient hybrids remains largely unknown. In some cases, hybrids will persist with both parental genomes in fairly equal proportions as new hybrid species or lineages, while in other instances, hybrid genomes will become biased towards one parent sub-genome over time (Albertin and Marullo, 2012; Buggs et al., 2010; Cheng et al., 2012; Emery et al., 2018; Louis et al., 2012; Prysycz et al., 2014; Schnable et al., 2011; Soltis et al., 2014; Wang et al., 2006). Untangling the genetic and environmental factors that lead to these outcomes is a burgeoning field.

Some hybrid genotypes will be unfit due to genetic hybrid incompatibilities or cytotype disadvantage; decades of work across many systems have illustrated examples of hybrid sterility and inviability (Coyne and Orr, 2004). Recent work has demonstrated that in hybrid genomes with a bias in parental composition like humans, in which most of the genome is comprised of modern human haplotypes with small fragments derived from archaic human, regions from the minor parent (e.g., Neanderthal or Denisovan) are decreased near functional elements and hybrid incompatibilities (Juric et al., 2016; Sankararaman et al., 2014; Schumer et al., 2018).

Conversely, there are examples of “adaptive introgression,” in which alleles from the minor parent confer a benefit, like wing patterning in butterflies, high altitude tolerance in the Tibetan human population, and winter color morphs in the snowshoe hare (Dasmahapatra et al., 2012; Huerta-Sánchez et al., 2014; Jones et al., 2018; Norris et al., 2015; Oziolor et al., 2019; Racimo

et al., 2015; Richards and Martin, 2017; Song et al., 2011; Suarez-Gonzalez et al., 2018). The environment undoubtedly plays a significant role in hybrid fitness, and genotype by environment interactions will shape hybrid fitness in a similar manner as they shape non-hybrid fitness. For example, there is general acceptance that the *Saccharomyces* species complex is largely void of genic incompatibilities (with exceptions (Lee et al., 2008)), however most experiments looking for incompatibilities have used laboratory conditions. Hou *et al.* utilized different carbon sources, chemicals, and temperatures to show that over one-fourth of intraspecific crosses show condition-specific loss of offspring viability (Hou et al., 2015). This is echoed by many examples of condition specific hybrid incompatibility in plants (Bombliet et al., 2007; Chen et al., 2014; Fu et al., 2013; Jeuken et al., 2009; Saito et al., 2007; Shii et al., 1980). Similarly, there are numerous examples of environment dependent high fitness hybrid genotypes (Anderson et al., 2009; Arnold et al., 2012; Grant and Grant, 2010, 2002; Johnson et al., 2010; Martin et al., 2006; Rieseberg et al., 2003; Salzburger et al., 2002; Schwarz et al., 2005; Seehausen, 2004; Zhang et al., 2020), exemplified by classic research showing Darwin's finch hybrids with different beak shapes gained a fitness benefit during and after an El Niño event (Grant and Grant, 2002).

The budding yeasts in the genus *Saccharomyces* have emerged as a particularly adept system to study genome evolution following hybridization. Recent evidence supports the hypothesis that the long-recognized whole genome duplication that occurred in the common ancestor that gave rise to *Saccharomyces* resulted from hybridization (Marcet-Houben and Gabaldón, 2015), and led to speculation that ancient hybridization could also explain other whole genome duplications in plants and animals (Wolfe, 2015). Introgression and hybridization have also been detected across the *Saccharomyces* clade (Barbosa et al., 2016; Belloch et al., 2009; González et al., 2006; Hittinger, 2013; Leducq et al., 2016; Marsit et al., 2017; Selmecki et al.,

2015); most famously, the lager brewing lineage *S. pastorianus* is a hybrid between *S. cerevisiae* and *S. eubayanus* (Baker et al., 2015; Dunn and Sherlock, 2008; Gibson and Liti, 2015; Nakao et al., 2009; Peris et al., 2016; Walther et al., 2014). A bias towards one parent sub-genome was identified in the ancient hybridization event and in *S. pastorianus*, and selection is inferred to be important in this process (Emery et al., 2018; Marcet-Houben and Gabaldón, 2015).

Experimental evolution of lab derived hybrids has provided significant new insights into the genetic architecture and influence of the environment on hybrid genome evolution (Dunn et al., 2013; Peris et al., 2020; Piotrowski et al., 2012; Zhang et al., 2020).

To empirically understand the genomic changes that occur as a hybrid adapts to a new environment, we previously created *de novo* interspecific hybrids between two yeast species, *S. cerevisiae* and *S. uvarum*, which are approximately 20 million years divergent and differ in a range of phenotypes, notably in preferred growth temperature. *S. uvarum* has been isolated primarily from *Nothofagus* (beech) and associated soil in Patagonia and similar habitats across the world, and is specifically known for fermentation of cider and wines at cold temperatures (Almeida et al., 2014; Fernandez-Espinar et al., 2003; Pérez-Torrado et al., 2018; Rainieri et al., 1999; Rodríguez et al., 2017). Many *S. uvarum* strains show evidence of introgression from several other yeast species, and *S. cerevisiae* x *S. uvarum* hybrids have been isolated from fermentation environments (Almeida et al., 2014; Krogerus et al., 2018).

We previously evolved *S. cerevisiae* x *S. uvarum* hybrids in the laboratory in several nutrient-limited environments at the preferred growth temperature of *S. cerevisiae* (Smukowski Heil et al., 2017). We frequently observed a phenomenon known as loss of heterozygosity (LOH) in these evolved hybrids, in which an allele from one species is lost while the other species' allele is maintained. The outcome of such events is the homogenization of the hybrid

genome at certain loci, and represents a way in which a hybrid genome may become biased toward one parent's sub-genome. This type of mutation can occur due to gene conversion or break induced replication, and as previously noted, has also been observed in organisms including *S. pastorianus*, pathogenic hybrid yeast, and hybrid plants, but its role in adaptation has been unclear (Li and Zhang, 2013; Marsit et al., 2017; Schröder et al., 2016). We used genetic manipulation and competitive fitness assays to show that a particular set of LOH events was the result of selection on the loss of the *S. uvarum* allele and amplification of the *S. cerevisiae* allele at the high affinity phosphate transporter *PHO84* in phosphate limited conditions. By empirically demonstrating that LOH can be the product of selection, we illuminated how an underappreciated mutation class can underlie adaptive hybrid phenotypes.

This prior study described an example of how the environment (differences in nutrient availability) can bias a hybrid genome towards one parent's sub-genome. Due to many examples of genotype by temperature interaction in hybrids across many taxa, and in particular difference in species temperature preference in our hybrids, we speculated that temperature is an important environmental modifier which may influence parental sub-genome representation in hybrids. Temperature can perturb fundamentally all physiological, developmental, and ecological processes, and as such, temperature is an essential factor in determining species distribution and biodiversity at temporal and spatial scales (Chen et al., 2011; Guisan and Thuiller, 2005; Stuart-Smith et al., 2017). We hypothesized that in *S. cerevisiae* x *S. uvarum* hybrids, *S. cerevisiae* alleles may be favored at warmer temperatures, whereas *S. uvarum* alleles may be preferred at colder temperatures, giving the hybrid an expanded capacity to adapt. To test how temperature influences hybrid genome composition over time, we evolved the same interspecific hybrid yeast in the laboratory at 15°C for 200 generations. In comparing laboratory evolution at 15°C and

30°C, we present evidence that temperature can indeed bias hybrid genome composition towards one parental sub-genome, and we focus on a reciprocal LOH event at the *PHO84* locus. We show that which species' allele is lost or maintained at this locus is dependent on the parental species' temperature preference and the temperature at which the hybrid was evolved, thus revealing a genotype by environment interaction. Our results are one of the first clear examples with a molecular genetic explanation of how hybrids have expanded adaptive potential by maintaining two genomes, but also how adapting to one condition may abrogate evolutionary possibilities in heterogeneous environments.

3.2 Results

3.2.1 *Laboratory evolution of hybrids and their parents at cold temperatures*

To test whether temperature can influence the direction of resolution of hybrid genomes, we evolved 14 independent populations of a *S. cerevisiae* x *S. uvarum* hybrid in nutrient-limited media at 15° C for 200 generations (phosphate-limited: 6 populations; glucose-limited: 4 populations; sulfate-limited: 4 populations; see **Table B.4** for strain details). Diploid *S. cerevisiae* and *S. uvarum* populations were evolved in parallel (4 populations of *S. cerevisiae* and 2 populations of *S. uvarum* in each of the three nutrient limited conditions; see **Table B.4** for strain details). Populations were sampled from the final timepoint and submitted for whole genome sequencing and analysis.

3.2.2 *Loss of *S. cerevisiae* alleles in cold evolved hybrids*

We detected large scale copy number variants in our cold evolved populations, including whole and partial chromosome aneuploidy and loss of heterozygosity (**Table 3.1**; **Tables B.1-B.2**;

Figures B.1-B.7). Copy number changes, and specifically amplification of nutrient transporter genes, are well-recognized paths to adaptation in laboratory evolution in nutrient limited conditions (Dunham et al., 2002; Dunn et al., 2013; Gresham et al., 2010, 2008; Hong et al., 2018; Lauer et al., 2018; Payen et al., 2014; Piotrowski et al., 2012; Sanchez et al., 2017; Selmecki et al., 2015; Smukowski Heil et al., 2019; Sunshine et al., 2015). We find a preference for *S. cerevisiae* partial and whole chromosome amplification in hybrids evolved at both 15°C and 30°C, which may reflect an increased capacity for *S. cerevisiae* to acquire this type of mutation (**Table 3.1**) (Bergström et al., 2014). In contrast, we observe a bias in the direction of LOH resolution dependent on temperature. Previously, we observed more LOH events in hybrids evolved at 30°C in which the *S. uvarum* allele was lost (5/9 LOH events) (Smukowski Heil et al., 2017). In this study, we observe 6/6 LOH events in hybrids evolved at 15°C in which the *S. cerevisiae* allele is lost and the *S. uvarum* allele is maintained, suggestive of a *S. uvarum* cold temperature benefit. While our sample sizes are modest, together these results indicate that temperature can determine hybrid genomic composition in the generations following a hybridization event.

Table 3.1. Mutations in cold-evolved hybrid populations

Population	Location	Gene(s)	Mutation
P1-15°	<i>S. cerevisiae</i> chrXVI: 772650	<i>CLB2</i>	coding-nonsynonymous: D333A
	<i>S. uvarum</i> chrVII: 818275	<i>UBR1</i>	coding-nonsynonymous: F1634C
	<i>S. uvarum</i> chrXI: 5832	<i>JEN1</i>	5'-upstream
	<i>S. cerevisiae</i> chrXIII: 1-81102 <i>S. uvarum</i> chrXIII: 1-82283	41 genes including <i>PHO84</i>	LOH: loss of <i>S. cerevisiae</i> allele and amplification of <i>S. uvarum</i> allele

	<i>S. cerevisiae</i> chrXIII: 81102-168343	47 genes	CNV: Segmental amplification of <i>S. cerevisiae</i>
P2-15°	<i>S. uvarum</i> chrIV: 903941	<i>YBR259W</i>	coding-nonsynonymous: S624Y
P2F-15°	<i>S. uvarum</i> chrV: 179951	<i>YAT2</i>	coding-synonymous
P3-15°	<i>S. uvarum</i> chrXI: 101238	<i>LST4</i>	coding-nonsynonymous: S533A
	<i>S. cerevisiae</i> chrXIII: 1-79085 <i>S. uvarum</i> chrXIII: 1-80181	40 genes including <i>PHO84</i>	LOH: loss of <i>S. cerevisiae</i> allele and amplification of <i>S. uvarum</i> allele
	<i>S. cerevisiae</i> chrXIII:79085-168343	48 genes	Segmental amplification of <i>S. cerevisiae</i>
G7-15°	<i>S. cerevisiae</i> chrXI:80553	<i>ACPI</i>	5' upstream
	<i>S. cerevisiae</i> chrIV:651345-871844	118 genes	Segmental amplification <i>S. cerevisiae</i> allele
	<i>S. uvarum</i> chrII: 554234-1289935	159 genes	Segmental amplification <i>S. uvarum</i> allele
	<i>S. cerevisiae</i> chrXV:976083-1071297	46 genes	LOH: loss of <i>S. cerevisiae</i> allele
G8-15°	<i>S. cerevisiae</i> chrIV:955826	<i>VHS1</i>	5'-upstream
	<i>S. cerevisiae</i> chrV:321068	<i>AIM9</i>	coding-nonsynonymous: A369V
	<i>S. cerevisiae</i> chrXI:80553	<i>CCPI</i>	5'-upstream
	<i>S. cerevisiae</i> chrXV:977571	<i>TYE7</i>	coding-nonsynonymous: E167K
	<i>S. uvarum</i> chrXV:685069	<i>IKI1</i>	coding-nonsynonymous: A2E
	<i>S. cerevisiae</i> chrIII:169495-316620	82 genes	LOH: loss of <i>S. cerevisiae</i> allele
	<i>S. cerevisiae</i> chrXII:732111-1078177	181 genes	Segmental amplification of <i>S. cerevisiae</i> allele
	<i>S. cerevisiae</i> chrXV: 340969-464306,464306-594878	71 genes, 72 genes	LOH: loss of <i>S. cerevisiae</i> allele

G9-15°	<i>S. cerevisiae</i> chrXII:812389	<i>FKSI</i>	coding-nonsynonymous: S798Y
	<i>S. cerevisiae</i> chrXII:818575-1078177	136 genes	Segmental amplification of <i>S. cerevisiae</i> allele
	<i>S. cerevisiae</i> chrXV:976083-1071297	46 genes	LOH: loss of <i>S. cerevisiae</i> allele
G10-15°	<i>S. cerevisiae</i> chrXV:1034298	<i>GPB1</i>	5' upstream
S7-15°	<i>S. cerevisiae</i> chrXII:238463	<i>YLR046C</i>	coding-nonsynonymous: M117I
	<i>S. cerevisiae</i> chrXII:1047895	<i>FMP27</i>	coding-nonsynonymous: P1300S
	<i>S. cerevisiae</i> chrII:786030-813184	12 genes including <i>SUL1</i>	Segmental amplification of <i>S. cerevisiae</i> allele
S8-15°	<i>S. cerevisiae</i> chrIX:212119	<i>AIR1</i>	5' upstream
	<i>S. cerevisiae</i> chrIX:212130	<i>AIR1</i>	5' upstream
	<i>S. cerevisiae</i> chrII:786025-813184	12 genes including <i>SUL1</i>	Segmental amplification of <i>S. cerevisiae</i> allele
S9-15°	<i>S. cerevisiae</i> chrII:786017-813184	12 genes including <i>SUL1</i>	Segmental amplification of <i>S. cerevisiae</i> allele
S10-15°	<i>S. uvarum</i> chrXIII: 752118	<i>GTO3</i>	5' upstream
	<i>S. uvarum</i> chrXVI: 456125	<i>SUR1</i>	5' upstream
	<i>S. cerevisiae</i> chrII:770240-813184	21 genes including <i>SUL1</i>	Segmental amplification of <i>S. cerevisiae</i> allele

LOH: loss of heterozygosity; CNV: copy number variant. No mutations were detected in populations P4-15°, P5-15°, or P6-15°. Breakpoints of CNV and LOH are approximate.

In line with previous studies, we find both chromosomal aneuploidy and LOH are nutrient limitation specific, with repeatable genomic changes occurring in replicate populations under the same nutrient condition, but no changes shared across nutrients. In glucose limitation, 3/4 hybrid populations experienced chromosome XV LOH, losing the *S. cerevisiae* allele for

portions of the chromosome. Haploidization of one of these implicated regions on chromosome XV was previously observed in *S. cerevisiae* diploids evolved at 30°C in glucose limitation (Dunham et al., 2002; Smukowski Heil et al., 2017), but it was not observed in any previously evolved hybrids, and which genes may be responsible for fitness increases are unclear. In sulfate limitation, we recapitulate previous hybrid laboratory evolution results (Smukowski Heil et al., 2017), observing the amplification of the *S. cerevisiae* high affinity sulfate transporter gene *SUL1* in low sulfate conditions (4/4 hybrids, **Figures B.1, B.2**). Amplification of *S. cerevisiae* *SUL1* therefore seems to confer a high relative fitness regardless of temperature (see section below, “Pleiotropic fitness costs resulting from loss of heterozygosity”). Though prior work showed highly repeatable amplification of *S. cerevisiae* *SUL1* at 30°C in *S. cerevisiae* haploids and diploids (Dunham et al., 2002; Gresham et al., 2008; Payen et al., 2014; Sanchez et al., 2017; Smukowski Heil et al., 2017), and amplification of *S. uvarum* *SUL2* after approximately 500 generations at 25°C in *S. uvarum* diploids (Sanchez et al., 2017), we never observed amplification of *SUL1* or *SUL2* in *S. cerevisiae* or *S. uvarum* diploids at 15°C, albeit our experiments were terminated at 200 generations.

Finally and most notably, in low phosphate conditions, we discovered a LOH event in which the *S. cerevisiae* allele is lost and *S. uvarum* allele is amplified on chromosome XIII, which encompasses the high affinity phosphate transporter *PHO84* locus (2/6 hybrid populations; **Figure 3.1A**). The LOH tract length extends approximately 80kb from the telomere in both cold evolved populations (P1-15°C: 0-82,283; P3-15°C: 0-79,085), and the breakpoints are potentially due to microhomology, located in the genes *GIM5* and *VPS9*, respectively. This LOH event is of high interest, as we previously identified a repeated LOH event encompassing the same genomic region when hybrid populations were evolved at 30°C (3/6 populations,

Figure 3.1A). Furthermore, the directionality of this LOH event is the opposite outcome of our observations of hybrids evolved at 30° C, in which the *S. cerevisiae* allele was amplified and the *S. uvarum* allele was lost. We are unfortunately limited by sample size in determining if these LOH events are statistically significant; however, the repeatability and directionality in resolution of these LOH events suggest they are modulated by temperature and worthy of further investigation.

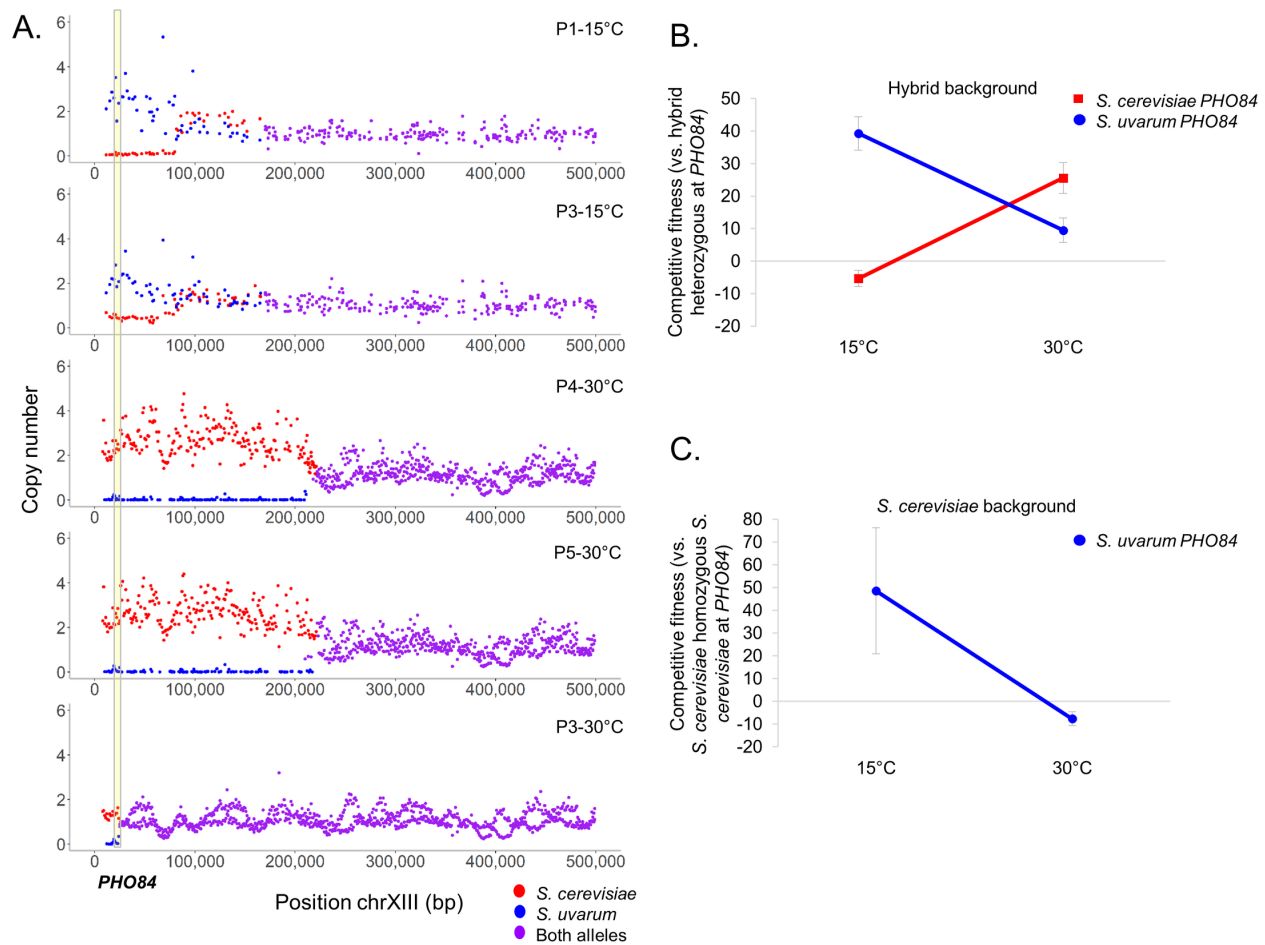


Figure 3.1. Loss of heterozygosity directionality results from selection on different species' alleles at different temperatures. **A)** Evolved hybrids exhibit reciprocal loss of heterozygosity on chromosome XIII encompassing the high affinity phosphate transporter gene *PHO84* (located in region shaded with yellow) in phosphate limited conditions at different temperatures. 2/6 independent populations lost the *S. cerevisiae* allele when evolved at 15°C (top 2 panels, breakpoints in *S. cerevisiae* coordinates P1-15°C: 82,283; P3-15°C: 79,085), 3/6 independent populations lost the *S. uvarum* allele when evolved at 30°C (bottom 3 panels, breakpoints in *S. cerevisiae* coordinates P4-30°C: 221753; P5-30°C: 234112; P3-30°C: 24,562). Purple denotes a region where both alleles are present at a single copy, blue denotes a *S. uvarum* change in copy number, red denotes a *S. cerevisiae* change in copy number. Note, copy number was derived from sequencing read depth at homologous ORFs. Clone sequencing was utilized for experiments at 30°C and population sequencing was utilized for experiments at 15°C, so exact population frequency and copy number changes are unclear for experiments at 15°C. **B)** Allele swap experiments in which a hybrid with one allele of *PHO84* from each species is competed against a hybrid with both copies of *PHO84* either from *S. cerevisiae* (Sc*PHO84*/Sc*PHO84*; red) or *S. uvarum* (Su*PHO84*/Su*PHO84*; blue) reveal a fitness effect dependent on temperature. Error bars denote 95% confidence intervals. **C)** Allele swap experiments in which a diploid *S. cerevisiae* homozygous for *S. cerevisiae* alleles of *PHO84* is competed against a diploid *S. cerevisiae* with both copies of *PHO84* from *S. uvarum* (Su*PHO84*/Su*PHO84*; blue) revealing a fitness effect dependent on temperature. Error bars denote 95% confidence intervals.

3.2.3 Environment-dependent loss of heterozygosity aids in temperature adaptation in hybrids

Based on previous results that demonstrated that LOH at the *PHO84* locus conferred a high competitive fitness benefit at warm temperatures (measured by direct competition of strains carrying the LOH vs an ancestral strain labeled with a neutral GFP marker), we hypothesized that this apparent preference for the alternate species' allele in different environments is explained by a genotype by environment interaction at the *PHO84* locus itself. Pho84 is a H⁺-coupled inorganic phosphate transporter, responsible for both sensing of phosphate in the environment and phosphate uptake, particularly when phosphate is scarce. The two species' proteins have a pairwise identity of 90% and are conserved at key residues identified as essential in phosphate transport, but do differ in several residues in transmembrane domains and notably in the large loop VI in the cytoplasm (**Figures B.8-B.9**) (Lagerstedt et al., 2004; Popova et al., 2010; Samyn et al., 2016, 2012).

To test the hypothesis that there is a genotype by environment interaction involving the *PHO84* locus, we repeated the competitive growth assays of allele-swapped strains from Smukowski Heil *et al.* (2017) at 15°C. These strains are either homozygous *S. cerevisiae*, homozygous *S. uvarum*, or heterozygous for both species at the *PHO84* locus (including both promoter and coding sequences) in an otherwise isogenic hybrid background. Indeed, we find a fitness tradeoff dependent on temperature, in which hybrids homozygous for *S. uvarum PHO84* show a fitness increase of 39.30% (+/-5.16; 95% C.I.) at 15°C relative to their hybrid ancestor, which carries a copy of each species' *PHO84* allele. In contrast, hybrids homozygous for *S. cerevisiae PHO84* show a slight relative fitness decrease (-5.36% +/-2.54; 95% C.I.) at this temperature (**Figure 3.1B**). There is a significant difference between fitness of hybrids homozygous for *S. cerevisiae PHO84* at different temperatures ($p < 0.001$, Welch Two Sample t-

test), and between fitness of hybrids homozygous for *S. uvarum* *PHO84* at different temperatures ($p < 0.0001$, Welch Two Sample t-test) suggesting that both species' alleles of *PHO84* are temperature sensitive.

To further explore how genetic interactions in the hybrid influence strain fitness, we created a *S. cerevisiae* diploid homozygous for *S. uvarum* *PHO84* (including both promoter and coding sequence) in an otherwise isogenic background. This strain exhibits a fitness increase of 48.56% (+/-27.72, 95% C.I.) at 15°C and a fitness decrease of -7.61% (+/-3.04, 95% C.I.) at 30°C relative to a diploid *S. cerevisiae* homozygous for *S. cerevisiae* *PHO84* (**Figure 3.1C**; $p = 0.0071$, Welch Two Sample t-test). These results remain consistent with our previous results in the hybrid background, in which the *S. uvarum* allele is more beneficial at cold temperatures. This suggests that the *PHO84* locus alone is sufficient to confer a temperature dependent fitness benefit and that no sizable genetic interactions contribute to this effect. Technical issues prevented us from testing the reciprocal combination (*S. uvarum* diploid with *S. cerevisiae* *PHO84* alleles).

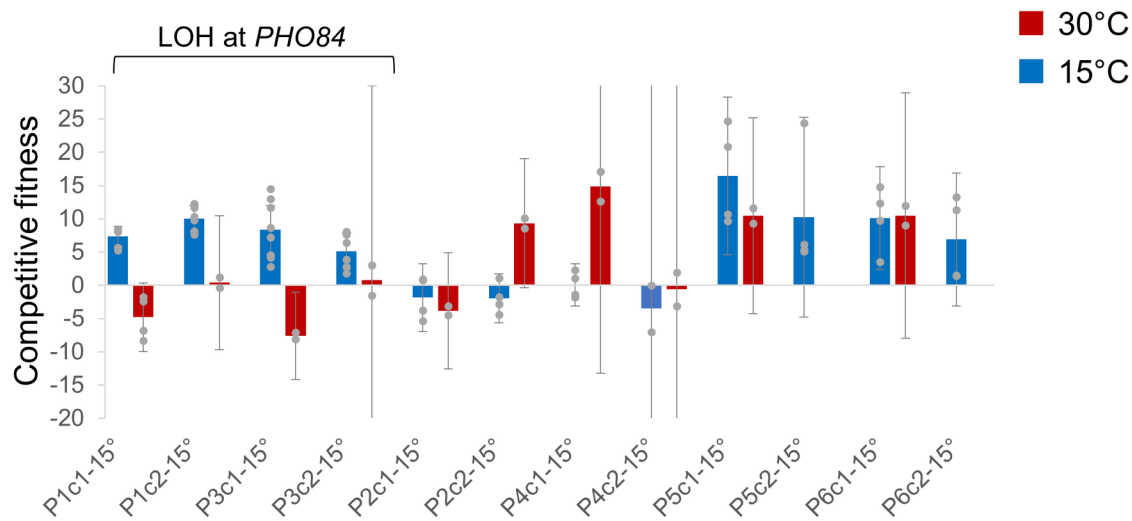
3.2.4 Pleiotropic fitness costs resulting from loss of heterozygosity

We clearly demonstrate a fitness trade-off dependent on temperature at the *PHO84* locus. To explore if other mutations in evolved hybrids show antagonistic pleiotropy at divergent temperatures, we conducted a series of competitive fitness assays at 15°C and 30°C. We isolated two clones from each hybrid population evolved at 15°C, and competed the clone against a common GFP-marked unevolved hybrid ancestor in the nutrient limitation it was evolved in at both 15°C and 30°C. We observe that clones isolated from the same population often have differences in competitive fitness, which we attribute to genetically different subpopulations coexisting in the population. As all of our analyses are conducted using population sequencing as

opposed to clone sequencing, the mutations present in an individual clone may be different than indicated in **Table 3.1** (and **Tables B.1** and **B.2**). However, we are still able to detect several trends, including examples of antagonistic pleiotropy and temperature independent high fitness genotypes.

First, we sought to identify how the chromosome XIII LOH event influences competitive fitness beyond the *PHO84* locus. We genotyped clones isolated from evolved populations and selected clones that have chromosome XIII LOH. Clones evolved in phosphate limitation with the chromosome XIII LOH event (homozygous *S. uvarum PHO84*; P1-15°C and P3-15°C) have higher competitive fitness at 15°C and decreased competitive fitness at 30°C, displaying antagonistic pleiotropy (**Figure 3.2A**, although note clones isolated from the same population have different magnitudes of fitness decreases). The competitive fitness increases seen in evolved hybrid clones at 15°C are much less extreme than the values observed for the allele swap strains (**Figure 3.1B**), suggesting that other genes included in the LOH event may have a negative fitness effect, and/or that genetic interactions dampen the magnitude of the fitness increase.

A. Populations evolved at 15°C



B. Populations evolved at 30°C

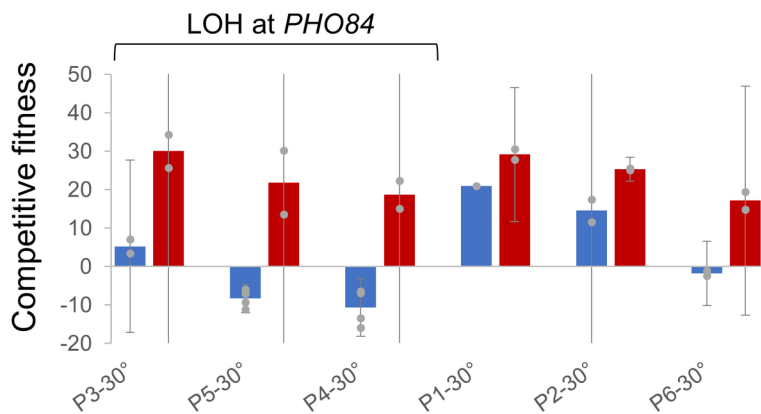


Figure 3.2. Fitness assays exhibit that loss of heterozygosity can result in antagonistic pleiotropy

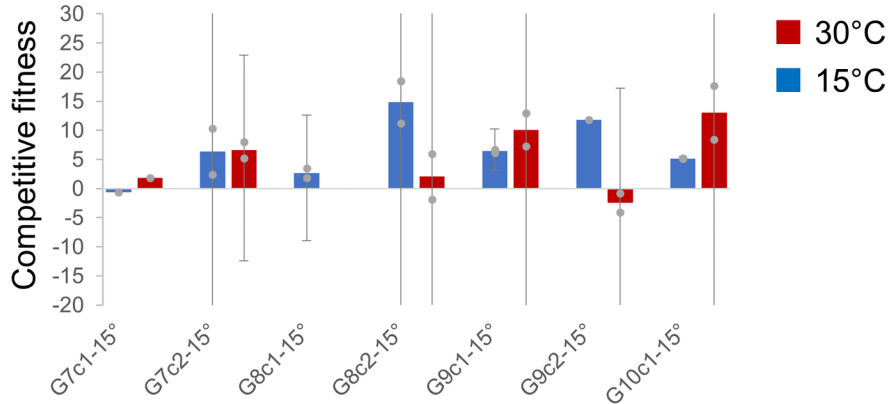
A) One or two clones were isolated from each population evolved in phosphate limitation at 15°C and competed against a common competitor, the fluorescently-labeled hybrid ancestor of the evolution experiments, at 15°C (blue) and 30°C (red) in phosphate limitation. Clones with chromosome XIII loss of heterozygosity exhibited higher fitness relative to their ancestor at 15°C and neutral or negative fitness at 30°C. Data for P5c2-15°C and P6c2-15°C competed at 30°C was not collected. The height of the bar represents the average competitive fitness value; gray points represent independent fitness measurements used to calculate the average. Error bars denote 95% confidence intervals; note where no cap of the error bar is apparent, the error bar is truncated for visualization purposes. **B)** Clones evolved in phosphate limitation at 30°C were competed against a common competitor, the hybrid ancestor of the evolution experiments, at 15°C and 30°C in phosphate limitation. Clones with chromosome XIII loss of heterozygosity exhibited higher fitness relative to their ancestor at 30°C and neutral or negative fitness at 15°C. The height of the bar represents the average competitive fitness value; gray points represent independent fitness measurements used to calculate the average. Error bars denote 95% confidence intervals; note where no cap of the error bar is apparent, the error bar is truncated for visualization purposes. No error bars are present for P1-30°C competed at 15°C as no replicates were successfully completed.

To compare these results to the reciprocal LOH event seen in hybrids evolved at 30°C in which the evolved strains became homozygous for *S. cerevisiae PHO84*, we competed clones from populations initially evolved at 30°C at 15°C. Indeed, clones with the LOH event homozygous for *S. cerevisiae PHO84* (P3-30°C, P4-30°C, P5-30°C) have increased fitness at 30°C and decreased fitness at 15°C (**Figure 3.2B**), consistent with the *PHO84* allele swap competitive fitness results. Of course, there are other mutations present in these clones, and some evidence that these fitness values may be influenced by the tract length of the LOH event, which ranges from approximately 79kb to 234kb. For example, P3-30°C has the shortest LOH tract at approximately 25kb in length and has a higher relative fitness at 15°C than either P4-30°C or P5-30°C, whose LOH tracts extend to 221kb and 234kb, respectively (**Figure 3.1A**). The LOH tract length is approximately 80kb in both cold evolved populations (P1-15°C: 82,283; P3-15°C: 79,085), but is made more complex by the amplification of a portion of the *S. cerevisiae* sub-genome adjacent to the LOH event (P1-15°C: 81,105-168,345; P3-15°C: 79,074-168,345; **Figure 3.1A**). Together, these results support a temperature sensitive fitness response at the *PHO84* locus, but also imply that there may be other genes modulating fitness in the chromosome XIII LOH events, something we hope to explore in future work.

In contrast, clones isolated from populations without chromosome XIII LOH (P2-15°C, P4-15°C, P5-15°C, P6-15°C, P1-30°C, P2-30°C, P6-30°C) generally show increased fitness at the temperature they were evolved at, but have variable fitness responses at the temperature they were not evolved at. Similarly, hybrid clones evolved in other media conditions at 15°C generally show an increase in fitness at 15°C, but variable responses at 30°C, with some clones having higher relative fitness at 15°C and lower fitness at 30°C, some clones showing the opposite trend, and some clones having similar fitness at both temperatures (**Figure 3.3**). It thus

appears that temperature specific antagonistic pleiotropy, in which a clone has high fitness at one temperature and low fitness at the other temperature, is relatively rare, with the LOH encompassing *PHO84* being the only clear example (although clones P2-C2 and G9-C2 display a pattern of antagonistic pleiotropy as well). The only other distinct pattern in the fitness data is that all hybrids evolved in sulfate limitation at 15°C show fitness gains at both 15°C and 30°C. All sulfate-limited hybrid clones have an increased fitness ranging from 23.66-41.01% relative to their hybrid ancestor at 30°C, except for the clone from population S9-15°C (**Figure 3.3B**). This result is in line with the observation of an amplification of *S. cerevisiae* *SUL1* at very low frequency and/or low copy number in population S9-15°C compared to other sulfate limited evolved populations, which display high copy number *S. cerevisiae* *SUL1* amplification (**Figure A3.1**). Previous work conducted at 30°C has illustrated that *SUL1* amplification in sulfate-limited conditions is highly advantageous. These new data suggest that an amplification of *S. cerevisiae* *SUL1* confers a fitness benefit at both cold and warm temperatures, but is most beneficial at warm temperatures. *SUL1* thus provides a clear example of a temperature independent high fitness genotype.

A. Populations evolved in glucose limitation at 15°C



B. Populations evolved in sulfate limitation at 15°C

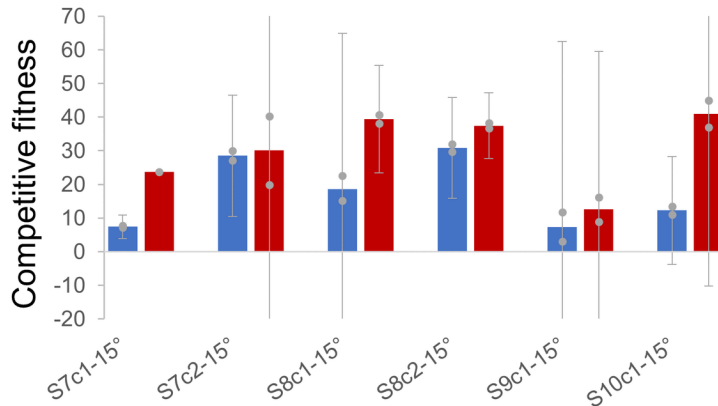


Figure 3.3. Fitness assays

A) One or two clones were isolated from each population evolved in glucose limitation at 15°C and competed against a common competitor, the fluorescently-labeled hybrid ancestor of the evolution experiments, at 15°C (blue) and 30°C (red) in glucose limitation. The height of the bar represents the average competitive fitness value; gray points represent independent fitness measurements used to calculate the average. Error bars denote 95% confidence intervals; note where no cap of the error bar is apparent, the error bar is truncated for visualization purposes. Where no error bars are shown, no replicates were successfully completed. **B)** One or two clones were isolated from each population evolved in sulfate limitation at 15°C and competed against a common competitor, the fluorescently-labeled hybrid ancestor of the evolution experiments, at 15°C (blue) and 30°C (red) in sulfate limitation. The height of the bar represents the average competitive fitness value; gray points represent independent fitness measurements used to calculate the average. Error bars denote 95% confidence intervals; note where no cap of the error bar is apparent, the error bar is truncated for visualization purposes. Where no error bars are shown, no replicates were successfully completed.

3.2.5 Mutations in *TPK2* are likely responsible for flocculation phenotype

Through comparison of the single nucleotide variants and indels called in the hybrid populations evolved at 15°C and 30°C, we observed a slight, though not significant, increase in the number of mutations in the *S. cerevisiae* portion of the genome when evolved at temperatures preferred by *S. uvarum* (12/19 mutations are in the *S. cerevisiae* sub-genome at 15°C compared to 16/30 mutations in the *S. cerevisiae* sub-genome at 30°C, Fisher's exact test $p=0.5636$; **Table B.3**).

There was no overlap in genes with variants identified in datasets from 15°C and 30°C.

We suspect that the low growth temperature is a selective pressure for both the hybrids and the parental populations, and we did observe mutations in two genes (*BNA7* and *OTUI*) that were previously identified in a study of transcriptional differences of *S. cerevisiae* in long-term, glucose-limited, cold chemostat exposure (Siew et al., 2007). We found no overlap with genes previously identified to be essential for growth in the cold (Abe and Minegishi, 2008; García-Ríos et al., 2016), or differentially expressed during short-term cold exposure (Kandror et al., 2004; Lashkari et al., 1997), though our screen is not saturated and growth conditions differ between these studies. Additionally, we observed some mutations in genes that are members of the cAMP-PKA pathway, which has previously been implicated in cold and nutrient-limitation adaptation (Sahara et al., 2002; Siew et al., 2007).

Based on the mutations observed in populations evolved at 30°C, we previously hypothesized that an intergenomic conflict between the nuclear and mitochondrial genome of *S. cerevisiae* and *S. uvarum* could be an important selection pressure during the evolution of these hybrids (Smukowski Heil et al., 2017). We find further circumstantial evidence for the possibility that mitochondrial conflicts are influential in hybrid evolution as 3/19 point mutations in the hybrids are related to mitochondrial function, whereas 1/20 are related in the parental

species populations (for a total of 7/46 point mutations in hybrids and 1/46 point mutations in parentals when both temperatures are considered; $p=0.0585$, Fisher's exact test).

Finally, we did observe one recurrent mutational target. Eight independent *S. cerevisiae* diploid lineages had a substitution occur at 1 of 3 different amino acid positions in Tpk2, a cAMP-dependent protein kinase catalytic subunit. Previously, it has been reported that Tpk2 is a key regulator of the cell sticking phenotype known as flocculation through inactivation of Sfl1, a negative regulator of *FLO11*, and activation of *FLO8*, a positive regulator of *FLO11* (Conlan and Tzamarias, 2001; Robertson and Fink, 1998). This mutation was detected exclusively in flocculent populations. We and others have previously established that flocculation evolves quite frequently in the chemostat, likely as an adaptation to the device itself, but we have not previously observed a flocculation phenotype caused by these mutations in other evolved populations of *S. cerevisiae* (Hope et al., 2017). While we have not definitively demonstrated causation, prior literature links *TPK2* to flocculation, and all evolved clones bearing a *TPK2* mutation flocculated within seconds of resuspension by vortexing (**Figure B.10**). Most mutations were heterozygous, but within several lineages, we observed evidence of a LOH event that caused the *TPK2* mutation to become homozygous. Clones bearing a homozygous mutation in *TPK2* showed a faster flocculation phenotype than their heterozygous counterparts. We similarly observed one lineage with a mutation causing a pre-mature stop and subsequent LOH in *SFL1*, whose isolated clones displayed a robust flocculation phenotype. We suspect that our previous lack of detection is likely due to the well-established genetic differences in the *FLO8* gene between the strains used in this study and previous studies, which would alter whether a *FLO8* dependent flocculation phenotype is possible (Liu et al., 1996).

3.3 Discussion

In summary, we evolved populations of interspecific hybrids at cold temperatures and show that temperature can influence parental representation in a hybrid genome. We find a variety of mutations whose annotated function is associated with temperature or nutrient limitation, including both previously described and novel genes. Most notably, we discover a temperature and species specific gene by environment interaction in hybrids, which empirically establishes that temperature can influence hybrid genome evolution.

Growth temperature appears to be one of the most definitive phenotypic differences between species of the *Saccharomyces* clade, with *S. cerevisiae* being exceptionally thermotolerant, while many other species exhibit cold tolerance (Gonçalves et al., 2011; Singer and Lindquist, 1998; Weiss et al., 2018). Significant work has focused on determining the genetic basis of thermotolerance in *S. cerevisiae* with less attention devoted to cold tolerance, though numerous genes and pathways have been implicated (Abe and Minegishi, 2008; Aguilera et al., 2007; García-Ríos et al., 2016; Homma et al., 2003; Kandrór et al., 2004; Lashkari et al., 1997; Paget et al., 2014; Phadtare et al., 1999; Rodriguez-Vargas et al., 2002). Hybrids may offer a unique pathway for coping with temperatures above or below the optimal growing temperature of one parent (Greig et al., 2002; Leducq et al., 2016; Li et al., 2019), and may aid in the identification of genes important in temperature tolerance. For example, it has long been speculated that the allopolyploid hybrid yeast *S. pastorianus* (*S. cerevisiae* x *S. eubayanus*) tolerates the cold temperatures utilized in lager beer production due to the sub-genome of the cold adapted *S. eubayanus* (Baker et al., 2015; Dunn and Sherlock, 2008; Gibson and Liti, 2015; Hebly et al., 2015; Libkind et al., 2011; Nakao et al., 2009; Nikulin et al., 2018; Peris et al., 2016; Walther et al., 2014). Indeed, creation of *de novo* hybrids between *S. cerevisiae* and cold

tolerant species *S. uvarum*, *S. eubayanus*, *S. arboricola*, and *S. mikatae* all show similar ability to ferment at 12°C (Nikulin et al., 2018). A pair of recent studies show that mitochondrial inheritance in hybrids is also important in heat and cold tolerance, with the *S. cerevisiae* mitotype conferring heat tolerance and *S. uvarum* and *S. eubayanus* mitotypes conferring cold tolerance (Baker et al., 2019; Li et al., 2019). The hybrid ancestor used for our laboratory evolution experiments at both 15°C and 30°C has *S. cerevisiae* mitochondria, but exploring how this has influenced the evolution of these hybrids is worthy of further work.

Though our work here is complicated by utilizing multiple selection pressures (nutrient limitation and cold temperature), several patterns are suggestive of temperature specific adaptations in evolved hybrids. We observe LOH events exclusively favoring the retention of the *S. uvarum* allele, and we demonstrate a fitness advantage of the *S. uvarum* allele compared to the *S. cerevisiae* allele at *PHO84*. The temperature sensitivity of the *PHO84* allele is a curious phenomenon for which we do not yet have a clear understanding. One potential connection is the need for inorganic phosphate for various processes involved in stress response, including heat shock and activation of the PKA pathway, for which *PHO84* is required (François and Parrou, 2001; Parrou et al., 1997; Popova et al., 2010; Secco et al., 2012). At the level of the protein, one potential region for further investigation of causal temperature sensitivity is the cytoplasmic loop VI of the Pho84 protein, from amino acid residues 283-324, a region which contains 13 radical substitutions between *S. cerevisiae* and *S. uvarum* (**Figures B.8-B.9**). These substitutions include changes from hydrophobic residues to charged residues, which could change temperature sensitivity. The promoter, which is quite divergent between the two species, may also be important. A genetic screen for *S. cerevisiae* growth at low temperatures found that uptake of phosphate is a growth limiting factor and implicated the overexpression of the genes *PHO84*,

PHO87, *PHO90* and *GTR1* in growth at 8°C (Vicent et al., 2015). More specifically, the authors found that both *PHO84* and *GTR1* (which are located close together on chromosome XIII) must be overexpressed to produce a growth phenotype at low temperatures. While we show that *S. uvarum* *PHO84* alone is sufficient to produce a fitness benefit at cold temperatures, we did not assay expression nor conduct promoter swaps, which could shine light on the basis of *PHO84* temperature sensitivity as well. However, our results do suggest that the introduction of *S. uvarum* *PHO84* into *S. cerevisiae* strains may prove useful for industrial applications of which growth at low temperatures is required. Overall, *PHO84* provides an interesting example of identifying a gene and pathway previously not appreciated for a role in temperature adaptation, and highlights using multiple environments to better understand parental species preferences and potentially environment specific incompatibilities.

More broadly, through the lens of *PHO84*, we establish LOH as an important molecular mechanism in hybrid adaptation, but we also show that this mutation type has fitness tradeoffs. The selection of a particular species' allele may confer a fitness advantage in a given environment, but at a risk of extinction if the environment changes. Furthermore, such mutations rarely affect single genes, and instead operate on multigenic genomic segments, leading to a further pleiotropic benefit and/or risk even in environments unrelated to the initial selective regime. Relatively constant environments such as those found in the production of beer and wine may offer fewer such risks, where hybrids may find a particular niche that is less variable than their natural environment. Future efforts are warranted to explore how variable environments influence hybrid evolution and the extent of antagonistic pleiotropy in hybrid genomes. However, because LOH has been documented in a variety of different genera and taxa that experience a range of environments, it's likely that our results have broad implications.

In conclusion, we illuminate pathways in which hybridization may allow adaptation to different temperature conditions. Mounting evidence suggests that anthropogenic climate change and habitat degradation are leading both to new niches that can be occupied by hybrids, as well as to new opportunities for hybridization due to changes in species distribution and breakdown of prezygotic reproductive isolation barriers (Abbott et al., 2013; Grabenstein and Taylor, 2018; Hoffmann and Sgró, 2011). Some researchers have speculated that this process is particularly likely in the arctic, where numerous hybrids have already been identified (Kelly et al., 2010). Our work supports the idea that portions of these hybrid genomes can be biased in parental representation by the environment in the initial generations following hybridization, and that this selection on species genetic variation may be beneficial or detrimental as conditions change.

3.4 Materials and Methods

Strains

Strains used to inoculate the laboratory evolution experiments were: *S. cerevisiae* diploid (YMD139, YMD140), *S. uvarum* diploid (YMD366), and a lab-derived diploid hybrid *S. cerevisiae* x *S. uvarum* (YMD129, YMD130). These strains and those used to gauge relative fitness of *PHO84* allele replacements in competition assays were previously utilized by Smukowski Heil et al. All strains are listed in **Table B.4**.

Evolution experiments

Continuous cultures were established using media and conditions previously described with several modifications to account for a temperature of 15°C (Gresham et al., 2008; Smukowski Heil et al., 2017). Individual cultures were maintained in a 4°C room in a heated water bath such

that the temperature the cultures experienced was 15°C, as monitored by a separate culture vessel containing a thermometer. The dilution rate was adjusted to approximately 0.08 volumes per hour (for 20 mL chemostats, 1.6 mL/hour), equating to about 3 generations per day. Samples were taken twice a week and measured for optical density at 600 nm and cell count; microscopy was performed to check for contamination; and archival glycerol stocks were made. By 200 generations, 2/16 hybrid populations, 10/12 *S. cerevisiae* diploid populations, and 0/6 *S. uvarum* diploid populations had evolved a cell-cell sticking phenotype consistent with flocculation. The experiment was terminated at 200 generations and flocculent and non-flocculent populations were sampled from the final timepoint and submitted for whole genome sequencing (40 populations total, some cultures had only a flocculent or non-flocculent population while some cultures had both sub-populations). Populations from vessels that experienced flocculation were isolated as described in (Hope et al., 2017), and are denoted with “F”. Briefly, 1 mL of each flocculent population was pipetted directly from the vessel upon the termination of the experiment and archived in glycerol stocks. Colonies were struck out from glycerol, inoculated into liquid culture and grown overnight at room temperature. From overnight cultures that displayed a clumping, and/or settling, phenotype, new glycerol stocks were made and one clone from each evolved population was selected for sequencing.

Genome sequencing and analysis

DNA was extracted from each population using the Hoffman–Winston protocol (Hoffman and Winston, 1987) and cleaned using the Clean & Concentrator kit (Zymo Research). Nextera libraries were prepared following the Nextera library kit protocol and sequenced using paired end 150 bp reads on the Illumina NextSeq 500 machine. The reference genomes used were *S.*

cerevisiae v3 (Engel et al., 2014), *S. uvarum* (Scannell et al., 2011), and a hybrid reference genome created by concatenating the two genomes.

Variant calling was conducted on each population using two separate pipelines. For the first pipeline, we trimmed reads using trimmomatic/0.32 and aligned reads to their respective genomes (*S. cerevisiae*., *S. uvarum*, or a concatenated hybrid genome) using the mem algorithm from BWA/0.7.13, and manipulated the resulting files using Samtools/1.7. Duplicates were then removed using picard/2.6.0, and the indels were realigned using GATK/3.7. Variants were then called using Samtools (bcftools/1.5 with the `-A` and `-B` arguments), freebayes and lofreq/2.1.2. The variants were then filtered using bcftools/1.5 for quality scores above 10 and read depth above 20. For the second pipeline, reads were trimmed using Trimmomatic/0.32 and aligned using Bowtie2/2.2.3, then preprocessed in the same manner as the first pipeline. Variants were then called using lofreq/2.1.2 and freebayes/1.0.2-6-g3ce827d (using the `--pooled-discrete --pooled-continuous --report-genotype-likelihood-max --allele-balance-priors-off --min-alternate-fraction 0.05` arguments from bcbio (<https://github.com/bcbio/bcbio-nextgen>)). Variants were then filtered using bedtools/2.25.0 and the following arguments (**Table B.6**). In both variant calling pipelines, variants were filtered against their sequenced ancestors and annotated for gene identity, mutation type, and amino acid change consequence. Final variant calls were manually confirmed through visual inspection in the Integrative Genomics Viewer (Robinson et al., 2011) (1550 mutations checked in total).

For comparisons with clones evolved at 30°C which were analyzed using a different pipeline (Smukowski Heil et al., 2017), we called variants on the previously published 30°C sequencing data using the same computational pipelines described here, and completely recapitulated the previous true positive variant calls.

Flocculation assays

Overnight cultures were resuspended by vortexing for three seconds. Highly flocculant clones settled out of solution within seconds of vortexing, complicating controlled quantitative measurement of the phenotype. Instead, we relied on visual observation within the first few seconds after vortexing.

Fitness assays

We utilize competitive growth as a measurement of strain fitness. The pairwise competition experiments were performed in replicate in 20 ml chemostats as previously described (Miller et al., 2013; Smukowski Heil et al., 2017). Briefly, a *S. cerevisiae* x *S. uvarum* hybrid tagged with a neutral GFP marker is grown to steady state in parallel with a query strain. When cultures have achieved steady state (approximately 10-15 generations), the GFP and non-GFP cultures are mixed at a 50:50 concentration. The proportion of GFP to non-GFP cells is monitored approximately every 2 generations for a total of five sampling points (approximately 10 generations, 25 total generations) using a BD Accuri C6 flow cytometer. Competitive fitness is calculated as the slope of the linear region of \ln [dark cells/GFP+ cells] versus generations. Efforts were made to have at least two replicates for each fitness measurement, but technical errors in the running of the fitness assays resulted in some clones having no replicates. Data used to estimate fitness can be found in the Supplementary Data, which is available online. The competition experiments performed at 15°C were modified as described above for the evolution experiments. For all cold-evolved hybrid populations, one to two clones were isolated for use in competition experiments. Clones from P1-15° and P3-15° were PCR validated to have the

chromosome XIII LOH event, but no other LOH, CNV, or single nucleotide variants were screened in these or any other clone tested.

CHAPTER 4 GENOMIC STABILITY AND ADAPTATION OF BEER BREWING YEASTS DURING SERIAL REPITCHING IN THE BREWERY

Ale brewing yeast are the result of admixture between diverse strains of *Saccharomyces cerevisiae*, resulting in a heterozygous tetraploid that has since undergone numerous genomic rearrangements. As a result, comparisons between the genomes of modern related ale brewing strains show both extensive aneuploidy and mitotic recombination that has resulted in a loss of intragenomic diversity. Similar patterns of intraspecific admixture and subsequent selection for one haplotype have been seen in many domesticated crops, potentially reflecting a general pattern of domestication syndrome between these systems. We set out to explore the evolution of the ale brewing yeast, to understand both polyploid evolution and the process of domestication in the ecologically relevant environment of the brewery. Utilizing a common brewery practice known as ‘repitching’, in which yeasts are reused over multiple beer fermentations, we generated population time courses from multiple breweries utilizing similar strains of ale yeast. Applying whole-genome sequencing to the time courses, we have found that the same structural variations in the form of aneuploidy and mitotic recombination of particular chromosomes reproducibly rise to detectable frequency during adaptation to brewing conditions across multiple related strains in different breweries. Our results demonstrate that domestication of ale strains is an ongoing process and that structural variation likely plays a critical role in ale brewing yeast evolution.

4.1 Introduction

Saccharomyces cerevisiae, the common budding yeast, occupies a diverse number of environments, from oak and fruit trees, to human-related industries such as baking and

fermentation (Marsit et al., 2017). Modern efforts to characterize the diversity of *S. cerevisiae* through large whole-genome sequencing efforts have found a somewhat discrete population structure, in which strains isolated from a particular fermented beverage or geography are more closely related to other yeasts from that environment (Gallone et al., 2016; Gonçalves et al., 2016; Peter et al., 2018; Strobe et al., 2015). Due to a tight association with humans, the genomes of yeast are thought to have been shaped by both historical migrations of humans and the environment in which they are reared. One of the best characterized examples of this human-associated adaptation or domestication is the beer brewing yeasts, which are divided into three large clades across the family tree of yeasts. The largest division is split over species barriers between the *S. cerevisiae* ale yeast and the lager yeasts, which are hybrids between *S. cerevisiae* and *S. eubayanus* (Libkind et al., 2011). The ale yeasts are further divided into two large groups coined as Beer 1 and Beer 2, with several smaller mixed origin groups containing yeast from the bread, wine, and spirits industries. While the Beer 2 group consists primarily of diploid individuals used in traditional Belgian styles, the Beer 1 yeasts (herein called ale yeasts) consist of a diverse group of mostly tetraploid strains from Germany, Belgium, the UK, the USA, and Norway (Gallone et al., 2016; Preiss et al., 2018). The origin of the ale yeasts is hypothesized to come from a historical admixture between several *S. cerevisiae* subpopulations who have similar genomic signatures as the extant populations of European and Asian wine strains with some beer brewing strains that are no longer in existence (Fay et al., 2019). The diversity and structure of these populations has allowed for extensive study of the specific molecular adaptations beer brewing yeasts have to their human-created environment, making them an excellent system in which to study the genetic basis of domestication.

Using a combination of genotype association and phenotyping in previous works, several specific genetic variations have been linked to traits that are either beneficial for the flavor of a particular beer or for growth and maintenance in a beer brewing environment. First, in comparison to wild strains, the ale brewing yeasts lack the ability to produce the flavor compound 4-vinylguaiacol (4-VG), which is undesirable in certain beer styles, through the inactivation of two genes, *PADI* and *FDCI* (Chen et al., 2015; Mukai et al., 2014). Interestingly, one lineage of ale yeasts which are specifically used for making wheat beers in which 4-VG is a desirable characteristic, retain functional alleles, highlighting the diversity and specialization of the domesticated strains (Gallone et al., 2016; Gonçalves et al., 2016). Second, ale yeasts encode an expansion of genes involved in the uptake and breakdown of maltose and maltotriose, two uniquely important sugar sources for beer brewing (Gallone et al., 2016; Gonçalves et al., 2016). Third, some ale and lager yeasts have been found to have an additional gene sequence likely formed from gene fusion, *Lg-FLOI* whose presence confers the increased ability to cellularly aggregate (flocculate) as fermentation completes (Kobayashi et al., 1998; Ogata et al., 2008; Van Mulders et al., 2010). Changes in flocculation behavior of beer brewing strains often allows for increased ease of separating the yeast from the liquid finished beer. Finally, both wine and ale brewing yeasts show evidence for loss of function alleles in *AQY1* and *AQY2* resulting in increased osmotolerance in high sugar content environments (Gonçalves et al., 2016; Will et al., 2010). As most of these putative adaptations have been identified because they are shared among most or all of the ale brewing yeasts (Beer 1), it is unclear to what extent there are additional genetic variations which are resultant from adaptive evolution or domestication within subsets of the beer brewing yeasts.

These single gene events have somewhat simplified the process of connecting them to potential phenotypes while other mutations prominent in the lineage are more difficult to interpret.

Likely as a result of the reduced ability of ale brewing yeasts to complete meiosis and the increased mutation rate of both aneuploidy and mitotic recombination in tetraploids (Mayer and Aguilera, 1990), tracts of homozygosity have been extensively observed in these yeasts. Similarly, in lager brewing yeasts, extensive aneuploidy and mitotic recombination between and within these two genomes have led to tracts of homozygosity favoring certain *S. cerevisiae* or *S. eubayanus* alleles (Libkind et al., 2011; Monerawela et al., 2015; Nakao et al., 2009; Salazar et al., 2019). Although it is unclear what the consequence of these intragenomic events are in ale and lager yeasts, previous studies from our group and others have shown that loss of heterozygosity (LOH) caused by mitotic recombination in a previously heterozygous strain can lead to drastic fitness consequences on the time scale of short-term experimental evolution (Dunn et al., 2013; Gorter De Vries et al., 2019; James et al., 2019; Smukowski Heil et al., 2019, 2017). Furthermore, in other yeasts, such as *Candida albicans* and *Cryptococcus neoformans*, extensive aneuploidy and LOH can lead to diverse phenotypic outcomes such as increased drug resistance and competitive growth (reviewed in (Bennett et al., 2014)). Finally, in mitotically dividing human cells, LOH of a non-functional tumor suppressor allele can lead to an increased risk of cancer progression including, among others, *BRCA1* mediated breast and ovarian cancer (Ryland et al., 2015). While LOH has been both observed frequently in ale yeasts and has been seen to have phenotypic consequences in other mitotic cell populations, it has yet to be linked conclusively to traits in ale brewing yeasts.

Additionally, ale yeasts' reduced ability to effectively go through meiosis complicates traditional quantitative trait mapping approaches for interpreting genetic variation. Alternative approaches that do not rely on meiosis, such as experimental evolution and genetic screens, have provided valuable insights into adaptation generally, including the importance of specific mutations, copy number variation (Lauer et al., 2018), and ploidy (Selmecki et al., 2015).

Therefore, we decided to study adaptation to the brewery by taking advantage of a form of experimental evolution already being conducted at breweries. Typically, professional brewers serially reuse populations of yeast to brew batches of beer in a practice known as repitching or backslopping to reduce the financial burden of constantly buying yeast and to give the yeast the opportunity to physiologically adapt to the brewery. The process begins when a brewery purchases a batch of a particular yeast strain at scale (population size of $\sim 2 \times 10^{13}$) from a propagation company. These yeasts have commonly been grown from a patch of yeast, derived from a clonal glycerol stock stored at -80°C . When a propagation company sends out these yeasts, they often grow the stock beyond the needs of a single brewery to meet the demand for a particular strain, meaning that there are several generations of yeast growth that occur before the yeast arrive in the brewery (minimum of ~ 50 yeast generations). Once the yeasts arrive at the brewery they are inoculated or 'pitched' into a cereal and grain derived beer medium or 'wort'. After the completion of fermentation at 10-14 days, the yeasts will flocculate to the bottom of the fermenter and are then collected. The brewer will typically collect approximately a third of the yeast, avoiding the trub that is made up of hop and protein particulates, and repitch the yeast into the next fermentation vessel with fresh wort. The actual number of yeast cells that are transferred varies from brewery to brewery and is often modified to match the starting sugar content of the media and the current viability of the yeasts. Historically, top-fermenting ale yeasts have also been collected from the top of the vessel earlier in fermentation in a practice known as top cropping or skimming.

Brewers often limit the number of times that yeast are repitched to ~ 8 reuses to reduce the possibility of a failed batch by contamination, physiological changes to viability and vitality (Jenkins et al., 2003; Kobayashi et al., 2007; Smart and Whisker, 1996), taste profile changes due to altered physiology (Powell et al., 2010; Verbelen et al., 2009), and the possibility of genetic

mutation (Deželak et al., 2014; Jenkins et al., 2009, 2008; Lawrence et al., 2012; Powell and Diacetis, 2007; Sato et al., 2001; Thorne, 1968). Despite the concern over the possibility of adaptive genetic mutations overtaking a population during a repitching regime, adaptive evolution has never been documented inside of a brewery using modern whole-genome sequencing. Furthermore, the mutational basis, timing, and consequence of any potential adaptive variation has not been fully assessed.

Herein we describe the effect of long-term repitching on brewing yeasts from samples collected in collaborations with multiple breweries across the United States and Canada that use an American brewing strain, serially-repitched for greater than 10 cycles. From these collaborations we either collected a time course across the pitches and sequenced several representative timepoints, or sequenced a starting and final population (**Figure 4.1**). Using a combination of short and long read (Illumina and Oxford Nanopore) sequencing, we found large-scale chromosomal rearrangements rising to a detectable frequency even within the first several generations of repitching. We also discovered a potential link between a specific mitotic recombination event and both a flocculation behavior change and flavor metabolite production. These results indicate both that ale yeasts are continuing to undergo domestication despite decades of growth in the brewing environment and that structural variation is likely important in these adaptations.

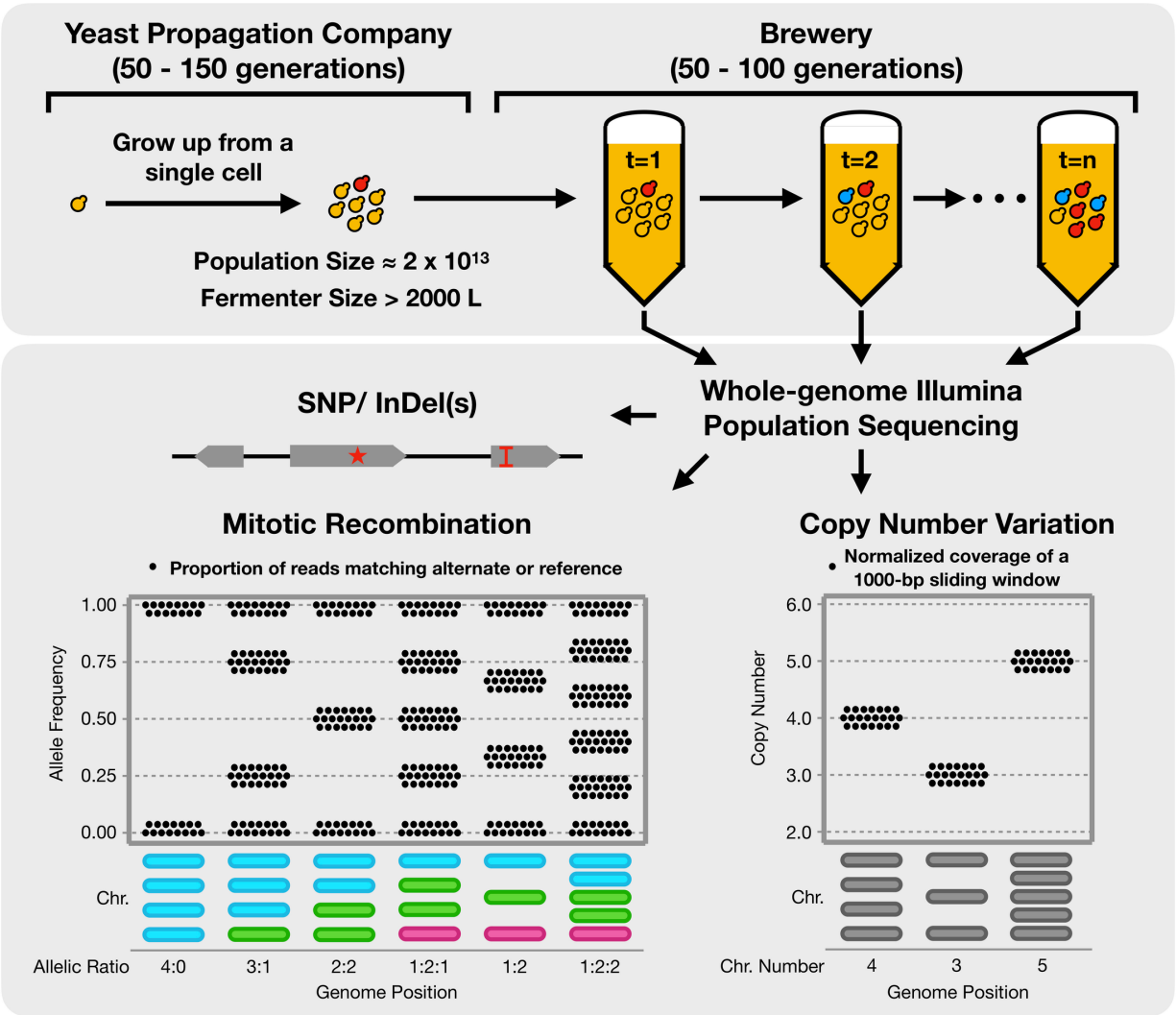


Figure 4.1. Research strategy to investigate a natural evolution experiment occurring in the brewery. Ale brewing yeast purchased from propagation companies at industrial scale and serially repitched for greater than ten beers are sequenced with whole-genome Illumina population sequencing to find signatures of evolution during brewery repitching. Mitotic recombination events are detected through allele frequency graphs (represented here), which denote every position of the genome as a point whose height is determined by the frequency of reads supporting either a reference or alternate allele. Copy number variation is detected and displayed as 1000-bp sliding windows, normalized by the average coverage across the genome.

4.2 Results

We set out to tap into the natural evolution experiment occurring at modern breweries to test whether domestication is actively occurring in ale yeasts (**Figure 4.1**). We established

collaborations with four breweries across the USA and Canada: Postdoc Brewing Co., Drake’s Brewing Co., Red Circle Brewing Co., and Elysian Brewing Co. All four breweries use a popular family of American yeast strains known as the ‘Chico’ yeasts and repitch for an extended number of cycles (>15), facilitating direct comparisons between the experiments. We confirmed both the ancestry and close genetic relationship between all strains using whole genome phylogenetics (see **Appendix C; Figure C.1**). Each brewery collected population samples of serially repitched yeast from independent beer lineages. For Postdoc Brewing Co. and Elysian Brewing Co. respectively we were able to collect two and three replicate beer lineages, plus one lineage each from the other two brewery partners. A complete record of the brewery populations is available in **Table 4.1**. Further information on recipe and fermentation performance is available in **Appendix C**. Using whole-genome sequencing, we compared the starting genotype assessed from either a clone or population depending on availability with the last time point population sample for each beer lineage. For one replicate from Postdoc Brewing Co. we sequenced multiple population time points, and several representative clones isolated from the beginning and end time points for further experimental use.

Table 4.1. Record of strains from brewery collaborations

Pop. Name	Brewery	Brewery ID	Strain	Rep.	Repitch Number	Variants Filtered By
PDB1	Postdoc Brewing Co.	PDB	Wyeast 1056	1	0	N/A
PDB6	Postdoc Brewing Co.	PDB	Wyeast 1056	1	6	PDB1
PDB15	Postdoc Brewing Co.	PDB	Wyeast 1056	1	15	PDB1
PDB19	Postdoc Brewing Co.	PDB	Wyeast 1056	1	19	PDB1
PDB26	Postdoc Brewing Co.	PDB	Wyeast 1056	1	26	PDB1
PDB1 Rep. 2	Postdoc Brewing Co.	PDB	Imperial A07	2	1	N/A
PDB29 Rep. 2	Postdoc Brewing Co.	PDB	Imperial A07	2	29	PDB1 Rep. 2

E01	Elysian Brewing Co.	Elysian.	BRY-96	1	0	N/A
E03	Elysian Brewing Co.	Elysian	BRY-96	1	15	E01
E08	Elysian Brewing Co.	Elysian	BRY-96	2	15	E01
E09	Elysian Brewing Co.	Elysian	BRY-96	2	17	E01
E05	Elysian Brewing Co.	Elysian	BRY-96	3	1	E07
E07	Elysian Brewing Co.	Elysian	BRY-96	3	0	N/A
E10	Elysian Brewing Co.	Elysian	BRY-96	3	14	E07
DK01	Drake's Brewing Co.	Drakes	White Labs WLP001	1	24	SRR7406282
RCB01	Red Circle Brewing Co.	Red Circle	Escarpment Cali Ale	1	36	SRR7406282
Clone Name	Brewery	Brewery ID	Strain	Rep.	Repitch Number	Variants Filtered By
PDB1 c1	Postdoc Brewing Co.	PDB	Wyeast 1056	1	1	PDB1
PDB1 c2	Postdoc Brewing Co.	PDB	Wyeast 1056	1	1	PDB1
PDB26 c1	Postdoc Brewing Co.	PDB	Wyeast 1056	1	26	PDB1
PDB26 c2	Postdoc Brewing Co.	PDB	Wyeast 1056	1	26	PDB1
PDB26 c3	Postdoc Brewing Co.	PDB	Wyeast 1056	1	26	PDB1
PDB26 c4	Postdoc Brewing Co.	PDB	Wyeast 1056	1	26	PDB1
PDB26 c5	Postdoc Brewing Co.	PDB	Wyeast 1056	1	26	PDB1
PDB26 c6	Postdoc Brewing Co.	PDB	Wyeast 1056	1	26	PDB1
PDB26 c7	Postdoc Brewing Co.	PDB	Wyeast 1056	1	26	PDB1
PDB26 c9	Postdoc Brewing Co.	PDB	Wyeast 1056	1	26	PDB1
PDB26 c10	Postdoc Brewing Co.	PDB	Wyeast 1056	1	26	PDB1
PDB26 c11	Postdoc Brewing Co.	PDB	Wyeast 1056	1	26	PDB1
PDB26 c12	Postdoc Brewing Co.	PDB	Wyeast 1056	1	26	PDB1
PDB26 c13	Postdoc Brewing Co.	PDB	Wyeast 1056	1	26	PDB1
PDB26 c20	Postdoc Brewing Co.	PDB	Wyeast 1056	1	26	PDB1
PDB26 c23	Postdoc Brewing Co.	PDB	Wyeast 1056	1	26	PDB1

Attempting to capture the full repertoire of genome variations that can occur and contribute to evolution, we investigated Single Nucleotide Polymorphisms (SNPs), Insertions and Deletions (InDels), Copy Number Variations (CNVs), and changes in allele frequency resulting from mitotic recombination. Scanning the whole genome, we found multiple instances of convergent SNPs and InDels that occurred in the same genes across multiple separate populations (See **Appendix C** and **Table C.6** for full details).

4.2.1 *Recurrent whole-chromosome copy number increase indicates adaptive evolution*

We investigated whether there were any large-scale genomic changes by plotting the read coverage across the genome for the Postdoc Brewing Co. time course. In line with previous work, we observed that the ‘Chico’ yeasts are largely tetraploid and have had several whole chromosome and segmental copy number changes (CNVs) that occurred at some point in its recent past (**Figure 4.2A**). We observed that during the Postdoc Brewing Co. time course, there was a copy number change of chromosome V which led to an increase from 3 to 4 chromosomal copies at a final estimated frequency in the population of 48.2% (**Figure 4.2B**). The second Postdoc Brewing experiment also replicated the increase in copy number on chromosome V (**Figure 4.2C**). Interestingly, unlike in the first Postdoc Brewing Co. replicate, the mutation entered the brewery at an estimated frequency of 27.6% and reached a frequency of 94.9% by the end of the experiment. For the population from Drake’s Brewing Co., we observed an estimated frequency of 27.9% for the chromosome V increase in copy number, indicating another replication of the same mutation. While no starting population was available for the sample, two separate sequences of WLP001 were uploaded two years apart by different groups and both shared 3 copies of chromosome V,

indicating that the starting strain likely had 3 copies. Additionally, the strain from Red Circle Brewing Co., which is of similar origin, maintained 3 copies of chromosome V.

Wanting to determine whether the potential benefit of the CNV was due to an increase in copy number of a particular haplotype or a restoration of a euploid copy number for dosage balance, we investigated whether one copy of chromosome V was recurrently amplified between populations. Through an investigation of both the clone sequences and the allele frequency of both the populations and the clones, we concluded that the increase in copy number of chromosome V occurred multiple times in both Postdoc Brewing Co. replicates, indicating a haplotype independent fitness benefit (See **Appendix C** and **Figure C.2**). Additionally, using phylogenomics to recreate the ancestry of the American brewing strains, we determined that the ancestral state of the chromosome V copy number for the strains that experienced a copy number increase was four copies (See **Appendix C** for full details).

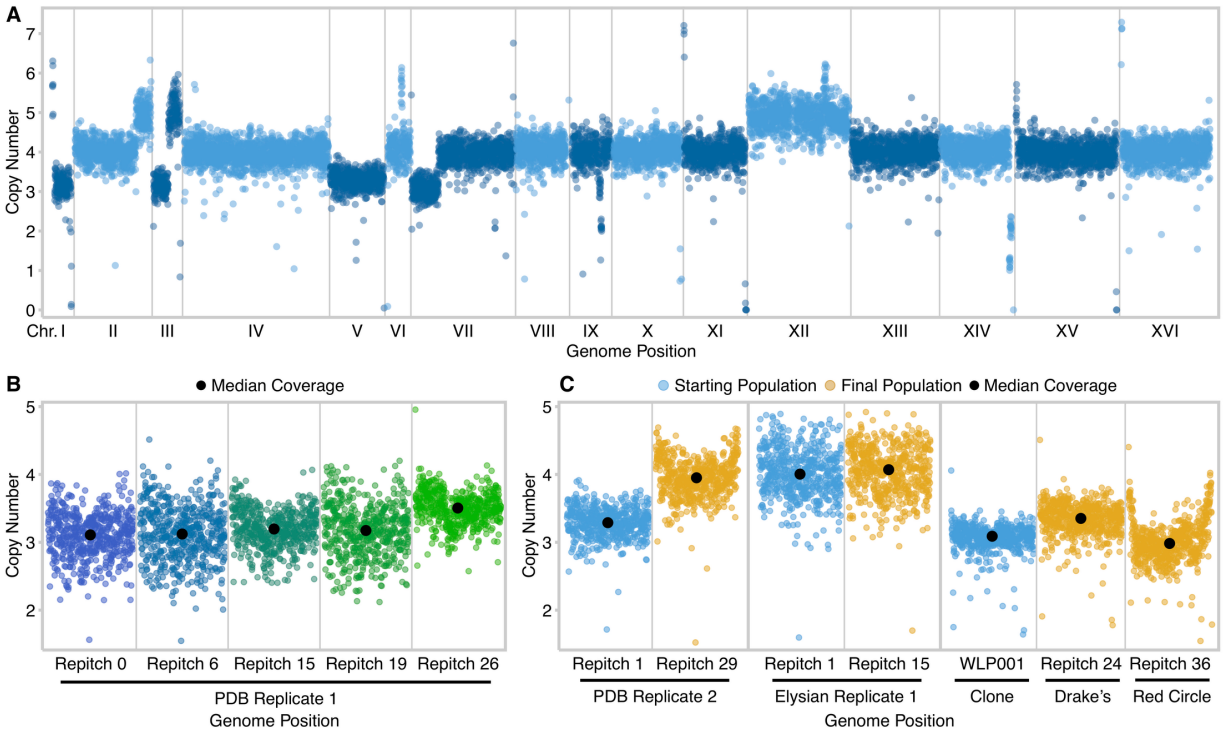


Figure 4.2. Copy number variation of chromosome V occurs multiple times between breweries and within the same brewery. (A) Whole-genome coverage of Imperial A07, highlighting the degree of chromosomal and sub-telomeric copy number alterations. (B) A time course of the Postdoc Brewing Co. replicate 1 is shown in 1000-bp coverage windows. A copy number change of chromosome V reaches 48.2% of the population by repitch 26. (C) The copy number increase of the second Postdoc Brewing Co. replicate population, starting at 27.6% of the population and reaching fixation by the 29th repitch. The strain BRY-96, which is used in Elysian Brewing Co. starts with a euploid copy number and remains constant during repitching. Drake's Brewing Co., which is from WLP001, has an aneuploid lineage which reaches 94.9% of the population. The sample from Red Circle Brewing Co. showed an increase coverage near the telomeres across its genome, but this is likely a well-documented artifact (Gallone et al., 2016).

4.2.2 *Recurrent de novo changes in heterozygosity on chromosome VIII suggests an adaptive benefit*

Given the admixed, tetraploid nature of the ale brewing strains, we next investigated whether there were copy number neutral changes in heterozygosity due to mitotic recombination by plotting the allele frequency of all positions in the genome. By looking at the allele frequency of the Postdoc Brewing Co. populations over the sampled repitches, we observed an allele frequency change on the right arm of chromosome VIII starting at repitch number 15 that appeared to angle towards an

allele frequency of 0.5 (**Figure 4.3A**). Looking at clones isolated from the last timepoint of the time course from Postdoc Brewing Co., we identified a private mitotic recombination breakpoint within each clone where the allele frequency changed from a haplotype ratio of 3:1 to 2:2 (**Figure 4.3C**; full list at **Figure C.4**). We determined that the signal from the individual clone breakpoints stacked in the population data to create the angled pattern, with all events sharing a 2:2 ratio at the most distal segment of the chromosome. From these data, we concluded that there are two chromosomal haplotypes on the right arm of chromosome VIII in a 3:1 major to minor ratio that are broken up by a mitotic recombination event that occurred numerous times independently in the population. Using the allele frequency of positions at the terminal end of the chromosome, we calculated that the allele frequency change reached a frequency of 43.8% by the end of the experiment.

Expanding our analysis to the other replicate populations, we observed that the second experiment from Postdoc Brewing Co. had a similar angled allele frequency change reaching 25.1% in the population, while all the Elysian Brewing Co. experiments showed sharp *de novo* breakpoints with different start locations (**Figure 4.3B**). Surprisingly, samples from breweries using either the WLP001 strain from White Labs or a derivative of it already had a starting fixed allele frequency change before entering the brewery. When we further investigated the rest of the American ale brewing strains within our phylogenetic dataset, we found that the entire branch leading to WLP001 shared this breakpoint (**Figure C.1**). Observing the same allele frequency change between multiple replicates at multiple breweries and independently within the American brewing yeasts, we concluded that this allele frequency change likely confers an adaptive benefit. From the Postdoc Brewing Co. replicate 1, for which we sequenced multiple intermediate samples, we estimated the selective benefit of the allele frequency change would be 5.70%, using a value

of 3 generations per repitch. Upon investigating the other replicate populations, we additionally observed several other recurrent mitotic recombination events spanning chromosomes XII and XV (**Figure C.5**).

4.2.3 *Loss of $BAT1^{A234D}$ as a candidate for a driver of an adaptive benefit*

We wanted to discover the basis of the selective benefit for the chromosome VIII mitotic recombination events as it was the most recurrent and tractable event. Therefore, we investigated whether any variation was eliminated as a result of this allele frequency change. We compared several clones from the first Postdoc Brewing Co. repitch experiment to identify the smallest candidate region in which the allele frequency change occurred and searched for positions inside of the region where variation was lost (**Figure 4.3C**). As the SacCer3 reference genome does not capture the genome structure at the end of chromosome VIII and breaks down at the *FLO5* gene (see below), our analysis spanned *YHR180W* to *FLO5* (**Figure 4.3D**). There was a single nonsynonymous mutation on one haplotype that was eliminated in every clone bearing a known allele frequency change and, notably, two clones without an allele frequency change (PDB26, clones 7 and 12). The mutation (an alanine-to-asparagine substitution) was found at position 234 in the gene *BATI*, which encodes a mitochondrial branched-chain amino acid (BCAA) aminotransferase Bat1 that is critical in the metabolism of BCAA (valine, leucine, and isoleucine). Due to the importance of Bat1 for BCAA metabolism even beyond the context of this study, we analyzed the function of the A234D variant in a companion study (Koonthongkaew et al., 2020). Briefly, we discovered that in an otherwise isogenic background, the *BATI* variant (*BATI^{A234D}*) leads to the same phenotype as a null allele in *BATI*. Specifically, we found that both the null allele and the *BATI^{A234D}* allele caused a growth defect in minimal medium, reduced levels of intracellular

valine and leucine during the logarithmic and stationary phases, respectively, and produced more fusel alcohols.

Interestingly, we found that in the Elysian Brewing Co. experiments, *BAT1* did not contain the A234D allele, but the allele frequency change on chromosome VIII still occurred. Investigating these populations, we found no additional variation that was lost because of the mitotic recombination, leading us to suspect that there was additional gene content at the end of chromosome VIII that could be further driving the benefit of the mitotic recombination. However, the level of structural divergence between the SacCer3 reference genome and the beer strain was too great to be bridged using short read sequencing, especially due to the repetitive and paralogous nature of *FLO5*. As there are not any currently available long-read sequencing data for the American brewing strains, we generated our own using clones isolated from the first Postdoc Brewing Co. experiment.

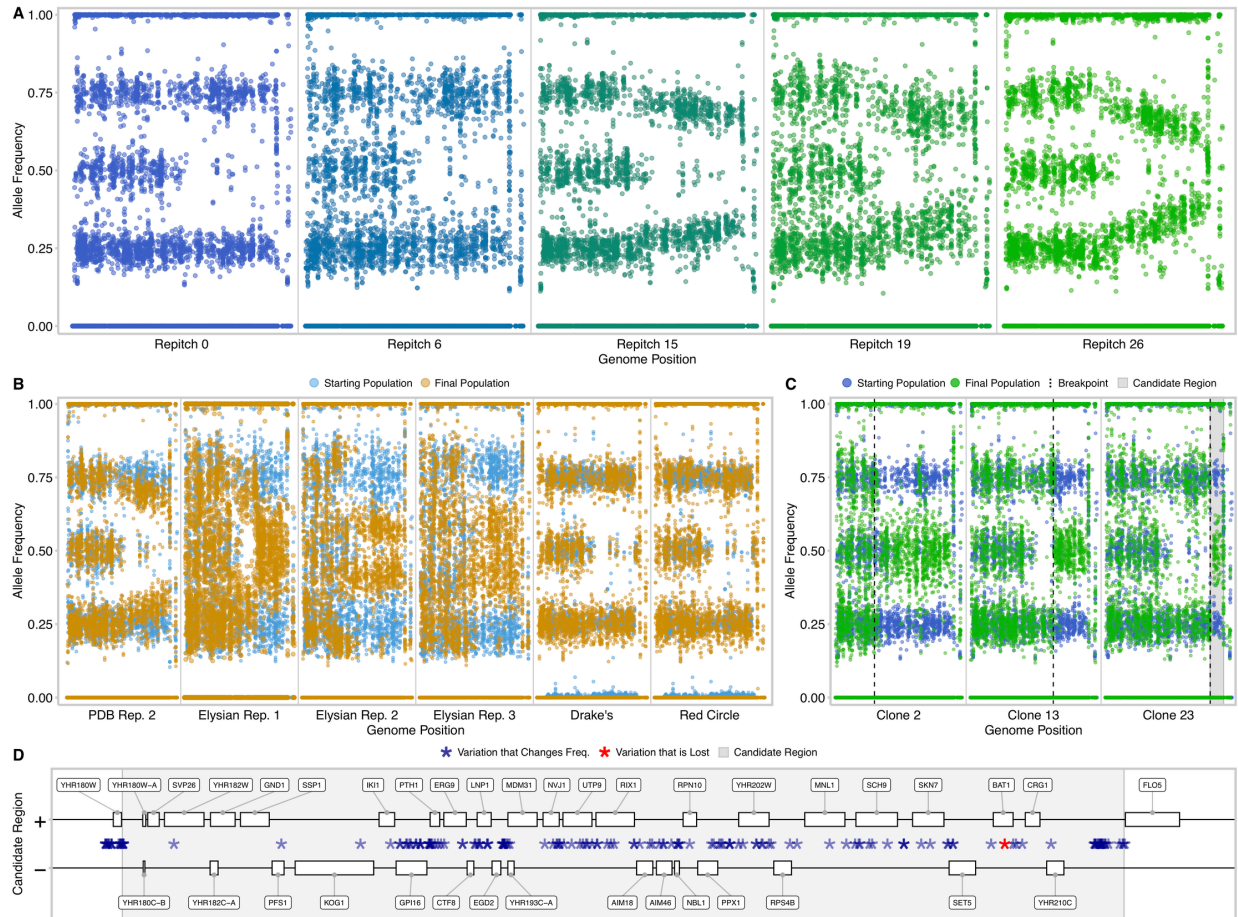


Figure 4.3. Mitotic recombination events spanning the same region recurrently mutated across multiple populations (A) Allele frequency plots of serially-repitched populations from the first Postdoc Brewing Co. replicate showing an allele frequency change, appearing at the 15th repitch and reaching a 43.8% frequency in the population by the 26th repitch. (B) Replicate populations from Postdoc Brewing Co., Elysian Brewing Co., Drake's Brewing Co., and Red Circle Brewing Co. showing the chromosome VIII allele frequency change. When the sample from Drake's and Red Circle Brewing were compared to their ancestors, WLP001 and Cali Ale, it was found that the allele frequency change had previously occurred and is fixed in the strain. (C) Chromosome VIII of three representative clones from the 26th repitch from the first Postdoc Brewing Co. experiment showing the different breakpoints of the mitotic recombination event. The region used to detect lost variation is highlighted in grey. (D) The minimal region, as detected from clone 23 is displayed with all known ORFs and variation that is either lost or changes frequency as a result of the mitotic recombination.

4.2.4 Long-read sequencing analysis reveals heterozygous genomic rearrangements at the end of chromosome VIII

Using a MinION sequencer, we generated long reads from a clone isolated from the first time point and three clones from the last time point (each with an allele frequency change). From these reads

we generated individual assemblies from each of the sequencing runs and polished them for quality using both the ONT and Illumina reads (see methods). Through comparisons between the assemblies and the SacCer3 reference genome, we found that multiple larger scale genome rearrangements had occurred at the telomeres of the beer strains. In particular, the right end of chromosome VIII had two separate rearrangements versus the SacCer3 reference that had occurred sometime in the ale brewing yeast past, one matching the left arm of chromosome I and the other the left end of chromosome IX. Furthermore, we found in the ancestral clones that one copy of chromosome I the sequence at the left arm had non-reciprocally transferred to the end of the right arm sometime in its past. Based on previous literature we suspect that the two intragenomic recombination events on chromosome VIII have been referred to as *Lg-Flo1* (chimera between *FLO5* and *YAL065C* originally discovered in lager yeast) and *ILF1* (chimera between *FLO5* and *YIL169C*). *Lg-FLO1* is of particular interest for its contribution to flocculation. Beyond the chimeric flocculins, we also discovered that additional gene content, extending to the telomere, was transferred. From the chromosome IX segment, *HXT12*, *IMA3*, *VTH1*, and *PAU14* were duplicated to chromosome VIII. From the chromosome I segment, *SEO1* and *PAU8* were duplicated.

Using alignments of the ONT reads back to polished assemblies, we established what variation and haplotypes were attached to which telomeric ends. Specifically, we found that the chromosome encoding the *BATI*^{A234D} allele is connected to the fragment from chromosome IX. Additionally, the minor haplotype is connected to the fragment from chromosome I, while the remaining two chromosomes are connected to the content from chromosome IX. While these observations were confirmed using ONT reads from clone isolates from the Postdoc Brewing Co. experiment, we have further found that the copy number of the chromosome I fragment containing

SEOI increases in both Postdoc Brewing Co. populations and the three Elysian Brewing Co. populations by the final timepoint, meaning that the copy number of *Lg-FLO1* and *SEOI* likely both increased in all populations that experienced a chromosome VIII mitotic recombination (See **Figure C.6**).

4.2.5 *Increase in yeast settling behavior correlated with an increase in Lg-FLO1 copy number*

Having found an increase in the copy number of *Lg-FLO1* because of the mitotic recombination on chromosome VIII, we tested whether there were any changes in flocculation behavior of clones isolated from the first replicate of the Postdoc Brewing Co experiment. Using a common assay known as a Helm's assay to determine yeast settling rate after six minutes in specific media conditions (Bendiak, 1994; D'Hautcourt and Smart, 1999), we found that the clones bearing the chromosome VIII mitotic recombination had an increase in flocculation behavior versus the ancestral clones (Mann-Whitney U Test: $p\text{-value} = 6.12 \times 10^{-7}$). Additionally, we found that two clones that had lost the *BATI*^{A234D} allele had shown no genomic evidence of experiencing a mitotic recombination between the major and minor haplotype maintained the ancestral flocculation rate (Clones 7 and 12).

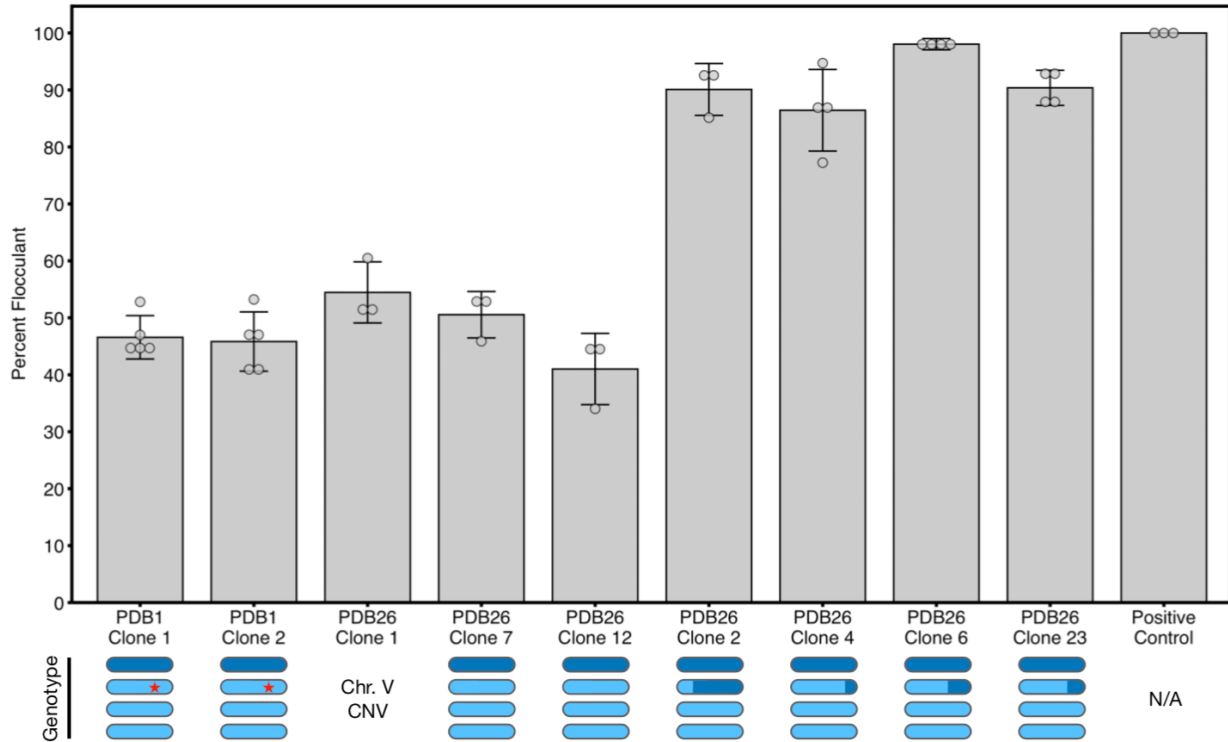


Figure 4.4. Flocculation rate increases correlated with mitotic recombination on chromosome VIII. Using the Helm’s assay to determine yeast settling behavior six minutes after agitation, it was found that clones bearing the chromosome VIII mitotic recombination had an increase in flocculation rate. A Mann-Whitney U Test between the ancestral clones and those bearing the mitotic recombination returned a significant result: $p\text{-value} = 6.12 \times 10^{-7}$.

4.2.6 *No observable change in growth rate of clones bearing the chromosome VIII mitotic recombination in simulated brewing conditions*

Given the potential of an evolutionary benefit of the allele frequency change on chromosome VIII, we tested for any growth rate changes of clones bearing this mutation. Briefly, the yeast were grown aerobically in freshly prepared brewers wort, and samples were taken on regular intervals to measure population density over 24 hours (**Figure C.7**). Under these conditions no changes in growth behavior were observed between clones bearing the mitotic recombination and the ancestral clones.

4.2.7 *Potential shifts in sensory profile of final timepoint yeast clones*

More than anything, the phenotype that is most important for brewers is the taste of their beer. To assay for any changes in flavor, we brewed beer with the ancestral strain and two of the clones described above and measured both the molecular profile of the beer and the sensory profile with a crowd-sourced panel from attendees at a Homebrewing Convention. Among the two fermentation replicates that we tested with chemical profiling, we found that there was an increased quantity of isobutanol isoamyl acetate and amyl alcohols in the beer produced by the clone lacking the *BATI*^{A234D} allele (**Table 4.2**). Notably, our prior investigation of the A234D allele in a laboratory strain background conclusively found this same pattern, potentially indicating *BATI* as the driver of the metabolite differences (Koonthongkaew et al., 2020).

Additionally, we observed from the specific gravity measurements that the fermentations with the clone that experienced the mitotic recombination on chromosome VIII (PDB26 clone 6) did not go to completion when compared to the fermentations from the clones containing the *BATI*^{A234D} allele (PDB1 clone 1, and PDB26 clone 1). While we don't know if this is linked to this specific allele or another mutation that the clone has, this feature overwhelmed the sensory panel, who found the beer to be different in both its maltiness and sweetness (**Table C.7**). As well, we found an increase in the production of total diacetyl, but we do not know definitively whether this was because of reduced ability to clean up the fermented product due to a fermentation delay. Further replicates and additional testing of clones genetically manipulated to alter the *BATI* allele identity are warranted to conclusively test the impact of the chromosome VIII allele frequency change, with and without the *BATI*^{A234D} allele, on beer characteristics.

Table 4.2. Sensory analysis of beers brewed with clones from the first Postdoc Brewing replicate

Sample Name	BAT1 Status	Ferment	Alcohol (%v/v)	Specific Gravity	Acetaldehyde (ppm)	1-Propanol (ppm)	Isobutanol (ppm)	Amyl Alcohols (ppm)	Iso-Amyl Acetate (ppm)	Total Diacetyl (ppb)	Total 2,3-Pentanedione (ppb)
PDB1 Clone 1	A234D	1	5.1	1.007552	5.89	28.78	18.12	66.29	0.42	44.32	<10
PDB26 Clone 6	+	1	4.72	1.010501	6.64	17.82	8.26	39.82	0.28	116.86	18.83
PDB26 Clone 1	A234D	1	5.1	1.007233	3.55	24.77	15.77	63.9	0.89	49.47	<10
PDB1 Clone 1	A234D	2	4.56	1.015936	3.03	24.8	43.28	93.42	0.18	89.61	<10
PDB26 Clone 6	+	2	4.5	1.016369	3.84	23.28	29.6	75.36	0.06	121.92	10.12
Wort Control	N/A	2	0	1.050506	0.65	5.28	0	0	0	41.66	<10

4.3 Discussion

Using whole-genome sequencing on yeast serially repitched across four breweries, seven populations, and three different strains, we observed the repeated occurrence of convergent mutations rising to high frequency in the populations. Notably, we observed multiple types of structural variation impacting chromosomes V, VIII, XII, and XV across multiple replicates. Through subsequent phenotyping of clones bearing some of these mutations, we have found a change flocculation behavior of strains carrying the mitotic recombination event on chromosome VIII. From these data we have concluded that these mutations are likely beneficial and selected for in the brewery, indicating that despite centuries of growth in the brewery, ale yeasts continue to show signatures of new adaptations.

Given the few numbers of convergent mutations, we sought to determine the driving force behind the potential adaptive benefit of the chromosome V copy number change and the chromosome VIII mitotic recombination. First, from clone and population sequencing, we were able to determine that the copy number change was not haplotype dependent (see **Appendix C**), meaning that any benefit likely originated from a dosage balance with the rest of the genome. Second, we found that because of the mitotic recombination on chromosome VIII a point mutation

in *BATI* in the Postdoc Brewing Co. populations was recurrently lost. Notably, the *BATI*^{A234D} allele was also recurrently lost in two clones wherein no evidence of mitotic recombination was found, indicating that its loss could have led to an adaptive benefit independent of the mitotic recombination event. Creating the *BATI*^{A234D} allele in a lab strain and comparing to an isogenic wild-type, we discovered that the mutation led to a number of phenotypes including a sensitivity to osmotic stress, reduced fermentation ability when grown in 20% glucose, and a growth defect in minimal media (Koonthongkaew et al., 2020). Attempting to measure one aspect of competitive benefit in brewing conditions of clones bearing the *BATI*^{A234D} allele, we generated multiple growth curves in wort medium of clones isolated from the first and last timepoint of the repitching regime. From these experiments, no obvious changes in growth patterns were observed, however we do note that the experiments were limited in scope and did not fully represent the brewing environment due to a lack of scale. Further experiments, utilizing competitive growth against a GFP tagged ancestor, grown across multiple brewery repitches, would more fully recreate the competitive environment of the brewery.

Additionally, the populations from Elysian Brewing Co. did not have the *BATI*^{A234D} allele, indicating there is likely to be additional adaptive consequences from the mitotic recombination event. Therefore, we applied long-read sequencing and *de novo* assembly on the clones from the first Postdoc Brewing Co. replicate to resolve the structure of the telomeric regions. As a result, we found that the mitotic recombination led to a copy number increase of *Lg-FLO1* and *SEO1* from the minor haplotype and reduction of *ILF1*, *HXT12*, *IMA3*, *VTH1*, and *PAUI4* from the major haplotype. Given the alteration in copy number of a flocculation associated gene, we tested several clones with and without the chromosome VIII mitotic recombination and found a clear increase in the flocculation behavior correlating with the increase in copy number of *Lg-FLO1*. Previous

reports comparing flocculation ability and Lg-*FLO1* copy number between distinct strains of *S. pastorianus* found a similar correlation, providing further evidence that Lg-*FLO1* gene copy number strongly impacts flocculation phenotype (van den Broek et al., 2015). Additionally, at the Sapporo Breweries in Japan, Sato et. al observed a decrease in flocculation behavior of three isolates of a *S. pastorianus* strain over three years of repitching correlated respectively with the loss of the terminal end of chromosome VIII, the loss of the messenger RNA of Lg-*FLO1*, and the a deletion in the internal portion of Lg-*FLO1* (Sato et al., 2001). Therefore, the alterations of flocculation behavior observed here are almost certainly tied to the copy number change of Lg-*FLO1*.

Considering the long history of beer brewing, one might presume that the yeast specialized in malt fermentation would already be pre-adapted to the brewery environment, meaning that new variation wouldn't provide a strong adaptive benefit. Especially given that repitching is not a new phenomenon with Louis Pasteur commenting in 1876 on the practice of passaging yeast within and between breweries:

[T]he wort is never left to ferment spontaneously, the fermentation being invariably produced by the addition of yeast formed on the spot in a preceding operation, or procured from some other working brewery, which, again, had at some time been supplied from a third brewery, which itself had derived it from another, and so on, as far back as the oldest brewery that can be imagined. ... [T]he interchange of yeasts amongst breweries is a time-honoured custom, which has been observed in all countries at all periods, as far back as we can trace the history of brewing. ((Pasteur, 1879), p. 186)

However, within our experiments we see multiple mutations overtaking the population in a relatively short period of time. The most parsimonious answer is that the brewing process has somehow changed in a way that creates new selective pressures, allowing for novel, highly beneficial mutations to evolve. One possibility is that the breweries which we partnered with utilize practices that the ‘Chico’ yeasts had not been extensively exposed to. Notably, with the introduction of long-term storage of beer brewing strains by either cryopreservation or freeze-drying, many of the strains that are currently used in commercial breweries have not seen a modern industrial brewery since they were preserved. Thus, any changes that have occurred in the common brewing practice since their preservation would be novel to these strains, allowing for new adaptive mutations. One relevant change in the last half century is the shift in preference by brewers for cylindroconical fermentation vessels, which easily allow for yeast to flocculate after fermentation is complete and collect in the cone at the bottom of the vessel (Maule, 1986). Before the shift in preference occurred, many styles of fermenter were in common use including the use of open fermentation vessels, where yeast could be collected by skimming the top of the culture. As the style of fermentation vessel and yeast collection technique shifted, we hypothesize that so too did the preference for certain flocculation behavior of brewing yeast strains.

Additionally, the brewing industry has shifted in the last several decades towards the use of pure clonal strains and propagation companies for yeast maintenance versus keeping yeast at scale in the brewery constantly through continual reuse. Often, to create a stock of a brewing strain the population is bottlenecked down to a very small size, often making a single representation of the population. Through this process it is likely that mutations that aren’t representative of the population at large and are potentially deleterious become genetically fixed. As well, given that the ales strains are mostly asexual, there is a lack of meiotic recombination that could separate

deleterious mutations that arise on otherwise adaptive genetic backgrounds. Therefore, when a strain with a deleterious mutation is grown to a massive population size in stressful brewing conditions, there is selection for *de novo* reversions of the deleterious mutations through structural variation. Within our brewing experiments, we have seen two examples that potentially fit this explanation. First, the copy number of chromosome V returned to a euploid copy number after growth in the brewery, which is its hypothesized ancestral state (see **Appendix C**). Second, the nonsynonymous mutation in *BATI* that is thought to be deleterious was genetically reverted. While the genetic drift then selection model is an attractive explanation for the data seen within, further work is required to rigorously test its veracity.

Another interesting complication for creating a single strain representation of a population was the occurrence of multiple lineages in the Postdoc Brewing Co. experiments that had the same or similar mutations within the population. We observed multiple independent occurrences of the CNV of chromosome V and the mitotic recombination on chromosome VIII. This phenomenon, called clonal interference, occurs when a new beneficial mutation is unable to completely overtake the population before another beneficial mutation occurs, creating competition between the new and old beneficial mutation and preventing a single lineage from taking over the population. Typically the parameters that are thought to control the degree of clonal interference during adaptive evolution are the mutation rate of beneficial mutations, the selective benefit of those mutations, and the population size (Gerrish and Lenski, 1998). As yeast population sizes inside of a brewery are immense, there is an ideal environment for clonal interference, potentially complicating the ability to create a single strain representative of a brewery. However, it is unclear why the non-Postdoc Brewing Co. populations did not experience the same degree of clonal interference. We suspect that the euploid nature of chromosome V of BRY-96 and the preexisting

mitotic recombination in WLP001 may have allowed for a different population dynamic that led to a single lineage dominating the population. The other possibility is that the beneficial mutations observed in the non-Postdoc Brewing Co. populations occurred earlier in their outgrowth, leading to a single lineage dominating the population.

Matching with this hypothesis, we found that on multiple instances the yeast entering the brewery already had undergone some amount of genetic divergence from the stock's genotype. This is likely due to the number of generations required for a stock of yeast to be grown to a population size needed by professional brewers. For example, given a 20 hectoliter batch of wort, the recommendation by White Labs, a prominent propagation company, is to add 2.4×10^{13} cells of yeast. The absolute minimum number of generations required to reach this number of yeast from a single cell, assuming a doubling per generation with no death, is 44.4 generations of yeast growth, which is almost certainly an underestimate. The number of generations occurring in the brewery, assuming 3 generations per beer fermentation, is 45 generations for 15 serial repitches and 78 for 26 serial repitches, meaning the growth period at the propagation company constitutes anywhere from half to a quarter of the yeasts growth in our experiments. As well, because mutations enter the population at a proportion of one over the total population size, beneficial mutations that occur earlier in the outgrowth have a higher probability of fixing in the population. Given the number of yeast cells needed by a brewer, it is likely inevitable that some amount of detectable evolution will occur prior to a batch of yeast even entering the brewery. These conclusions match with recent work that found phenotypic differences in subclonal lineages isolated from the same stock of yeast, purchased from commercial vendors (Rácz et al., 2021).

Typically, the professional brewer wants to know how long they can reuse their yeast before they will start to notice considerable difference in the characteristics of the yeast or beer.

Perhaps the most accurate but somewhat unsatisfying response is that it depends on a number of factors. Specifically, the timing might be different given the spectrum of adaptive mutations that a particular strain has access to, the individual mutation rate of that strain, and the number of generations that the population was grown at the propagation company. Even given replicates using the same strain, there is an element of stochastic mutation that can potentially drastically change how a brewery population evolves. Looking to the future and at methods to have serially repitched populations with fewer impactful mutations may begin with sequencing more populations and finding isolates that are better preadapted to the modern brewery. However, this strategy assumes these mutations do not have undesirable tradeoffs on other aspects of performance, such as on flavor profile, fermentation kinetics, and flocculation behavior. As well, if the possible spectrum of adaptive mutations is determined for a given strain it may be possible for a commercial service to track the frequency of these mutations over time and identify when they start impacting the beer. We note that due to the variability in beer styles employed during most of the time courses analyzed here, we were unable to rigorously track changes in fermentation characteristics and/or beer quality that may have happened in tandem with the rise of these mutations.

In conclusion, we observed multiple independent brewing yeast populations with high-frequency structural mutations that likely contributed to changes in yeast characteristics in the brewery. Discovering the likely adaptive benefit of mitotic recombination events in the brewery raises the possibility that historical ale brewing yeast adaptation was due in part to these kinds of structural mutations. Notably, the ale yeasts are thought to have originated from an admixture event which introduced intragenomic variation into the ancestor of the modern brewing strains (Fay et al., 2019). Potentially, ale yeasts have the capacity to adapt to new conditions using mitotic

recombination on existing variation to eliminate or fix deleterious or adaptive alleles respectively. Such events have been observed within the lager brewing yeasts wherein similar patterns of structural variation have been linked to phenotypic outcomes (Gallone et al., 2019; Usher and Bond, 2009). Furthermore, multiple mitotic recombination events were shown to lead to changes in both sugar utilization and flocculation when *de novo* hybrids between *S. cerevisiae* and *S. eubayanus* were evolved in simulated brewing conditions (Gorter De Vries et al., 2019). Given the prevalence of structural mutations in the history of the genome of brewing yeasts, and their link to adaptive phenotypic outcomes, further investigation into the consequences of this variation will likely provide additional insights into their domestication.

4.4 Materials and Methods

Origin, growth and collection of population samples from the breweries

Depending on the brewery, yeast cells were ordered from Wyeast, Imperial Yeast, White Labs, Escarpment Laboratories, or an internal propagation service (in the case of Elysian Brewing Co.). For some of the experiments, starting samples were collected either from the shipment or from the first beer brewed with the yeast. Otherwise these yeast cells were commonly grown for several generations in low density wort, then transferred into a cycle of several ale beer recipes ranging from barley wine to double IPAs. The precise recipe and conditions are proprietary for some of the breweries, however Postdoc Brewing Co. has provided the style in which the yeast were passaged through (**Table C.1**). For the Postdoc Brewing Co. samples, they were collected from the middle of the flocculated yeast after the runnings of hop and protein particulate was disposed of. Once samples were collected, they were stored at 4°C in a sterile, airtight container until

transfer to the laboratory was possible. Upon arrival in the laboratory, the samples were thoroughly mixed and 1 mL was transferred to a 25% glycerol stock that was subsequently frozen at -70°C.

Short-read genome sequencing of brewery yeast populations and clones

Populations of yeast cells, previously stored in 25% glycerol at -70°C were transferred to deionized water (diH₂O) and measured for cell density using a hemocytometer. Based on cell density counts in the diH₂O, the cell suspensions were diluted and plated to collect approximately 1,000 independent yeast colonies, grown for 4 days on yeast extract peptone dextrose (YEPD) plates with 2% glucose and 1.7% agar at room temperature. These plates were scraped for cells with a sterile glass rod, concentrated by centrifugation, and washed in diH₂O. DNA was then extracted from the cell pellets using a modified Hoffman-Winston preparation (Hoffman and Winston, 1987).

Single clone isolates were generated from a population glycerol stock. In short, the brewery populations were streaked onto a YEPD plate and grown at room temperature. A single colony was isolated and grown overnight in 5 mL of YEPD liquid medium with rotation. A portion of the overnight culture was stored in a 25% glycerol stock for archiving and subsequent analysis. The remaining cells were concentrated, washed with diH₂O and had their DNA extracted with a modified Hoffman-Winston preparation (Hoffman and Winston, 1987). Clones 13 through 23 were selected for sequencing based on their likelihood for bearing a chromosome VIII allele frequency change from genotyping using PCR and Sanger sequencing for a SNP frequency within a variable region on the end of the chromosome.

After measuring the concentration of DNA using a Qubit Fluorometer (Thermo Fisher Scientific), dual-indexed Illumina libraries were generated using a Nextera sample preparation kit

(Illumina, Inc.) with 50 ng of input DNA. The genomic libraries were sequenced using 150-bp paired end sequencing on an Illumina NextSeq 500 using the manufacturer's recommended protocols.

Whole genome analysis of copy number, allele frequency, and de novo variants

The Illumina reads were demultiplexed using bcl2fastq with default parameters. The reads were then aligned to the SacCer3 reference genome (R64-2-1) using BWA-mem (version 0.7.15) (Li, 2013). The alignments, after being sorted and indexed with SAMtools (Li et al., 2009) (version 1.9) were marked for duplicates using Picard Tools (version 2.6.0). When libraries were sequenced on multiple lanes or runs, the alignments were combined using SAMtools. Afterwards, the alignments had their InDels realigned using GATK (version 3.7).

Short mutations such as SNPs and InDels were then called using three separate variant calling software packages. First, BCFtools call using modified input parameters was used. Second, FreeBayes (version 1.0.2-6-g3ce827d) (Garrison and Marth, 2012) using input parameters (`-pooled-discrete -pooled-continuous -report-genotype-likelihood-max -allelebalance-priors-off -min-alternate-fraction 0.1`) were used to call both SNPs and InDels. Finally, in a paired mode with the sample's ancestor, LoFreq was used to call SNPs (Wilm et al., 2012). For all of the variant callers, BEDtools was used to filter the variants called for a sample versus its ancestor (Quinlan and Hall, 2010). Each variant file was subsequently filtered using standard parameters that are listed in Supp. Table 8. The three variant files were then filtered to exclude overlaps of the same variant and combined into one file using a custom script. Afterwards, the annotation and impact of the variants were determined using a script previously published in (Pashkova et al., 2013). Finally, each variant that passed all filters was manually checked for its authenticity in the

Integrative Genomics Viewer (IGV) (Robinson et al., 2011). When variant calls from BCFtools call exceeded 300 variants, these files were ignored, as they were found to contain primarily false-positives through manual inspection and comparisons with other software.

As noted earlier, there are multiple haplotypes containing varying degrees of shared variation between homologous chromosomes. To quantify and observe the degree that this variation has been altered through mitotic recombination, allele frequency was calculated and plotted for all genomic coordinates. Briefly, from the previously generated alignments, variant calls were generated using the GATK (version 3.7) HaplotypeCaller. These variant calls were passed to GATK VariantToTable and modified using an in-house java script into a per base allele ratio between a reference and alternate allele. Subsequently, the allele frequency was plotted using an R script with ggplot2. Changes in the ratios between haplotypes were visually determined through inspection of these plots. Precise values on the proportion of the allele frequency change of chromosome VIII in the population were generated using an average of the change in allele frequency of a set of SNPs that were highly representative of the mitotic recombination events in the clones at the end of chromosome VIII. These values were then used to calculate the selective benefit of the chromosome VIII allele frequency.

Using the alignments listed above, the copy number of the genome was determined and plotted using an in-house script. Briefly, the total genome coverage was calculated using GATK (version 2.6.5) DepthOfCoverage. Next, the per window average coverage across the genome was calculated using the command-line tools version of IGVtools, while filtering for windows with a high average mapping quality (MAPQ>30). These files were combined using a python script to generate a normalized coverage measure. As many of the samples included a ‘wavy’ coverage in which the coverage varied across the genome in an inconsistent and seemingly random pattern, the

per ORF coverage was unable to be accurately determined. In the cases that the coverage was too ‘wavy’ to accurately determine the coverage, the allele frequency plots that are described above were used to determine the copy number as the per allele coverage remained unchanged by the ‘wavy’ sequencing artifact.

Phylogenomic analysis to determine ancestry and structure of the American brewing yeasts

In order to properly understand the diversity and previous evolutionary history of the American brewing strains, all publicly available brewing strains whole genome sequencing were processed into a phylogenetic representation. Capturing the most amount of American diversity possible, some strains that had not previously been sequenced, but suspected to be part of the American yeast group (due to tips from professional and amateur brewers) were ordered and kindly donated from a variety of yeast propagation companies. As described above, the strains had their DNA extracted and sequenced using the paired-end Illumina technology. All of the sequencing reads were aligned using a similar strategy as previously described above with slight modifications, and called for variants in the GVCF mode using GATK (version 4.1.1.0) HaplotypeCaller on regions of high confidence (excluding the first and last 50 kb of each chromosome to avoid poorly assembled telomeric sequences). Individual variant calls were collected and jointly genotyped using GATK GenomicsDBImport and GenotypeGVCFs and filtered with GATK (version 4.1.3.0). Removing the influence of ancestral variation lost by mitotic recombination, the SNPs from the sample excluding BE051 were then filtered by SNPs called from BE051 using BEDtools (Quinlan and Hall, 2010). The SNP calls were then converted into two concatenated fasta files wherein the first fasta was the SacCer3 reference genome with the reference allele as listed if the strain was either heterozygous or homozygous for the reference allele. The second fasta also contained the

SacCer3 allele unless a heterozygous or homozygous variant position was detected in which case the alternate allele was outputted. This task was done using BCFtools. The concatenated fastas from all of the American brewing strains were passed to IQTree2 to generate a maximum-likelihood tree using GTR4 + gamma model (Minh et al., 2019). The tree was then modified for aesthetics and annotation using iTOL (Letunic and Bork, 2019).

Comparisons between the ‘Chico’ yeasts and BRY-96 for determination of the ancestry of the ‘Chico’ yeasts was done using the aforementioned SNP calls. First, the union of the SNPs called in WLP001 and Wyeast 1056 was generated using BEDtools. Second, the mutations unique to BRY-96 when compared with that union were generated. Finally, the remaining SNPs from BRY-96 were manually inspected for veracity using IGV.

Measurement of flocculation behavior using the Helm’s Assay

The flocculation behavior of clones isolated from the first replicate population from Postdoc Brewing Co. were measured similar to as described (Bendiak, 1994; D’Hautcourt and Smart, 1999). Briefly, single yeast colonies from a 2% YPD plate were grown in 5 mL of wort medium for 48 hours with rotation. The optical density of the cultures was measured at 600 nm (OD600) by taking a well-mixed derivative from the culture, deflocculating it in 250 mM EDTA (pH 7.5) and resuspending it in water for measurement. Afterwards, the cultures were backdiluted in wort to an OD600 of 0.5 in 50 mL of wort medium to match a final cell/mL density of 1.0×10^7 . The cultures were then shaken for 72 hours at room temperature. Next, 10 mL of the cultures were spun at 1500 rpm for 5 min., washed in 0.5 M EDTA (pH 7.5) to deflocculate the yeast cells, and resuspended in distilled water. The cultures were then diluted in a calculated amount of distilled water to bring the density of the cultures to an OD600 of 15 ($\sim 1 \times 10^8$ cells/mL). The final OD600

of this culture was measured to ensure accuracy for later calculations. Next, 10 mL of the culture was transferred to a 15 mL conical tube, where it was first washed in 4 mM CaCl₂, then resuspended in a suspension solution consisting of 4 mM CaCl₂, 4% ethanol, 4.05 g/L Glacial acetic acid, and 6.8 g/L sodium acetate. The cultures were then agitated for 25 seconds by vortexing before being allowed to settle for exactly 6 minutes. Afterwards, the top ten percent of the culture was collected using a micropipette, washed in 250 mM EDTA (pH 7.5) and resuspended in distilled water before being measured for its OD600. Finally, a summary metric called percent flocculant was generated from the ratio of OD600 measurements from the top ten percentage of the culture and the known OD600 of the culture.

Generation of laboratory brewers wort media

The brewers wort media, utilized for the growth phenotyping and fermentation analysis was made as previously mentioned in (Smukowski Heil et al., 2018) with slight modification. Briefly, 320 grams of amber liquid malt extract from Breiss Malt and Ingredients Co were mixed with 1.5 liters of distilled water and boiled for an hour. Fifteen minutes before the boil finished, 0.2 gram of the Wyeast Beer Nutrient Blend was added to the mixture according to the manufacture's guidelines. After the wort had been chilled to a workable temperature, the specific gravity was measured using a hydrometer (and the value read was corrected based on the temperature), and the media was passed through fresh Melitta filters to remove any large coagulants. Next, the media was passed through a 0.45 micron filter (Nalgene 500mL Rapid-Flow Bottle Top Filters) to completely sterilize the media. The specific gravity of all batches used herein were found to be the same value of 1.050.

Measurements of growth parameters of brewing yeast isolates in brewers wort

The growth characteristic of clones isolated from the first replicate population from Postdoc Brewing Co. was measured. First, single yeast colonies from a 2% YPD plate were grown in 5 mL of wort medium for 48 hours with rotation. The optical density of the cultures was measured at 600 nm (OD₆₀₀) by taking a well-mixed derivative from the culture, deflocculating it in 250 mM EDTA (pH 7.5) and resuspending it in water for measurement. Each culture was then diluted in an appropriate amount of wort to reach a final OD₆₀₀ of 0.05 in 50 mL of wort and shaken for 24 hours at room temperature. Samples were taken periodically during the growth curve from the 50 mL cultures, and the optical density was measured as mentioned above. Utilizing a script written in the R programming language, the growth data were analyzed using the *growthrates* package. Employing the *growthrates* implementation of fitting linear models to the exponential growth period outlined in (Hall et al., 2014), we extracted the maximum growth rate of the clones. To determine whether there was a difference in the growth rates between clones, we conducted a Kruskal Wallis rank sum test.

Sensory profiling of brewing yeasts

The isolated clones from the first Postdoc Brewing replicate were tested for differences in the production of flavor compounds and the effect these compounds had on the beer sensory profile. First, two separate beer batches (beer batches 1 and 2) were generated from fermentations carried out either at Postdoc Brewing (using an all grain pale ale recipe) or in the laboratory (using the malt extract wort mentioned earlier). The yeast that fermented the beer were grown in the laboratory from single colonies to the desired cell count in 2% YEPD liquid medium with shaking. For the first and second beer batch, the yeast were concentrated with centrifugation and pitched

into the wort at a rate of 3.5×10^5 and 1.0×10^6 cells per degree of plato (measure of sugar density) respectively.

Second, both beer batches were submitted to White Laboratories for analytical services including gas chromatography measurements of a number of flavor compounds and measurements of alcohol percentage and specific gravity. Next, the beers from batch 1 were submitted to an untrained judging panel (n=95) at the Homebrew Con 2018, who used a standardized beer scoresheet from the Beer Judge Certification Program to analyze the profile of the beer. The identity of the beers were kept masked from the participants while they filled out their analysis. Afterwards, the scoresheets were aggregated and analyzed for differences using a Kruskal Wallis rank sum statistical test.

Long read and genome assembly generation of an American brewing yeast

Yeast cell cultures were grown overnight at 30°C in 20 mL of YPD medium to early stationary phase before cells were harvested by centrifugation. Total genomic DNA was then extracted using the QIAGEN Genomic-tip 100/G according to the manufacturer's instructions. The extracted DNA was barcoded using the EXP-NBD104 native barcoding kit (Oxford Nanopore Technologies) and the concentration of the barcoded DNA was measured with a Qubit 1.0 fluorometer (Thermo Fisher Scientific). The barcoded DNA samples were pooled with an equal concentration for each strain. Using the SQK-LSK109 ligation sequencing kit (Oxford Nanopore Technologies), the adapters were ligated on the barcoded DNA. Finally, the sequencing mix was added to the R9.3 flowcell for a 48 hour run.

The ONT reads were demultiplexed using Guppy with default parameters. The adapters on the raw reads were removed using Porechop. Afterwards, each sample was independently run

through SMARTdenovo with default parameters to generate a draft genome assembly. To improve the quality of the assembly, the draft sequences were first run through racon then medaka. Next they were refined using pilon and the Illumina reads previously generated for the four clones sequenced on the MinION. The identity of the contigs was determined through pairwise alignment of the contigs (masked with RepeatMasker) to the SacCer3 reference genome using Minimap2 and plotted using an R package called DotPlotly. Confirmation of the contig identity, and the inferred identity of the ancestor was done using a combination of Minimap2 alignments of the SacCer3 reference ORFs, SacCer3 reference sequence, ONT reads, and Illumina reads, all visualized in IGV.

4.5 Acknowledgements

Massive thanks to Professor Mary Kuhner for advice on best practices for complicated phylogenetic inference. Sequencing analysis consultation was graciously provided by Mitchell Vollger and Dr. Glennis Logsdon. Thanks to Jess Caudill at Imperial Yeast for insight to the yeast propagation industry. Thanks to the attendees of Homebrew Con 2018 who participated in the sensory analysis. Thanks to Karen Fortmann and White Labs for metabolite profiling. This research was only made possible by the generous contribution of numerous unlisted, but greatly appreciated brewers, historians, and researchers.

CHAPTER 5 CONCLUSIONS AND FUTURE DIRECTIONS

Within this thesis, I have described three sets of experiments utilizing experimental evolution to garner new understanding about reproducibility in evolution, the influence of admixture in evolution, and the domestication of beer brewing yeasts. Each chapter has described a set of experiments with an increasing number of variables, with the hope of bridging the divide between evolution in the laboratory and evolution in nature. First, in **Chapter 2**, I discussed the use of the chemostat to produce a constant and reproducible environment with a laboratory strain in three different nutrient limitations. Therein, I found a set of highly reproducible targets of mutation that clustered within certain complexes and regions of the genome. However, I found heterogeneity in the mechanism and benefit of mutation that was potentially modulated by genome context. Second, in **Chapter 3**, I similarly explored evolution in the chemostat, except with the added variables of temperature and genome composition resulting from hybridization. Together with Dr. Caiti Smukowski Heil, I found that temperature modified the direction of hybrid genome retention coincident with ancestral temperature preference. Finally, in **Chapter 4**, I expanded the general methodology of experimental evolution to the industrial process of beer brewing to explore the domestication of beer brewing yeast. Similar to **Chapter 3**, I discovered that the admixed origin of the ale brewing yeasts likely influenced its domestication. In particular, I found that structural variation in the form of aneuploidy and mitotic recombination were the primary sources of adaptive variation, indicating the importance of this form of mutation in the domestication of beer brewing yeasts. These findings matched with what is observed both within the extant lager and ale brewing yeasts as well as the findings of **Chapter 3**. Below I discuss several future directions that would help generate a more predictive model of evolution, increase our understanding of the relevance of repitching and structural variation in

brewing yeast domestication, connect variation in phenotype to genotype for ale brewing yeast, and help reveal the origin of multiple life history traits of the ale brewing yeasts.

5.1 *Contingency and stochasticity in evolution*

Adaptive evolution in a mutation limited environment relies on the cooperative action of the formation of new beneficial variants and selection acting on those new variants. Thus, a more complete understanding of the mechanisms and rates of beneficial mutation occurrence as well as the influences of the selective benefit of those mutations would lead to a more predictive model of evolution. In **Chapter 2** I discussed multiple instances where the adaptive benefit and mutational frequency of specific CNVs and Ty element mobilizations respectively were likely influenced by genomic context. Below I propose new strategies to investigate whether the observational findings seen in **Chapter 2** hold when the conditions of the experiment are altered. Furthermore, I put forward new methods to categorize the extent of epistasis during chemostat experimental evolution.

5.1.1 *The influence of genome context on *SUL1* CNV*

During the evolution experiments in sulfur-limitation described in **Chapter 2**, I observed that the local sequence context likely impacts the span of chromosomal amplifications through a combination of fitness effects and mutational mechanism. One potential way to measure the impact of both mechanisms on the formation and selection of amplified *SUL1* alleles would be to translocate the *SUL1* locus to a different location in genome and repeat the evolution experiments. Through comparison of the rate and span of amplifications to the known benefits and costs of amplified regions of the genome available in Payen et al., 2016, *SUL1* could be used

as a tool to investigate genome context in CNV formation and evolution. Overall, these experiments would push our observational support of the contingency of CNV amplification towards a more mechanistic understanding.

5.1.2 *Probing the effect of Ty element mobilization bias on evolutionary outcomes*

The rate of Ty element mobilization towards a particular region of the genome depends on its position relative to a gene transcribed by Pol III (Baller et al., 2012; Bridier-Nahmias et al., 2015; Mularoni et al., 2012). In this way, tRNAs increase the mutation rate in their local sequence neighborhood. During experimental evolution, I found that the proximity of the recurrently targeted genes to predictors of mobilization likely influenced whether they were mutated by Ty elements versus SNP/InDels (See **Chapter 2** for more details). However, this pattern was most prominently observed in sulfate limitation, potentially due to the lack of proximity of recurrent targets of mutation in glucose and phosphate limitation. To extend these observations, three strategies could be taken: First, new tRNAs could be introduced proximal to the previously observed recurrent targets in phosphate and glucose limitations, such as *GSH1* and *RME1*. Then, once the evolution experiments were repeated in these conditions, we could monitor the rate of new Ty insertion versus SNP/InDel into the proximal gene to see whether the new insertion has biased the outcomes of evolution towards the most mutationally likely outcome. Special care would need to be taken to ensure that the introduction of the new tRNA would not disrupt the expression of the proximal gene through qPCR measurements of transcript levels in the relevant conditions (Hamdani et al., 2019). A second strategy would be to move a preexisting tRNA, such as tD(GUC)B away from proximity to *SPT7*, repeat the evolution experiments, and similarly observe whether the rates of Ty insertions versus SNP/InDel are

altered. Using any of these strategies would create a more direct link between the influence of tRNA on local sequence context and long-term evolutionary outcomes.

5.1.3 *Epistasis in adaptive evolution*

Within the three nutrient-limited conditions highlighted in **Chapter 2**, I observed under 20 recurrent targets of mutation across 32 replicates in each condition. These data would suggest that there is a narrow pathway to adaptation that occurs through the mutation of a quantized number of genes. However, previous measurements of the competitive fitness of nearly every gene in the yeast genome using the yeast deletion collection revealed there are many more possible beneficial mutations that are not explored (Payen et al., 2016). When looking at phosphate-limited conditions specifically, there are 195 possible mutations that provide at least a 5% competitive fitness increase, but only 14 are observed across 32 evolution experiment replicates. Similar numbers exist for sulfate and glucose limited conditions (Sulfate-limited 8/123; Glucose-limited 18/143). One possible explanation for this incongruency is that the measurements in Payen et al. only captured the adaptive benefit of the mutations in isolation, without looking at how they interact with possible secondary mutations. Possible epistatic effects between the mutations could alter the long-term benefit of any single mutation during experimental evolution.

A comprehensive way to categorize the effects of epistasis on evolutionary outcomes would be to measure the competitive fitness of the unobserved mutations in the genetic background of a strain that contains one of the observed high impact mutations. Subsequent comparisons between the competitive fitness measurements of the same gene in different genetic backgrounds would yield insights into the extent by which epistasis shapes evolutionary

trajectories. Given the tools available to yeast genetics, this could be achieved through first genetically replacing the known highly recurrent genes, such as *GSH1* with a selectable marker. Subsequently, these strains could be mated in mass to the haploid yeast deletion collection (Giaever et al., 2002). Afterwards, the mated diploids could be sporulated, generating haploids that could then be selected for the correct mating type using a set of genetic markers. The resulting libraries would consist of the yeast deletion collection in the genetic background of a knockout of a highly recurrent gene. These libraries would then be competed in the chemostat in their relevant nutrient limitation. Comparisons between the input frequency of the barcodes associated with yeast deletion collection and further time points would yield a measure of the competitive fitness. The same general strategy could be applied for the known beneficial CNV that occur during experimental evolution such as *SUL1* and *PHO84* through transformation of the yeast deletion collection with a selectable plasmid encoding additional copies of the gene of interest. Further evaluation of the differences in competitive fitness of the deletion collection in different genetic backgrounds would allow for direct measurement of the effects of epistasis. Overall, these experiments would yield greater insight into the effect that epistasis has in determining the trajectory of adaptation during experimental evolution in the chemostat.

5.2 Further relevance of structural variation in brewing

In **Chapter 4**, I used the common brewery practice of repitching to investigate the domestication of beer brewing yeasts. Through partnerships with multiple breweries using the same or similar strain of yeast, I was able to observe replication of the same type of structural variation rising in frequency in experimental populations, indicating its adaptive benefit in the brewery. While the primary focus of the work ended up being on the most recurrent of these events, a mitotic

recombination on the right arm of chromosome VIII there were additionally several other recurrent mitotic recombination events whose function or relevance has not been extensively investigated. One limitation to further investigation of these events is the lack of a high-quality genome assembly that well represents the sometimes nonsyntenic and divergent ale yeast genome. In **Chapter 4**, I discussed the use of error-probe long reads generated through Oxford Nanopore Technologies for the *de novo* assembly and haplotype matching of the mitotic recombination of chromosome VIII. While it was possible in this instance to use the ONT reads to resolve the structure of chromosome VIII, subsequent work should be put towards the generation of a higher quality *de novo* assembly of the ale strains, generated from higher accuracy PacBio HiFi reads, such that the identification of structural variation, *de novo* SNPs and InDels, and Ty element mobilization can be probed with greater specificity and efficiency (Hon et al., 2020). Furthermore, having high quality long reads would enable the investigation of difficult-to-resolve regions of the genome, such as the duplicated *MAL* and flocculin genes.

Additionally, the work presented in **Chapter 4** exclusively utilized strains from the American brewing yeast clade to allow for comparisons to be made between the replicate experiments. Given the similar genome structure, and the recent common ancestor, I predict that the same forms of structural variation would be relevant during the repitching of other ale brewing yeasts, however the specific chromosomal regions may likely be different due to genetic background effects. Further investigation of repitching using strains from the English, German, and Belgian ale beer clades should be undertaken to understand the broader applicability of the findings presented in **Chapter 4**. Additionally, with the increased use of farmhouse beer strains, such as the Kveik yeast, it may be possible to observe how previously unindustrialized yeast adapt to the modern brewery (Preiss et al., 2018). However, the limitation in expanding the study

cohort to include breweries that use non-American strains is finding breweries that repitch for an extended period. One alternative approach would be to partner with the propagation companies who cultivate the yeast for the breweries. From several of the populations in **Chapter 4**, there was preexisting population variation, observable by population sequencing from the first time point in brewery, indicating that it is possible to observe evolution during the propagation itself. Given that the propagation companies commonly cultivate their yeast in conditions that are similar to that of the brewery, they are likely representative of the conditions inside of the brewery. Due to the few number of generations that occur at the propagation company some experiments would likely yield no insight as no new variation would be detectable on the population level, however more replication would be possible as the throughput of propagation companies is higher. Additionally, as the process is more controlled at a propagation company, it would be possible to accurately track the number of yeast generations occurring during propagation, allowing for selection of certain populations to analyze depending on their generation number. Overall, by increasing the repitching study cohort we can determine the relevance of the findings of **Chapter 4** to other brewing clades, and potentially generate new insights into the domestication of beer brewing yeasts.

5.3 *Mapping functional variation in brewing yeast*

Large scale phenotyping has shown that despite the shared origin of the ale brewing strains, there is extensive variation in many traits that are highly relevant to brewing conditions (Gallone et al., 2016; Peter et al., 2018). Understanding the genetic basis of this phenotypic variation may provide key insight to the specific genetic mechanisms by which yeast have become domesticated. Despite the availability of these data and the accompanying whole genome

sequencing, there has been limited success in connecting specific variation in genotype to variation in phenotype using traditional genome wide association studies. Alternative methods, such as experimental evolution have been discussed and implemented in **Chapter 4** of this thesis. While this strategy is effective in connecting *de novo* variation to phenotype, it has limited ability to connect existing variation to phenotype. A powerful method to connect genotype to phenotype across a broad range of model systems is quantitative trait loci mapping (reviewed in Rockman, 2008). However, the lack of functional meiosis among the ale brewing strains limits the utility of this strategy. To overcome this, two alternatives would be to either to find a strain that has somehow retained the ability to successfully complete meiosis or to genetically manipulate the yeast to reintroduce sporulation.

Regarding the first strategy, a recent publication found, through large scale phenotyping of the yeast 1,011 strain collection, that five of the ale strains showed some evidence of sporulation (Peter et al., 2018). Currently, these strains are being investigated for their ability to survive meiosis and are promising candidates for subsequent analysis. Considering the second strategy, to ameliorate whatever deficiency is responsible for the lack of meiosis, we must understand something about its genetic basis. While it is suspected that the ale strains are unable to conduct meiosis due to do high presence of aneuploidy (Gallone et al., 2016), it is likely that there is additional disruptive variation in some part of the pathway controlling meiosis as fully euploid beer strains still cannot successfully complete meiosis (De Chiara et al., 2020). Additionally, several other members of the Sake, French dairy and French Guyana clades have lost sporulation due to loss of function variants in members of the meiosis pathway, indicating this as a common mechanism of sterility (De Chiara et al., 2020). Therefore, one potential strategy would be to complement any loss of function variation in the ale strains with a wild-type allele to cure

meiosis. One effective method to generate complementation across the genome would be to mate the tetraploid ale strain with a lab strain that is fully capable of completing meiosis, and thus generate an octoploid strain with full a complement of the entire meiosis pathway. Previous work has found that generation of higher ploidy *Saccharomyces* is possible up to twelve genome copies (Peris et al., 2020). However, this strategy would require the genetic manipulation of the ale strain such that it was homozygous for its sex determination locus and depend on the variation impeding meiosis to be recessive. If either of these strategies are effective in generating a meiosis competent ale strain, new links between variation and phenotype could be explored in much higher throughput and resolution. Overall, this would unlock key insights into the evolutionary history of the domestication of the ale brewing strains and the variation that led to its vital role in human life.

5.4 *What are the consequences of life history trait shifts?*

Despite the discovery of the admixed beginnings of the ale and lager brewing strains, there are still several open questions surrounding the origin of their life history traits (Fay et al., 2019). First, it is unclear when exactly the ale brewing yeast lost their ability to successfully complete meiosis, and whether the transition was due to adaptation. One prominent hypothesis in the field is that the loss of sexual reproduction could be correlated with the transition to a tetraploid lifestyle, as aneuploidy, which is more common in tetraploids, leads to disruptions to the faithful segregation of chromosomes (Gallone et al., 2016). Another idea is that sporulation was lost by a lack of selection for its maintenance as sporulation is only induced upon starvation for both nitrogen and carbon, which would likely be unusual in an industrial brewing setting. Second, it is unclear based on current evidence the genetic mechanism by which the strains became tetraploid

and what long-term effect it has had on their evolution. Previous work using a tetraploid laboratory strain during asexual experimental evolution discovered that while tetraploidy initially reduced fitness, it accelerated future fitness gains (Selmecki et al., 2015). Therefore, tetraploidy could have been favored as the result of positive fitness outcomes during a rapid adaptation to the brewing environment. An alternative hypothesis is that tetraploidy could have allowed for a greater amount of intragenomic diversity to be locked into a single lineage, which could be advantageous when outcrossing is either rare or absent.

Unfortunately, many of the primary events that would give credence to one hypothesis over another for both the loss of sporulation and gain of tetraploidy occurred likely 400-500 years ago (Gallone et al., 2016). Without the fortuitous discovery of an ale yeast locked away in the belly of a sunken ship, there is little hope that the ancestral state of the ale yeast can be directly observed (Thomas et al., 2021). Therefore, to answer these questions, inference using extant yeast strains must be used to recreate these early events. One promising advancement that could lead to answers to these questions is the application of long-read sequencing to the phasing of higher ploidy genomes (Abou Saada et al., 2021). Perhaps through the collective analysis of the haplotype patterns of many ale brewing strains, the timing of loss of meiosis, and the gain of tetraploidy could be determined. However, the answers that are locked away in the ancestral haplotype might simply be lost to the homogenizing influence of mitotic recombination and aneuploidy. Hopefully, as sequencing technology and computational algorithms improve, we will someday have an answer to the complete origin story of the ale brewing yeasts.

BIBLIOGRAPHY

- Abbott R, Albach D, Ansell S, Arntzen JW, Baird SJE, Bierne N, Boughman J, Brelsford A, Buerkle CA, Buggs R, Butlin RK, Dieckmann U, Eroukhmanoff F, Grill A, Cahan SH, Hermansen JS, Hewitt G, Hudson AG, Jiggins C, Jones J, Keller B, Marczewski T, Mallet J, Martinez-Rodriguez P, Möst M, Mullen S, Nichols R, Nolte AW, Parisod C, Pfennig K, Rice AM, Ritchie MG, Seifert B, Smadja CM, Stelkens R, Szymura JM, Väinölä R, Wolf JBW, Zinner D. 2013. Hybridization and speciation. *J Evol Biol.* doi:10.1111/j.1420-9101.2012.02599.x
- Abe F, Minegishi H. 2008. Global screening of genes essential for growth in high-pressure and cold environments: Searching for basic adaptive strategies using a yeast deletion library. *Genetics* **178**:851–872. doi:10.1534/genetics.107.083063
- Abou Saada O, Tsouris A, Eberlein C, Friedrich A, Schacherer J. 2021. nPhase: an accurate and contiguous phasing method for polyploids. *Genome Biol* **22**:1–27. doi:10.1186/s13059-021-02342-x
- Aguilera J, Randez-Gil F, Prieto JA. 2007. Cold response in *Saccharomyces cerevisiae*: New functions for old mechanisms. *FEMS Microbiol Rev.* doi:10.1111/j.1574-6976.2007.00066.x
- Albertin W, Marullo P. 2012. Polyploidy in fungi: Evolution after whole-genome duplication. *Proc R Soc B Biol Sci.* doi:10.1098/rspb.2012.0434
- Almeida P, Gonçalves C, Teixeira S, Libkind D, Bontrager M, Masneuf-Pomarède I, Albertin W, Durrens P, Sherman DJ, Marullo P, Todd Hittinger C, Gonçalves P, Sampaio JP. 2014. A Gondwanan imprint on global diversity and domestication of wine and cider yeast *Saccharomyces uvarum*. *Nat Commun* **5**. doi:10.1038/ncomms5044

- Alsammar H, Delneri D. 2020. An update on the diversity, ecology and biogeography of the *Saccharomyces* genus. *FEMS Yeast Res* **20**:13. doi:10.1093/FEMSYR/FOAA013
- Anderson TM, VonHoldt BM, Candille SI, Musiani M, Greco C, Stahler DR, Smith DW, Padhukasahasram B, Randi E, Leonard JA, Bustamante CD, Ostrander EA, Tang H, Wayne RK, Barsh GS. 2009. Molecular and evolutionary history of melanism in North American gray wolves. *Science* **323**:1339–1343. doi:10.1126/science.1165448
- Aouizerat T, Gelman D, Szitenberg A, Gutman I, Glazer S, Reich E, Schoemann M, Kaplan R, Saragovi A, Hazan R, Klutstein M. 2019. Eukaryotic Adaptation to Years-Long Starvation Resembles that of Bacteria. *iScience* **19**:545–558. doi:10.1016/j.isci.2019.08.002
- Arnold ML, Ballerini ES, Brothers AN. 2012. Hybrid fitness, adaptation and evolutionary diversification: Lessons learned from Louisiana Irises. *Heredity (Edinb)*. doi:10.1038/hdy.2011.65
- Baker E, Wang B, Bellora N, Peris D, Hulfachor AB, Koshalek JA, Adams M, Libkind D, Hittinger CT. 2015. The Genome Sequence of *Saccharomyces eubayanus* and the Domestication of Lager-Brewing Yeasts. *Mol Biol Evol* **32**:2818–2831. doi:10.1093/molbev/msv168
- Baker ECP, Peris D, Moriarty R V., Li XC, Fay JC, Hittinger CT. 2019. Mitochondrial DNA and temperature tolerance in lager yeasts. *Sci Adv* **5**. doi:10.1126/sciadv.aav1869
- Baller JA, Gao J, Stamenova R, Curcio MJ, Voytas DF. 2012. A nucleosomal surface defines an integration hotspot for the *Saccharomyces cerevisiae* Ty1 retrotransposon. *Genome Res* **22**:704–713. doi:10.1101/GR.129585.111
- Barbosa R, Almeida P, Safar SVB, Santos RO, Morais PB, Nielly-Thibault L, Leducq JB, Landry CR, Gonçalves P, Rosa CA, Sampaio JP. 2016. Evidence of natural hybridization in

- Brazilian wild lineages of *Saccharomyces cerevisiae*. *Genome Biol Evol* **8**:317–329.
doi:10.1093/gbe/evv263
- Barrio E, González SS, Arias A, Belloch C, Querol A. 2006. Molecular Mechanisms Involved in the Adaptive Evolution of Industrial Yeasts. *Yeasts in Food and Beverages*. Springer, Berlin, Heidelberg. pp. 153–174. doi:10.1007/978-3-540-28398-0_6
- Barros Lopes M, Bellon JR, Shirley NJ, Ganter PF. 2002. Evidence for multiple interspecific hybridization in *Saccharomyces sensu stricto* species. *FEMS Yeast Res* **1**:323–331.
doi:10.1111/j.1567-1364.2002.tb00051.x
- Belloch C, Pérez-Torrado R, González SS, José E. Pérez-Ortín, García-Martínez J, Querol A, Barrio E. 2009. Chimeric genomes of natural hybrids of *Saccharomyces cerevisiae* and *Saccharomyces kudriavzevii*. *Appl Environ Microbiol* **75**:2534–2544.
doi:10.1128/AEM.02282-08
- Bendiak DS. 1994. Quantification of the Helm's Flocculation Test. *J Am Soc Brew Chem* **52**:120–122. doi:10.1094/ASBCJ-52-0120
- Bennett RJ, Forche A, Berman J. 2014. Rapid mechanisms for generating genome diversity: Whole ploidy shifts, aneuploidy, and loss of heterozygosity. *Cold Spring Harb Perspect Med* **4**. doi:10.1101/cshperspect.a019604
- Bergström A, Simpson JT, Salinas F, Barré B, Parts L, Zia A, Nguyen Ba AN, Moses AM, Louis EJ, Mustonen V, Warringer J, Durbin R, Liti G. 2014. A high-definition view of functional genetic variation from natural yeast genomes. *Mol Biol Evol* **31**:872–888.
doi:10.1093/molbev/msu037
- Bomblies K, Lempe J, Epple P, Warthmann N, Lanz C, Dangl JL, Weigel D. 2007. Autoimmune response as a mechanism for a Dobzhansky-Muller-type incompatibility syndrome in

- plants. *PLoS Biol* **5**:1962–1972. doi:10.1371/journal.pbio.0050236
- Borneman AR, Forgan AH, Kolouchova R, Fraser JA, Schmidt SA. 2016. Whole genome comparison reveals high levels of inbreeding and strain redundancy across the spectrum of commercial wine strains of *Saccharomyces cerevisiae*. *G3 Genes, Genomes, Genetics* **6**:957–971. doi:10.1534/g3.115.025692
- Borneman AR, Pretorius IS. 2015. Genomic insights into the *Saccharomyces sensu stricto* complex. *Genetics* **199**:281–291. doi:10.1534/genetics.114.173633
- Botstein D, Fink GR. 2011. Yeast: An Experimental Organism for 21st Century Biology. *Genetics* **189**:695–704. doi:10.1534/GENETICS.111.130765
- Brewer BJ, Payen C, Di Rienzi SC, Higgins MM, Ong G, Dunham MJ, Raghuraman MK. 2015. Origin-Dependent Inverted-Repeat Amplification: Tests of a Model for Inverted DNA Amplification. *PLoS Genet* **11**:e1005699. doi:10.1371/journal.pgen.1005699
- Brewer BJ, Payen C, Raghuraman MK, Dunham MJ. 2011. Origin-dependent inverted-repeat amplification: A replication-based model for generating palindromic amplicons. *PLoS Genet* **7**:e1002016. doi:10.1371/journal.pgen.1002016
- Bridier-Nahmias A, Tchalikian-Cosson A, Baller JA, Menouni R, Fayol H, Flores A, Saïb A, Werner M, Voytas DF, Lesage P. 2015. An RNA polymerase III subunit determines sites of retrotransposon integration. *Science* **348**:585–588. doi:10.1126/science.1259114
- Brown CJ, Todd KM, Rosenzweig RF. 1998. Multiple duplications of yeast hexose transport genes in response to selection in a glucose-limited environment. *Mol Biol Evol* **15**:931–942. doi:10.1093/oxfordjournals.molbev.a026009
- Bud R. 1994. *The Uses of Life: A History of Biotechnology*. Cambridge, UK: Cambridge University Press.

- Buggs RJA, Chamala S, Wu W, Gao L, May GD, Schnable PS, Soltis DE, Soltis PS, Barbazuk WB. 2010. Characterization of duplicate gene evolution in the recent natural allopolyploid *Tragopogon miscellus* by next-generation sequencing and Sequenom iPLEX MassARRAY genotyping. *Mol Ecol* **19**:132–146. doi:10.1111/j.1365-294X.2009.04469.x
- Carrau F, Gaggero C, Aguilar PS. 2015. Yeast diversity and native vigor for flavor phenotypes. *Trends Biotechnol.* doi:10.1016/j.tibtech.2014.12.009
- Chapman AC. 1931. The yeast cell: what did Leeuwenhoeck see? *J Inst Brew* **37**:433–436. doi:10.1002/j.2050-0416.1931.tb05346.x
- Chen C, Chen H, Lin YS, Shen JB, Shan JX, Qi P, Shi M, Zhu MZ, Huang XH, Feng Q, Han B, Jiang L, Gao JP, Lin HX. 2014. A two-locus interaction causes interspecific hybrid weakness in rice. *Nat Commun* **5**:3357. doi:10.1038/ncomms4357
- Chen IC, Hill JK, Ohlemüller R, Roy DB, Thomas CD. 2011. Rapid range shifts of species associated with high levels of climate warming. *Science* **333**:1024–1026. doi:10.1126/science.1206432
- Chen P, Dong J, Yin H, Bao X, Chen L, He Y, Wan X, Chen R, Zhao Y, Hou X. 2015. Single nucleotide polymorphisms and transcription analysis of genes involved in ferulic acid decarboxylation among different beer yeasts. *J Inst Brew* **121**:481–489. doi:10.1002/jib.249
- Chen P, Zhang J. 2021. Asexual Experimental Evolution of Yeast Does Not Curtail Transposable Elements. *Mol Biol Evol* **38**:2831–2842. doi:10.1093/molbev/msab073
- Cheng F, Wu J, Fang L, Sun S, Liu B, Lin K, Bonnema G, Wang X. 2012. Biased gene fractionation and dominant gene expression among the subgenomes of *Brassica rapa*. *PLoS One* **7**:e36442. doi:10.1371/journal.pone.0036442
- Cheon Y, Kim H, Park K, Kim M, Lee D. 2020. Dynamic modules of the coactivator SAGA in

- eukaryotic transcription. *Exp Mol Med*. doi:10.1038/s12276-020-0463-4
- Conlan RS, Tzamarias D. 2001. Sfl1 functions via the co-repressor Ssn6-Tup1 and the cAMP-dependent protein kinase Tpk2. *J Mol Biol* **309**:1007–1015. doi:10.1006/jmbi.2001.4742
- Costanzo M, Baryshnikova A, Bellay J, Kim Y, Spear ED, Sevier CS, Ding H, Koh JLY, Toufighi K, Mostafavi S, Prinz J, St. Onge RP, Vandersluis B, Makhnevych T, Vizeacoumar FJ, Alizadeh S, Bahr S, Brost RL, Chen Y, Cokol M, Deshpande R, Li Z, Lin ZY, Liang W, Marback M, Paw J, Luis BJS, Shuteriqi E, Tong AHY, Van Dyk N, Wallace IM, Whitney JA, Weirauch MT, Zhong G, Zhu H, Houry WA, Brudno M, Ragibizadeh S, Papp B, Pál C, Roth FP, Giaever G, Nislow C, Troyanskaya OG, Bussey H, Bader GD, Gingras AC, Morris QD, Kim PM, Kaiser CA, Myers CL, Andrews BJ, Boone C. 2010. The genetic landscape of a cell. *Science* **327**:425–431. doi:10.1126/science.1180823
- Coyne JA, Orr HA. 2004. Speciation. Sunderland, MA: Sinauer Associates.
- Cubillos FA, Gibson B, Grijalva-Vallejos N, Krogerus K, Nikulin J. 2019. Bioprospecting for brewers: Exploiting natural diversity for naturally diverse beers. *Yeast* **36**:383–398. doi:10.1002/yea.3380
- D’Hautcourt O, Smart KA. 1999. The Measurement of Brewing Yeast Flocculation. *J Am Soc Brew Chem* **57**:123–128. doi:10.1094/ASBCJ-57-0129
- Dasmahapatra KK, Walters JR, Briscoe AD, Davey JW, Whibley A, Nadeau NJ, Zimin A V., Salazar C, Ferguson LC, Martin SH, Lewis JJ, Adler S, Ahn SJ, Baker DA, Baxter SW, Chamberlain NL, Ritika C, Counterman BA, Dalmay T, Gilbert LE, Gordon K, Heckel DG, Hines HM, Hoff KJ, Holland PWH, Jacquín-Joly E, Jiggins FM, Jones RT, Kapan DD, Kersey P, Lamas G, Lawson D, Mapleson D, Maroja LS, Martin A, Moxon S, Palmer WJ, Papa R, Papanicolaou A, Pauchet Y, Ray DA, Rosser N, Salzberg SL, Supple MA,

- SurrIDGE A, Tenger-Trolander A, Vogel H, Wilkinson PA, Wilson D, Yorke JA, Yuan F, Balmuth AL, Eland C, Gharbi K, Thomson M, Gibbs RA, Han Y, Jayaseelan JC, Kovar C, Mathew T, Muzny DM, Ogeri F, Pu LL, Qu J, Thornton RL, Worley KC, Wu YQ, Linares M, Blaxter ML, French-Constant RH, Joron M, Kronforst MR, Mullen SP, Reed RD, Scherer SE, Richards S, Mallet J, Mc Millan WO, Jiggins CD. 2012. Butterfly genome reveals promiscuous exchange of mimicry adaptations among species. *Nature* **487**:94–98. doi:10.1038/nature11041
- De Chiara M, Barré B, Persson K, Chioma AO, Irizar A, Schacherer J, Warringer J, Liti G. 2020. Domestication reprogrammed the budding yeast life cycle. *bioRxiv* 2020.02.08.939314. doi:10.1101/2020.02.08.939314
- Denby CM, Li RA, Vu VT, Costello Z, Lin W, Chan LJG, Williams J, Donaldson B, Bamforth CW, Petzold CJ, Scheller H V., Martin HG, Keasling JD. 2018. Industrial brewing yeast engineered for the production of primary flavor determinants in hopped beer. *Nat Commun* **9**:965. doi:10.1038/s41467-018-03293-x
- Deželak M, Gebremariam MM, Čadež N, Zupan J, Raspor P, Zarnkow M, Becker T, Košir IJ. 2014. The influence of serial repitching of *Saccharomyces pastorianus* on its karyotype and protein profile during the fermentation of gluten-free buckwheat and quinoa wort. *Int J Food Microbiol* **185**:93–102. doi:10.1016/j.ijfoodmicro.2014.05.023
- Donczew R, Warfield L, Pacheco D, Erijman A, Hahn S. 2020. Two roles for the yeast transcription coactivator SAGA and a set of genes redundantly regulated by TFIID and SAGA. *Elife* **9**. doi:10.7554/eLife.50109
- Duan SF, Han PJ, Wang QM, Liu WQ, Shi JY, Li K, Zhang XL, Bai FY. 2018. The origin and adaptive evolution of domesticated populations of yeast from Far East Asia. *Nat Commun*

9:2690. doi:10.1038/s41467-018-05106-7

Dunham MJ, Badrane H, Ferea T, Adams J, Brown PO, Rosenzweig F, Botstein D. 2002.

Characteristic genome rearrangements in experimental evolution of *Saccharomyces cerevisiae*. *Proc Natl Acad Sci U S A* **99**:16144–16149. doi:10.1073/pnas.242624799

Dunn B, Paulish T, Stanbery A, Piotrowski J, Koniges G, Kroll E, Louis EJ, Liti G, Sherlock G,

Rosenzweig F. 2013. Recurrent Rearrangement during Adaptive Evolution in an Interspecific Yeast Hybrid Suggests a Model for Rapid Introgression. *PLoS Genet* **9**.

doi:10.1371/journal.pgen.1003366

Dunn B, Sherlock G. 2008. Reconstruction of the genome origins and evolution of the hybrid

lager yeast *Saccharomyces pastorianus*. *Genome Res* **18**:1610–23.

doi:10.1101/gr.076075.108

Emery M, Willis MMS, Hao Y, Barry K, Oakgrove K, Peng Y, Schmutz J, Lyons E, Pires JC,

Edger PP, Conant GC. 2018. Preferential retention of genes from one parental genome after polyploidy illustrates the nature and scope of the genomic conflicts induced by

hybridization. *PLoS Genet* **14**. doi:10.1371/journal.pgen.1007267

Engel SR, Dietrich FS, Fisk DG, Binkley G, Balakrishnan R, Costanzo MC, Dwight SS, Hitz

BC, Karra K, Nash RS, Weng S, Wong ED, Lloyd P, Skrzypek MS, Miyasato SR, Simison

M, Cherry JM. 2014. The Reference Genome Sequence of *Saccharomyces cerevisiae*: Then and Now. *G3 Genes, Genomes, Genetics* **4**:389–398. doi:10.1534/g3.113.008995

Fay JC, Liu P, Ong GT, Dunham MJ, Cromie GA, Jeffery EW, Ludlow CL, Dudley AM. 2019.

A polyploid admixed origin of beer yeasts derived from European and Asian wine populations. *PLOS Biol* **17**:e3000147. doi:10.1371/journal.pbio.3000147

Fernandez-Espinar TT, Barrio E, Querol A. 2003. Analysis of the genetic variability in the

species of the *Saccharomyces sensu stricto* complex. *Yeast* **20**:1213–1226.

doi:10.1002/yea.1034

François J, Parrou JL. 2001. Reserve carbohydrates metabolism in the yeast *Saccharomyces cerevisiae*. *FEMS Microbiol Rev* **25**:125–145. doi:10.1111/j.1574-6976.2001.tb00574.x

Fu CY, Wang F, Sun BR, Liu WG, Li JH, Deng RF, Liu DL, Liu ZR, Zhu MS, Liao YL, Chen JW. 2013. Genetic and Cytological Analysis of a Novel Type of Low Temperature-Dependent Intraspecific Hybrid Weakness in Rice. *PLoS One* **8**.

doi:10.1371/journal.pone.0073886

Gallone B, Steensels J, Mertens S, Dzialo MC, Gordon JL, Wauters R, Theßeling FA, Bellinazzo F, Saels V, Herrera-Malaver B, Prah T, White C, Hutzler M, Meußdoerffer F, Malcorps P, Souffriau B, Daenen L, Baele G, Maere S, Verstrepen KJ. 2019. Interspecific hybridization facilitates niche adaptation in beer yeast. *Nat Ecol Evol* **3**:1562–1575. doi:10.1038/s41559-019-0997-9

Gallone B, Steensels J, Prah T, Soriaga L, Saels V, Herrera-Malaver B, Merlevede A, Roncoroni M, Voordeckers K, Miraglia L, Teiling C, Steffy B, Taylor M, Schwartz A, Richardson T, White C, Baele G, Maere S, Verstrepen KJ. 2016. Domestication and Divergence of *Saccharomyces cerevisiae* Beer Yeasts. *Cell* **166**:1397-1410.e16.

doi:10.1016/J.CELL.2016.08.020

García-Ríos E, Ramos-Alonso L, Guillamón JM. 2016. Correlation between low temperature adaptation and oxidative stress in *Saccharomyces cerevisiae*. *Front Microbiol* **7**.

doi:10.3389/fmicb.2016.01199

Garrison E, Marth G. 2012. Haplotype-based variant detection from short-read sequencing. doi:
<http://arxiv.org/abs/1207.3907>

- Gerrish PJ, Lenski RE. 1998. The fate of competing beneficial mutations in an asexual population. *Genetica* **102/103**:127–144. doi:10.1023/A:1017067816551
- Giaever G, Chu AM, Ni L, Connelly C, Riles L, Véronneau S, Dow S, Lucau-Danila A, Anderson K, André B, Arkin AP, Astromoff A, El Bakkoury M, Bangham R, Benito R, Brachat S, Campanaro S, Curtiss M, Davis K, Deutschbauer A, Entian KD, Flaherty P, Foury F, Garfinkel DJ, Gerstein M, Gotte D, Güldener U, Hegemann JH, Hempel S, Herman Z, Jaramillo DF, Kelly DE, Kelly SL, Kötter P, LaBonte D, Lamb DC, Lan N, Liang H, Liao H, Liu L, Luo C, Lussier M, Mao R, Menard P, Ooi SL, Revuelta JL, Roberts CJ, Rose M, Ross-Macdonald P, Scherens B, Schimmack G, Shafer B, Shoemaker DD, Sookhai-Mahadeo S, Storms RK, Strathern JN, Valle G, Voet M, Volckaert G, Wang CY, Ward TR, Wilhelmy J, Winzeler EA, Yang Y, Yen G, Youngman E, Yu K, Bussey H, Boeke JD, Snyder M, Philippsen P, Davis RW, Johnston M. 2002. Functional profiling of the *Saccharomyces cerevisiae* genome. *Nature* **418**:387–391. doi:10.1038/nature00935
- Gibson B, Dahabieh M, Krogerus K, Jouhten P, Magalhães F, Pereira R, Siewers V, Vidgren V. 2020. Adaptive Laboratory Evolution of Ale and Lager Yeasts for Improved Brewing Efficiency and Beer Quality. *Annu Rev Food Sci Technol*. doi:10.1146/annurev-food-032519-051715
- Gibson B, Geertman J-MMA, Hittinger CT, Krogerus K, Libkind D, Louis EJ, Magalhães F, Sampaio JP. 2017. New yeasts-new brews: Modern approaches to brewing yeast design and development. *FEMS Yeast Res* **17**. doi:10.1093/femsyr/fox038
- Gibson B, Liti G. 2015. *Saccharomyces pastorianus*: Genomic insights inspiring innovation for industry. *Yeast* **32**:17–27. doi:10.1002/yea.3033
- Gibson B, Vidgren V, Peddinti G, Krogerus K. 2018. Diacetyl control during brewery

- fermentation via adaptive laboratory engineering of the lager yeast *Saccharomyces pastorianus*. *J Ind Microbiol Biotechnol* **45**:1103–1112. doi:10.1007/s10295-018-2087-4
- Gonçalves M, Pontes A, Almeida P, Barbosa R, Serra M, Libkind D, Hutzler M, Gonçalves P, Sampaio JP. 2016. Distinct Domestication Trajectories in Top-Fermenting Beer Yeasts and Wine Yeasts. *Curr Biol* **26**:2750–2761. doi:10.1016/j.cub.2016.08.040
- Gonçalves P, Valério E, Correia C, de Almeida JMGCF, Sampaio JP. 2011. Evidence for divergent evolution of growth temperature preference in sympatric *Saccharomyces* species. *PLoS One* **6**. doi:10.1371/journal.pone.0020739
- González SS, Barrio E, Gafner J, Querol A. 2006. Natural hybrids from *Saccharomyces cerevisiae*, *Saccharomyces bayanus* and *Saccharomyces kudriavzevii* in wine fermentations. *FEMS Yeast Res* **6**:1221–1234. doi:10.1111/j.1567-1364.2006.00126.x
- Gorter De Vries AR, Voskamp MA, Van Aalst ACA, Kristensen LH, Jansen L, Van Den Broek M, Salazar AN, Brouwers N, Abeel T, Pronk JT, Daran JMG. 2019. Laboratory evolution of a *Saccharomyces cerevisiae* × *S. eubayanus* hybrid under simulated lager-brewing conditions. *Front Genet* **10**. doi:10.3389/fgene.2019.00242
- Grabenstein KC, Taylor SA. 2018. Breaking Barriers: Causes, Consequences, and Experimental Utility of Human-Mediated Hybridization. *Trends Ecol Evol*. doi:10.1016/j.tree.2017.12.008
- Grant PR, Grant BR. 2010. Natural selection, speciation and Darwin's finches. *Proc Calif Acad Sci* **61**:245–260.
- Grant PR, Grant BR. 2002. Unpredictable evolution in a 30-year study of Darwin's finches. *Science* **296**:707–711. doi:10.1126/science.1070315
- Greig D, Louis EJ, Borts RH, Travisano M. 2002. Hybrid speciation in experimental populations

- of yeast. *Science* **298**:1773–1775. doi:10.1126/science.1076374
- Gresham D, Desai MM, Tucker CM, Jenq HT, Pai DA, Ward A, DeSevo CG, Botstein D, Dunham MJ. 2008. The Repertoire and Dynamics of Evolutionary Adaptations to Controlled Nutrient-Limited Environments in Yeast. *PLoS Genet* **4**:e1000303. doi:10.1371/journal.pgen.1000303
- Gresham D, Dunham MJ. 2014. The enduring utility of continuous culturing in experimental evolution. *Genomics* **104**:399–405. doi:10.1016/j.ygeno.2014.09.015
- Gresham D, Usaite R, Germann SM, Lisby M, Botstein D, Regenbreg B. 2010. Adaptation to diverse nitrogen-limited environments by deletion or extrachromosomal element formation of the *GAPI* locus. *Proc Natl Acad Sci U S A* **107**:18551–18556. doi:10.1073/pnas.1014023107
- Guisan A, Thuiller W. 2005. Predicting species distribution: Offering more than simple habitat models. *Ecol Lett.* doi:10.1111/j.1461-0248.2005.00792.x
- Hall BG, Acar H, Nandipati A, Barlow M. 2014. Growth rates made easy. *Mol Biol Evol* **31**:232–238. doi:10.1093/molbev/mst187
- Hamdani O, Dhillon N, Hsieh T-HS, Fujita T, Ocampo J, Kirkland JG, Lawrimore J, Kobayashi TJ, Friedman B, Fulton D, Wu KY, Chereji R V., Oki M, Bloom K, Clark DJ, Rando OJ, Kamakaka RT. 2019. tRNA Genes Affect Chromosome Structure and Function via Local Effects. *Mol Cell Biol* **39**. doi:10.1128/mcb.00432-18
- Han E-K, Cotty F, Sottas C, Jiang H, Michels CA. 1995. Characterization of *AGT1* encoding a general α -glucoside transporter from *Saccharomyces*. *Mol Microbiol* **17**:1093–1107. doi:10.1111/J.1365-2958.1995.MMI_17061093.X
- Hansen EC. 1883. Recherches sur la physiologie et la morphologie des ferments alcooliques. V.

- Methodes pour obtenir des cultures pures de *Saccharomyces* et de mikroorganismes analogues. *Compt Rend Trav Lab Carlsb* **2**:92–105.
- Hartwell LH, Culotti J, Reid B. 1970. Genetic control of the cell-division cycle in yeast. I. Detection of mutants. *Proc Natl Acad Sci U S A* **66**:352–359. doi:10.1073/pnas.66.2.352
- Hebly M, Brickwedde A, Bolat I, Driessen MRM, de Hulster EAF, van den Broek M, Pronk JT, Geertman JM, Daran JM, Daran-Lapujade P. 2015. *S. cerevisiae* × *S. eubayanus* interspecific hybrid, the best of both worlds and beyond. *FEMS Yeast Res* **15**:1–14. doi:10.1093/femsyr/fov005
- Hewitt SK, Donaldson IJ, Lovell SC, Delneri D. 2014. Sequencing and Characterisation of Rearrangements in Three *S. pastorianus* Strains Reveals the Presence of Chimeric Genes and Gives Evidence of Breakpoint Reuse. *PLoS One* **9**:e92203. doi:10.1371/JOURNAL.PONE.0092203
- Hittinger CT. 2013. *Saccharomyces* diversity and evolution: A budding model genus. *Trends Genet.* doi:10.1016/j.tig.2013.01.002
- Ho CH, Magtanong L, Barker SL, Gresham D, Nishimura S, Natarajan P, Koh JLY, Porter J, Gray CA, Andersen RJ, Giaever G, Nislow C, Andrews B, Botstein D, Graham TR, Yoshida M, Boone C. 2009. A molecular barcoded yeast ORF library enables mode-of-action analysis of bioactive compounds. *Nat Biotechnol* **27**:369–377. doi:10.1038/nbt.1534
- Hockings K, Dunbar R. 2019. Alcohol and Humans: A Long and Social Affair. Oxford, UK: Oxford University Press. doi:10.1093/oso/9780198842460.001.0001
- Hoffman CS, Winston F. 1987. A ten-minute DNA preparation from yeast efficiently releases autonomous plasmids for transformiaon of *Escherichia coli*. *Gene* **57**:267–272. doi:10.1016/0378-1119(87)90131-4

- Hoffmann AA, Sgró CM. 2011. Climate change and evolutionary adaptation. *Nature*.
doi:10.1038/nature09670
- Homma T, Iwahashi H, Komatsu Y. 2003. Yeast gene expression during growth at low temperature. *Cryobiology* **46**:230–237. doi:10.1016/S0011-2240(03)00028-2
- Hon T, Mars K, Young G, Tsai Y-C, Karalius JW, Landolin JM, Maurer N, Kudrna D, Hardigan MA, Steiner CC, Knapp SJ, Ware D, Shapiro B, Peluso P, Rank DR. 2020. Highly accurate long-read HiFi sequencing data for five complex genomes. *Sci Data* 2020 71 **7**:1–11.
doi:10.1038/s41597-020-00743-4
- Hong J, Brandt N, Abdul-Rahman F, Yang A, Hughes T, Gresham D. 2018. An incoherent feedforward loop facilitates adaptive tuning of gene expression. *Elife* **7**.
doi:10.7554/eLife.32323
- Hope EA, Amorosi CJ, Miller AW, Dang K, Heil CS, Dunham MJ. 2017. Experimental evolution reveals favored adaptive routes to cell aggregation in yeast. *Genetics* **206**:1153–1167. doi:10.1534/genetics.116.198895
- Hornsey IS. 2003. A history of beer and brewing. Cambridge, UK: The Royal Society of Chemistry.
- Hou J, Friedrich A, Gounot JS, Schacherer J. 2015. Comprehensive survey of condition-specific reproductive isolation reveals genetic incompatibility in yeast. *Nat Commun* **6**.
doi:10.1038/ncomms8214
- Huerta-Sánchez E, Jin X, Asan, Bianba Z, Peter BM, Vinckenbosch N, Liang Y, Yi X, He M, Somel M, Ni P, Wang B, Ou X, Huasang, Luosang J, Cuo ZXP, Li K, Gao G, Yin Y, Wang W, Zhang X, Xu X, Yang H, Li Y, Wang Jian, Wang Jun, Nielsen R. 2014. Altitude adaptation in Tibetans caused by introgression of Denisovan-like DNA. *Nature* **512**:194–

197. doi:10.1038/nature13408

Huh WK, Falvo J V., Gerke LC, Carroll AS, Howson RW, Weissman JS, O'Shea EK. 2003.

Global analysis of protein localization in budding yeast. *Nature* **425**:686–691.

doi:10.1038/nature02026

James TY, Michelotti LA, Glasco AD, Clemons RA, Powers RA, James ES, Rabern Simmons

D, Bai F, Ge S. 2019. Adaptation by loss of heterozygosity in *Saccharomyces cerevisiae*

clones under divergent selection. *Genetics* **213**:665–683. doi:10.1534/genetics.119.302411

Jenkins CL, Kennedy AI, Hodgson JA, Thurston P, Smart KA. 2003. Impact of Serial Repitching

on Lager Brewing Yeast Quality. *J Am Soc Brew Chem* **61**:1–9. doi:10.1094/ASBCJ-61-

0001

Jenkins CL, Kennedy AI, Thurston P, Hodgson JA, Smart KA. 2008. Serial Repitching

Fermentation Performance and Functional Biomarkers Brewing Yeast Fermentation

Performance. Oxford, UK: Blackwell Science. pp. 257–271.

doi:10.1002/9780470696040.ch24

Jenkins CL, Lawrence SJ, Kennedy AI, Thurston P, Hodgson JA, Smart KA. 2009. Incidence

and Formation of Petite Mutants in Lager Brewing Yeast *Saccharomyces cerevisiae* (Syn. *S. pastorianus*) Populations. *J Am Soc Brew Chem* **67**:72–80.

Jerison ER, Desai MM. 2015. Genomic investigations of evolutionary dynamics and epistasis in

microbial evolution experiments. *Curr Opin Genet Dev* **35**:33–39.

doi:10.1016/j.gde.2015.08.008

Jeuken MJW, Zhang NW, McHale LK, Pelgrom K, Den Boer E, Lindhout P, Michelmore RW,

Visser RGF, Niks RE. 2009. Rin4 causes hybrid necrosis and race-specific resistance in an

interspecific lettuce hybrid. *Plant Cell* **21**:3368–3378. doi:10.1105/tpc.109.070334

- Johnson WE, Onorato DP, Roelke ME, Land ED, Cunningham M, Belden RC, McBride R, Jansen D, Lotz M, Shindle D, Howard JG, Wildt DE, Penfold LM, Hostetler JA, Oli MK, O'Brien SJ. 2010. Genetic restoration of the Florida panther. *Science* **329**:1641–1645. doi:10.1126/science.1192891
- Jones MR, Scott Mills L, Alves PC, Callahan CM, Alves JM, Lafferty DJR, Jiggins FM, Jensen JD, Melo-Ferreira J, Good JM. 2018. Adaptive introgression underlies polymorphic seasonal camouflage in snowshoe hares. *Science* **360**:1355–1358. doi:10.1126/science.aar5273
- Juric I, Aeschbacher S, Coop G. 2016. The Strength of Selection against Neanderthal Introgression. *PLoS Genet* **12**:e1006340. doi:10.1371/journal.pgen.1006340
- Kandror O, Bretschneider N, Kreydin E, Cavalieri D, Goldberg AL. 2004. Yeast adapt to near-freezing temperatures by STRE/Msn2,4-dependent induction of trehalose synthesis and certain molecular chaperones. *Mol Cell* **13**:771–781. doi:10.1016/S1097-2765(04)00148-0
- Kao KC, Sherlock G. 2008. Molecular characterization of clonal interference during adaptive evolution in asexual populations of *Saccharomyces cerevisiae*. *Nat Genet* **40**:1499–1504. doi:10.1038/ng.280
- Kelly BP, Whiteley A, Tallmon D. 2010. The Arctic melting pot. *Nature*. doi:10.1038/468891a
- Kobayashi M, Shimizu H, Shioya S. 2007. Physiological analysis of yeast cells by flow cytometry during serial-repitching of low-malt beer fermentation. *J Biosci Bioeng* **103**:451–456. doi:10.1263/jbb.103.451
- Kobayashi O, Hayashi N, Kuroki R, Sone H. 1998. Region of Flo1 proteins responsible for sugar recognition. *J Bacteriol* **180**:6503–6510. doi:10.1128/jb.180.24.6503-6510.1998
- Koonthongkaew J, Toyokawa Y, Ohashi M, Large CRL, Dunham MJ, Takagi H. 2020. Effect of

- the Ala234Asp replacement in mitochondrial branched-chain amino acid aminotransferase on the production of BCAAs and fusel alcohols in yeast. *Appl Microbiol Biotechnol*. doi:10.1007/s00253-020-10800-y
- Krogerus K, Gibson B. 2020. A re-evaluation of diastatic *Saccharomyces cerevisiae* strains and their role in brewing. *Appl Microbiol Biotechnol* 2020 1049 **104**:3745–3756. doi:10.1007/S00253-020-10531-0
- Krogerus K, Gibson BR. 2013. 125th anniversary review: Diacetyl and its control during brewery fermentation. *J Inst Brew* **119**:86–97. doi:10.1002/jib.84
- Krogerus K, Magalhães F, Kuivanen J, Gibson B. 2019. A deletion in the *STAI* promoter determines maltotriose and starch utilization in *STAI+* *Saccharomyces cerevisiae* strains. *Appl Microbiol Biotechnol* 2019 10318 **103**:7597–7615. doi:10.1007/S00253-019-10021-Y
- Krogerus K, Magalhães F, Vidgren V, Gibson B. 2017. Novel brewing yeast hybrids: creation and application. *Appl Microbiol Biotechnol* **101**:65–78. doi:10.1007/s00253-016-8007-5
- Krogerus K, Magalhães F, Vidgren V, Gibson B. 2015. New lager yeast strains generated by interspecific hybridization. *J Ind Microbiol Biotechnol* **42**:769–778. doi:10.1007/s10295-015-1597-6
- Krogerus K, Preiss R, Gibson B. 2018. A unique *Saccharomyces cerevisiae* x *Saccharomyces uvarum* hybrid isolated from norwegian farmhouse beer: Characterization and reconstruction. *Front Microbiol* **9**. doi:10.3389/fmicb.2018.02253
- Kryazhimskiy S, Rice DP, Jerison ER, Desai MM. 2014. Global epistasis makes adaptation predictable despite sequence-level stochasticity. *Science* **344**:1519–1522. doi:10.1126/science.1250939
- Kvitek DJ, Sherlock G. 2011. Reciprocal sign epistasis between frequently experimentally

- evolved adaptive mutations causes a rugged fitness landscape. *PLoS Genet* **7**.
doi:10.1371/journal.pgen.1002056
- Lagerstedt JO, Voss JC, Wieslander Å, Persson BL. 2004. Structural modeling of dual-affinity purified Pho84 phosphate transporter. *FEBS Lett* **578**:262–268.
doi:10.1016/j.febslet.2004.11.012
- Lang GI, Rice DP, Hickman MJ, Sodergren E, Weinstock GM, Botstein D, Desai MM. 2013. Pervasive genetic hitchhiking and clonal interference in forty evolving yeast populations. *Nature* **500**:571–4. doi:10.1038/nature12344
- Langdon QK, Peris D, Baker ECP, Opulente DA, Nguyen HV, Bond U, Gonçalves P, Sampaio JP, Libkind D, Hittinger CT. 2019. Fermentation innovation through complex hybridization of wild and domesticated yeasts. *Nat Ecol Evol* **3**:1576–1586. doi:10.1038/s41559-019-0998-8
- Larroque MN, Carrau F, Fariña L, Boido E, Dellacassa E, Medina K. 2021. Effect of *Saccharomyces* and non-*Saccharomyces* native yeasts on beer aroma compounds. *Int J Food Microbiol* **337**:108953. doi:10.1016/j.ijfoodmicro.2020.108953
- Lashkari DA, Derisi JL, Mccusker JH, Namath AF, Gentile C, Hwang SY, Brown PO, Davis RW. 1997. Yeast microarrays for genome wide parallel genetic and gene expression analysis. *Proc Natl Acad Sci U S A* **94**:13057–13062. doi:10.1073/pnas.94.24.13057
- Lauer S, AVECILLA G, Spealman P, Sethia G, Brandt N, Levy SF, Gresham D. 2018. Single-cell copy number variant detection reveals the dynamics and diversity of adaptation. *PLoS Biol* **16**:e3000069. doi:10.1371/journal.pbio.3000069
- Lawrence SJ, Wimalasena TT, Nicholls SM, Box WG, Boulton C, Smart KA. 2012. Incidence and characterization of petites isolated from lager brewing yeast *Saccharomyces cerevisiae*

- populations. *J Am Soc Brew Chem* **70**:268–274. doi:10.1094/ASBCJ-2012-0917-01
- Leducq JB, Nielly-Thibault L, Charron G, Eberlein C, Verta JP, Samani P, Sylvester K, Hittinger CT, Bell G, Landry CR. 2016. Speciation driven by hybridization and chromosomal plasticity in a wild yeast. *Nat Microbiol* **1**. doi:10.1038/nmicrobiol.2015.3
- Lee HY, Chou JY, Cheong L, Chang NH, Yang SY, Leu JY. 2008. Incompatibility of Nuclear and Mitochondrial Genomes Causes Hybrid Sterility between Two Yeast Species. *Cell* **135**:1065–1073. doi:10.1016/j.cell.2008.10.047
- Letunic I, Bork P. 2019. Interactive Tree of Life (iTOL) v4: Recent updates and new developments. *Nucleic Acids Res* **47**. doi:10.1093/nar/gkz239
- Li H. 2013. Aligning sequence reads, clone sequences and assembly contigs with BWA-MEM. *arXiv*.
- Li H, Handsaker B, Wysoker A, Fennell T, Ruan J, Homer N, Marth G, Abecasis G, Durbin R. 2009. The Sequence Alignment/Map format and SAMtools. *Bioinformatics* **25**:2078–2079. doi:10.1093/bioinformatics/btp352
- Li XC, Peris D, Hittinger CT, Sia EA, Fay JC. 2019. Mitochondria-encoded genes contribute to evolution of heat and cold tolerance in yeast. *Sci Adv* **5**. doi:10.1126/sciadv.aav1848
- Li Y, Venkataram S, Agarwala A, Dunn B, Petrov DA, Sherlock G, Fisher DS. 2018. Hidden Complexity of Yeast Adaptation under Simple Evolutionary Conditions. *Curr Biol* **28**:515–525.e6. doi:10.1016/j.cub.2018.01.009
- Li ZK, Zhang F. 2013. Rice breeding in the post-genomics era: From concept to practice. *Curr Opin Plant Biol*. doi:10.1016/j.pbi.2013.03.008
- Libkind D, Hittinger CT, Valério E, Gonçalves C, Dover J, Johnston M, Gonçalves P, Sampaio JP. 2011. Microbe domestication and the identification of the wild genetic stock of lager-

- brewing yeast. *Proc Natl Acad Sci U S A* **108**:14539–44. doi:10.1073/pnas.1105430108
- Liti G, Peruffo A, James SA, Roberts IN, Louis EJ. 2005. Inferences of evolutionary relationships from a population survey of LTR-retrotransposons and telomeric-associated sequences in the *Saccharomyces sensu stricto* complex. *Yeast* **22**:177–192. doi:10.1002/yea.1200
- Liti G, Schacherer J. 2011. The rise of yeast population genomics. *Comptes Rendus - Biol* **334**:612–619. doi:10.1016/j.crvi.2011.05.009
- Liu H, Styles CA, Fink GR. 1996. *Saccharomyces cerevisiae* S288C has a mutation in *FLO8*, a gene required for filamentous growth. *Genetics* **144**:967–978. doi:10.1093/genetics/144.3.967
- Louis VL, Despons L, Friedrich A, Martin T, Durrens P, Casarégola S, Neuvéglise C, Fairhead C, Marck C, Cruz JA, Straub ML, Kugler V, Sacerdot C, Uzunov Z, Thierry A, Weiss S, Bleykasten C, Montigny J De, Jacques N, Jung P, Lemaire M, Mallet S, Morel G, Richard GF, Sarkar A, Savel G, Schacherer J, Seret ML, Talla E, Samson G, Jubin C, Poulain J, Vacherie B, Barbe V, Pelletier E, Sherman DJ, Westhof E, Weissenbach J, Baret P V, Wincker P, Gaillardin C, Dujon B, Souciet JL. 2012. *Pichia sorbitophila*, an Interspecies Yeast Hybrid, Reveals Early Steps of Genome Resolution After Polyploidization. *G3 Genes, Genomes, Genetics* **2**:299–311. doi:10.1534/g3.111.000745
- Marcet-Houben M, Gabaldón T. 2015. Beyond the whole-genome duplication: Phylogenetic evidence for an ancient interspecies hybridization in the baker's yeast lineage. *PLoS Biol* **13**. doi:10.1371/journal.pbio.1002220
- Marsit S, Leducq J-B, Durand É, Marchant A, Filteau M, Landry CR. 2017. Evolutionary biology through the lens of budding yeast comparative genomics. *Nat Rev Genet* **18**:581–

598. doi:10.1038/nrg.2017.49
- Martin NH, Bouck AC, Arnold ML. 2006. Detecting adaptive trait introgression between *Iris fulva* and *I. brevicaulis* in highly selective field conditions. *Genetics* **172**:2481–2489. doi:10.1534/genetics.105.053538
- Maule DR. 1986. A Century Of Fermenter Design. *J Inst Brew* **92**:137–145. doi:10.1002/j.2050-0416.1986.tb04387.x
- Mayer VW, Aguilera A. 1990. High levels of chromosome instability in polyploids of *Saccharomyces cerevisiae*. *Mutat Res Mol Mech Mutagen* **231**:177–186. doi:10.1016/0027-5107(90)90024-X
- Mcdonald MJ, Rice DP, Desai MM. 2016. Sex speeds adaptation by altering the dynamics of molecular evolution. *Nature* **531**. doi:10.1038/nature17143
- McGovern PE. 2019a. Alcoholic Beverages as the Universal Medicine before SyntheticsACS Symposium Series. American Chemical Society. pp. 111–127. doi:10.1021/bk-2019-1314.ch008
- McGovern PE. 2019b. Uncorking the Past: Alcoholic Fermentation as Humankind’s First Biotechnology Alcohol and Humans: A Long and Social Affair. Oxford, UK: Oxford University Press. pp. 81–92. doi:10.1093/oso/9780198842460.003.0006
- McGovern PE. 2009. Uncorking the Past : the Quest for Wine, Beer, and Other Alcoholic Beverages. Berkeley, CA, USA: University of California Press.
- Miller AW, Befort C, Kerr EO, Dunham MJ. 2013. Design and Use of Multiplexed Chemostat Arrays. *J Vis Exp* 50262. doi:10.3791/50262
- Minh BQ, Schmidt H, Chernomor O, Schrempf D, Woodhams M, von Haeseler A, Lanfear R. 2019. IQ-TREE 2: New models and efficient methods for phylogenetic inference in the

- genomic era. *Mol Biol Evol* **37**:1530–1534. doi:10.1093/molbev/msaa015
- Monerawela C, Bond U. 2017. Brewing up a storm: The genomes of lager yeasts and how they evolved. *Biotechnol Adv* **35**:512–519. doi:10.1016/J.BIOTECHADV.2017.03.003
- Monerawela C, James TC, Wolfe KH, Bond U. 2015. Loss of lager specific genes and subtelomeric regions define two different *Saccharomyces cerevisiae* lineages for *Saccharomyces pastorianus* Group I and II strains. *FEMS Yeast Res* **15**. doi:10.1093/femsyr/fou008
- Monod J. 1950. Technique, Theory and Applications of Continuous Culture. *Ann Inst Pasteur* **79**:390–410.
- Morales L, Dujon B. 2012. Evolutionary role of interspecies hybridization and genetic exchanges in yeasts. *Microbiol Mol Biol Rev* **76**:721–39. doi:10.1128/MMBR.00022-12
- Mukai N, Masaki K, Fujii T, Iefuji H. 2014. Single nucleotide polymorphisms of *PAD1* and *FDC1* show a positive relationship with ferulic acid decarboxylation ability among industrial yeasts used in alcoholic beverage production. *J Biosci Bioeng* **118**:50–55. doi:10.1016/j.jbiosc.2013.12.017
- Mularoni L, Zhou Y, Bowen T, Gangadharan S, Wheelan SJ, Boeke JD. 2012. Retrotransposon Ty1 integration targets specifically positioned asymmetric nucleosomal DNA segments in tRNA hotspots. *Genome Res* **22**:693–703. doi:10.1101/gr.129460.111
- Nakao Y, Kanamori T, Itoh T, Kodama Y, Rainieri S, Nakamura N, Shimonaga T, Hattori M, Ashikari T. 2009. Genome sequence of the lager brewing yeast, an interspecies hybrid. *DNA Res* **16**:115–129. doi:10.1093/dnares/dsp003
- Naumov GI, Naumova ES, Michels CA. 1994. Genetic variation of the repeated *MAL* loci in natural populations of *Saccharomyces cerevisiae* and *Saccharomyces paradoxus*. *Genetics*

136.

- Nelson MG, Linheiro RS, Bergman CM. 2017. McClintock: An integrated pipeline for detecting transposable element insertions in whole-genome shotgun sequencing data. *G3 Genes, Genomes, Genetics* **7**:2763–2778. doi:10.1534/g3.117.043893
- Nguyen HV, Legras JL, Neuvéglise C, Gaillardin C. 2011. Deciphering the hybridisation history leading to the lager lineage based on the mosaic genomes of *Saccharomyces bayanus* strains NBRC1948 and CBS380 T. *PLoS One* **6**:e25821. doi:10.1371/journal.pone.0025821
- Nikulin J, Krogerus K, Gibson B. 2018. Alternative *Saccharomyces* interspecies hybrid combinations and their potential for low-temperature wort fermentation. *Yeast* **35**:113–127. doi:10.1002/yea.3246
- Norris LC, Main BJ, Lee Y, Collier TC, Fofana A, Cornel AJ, Lanzaro GC. 2015. Adaptive introgression in an African malaria mosquito coincident with the increased usage of insecticide-treated bed nets. *Proc Natl Acad Sci U S A* **112**:815–820. doi:10.1073/pnas.1418892112
- Novick A, Szilard L. 1950. Description of the chemostat. *Science* **112**:715–716. doi:10.1126/science.112.2920.715
- Ogata T, Izumikawa M, Kohno K, Shibata K. 2008. Chromosomal location of Lg-*FLO1* in bottom-fermenting yeast and the *FLO5* locus of industrial yeast. *J Appl Microbiol* **105**:1186–1198. doi:10.1111/j.1365-2672.2008.03852.x
- Ogata T, Ohtake A, Takeuchi S, Tabuchi M, Nakamura K. 2020. Flocculation Type and the Lg-*FLO1* Gene of Bottom-Fermenting Yeast Are Derived from Top-Fermenting Yeast. *Journal of the American Society of Brewing Chemists* **79**:306–313. doi:10.1080/03610470.2020.1843944

- Okuno M, Kajitani R, Ryusui R, Morimoto H, Kodama Y, Itoh T. 2016. Next-generation sequencing analysis of lager brewing yeast strains reveals the evolutionary history of interspecies hybridization. *DNA Res* **23**:67–80. doi:10.1093/DNARES/DSV037
- Omasits U, Ahrens CH, Müller S, Wollscheid B. 2014. Protter: Interactive protein feature visualization and integration with experimental proteomic data. *Bioinformatics* **30**:884–886. doi:10.1093/bioinformatics/btt607
- Oziolor EM, Reid NM, Yair S, Lee KM, VerPloeg SG, Bruns PC, Shaw JR, Whitehead A, Matson CW. 2019. Adaptive introgression enables evolutionary rescue from extreme environmental pollution. *Science* **364**:455–457. doi:10.1126/science.aav4155
- Paget CM, Schwartz JM, Delneri D. 2014. Environmental systems biology of cold-tolerant phenotype in *Saccharomyces* species adapted to grow at different temperatures. *Mol Ecol* **23**:5241–5257. doi:10.1111/mec.12930
- Parrou JL, Teste MA, François J. 1997. Effects of various types of stress on the metabolism of reserve carbohydrates in *Saccharomyces cerevisiae*: Genetic evidence for a stress-induced recycling of glycogen and trehalose. *Microbiology* **143**:1891–1900. doi:10.1099/00221287-143-6-1891
- Pashkova N, Gakhar L, Winistorfer SC, Sunshine AB, Rich M, Dunham MJ, Yu L, Piper RC. 2013. The yeast alix homolog bro1 functions as a ubiquitin receptor for protein sorting into multivesicular endosomes. *Dev Cell* **25**:520–533. doi:10.1016/j.devcel.2013.04.007
- Pasteur L. 1879. *Studies on Fermentation: The diseases of beer, their causes, and the means of preventing them.* London: Macmillan and Co.
- Payen C, Di Rienzi SC, Ong GT, Pogachar JL, Sanchez JC, Sunshine AB, Raghuraman MK, Brewer BJ, Dunham MJ. 2014. The Dynamics of Diverse Segmental Amplifications in

- Populations of *Saccharomyces cerevisiae* Adapting to Strong Selection. *G3 Genes, Genomes, Genetics* **4**.
- Payen C, Sunshine AB, Ong GT, Pogachar JL, Zhao W, Dunham MJ. 2016. High-Throughput Identification of Adaptive Mutations in Experimentally Evolved Yeast Populations. *PLoS Genet* **12**. doi:10.1371/journal.pgen.1006339
- Pérez-Torrado R, Barrio E, Querol A. 2018. Alternative yeasts for winemaking: *Saccharomyces non-cerevisiae* and its hybrids. *Crit Rev Food Sci Nutr* **58**:1780–1790. doi:10.1080/10408398.2017.1285751
- Pérez-Través L, Lopes CA, Querol A, Barrio E. 2014. On the complexity of the *Saccharomyces bayanus* taxon: Hybridization and potential hybrid speciation. *PLoS One* **9**:e93729. doi:10.1371/journal.pone.0093729
- Peris D, Alexander WG, Fisher KJ, Moriarty R V., Basuino MG, Ubbelohde EJ, Wrobel RL, Hittinger CT. 2020. Synthetic hybrids of six yeast species. *Nat Commun* **11**:1–11. doi:10.1038/s41467-020-15559-4
- Peris D, Langdon QK, Moriarty R V., Sylvester K, Bontrager M, Charron G, Leducq JB, Landry CR, Libkind D, Hittinger CT. 2016. Complex Ancestries of Lager-Brewing Hybrids Were Shaped by Standing Variation in the Wild Yeast *Saccharomyces eubayanus*. *PLoS Genet* **12**:e1006155. doi:10.1371/journal.pgen.1006155
- Peter J, De Chiara M, Friedrich A, Yue JX, Pflieger D, Bergström A, Sigwalt A, Barre B, Freel K, Llored A, Cruaud C, Labadie K, Aury JM, Istace B, Lebrigand K, Barbry P, Engelen S, Lemainque A, Wincker P, Liti G, Schacherer J. 2018. Genome evolution across 1,011 *Saccharomyces cerevisiae* isolates. *Nature* **556**:339–344. doi:10.1038/s41586-018-0030-5
- Phadtare S, Alsina J, Inouye M. 1999. Cold-shock response and cold-shock proteins. *Curr Opin*

- Microbiol* **2**:175–180. doi:10.1016/S1369-5274(99)80031-9
- Piotrowski JS, Nagarajan S, Kroll E, Stanbery A, Chiotti KE, Kruckeberg AL, Dunn B, Sherlock G, Rosenzweig F. 2012. Different selective pressures lead to different genomic outcomes as newly-formed hybrid yeasts evolve. *BMC Evol Biol* **12**:46. doi:10.1186/1471-2148-12-46
- Popova Y, Thayumanavan P, Lonati E, Agrochão M, Thevelein JM. 2010. Transport and signaling through the phosphate-binding site of the yeast Pho84 phosphate transceptor. *Proc Natl Acad Sci U S A* **107**:2890–2895. doi:10.1073/pnas.0906546107
- Powell C, Fischborn T, Id CREF, Wau ML, Library S. 2010. Serial Repitching of Dried Lager Yeast. *J Am Soc Brew Chem* **68**:48–56. doi:10.1094/ASBCJ-2010-0125-01
- Powell CD, Diacetis AN. 2007. Long term serial repitching and the genetic and phenotypic stability of brewer's yeast. *J Inst Brew* **113**:67–74. doi:10.1002/j.2050-0416.2007.tb00258.x
- Preiss R, Tyrawa C, Krogerus K, Garshol LM, van der Merwe G. 2018. Traditional Norwegian Kveik Are a Genetically Distinct Group of Domesticated *Saccharomyces cerevisiae* Brewing Yeasts. *Front Microbiol* **9**:2137. doi:10.3389/fmicb.2018.02137
- Pryszcz LP, Németh T, Gácsér A, Gabaldón T. 2014. Genome comparison of *Candida orthopsilosis* clinical strains reveals the existence of hybrids between two distinct subspecies. *Genome Biol Evol* **6**:1069–1078. doi:10.1093/gbe/evu082
- Quinlan AR, Hall IM. 2010. BEDTools: A flexible suite of utilities for comparing genomic features. *Bioinformatics* **26**:841–842. doi:10.1093/bioinformatics/btq033
- Racimo F, Sankararaman S, Nielsen R, Huerta-Sánchez E. 2015. Evidence for archaic adaptive introgression in humans. *Nat Rev Genet*. doi:10.1038/nrg3936
- Rác HV, Mukhtar F, Imre A, Rádai Z, Gombert AK, Rátónyi T, Nagy J, Pócsi I, Pfliegler WP. 2021. How to characterize a strain? Clonal heterogeneity in industrial *Saccharomyces*

- influences both phenotypes and heterogeneity in phenotypes. *Yeast*. doi:10.1002/yea.3562
- Rainieri S, Kodama Y, Kaneko Y, Mikata K, Nakao Y, Ashikari T. 2006. Pure and mixed genetic lines of *Saccharomyces bayanus* and *Saccharomyces pastorianus* and their contribution to the lager brewing strain genome. *Appl Environ Microbiol* **72**:3968–3974. doi:10.1128/AEM.02769-05
- Rainieri S, Zambonelli C, Hallsworth JE, Pulvirenti A, Giudici P. 1999. *Saccharomyces uvarum*, a distinct group within *Saccharomyces sensu stricto*. *FEMS Microbiol Lett* **177**:177–185. doi:10.1111/j.1574-6968.1999.tb13729.x
- Raynes Y, Wylie CS, Sniegowski PD, Weinreich DM. 2018. Sign of selection on mutation rate modifiers depends on population size. *Proc Natl Acad Sci* **115**:3422–3427. doi:10.1073/pnas.1715996115
- Richards EJ, Martin CH. 2017. Adaptive introgression from distant Caribbean islands contributed to the diversification of a microendemic adaptive radiation of trophic specialist pupfishes. *PLoS Genet* **13**. doi:10.1371/journal.pgen.1006919
- Richardson SM, Mitchell LA, Stracquadanio G, Yang K, Dymond JS, DiCarlo JE, Lee D, Huang CLV, Chandrasegaran S, Cai Y, Boeke JD, Bader JS. 2017. Design of a synthetic yeast genome. *Science* **355**:1040–1044. doi:10.1126/SCIENCE.AAF4557
- Rieseberg LH, Raymond O, Rosenthal DM, Lai Z, Livingstone K, Nakazato T, Durphy JL, Schwarzbach AE, Donovan LA, Lexer C. 2003. Major ecological transitions in wild sunflowers facilitated by hybridization. *Science* **301**:1211–1216. doi:10.1126/science.1086949
- Robertson LS, Fink GR. 1998. The three yeast A kinases have specific signaling functions in pseudohyphal growth. *Proc Natl Acad Sci U S A* **95**:13783–13787.

doi:10.1073/pnas.95.23.13783

Robinson JT, Thorvaldsdóttir H, Wenger AM, Zehir A, Mesirov JP. 2017. Variant Review with the Integrative Genomics Viewer (IGV). *Cancer Res* **77**:e31. doi:10.1158/0008-5472.CAN-17-0337

Robinson JT, Thorvaldsdóttir H, Winckler W, Guttman M, Lander ES, Getz G, Mesirov JP. 2011. Integrative genomics viewer. *Nat Biotechnol* **29**:24–26. doi:10.1038/nbt.1754

Rockman M V. 2008. Reverse engineering the genotype-phenotype map with natural genetic variation. *Nature* **456**:738-744. doi:10.1038/nature07633

Rodríguez-Vargas S, Estruch F, Ranz-Gil F. 2002. Gene expression analysis of cold and freeze stress in Baker's yeast. *Appl Environ Microbiol* **68**:3024–3030. doi:10.1128/AEM.68.6.3024-3030.2002

Rodríguez ME, Pérez-Través L, Sangorrín MP, Barrio E, Querol A, Lopes CA. 2017. *Saccharomyces uvarum* is responsible for the traditional fermentation of apple chicha in Patagonia. *FEMS Yeast Res* **17**:109. doi:10.1093/femsyr/fow109

Ryland GL, Doyle MA, Goode D, Boyle SE, Choong DYH, Rowley SM, Li J, Bowtell DD, Tothill RW, Campbell IG, Gorringer KL. 2015. Loss of heterozygosity: What is it good for? *BMC Med Genomics* **8**. doi:10.1186/s12920-015-0123-z

Sahara T, Goda T, Ohgiya S. 2002. Comprehensive expression analysis of time-dependent genetic responses in yeast cells to low temperature. *J Biol Chem* **277**:50015–50021. doi:10.1074/jbc.M209258200

Saito T, Ichitani K, Suzuki T, Marubashi W, Kuboyama T. 2007. Developmental observation and high temperature rescue from hybrid weakness in a cross between Japanese rice cultivars and Peruvian rice cultivar “Jamaica.” *Breed Sci* **57**:281–288.

doi:10.1270/jsbbs.57.281

- Salazar AN, Gorter De Vries AR, Van Den Broek M, Brouwers N, De La Torre Cortès P, Kuijpers NGA, Daran JMG, Abeel T. 2019. Chromosome level assembly and comparative genome analysis confirm lager-brewing yeasts originated from a single hybridization. *BMC Genomics* **20**. doi:10.1186/s12864-019-6263-3
- Salzburger W, Baric S, Sturmbauer C. 2002. Speciation via introgressive hybridization in East African cichlids? *Mol Ecol* **11**:619–625. doi:10.1046/j.0962-1083.2001.01438.x
- Samyn DR, Ruiz-Pávon L, Andersson MR, Popova Y, Thevelein JM, Persson BL. 2012. Mutational analysis of putative phosphate- and proton-binding sites in the *Saccharomyces cerevisiae* Pho84 phosphate:H⁺ transceptor and its effect on signalling to the PKA and PHO pathways. *Biochem J* **445**:413–422. doi:10.1042/BJ20112086
- Samyn DR, Van Der Veken J, Van Zeebroeck G, Persson BL, Karlsson BCG. 2016. Key residues and phosphate release routes in the *Saccharomyces cerevisiae* Pho84 transceptor: The role of TYR179 in functional regulation. *J Biol Chem* **291**:26388–26398. doi:10.1074/jbc.M116.738112
- Sanchez MR, Miller AW, Liachko I, Sunshine AB, Lynch B, Huang M, Alcantara E, DeSevo CG, Pai DA, Tucker CM, Hoang ML, Dunham MJ. 2017. Differential paralog divergence modulates genome evolution across yeast species. *PLoS Genet* **13**. doi:10.1371/journal.pgen.1006585
- Sankararaman S, Mallick S, Dannemann M, Prüfer K, Kelso J, Pääbo S, Patterson N, Reich D. 2014. The genomic landscape of Neanderthal ancestry in present-day humans. *Nature* **507**:354–357. doi:10.1038/nature12961
- Sato M, Watari J, Shinotsuka K. 2001. Genetic Instability in Flocculation of Bottom-Fermenting

- Yeast. *J Am Soc Brew Chem* **59**:130–134. doi:10.1094/ASBCJ-59-0130
- Scannell DR, Zill OA, Rokas A, Payen C, Dunham MJ, Eisen MB, Rine J, Johnston M, Hittinger CT. 2011. The awesome power of yeast evolutionary genetics: New genome sequences and strain resources for the *Saccharomyces sensu stricto* genus. *G3 Genes, Genomes, Genetics* **1**:11–25. doi:10.1534/g3.111.000273
- Schlenk F. 1985. Early research on fermentation - a story of missed opportunities. *Trends Biochem Sci* **10**:252–254. doi:10.1016/0968-0004(85)90145-8
- Schnable JC, Springer NM, Freeling M. 2011. Differentiation of the maize subgenomes by genome dominance and both ancient and ongoing gene loss. *Proc Natl Acad Sci U S A* **108**:4069–4074. doi:10.1073/pnas.1101368108
- Schrader L, Schmitz J. 2019. The impact of transposable elements in adaptive evolution. *Mol Ecol* **28**:1537–1549. doi:10.1111/mec.14794
- Schröder MS, Martinez de San Vicente K, Prandini THR, Hammel S, Higgins DG, Bagagli E, Wolfe KH, Butler G. 2016. Multiple Origins of the Pathogenic Yeast *Candida orthopsilosis* by Separate Hybridizations between Two Parental Species. *PLoS Genet* **12**. doi:10.1371/journal.pgen.1006404
- Schumer M, Xu C, Powell DL, Durvasula A, Skov L, Holland C, Blazier JC, Sankararaman S, Andolfatto P, Rosenthal GG, Przeworski M. 2018. Natural selection interacts with recombination to shape the evolution of hybrid genomes. *Science* **360**:656–660. doi:10.1126/science.aar3684
- Schwarz D, Matta BM, Shakir-Botteri NL, McPherson BA. 2005. Host shift to an invasive plant triggers rapid animal hybrid speciation. *Nature* **436**:546–549. doi:10.1038/nature03800
- Secco D, Wang C, Shou H, Whelan J. 2012. Phosphate homeostasis in the yeast *Saccharomyces*

- cerevisiae*, the key role of the SPX domain-containing proteins. *FEBS Lett.*
doi:10.1016/j.febslet.2012.01.036
- Seehausen O. 2004. Hybridization and adaptive radiation. *Trends Ecol Evol.*
doi:10.1016/j.tree.2004.01.003
- Selmecki AM, Maruvka YE, Richmond PA, Guillet M, Shoresh N, Sorenson AL, De S, Kishony R, Michor F, Dowell R, Pellman D. 2015. Polyploidy can drive rapid adaptation in yeast. *Nature* **519**:349–351. doi:10.1038/nature14187
- Shampay J, Szostak JW, Blackburn EH. 1984. DNA sequences of telomeres maintained in yeast. *Nature* **310**:154–157. doi:10.1038/310154a0
- Shii CT, Mok MC, Temple SR, Mok DWS. 1980. Expression of developmental abnormalities in hybrids of *Phaseolus vulgaris* L.: Interaction between temperature and allelic dosage. *J Hered* **71**:218–222. doi:10.1093/oxfordjournals.jhered.a109353
- Siew LT, Daran-Lapujade P, Walsh MC, Pronk JT, Daran JM. 2007. Acclimation of *Saccharomyces cerevisiae* to low temperature: A chemostat-based transcriptome analysis. *Mol Biol Cell* **18**:5100–5112. doi:10.1091/mbc.E07-02-0131
- Singer MA, Lindquist S. 1998. Thermotolerance in *Saccharomyces cerevisiae*: The Yin and Yang of trehalose. *Trends Biotechnol.* doi:10.1016/S0167-7799(98)01251-7
- Smart KA, Whisker SW. 1996. Effect of Serial Repitching on the Fermentation Properties and Condition of Brewing Yeast. *J Am Soc Brew Chem* **54**:41–44. doi:10.1094/ASBCJ-54-0041
- Smukowski Heil C, Burton JN, Liachko I, Friedrich A, Hanson NA, Morris CL, Schacherer J, Shendure J, Thomas JH, Dunham MJ. 2018. Identification of a novel interspecific hybrid yeast from a metagenomic spontaneously inoculated beer sample using Hi-C. *Yeast* **35**:71–84. doi:10.1002/yea.3280

- Smukowski Heil CS, DeSevo CG, Pai DA, Tucker CM, Hoang ML, Dunham MJ. 2017. Loss of Heterozygosity Drives Adaptation in Hybrid Yeast. *Mol Biol Evol* **34**:1596–1612.
doi:10.1093/molbev/msx098
- Smukowski Heil CS, Large CRL, Patterson K, Hickey ASM, Yeh CLC, Dunham MJ. 2019. Temperature preference can bias parental genome retention during hybrid evolution. *PLoS Genet* **15**:e1008383. doi:10.1371/journal.pgen.1008383
- Soltis DE, Visger CJ, Soltis PS. 2014. The polyploidy revolution then...and now: Stebbins revisited. *Am J Bot* **101**:1057–1078. doi:10.3732/ajb.1400178
- Song Y, Endepols S, Klemann N, Richter D, Matuschka FR, Shih CH, Nachman MW, Kohn MH. 2011. Adaptive introgression of anticoagulant rodent poison resistance by hybridization between old world mice. *Curr Biol* **21**:1296–1301.
doi:10.1016/j.cub.2011.06.043
- Steensels J, Meersman E, Snoek T, Saels V, Verstrepen KJ. 2014a. Large-scale selection and breeding to generate industrial yeasts with superior aroma production. *Appl Environ Microbiol* **80**:6965–6975. doi:10.1128/AEM.02235-14
- Steensels J, Snoek T, Meersman E, Nicolino MP, Voordeckers K, Verstrepen KJ. 2014b. Improving industrial yeast strains: Exploiting natural and artificial diversity. *FEMS Microbiol Rev* **38**:947–995. doi:10.1111/1574-6976.12073
- Steenwyk J, Rokas A. 2017. Extensive Copy Number Variation in Fermentation-Related Genes Among *Saccharomyces cerevisiae* Wine Strains. *G3 Genes, Genomes, Genetics* **7**:1475–1485. doi:10.1534/G3.117.040105
- Storchova Z. 2014. Ploidy changes and genome stability in yeast. *Yeast* **31**:421–430.
doi:10.1002/yea.3037

- Strope PK, Skelly DA, Kozmin SG, Mahadevan G, Stone EA, Magwene PM, Dietrich FS, McCusker JH. 2015. The 100-genomes strains, an *S. cerevisiae* resource that illuminates its natural phenotypic and genotypic variation and emergence as an opportunistic pathogen. *Genome Res* **25**:762–74. doi:10.1101/gr.185538.114
- Stuart-Smith RD, Edgar GJ, Bates AE. 2017. Thermal limits to the geographic distributions of shallow-water marine species. *Nat Ecol Evol* **1**:1846–1852. doi:10.1038/s41559-017-0353-x
- Suarez-Gonzalez A, Lexer C, Cronk QCB. 2018. Adaptive introgression: A plant perspective. *Biol Lett* **14**. doi:10.1098/rsbl.2017.0688
- Sunshine AB, Payen C, Ong GT, Liachko I, Tan KM, Dunham MJ. 2015. The Fitness Consequences of Aneuploidy Are Driven by Condition-Dependent Gene Effects. *PLoS Biol* **13**. doi:10.1371/journal.pbio.1002155
- Takeshige K, Baba M, Tsuboi S, Noda T, Ohsumi Y. 1992. Autophagy in yeast demonstrated with proteinase-deficient mutants and conditions for its induction. *J Cell Biol* **119**:301–312. doi:10.1083/jcb.119.2.301
- Thomas K, Ironside K, Clark L, Bingle L. 2021. Preliminary microbiological and chemical analysis of two historical stock ales from Victorian and Edwardian brewing. *J Inst Brew* **127**:167–175. doi:10.1002/jib.641
- Thorne RSW. 1968. Some Observations on Yeast Mutation During Continuous Fermentation. *J Inst Brew* **74**:516–524. doi:10.1002/j.2050-0416.1968.tb03167.x
- Usher J, Bond U. 2009. Recombination between homoeologous chromosomes of lager yeasts leads to loss of function of the hybrid *GPH1* gene. *Appl Environ Microbiol* **75**:4573–4579. doi:10.1128/AEM.00351-09
- van den Broek M, Bolat I, Nijkamp JF, Ramos E, Luttk MAH, Koopman F, Geertman JM, de

- Ridder D, Pronk JT, Daran J-M. 2015. Chromosomal Copy Number Variation in *Saccharomyces pastorianus* Is Evidence for Extensive Genome Dynamics in Industrial Lager Brewing Strains. *Appl Environ Microbiol* **81**:6253–67. doi:10.1128/AEM.01263-15
- Van Mulders SE, Ghequire M, Daenen L, Verbelen PJ, Verstrepen KJ, Delvaux FR. 2010. Flocculation gene variability in industrial brewer's yeast strains. *Appl Microbiol Biotechnol* **88**:1321–1331. doi:10.1007/s00253-010-2843-5
- Van Wyk N, Grossmann M, Wendland J, Von Wallbrunn C, Pretorius IS. 2019. The Whiff of Wine Yeast Innovation: Strategies for Enhancing Aroma Production by Yeast during Wine Fermentation. *J Agric Food Chem*. doi:10.1021/acs.jafc.9b06191
- Verbelen PJ, Dekoninck TML, Saerens SMG, Van Mulders SE, Thevelein JM, Delvaux FR. 2009. Impact of pitching rate on yeast fermentation performance and beer flavour. *Appl Microbiol Biotechnol* **82**:155–167. doi:10.1007/s00253-008-1779-5
- Verstrepen KJ, Derdelinckx G, Verachtert H, Delvaux FR. 2003. Yeast flocculation: what brewers should know. *Appl Microbiol Biotechnol* **61**:197–205. doi:10.1007/S00253-002-1200-8
- Vicent I, Navarro A, Mulet JM, Sharma S, Serrano R. 2015. Uptake of inorganic phosphate is a limiting factor for *Saccharomyces cerevisiae* during growth at low temperatures. *FEMS Yeast Res* **15**:1–13. doi:10.1093/femsyr/fov008
- Walther A, Hesselbart A, Wendland J. 2014. Genome sequence of *Saccharomyces carlsbergensis*, the world's first pure culture lager yeast. *G3 Genes, Genomes, Genetics* **4**:783–793. doi:10.1534/g3.113.010090
- Wang J, Tian L, Lee HS, Wei NE, Jiang H, Watson B, Madlung A, Osborn TC, Doerge RW, Comai L, Chen ZJ. 2006. Genomewide nonadditive gene regulation in *Arabidopsis*

- allotetraploids. *Genetics* **172**:507–517. doi:10.1534/genetics.105.047894
- Weiss C V., Roop JI, Hackley RK, Chuong JN, Grigoriev I V., Arkin AP, Skerker JM, Brem RB. 2018. Genetic dissection of interspecific differences in yeast thermotolerance. *Nat Genet.* doi:10.1038/s41588-018-0243-4
- Wendland J. 2014. Lager yeast comes of age. *Eukaryot Cell* **13**:1256–1265. doi:10.1128/EC.00134-14
- Will JL, Kim HS, Clarke J, Painter JC, Fay JC, Gasch AP. 2010. Incipient balancing selection through adaptive loss of aquaporins in natural *Saccharomyces cerevisiae* populations. *PLoS Genet* **6**. doi:10.1371/journal.pgen.1000893
- Wilm A, Aw PPK, Bertrand D, Yeo GHT, Ong SH, Wong CH, Khor CC, Petric R, Hibberd ML, Nagarajan N. 2012. LoFreq: A sequence-quality aware, ultra-sensitive variant caller for uncovering cell-population heterogeneity from high-throughput sequencing datasets. *Nucleic Acids Res* **40**:11189–11201. doi:10.1093/nar/gks918
- Wolfe KH. 2015. Origin of the yeast whole-genome duplication. *PLoS Biol* **13**. doi:10.1371/journal.pbio.1002221
- Zhang Z, Bendixsen DP, Janzen T, Nolte AW, Greig D, Stelkens R. 2020. Recombining Your Way out of Trouble: The Genetic Architecture of Hybrid Fitness under Environmental Stress. *Mol Biol Evol* **37**:167–182. doi:10.1093/molbev/msz211
- Ziv N, Brandt NJ, Gresham D. 2013. The use of chemostats in microbial systems biology. *J Vis Exp.* doi:10.3791/50168

APPENDIX A: Supplementary materials for Chapter 2

Table A.1. All mutations observed during the chemostat evolution experiments

Sample	Chr	Position	Type	Effect	ORF	Gene	Mutation
G1	chrV	520259	SNP/INDEL	nonsynonymous	YER167W	BCK2	G682*
G1	chrX	235587	SNP/INDEL	nonsynonymous	YJL101C	GSH1	S257F
G10	chrIX	69868	SNP/INDEL	nonsynonymous	YIL147C	SLN1	P1196T
G10	chrV	520259	SNP/INDEL	nonsynonymous	YER167W	BCK2	G682*
G10	chrX	236338	SNP/INDEL	nonsynonymous	YJL101C	GSH1	G7S
G10	chrXIII	218547	SNP/INDEL	nonsynonymous	YML029W	USA1	R396indel
G10	chrXV	411326	SNP/INDEL	nonsynonymous	YOR043W	WHI2	E153*
G11	chrII	330958	SNP/INDEL	nonsynonymous	YBR046C	ZTA1	K185R
G11	chrVIII	116838	SNP/INDEL	intergenic	NA	NA	NA
G11	chrX	234549	SNP/INDEL	nonsynonymous	YJL101C	GSH1	A603E
G12	chrM	20663	SNP/INDEL	synonymous	Q0065	AI4	L133L
G12	chrM	20663	SNP/INDEL	synonymous	Q0070	AI5_ALPHA	L133L
G12	chrM	20663	SNP/INDEL	synonymous	Q0045	COX1	L133L
G12	chrXV	411594	SNP/INDEL	nonsynonymous	YOR043W	WHI2	S242*
G13	chrIV	836608	SNP/INDEL	nonsynonymous	YDR188W	CCT6	L63R
G13	chrIV	836608	SNP/INDEL	nonsynonymous	YDR187C	YDR187C	S47R
G14	chrIX	342202	SNP/INDEL	intergenic	NA	NA	NA
G14	chrXII	863973	SNP/INDEL	nonsynonymous	YLR371W	ROM2	L420F
G14	chrXV	412193	SNP/INDEL	nonsynonymous	YOR043W	WHI2	E442*
G15	chrIX	84074	SNP/INDEL	nonsynonymous	YIL142W	CCT2	L258W
G15	chrXII	164066	Ty	Upstream	YLR007W	NSE1	
G15	chrXII	164066	Ty	Upstream	YLR006C	SSK1	
G16	chrV	520259	SNP/INDEL	nonsynonymous	YER167W	BCK2	G682*
G16	chrXIII	302619	Ty	Upstream	YMR015C	ERG5	
G16	chrXIII	302619	Ty	Downstream	YMR016C	SOK2	
G17	chrIII	190027	SNP/INDEL	nonsynonymous	YCR033W	SNT1	L1180*
G17	chrIX	84075	SNP/INDEL	nonsynonymous	YIL142W	CCT2	L258F
G17	chrV	335088	SNP/INDEL	nonsynonymous	YER088C	DOT6	S34*
G17	chrVII	989653	SNP/INDEL	intergenic	NA	NA	NA
G17	chrVII	1035088	SNP/INDEL	nonsynonymous	YGR271W	SLH1	F1100V
G17	chrVIII	246342	SNP/INDEL	synonymous	YHR074W	QNS1	G50G
G17	chrX	235255	SNP/INDEL	nonsynonymous	YJL101C	GSH1	F368I
G17	chrX	236506	Ty	Upstream	YJL101C	GSH1	

G17	chrX	236506	Ty	Upstream	YJL100W	LSB6	
G17	chrXII	898374	SNP/INDEL	five_prime_UTR_intron	YLR388W	NA	NA
G17	chrXIII	889769	SNP/INDEL	nonsynonymous	YMR308C	PSE1	E818G
G17	chrXIV	413774	SNP/INDEL	nonsynonymous	YNL112W	DBP2	F46I
G17	chrXV	1013449	SNP/INDEL	nonsynonymous	YOR360C	PDE2	S458*
G18	chrIX	132917	SNP/INDEL	nonsynonymous	YIL121W	QDR2	G225E
G18	chrV	479831	SNP/INDEL	nonsynonymous	YER155C	BEM2	Y1006*
G18	chrV	479940	SNP/INDEL	nonsynonymous	YER155C	BEM2	S970*
G18	chrVII	795136	Ty	Upstream	YGR153W	None	
G18	chrVII	795136	Ty	Downstream	tA(UGC)G	None	
G18	chrVII	795136	Ty	Inside	YGR152C	RSR1	
G18	chrVIII	513052	SNP/INDEL	synonymous	YHR206W	SKN7	T107T
G18	chrX	236005	SNP/INDEL	nonsynonymous	YJL101C	GSH1	V118F
G18	chrXII	676499	SNP/INDEL	nonsynonymous	YLR266C	PDR8	H409R
G18	chrXV	642294	SNP/INDEL	intergenic	NA	NA	NA
G19	chrV	480767	SNP/INDEL	nonsynonymous	YER155C	BEM2	W694*
G19	chrVII	103191	SNP/INDEL	nonsynonymous	YGL206C	CHC1	I1438M
G19	chrX	235587	SNP/INDEL	nonsynonymous	YJL101C	GSH1	S257F
G19	chrXI	47013	Ty	Upstream	YKL208W	CBT1	
G19	chrXI	47013	Ty	Upstream	YKL209C	STE6	
G19	chrXI	47013	Ty	Upstream	t(CGU)K	TRT2	
G19	chrXI	618062	SNP/INDEL	synonymous	YKR094C	RPL40b	A107A
G19	chrXII	406479	SNP/INDEL	nonsynonymous	YLR131C	ACE2	S115indel
G19	chrXII	489897	SNP/INDEL	nonsynonymous	YLR162W	YLR162W	P109indel
G19	chrXII	489911	SNP/INDEL	nonsynonymous	YLR162W	YLR162W	R113indel
G19	chrXIII	244303	SNP/INDEL	nonsynonymous	YML013W	UBX2	A52E
G2	chrM	34945	SNP/INDEL	intergenic	NA	NA	NA
G2	chrV	195642	SNP/INDEL	nonsynonymous	YER020W	GPA2	Y159D
G2	chrX	236492	Ty	Upstream	YJL101C	GSH1	
G2	chrX	236492	Ty	Upstream	YJL100W	LSB6	
G2	chrXVI	219885	SNP/INDEL	nonsynonymous	YPL175W	SPT14	D386Y
G20	chrII	807169	Ty	Downstream	YBR299W	MAL32	
G20	chrIV	617412	SNP/INDEL	intergenic	NA	NA	NA
G20	chrX	235571	SNP/INDEL	nonsynonymous	YJL101C	GSH1	M262I
G20	chrXII	406838	SNP/INDEL	5'-upstream	YLR131C	ACE2	NA
G21	chrI	203245	Ty	Upstream	YAR050W	FLO1	
G21	chrII	524665	SNP/INDEL	nonsynonymous	YBR140C	IRA1	L655W
G21	chrIV	568755	Ty	Upstream	tD(GUC)D	None	
G21	chrIV	568755	Ty	Upstream	tR(UCU)D	None	

G21	chrIV	568755	Ty	Upstream	YDR058C	TGL2	
G21	chrIV	568755	Ty	Downstream	YDR059C	UBC5	
G21	chrIV	1433679	SNP/INDEL	nonsynonymous	YDR490C	PKH1	A197E
G21	chrM	34945	SNP/INDEL	intergenic	NA	NA	NA
G21	chrXVI	100747	SNP/INDEL	synonymous	YPL237W	SUI3	K84K
G21	chrXVI	100747	SNP/INDEL	synonymous	YPL238C	YPL238C	F39F
G22	chrV	480741	SNP/INDEL	nonsynonymous	YER155C	BEM2	S703*
G22	chrX	235723	SNP/INDEL	nonsynonymous	YJL101C	GSH1	V212F
G22	chrX	577865	SNP/INDEL	nonsynonymous	YJR077C	MIR1	T109S
G22	chrXII	406111	SNP/INDEL	nonsynonymous	YLR131C	ACE2	Q238*
G22	chrXIII	192633	Ty	Upstream	YML042W	CAT2	
G22	chrXIII	192633	Ty	Upstream	YML043C	RRN11	
G22	chrXIII	740362	SNP/INDEL	nonsynonymous	YMR234W	RNH1	G33C
G22	chrXV	282045	Ty	Downstream	YOL021C	DIS3	
G22	chrXV	282045	Ty	Upstream	tG(GCC)O2	SUF17	
G22	chrXV	282045	Ty	Upstream	YOL022C	TSR4	
G22	chrXV	412237	Ty	Upstream	YOR044W	IRC23	
G22	chrXV	412237	Ty	Inside	YOR043W	WHI2	
G22	chrXVI	775856	SNP/INDEL	intergenic	NA	NA	NA
G23	chrI	180855	Ty	Upstream	tL(CAA)A	SUP56	
G23	chrII	692619	SNP/INDEL	nonsynonymous	YBR237W	PRP5	N217K
G23	chrIX	248401	Ty	Upstream	YIL057C	RGI2	
G23	chrIX	248401	Ty	Upstream	tS(UGA)I	SUP17	
G23	chrV	418254	SNP/INDEL	nonsynonymous	YER129W	SAK1	T325M
G23	chrV	476603	SNP/INDEL	nonsynonymous	YER155C	BEM2	Y2082*
G23	chrVI	210849	Ty	Upstream	YFR028C	CDC14	
G23	chrVI	210849	Ty	Upstream	YFR029W	PTR3	
G23	chrVI	210849	Ty	Upstream	tY(GUA)F2	SUP6	
G23	chrXI	50235	SNP/INDEL	nonsynonymous	YKL205W	LOS1	T62I
G23	chrXII	406820	SNP/INDEL	nonsynonymous	YLR131C	ACE2	M1I
G23	chrXVI	744093	Ty	Upstream	YPR109W	GLD1	
G23	chrXVI	744093	Ty	Upstream	tT(UGU)P	None	
G23	chrXVI	744093	Ty	Upstream	YPR108W-A	None	
G23	chrXVI	744093	Ty	Downstream	YPR108W	RPN7	
G24	chrV	480262	SNP/INDEL	nonsynonymous	YER155C	BEM2	Q863*
G24	chrXII	288034	Ty	Inside	YLR080W	EMP46	
G24	chrXII	288034	Ty	Downstream	YLR079W	SIC1	
G24	chrXIV	291012	SNP/INDEL	nonsynonymous	YNL186W	UBP10	S505R
G24	chrXV	411401	SNP/INDEL	nonsynonymous	YOR043W	WHI2	E178*

G25	chrI	203094	Ty	Upstream	YAR050W	FLO1	
G25	chrIX	70005	SNP/INDEL	nonsynonymous	YIL147C	SLN1	V1150G
G25	chrV	195642	SNP/INDEL	nonsynonymous	YER020W	GPA2	Y159D
G25	chrX	556731	SNP/INDEL	nonsynonymous	YJR064W	CCT5	T273M
G25	chrXVI	219885	SNP/INDEL	nonsynonymous	YPL175W	SPT14	D386Y
G26	chrI	39261	SNP/INDEL	nonsynonymous	YAL056W	GPB2	M1I
G26	chrI	180967	Ty	Upstream	tI(CAA)A	SUP56	
G26	chrI	202951	Ty	Upstream	YAR050W	FLO1	
G26	chrIV	1458624	SNP/INDEL	nonsynonymous	YDR505C	PSP1	S199R
G26	chrIX	71790	SNP/INDEL	nonsynonymous	YIL147C	SLN1	A555V
G26	chrIX	372266	Ty	Inside	YIR007W	EGH1	
G26	chrIX	372266	Ty	Downstream	YIR008C	PRI1	
G26	chrVI	226854	Ty	Upstream	YFR036W	CDC26	
G26	chrVI	226854	Ty	Upstream	YFR035C	None	
G26	chrVI	226854	Ty	Upstream	tK(CUU)F	None	
G26	chrVI	226854	Ty	Upstream	YFR034C	PHO4	
G26	chrVI	226854	Ty	Downstream	YFR037C	RSC8	
G26	chrVIII	300573	SNP/INDEL	nonsynonymous	YHR098C	SFB3	R454S
G26	chrX	235519	SNP/INDEL	nonsynonymous	YJL101C	GSH1	R280G
G26	chrXII	372615	SNP/INDEL	nonsynonymous	YLR113W	HOG1	W332*
G26	chrXII	675074	SNP/INDEL	nonsynonymous	YLR265C	NEJ1	D128N
G26	chrXVI	491553	Ty	Downstream	YPL031C	PHO85	
G26	chrXVI	491553	Ty	Upstream	YPL032C	SVL3	
G27	chrI	203250	Ty	Upstream	YAR050W	FLO1	
G27	chrIX	31275	SNP/INDEL	nonsynonymous	YIL166C	YIL166C	S431C
G27	chrVII	730992	Ty	Upstream	YGR120C	COG2	
G27	chrVII	730992	Ty	Downstream	YGR121C	MEP1	
G27	chrVII	730992	Ty	Upstream	tN(GUU)G	None	
G27	chrXII	405786	SNP/INDEL	nonsynonymous	YLR131C	ACE2	Y346indel
G27	chrXII	605174	Ty	Downstream	YLR231C	BNA5	
G27	chrXII	605174	Ty	Upstream	YLR229C	CDC42	
G27	chrXII	605174	Ty	Downstream	tI(UAU)L	None	
G27	chrXIV	201917	SNP/INDEL	nonsynonymous	YNL239W	LAP3	G450V
G27	chrXIV	682813	SNP/INDEL	nonsynonymous	YNR031C	SSK2	S874*
G27	chrXV	170924	Ty	Downstream	YOL082W	ATG19	
G27	chrXV	170924	Ty	Upstream	YOL081W	IRA2	
G27	chrXV	411452	SNP/INDEL	nonsynonymous	YOR043W	WHI2	R195*
G27	chrXV	411557	SNP/INDEL	nonsynonymous	YOR043W	WHI2	Q230indel
G27	chrXV	411563	SNP/INDEL	nonsynonymous	YOR043W	WHI2	Q232K

G27	chrXV	1036390	SNP/INDEL	nonsynonymous	YOR372C	NDD1	N28indel
G28	chrI	202932	Ty	Upstream	YAR050W	FLO1	
G29	chrI	41731	SNP/INDEL	nonsynonymous	YAL056W	GPB2	E825*
G29	chrV	479338	SNP/INDEL	nonsynonymous	YER155C	BEM2	A1171indel
G29	chrV	481111	SNP/INDEL	nonsynonymous	YER155C	BEM2	E580*
G29	chrV	557749	SNP/INDEL	nonsynonymous	YER184C	TOG1	F311S
G29	chrVI	167559	Ty	Upstream	YFR012W	DCV1	
G29	chrVI	167559	Ty	Upstream	YFR011C	MIC19	
G29	chrVI	167559	Ty	Downstream	tY(GUA)F1	SUP11	
G29	chrVI	167559	Ty	Downstream	YFR010W	UBP6	
G29	chrX	234451	SNP/INDEL	nonsynonymous	YJL101C	GSH1	Y636D
G29	chrXII	404817	SNP/INDEL	nonsynonymous	YLR131C	ACE2	R669indel
G29	chrXII	706384	SNP/INDEL	nonsynonymous	YLR284C	ECI1	E219D
G3	chrM	85596	SNP/INDEL	nonsynonymous	Q0297	Q0297	A15indel
G31	chrX	234356	Ty	Inside	YJL101C	GSH1	
G31	chrX	234356	Ty	Downstream	YJL102W	MEF2	
G31	chrX	234356	Ty	Downstream	tR(ACG)J	None	
G31	chrX	235539	SNP/INDEL	nonsynonymous	YJL101C	GSH1	A273E
G31	chrX	236005	SNP/INDEL	nonsynonymous	YJL101C	GSH1	V118F
G31	chrXII	62340	SNP/INDEL	nonsynonymous	YLL040C	VPS13	S436A
G31	chrXV	1036451	SNP/INDEL	nonsynonymous	YOR372C	NDD1	Y7*
G31	chrXVI	105441	SNP/INDEL	5'-upstream	YPL234C	VMA11	NA
G32	chrI	203003	Ty	Upstream	YAR050W	FLO1	
G32	chrM	85596	SNP/INDEL	nonsynonymous	Q0297	Q0297	A15indel
G32	chrX	228863	SNP/INDEL	ARS	ARS1009	NA	NA
G32	chrXIV	684135	SNP/INDEL	nonsynonymous	YNR031C	SSK2	W433*
G4	chrI	203250	Ty	Upstream	YAR050W	FLO1	
G4	chrIV	1014796	SNP/INDEL	nonsynonymous	YDR277C	MTH1	E303*
G4	chrIX	69868	SNP/INDEL	nonsynonymous	YIL147C	SLN1	P1196T
G5	chrI	106877	SNP/INDEL	nonsynonymous	YAL023C	PMT2	M559L
G5	chrX	235994	SNP/INDEL	nonsynonymous	YJL101C	GSH1	N121K
G5	chrXIII	301642	SNP/INDEL	nonsynonymous	YMR015C	ERG5	A282P
G5	chrXIV	281414	Ty	Inside	YNL191W	DUG3	
G5	chrXIV	281414	Ty	Upstream	YNL190W	None	
G6	chrIV	630265	SNP/INDEL	nonsynonymous	YDR092W	UBC13	G41D
G6	chrVI	71985	SNP/INDEL	nonsynonymous	YFL033C	RIM15	L815indel
G7	chrV	517729	SNP/INDEL	intergenic	NA	NA	NA
G7	chrVI	256035	SNP/INDEL	intergenic	NA	NA	NA
G7	chrX	194443	SNP/INDEL	nonsynonymous	YJL116C	NCA3	D144A

G7	chrXIII	557091	SNP/INDEL	intergenic	NA	NA	NA
G7	chrXIV	710260	SNP/INDEL	nonsynonymous	YNR047W	FPK1	E580Q
G7	chrXVI	315823	SNP/INDEL	synonymous	YPL125W	KAP120	I812I
G8	chrI	131089	SNP/INDEL	synonymous	YAL012W	CYS3	A97A
G8	chrII	90872	SNP/INDEL	nonsynonymous	YBL069W	AST1	H44Q
G8	chrII	90872	SNP/INDEL	synonymous	YBL070C	YBL070C	T18T
G8	chrII	259459	SNP/INDEL	synonymous	YBR012C	YBR012C	A36A
G8	chrII	288489	SNP/INDEL	intergenic	NA	NA	NA
G8	chrII	630993	SNP/INDEL	nonsynonymous	YBR203W	COS111	I609T
G8	chrII	664345	SNP/INDEL	synonymous	YBR220C	YBR220C	G111G
G8	chrII	687343	SNP/INDEL	nonsynonymous	YBR235W	VHC1	L148P
G8	chrVII	144793	SNP/INDEL	5'-upstream	YGL191W	COX13	NA
G8	chrVIII	289326	SNP/INDEL	nonsynonymous	YHR093W	AHT1	K62T
G8	chrXI	137514	SNP/INDEL	intergenic	NA	NA	NA
G8	chrXII	695580	SNP/INDEL	synonymous	YLR276C	DBP9	G417G
G8	chrXIV	258371	SNP/INDEL	nonsynonymous	YNL205C	YNL205C	H69Q
G8	chrXIV	322133	SNP/INDEL	ARS	ARS1415	NA	NA
G8	chrXV	88058	SNP/INDEL	nonsynonymous	YOL123W	HRP1	T72R
G8	chrXV	148622	SNP/INDEL	nonsynonymous	YOL090W	MSH2	D414A
G8	chrXV	412193	SNP/INDEL	nonsynonymous	YOR043W	WHI2	E442*
G9	chrM	66892	SNP/INDEL	intergenic	NA	NA	NA
G9	chrM	81992	SNP/INDEL	intergenic	NA	NA	NA
G9	chrXII	1020334	Ty	Inside	YLR442C	SIR3	
P1	chrIV	1159597	SNP/INDEL	intergenic	NA	NA	NA
P1	chrV	506640	SNP/INDEL	nonsynonymous	YER164W	CHD1	W417indel
P1	chrX	204071	SNP/INDEL	ARS	ARS1008	NA	NA
P1	chrXIII	25025	SNP/INDEL	nonsynonymous	YML123C	PHO84	L259P
P1	chrXIV	149883	SNP/INDEL	nonsynonymous	YNL262W	POL2	V558L
P10	chrVI	24499	SNP/INDEL	nonsynonymous	YFL053W	DAK2	K359N
P10	chrVII	625324	SNP/INDEL	nonsynonymous	YGR068C	ART5	*587C
P10	chrX	264748	SNP/INDEL	nonsynonymous	YJL090C	DPB11	E102K
P10	chrX	544126	SNP/INDEL	nonsynonymous	YJR057W	CDC8	C22F
P10	chrXIII	25025	SNP/INDEL	nonsynonymous	YML123C	PHO84	L259P
P10	chrXIV	556263	SNP/INDEL	nonsynonymous	YNL039W	BDP1	Y406D
P10	chrXV	442477	SNP/INDEL	nonsynonymous	YOR061W	CKA2	L315*
P11	chrXIII	25025	SNP/INDEL	nonsynonymous	YML123C	PHO84	L259P
P12	chrVII	870194	SNP/INDEL	intergenic	NA	NA	NA
P12	chrXI	47292	Ty	Inside	YKL208W	CBT1	
P12	chrXI	47292	Ty	Upstream	YKL207W	EMC3	

P12	chrXI	47292	Ty	Upstream	YKL209C	STE6	
P12	chrXI	47292	Ty	Upstream	tT(CGU)K	TRT2	
P12	chrXII	1021221	SNP/INDEL	nonsynonymous	YLR442C	SIR3	S344*
P12	chrXIII	25025	SNP/INDEL	nonsynonymous	YML123C	PHO84	L259P
P13	chrIV	918933	SNP/INDEL	nonsynonymous	YDR227W	SIR4	E455*
P13	chrXIII	25025	SNP/INDEL	nonsynonymous	YML123C	PHO84	L259P
P13	chrXV	442315	SNP/INDEL	nonsynonymous	YOR061W	CKA2	G261V
P14	chrIX	342202	SNP/INDEL	intergenic	NA	NA	NA
P14	chrXI	642185	SNP/INDEL	nonsynonymous	YKR101W	SIR1	L549*
P14	chrXII	1019664	SNP/INDEL	nonsynonymous	YLR442C	SIR3	R863I
P14	chrXII	1022219	SNP/INDEL	nonsynonymous	YLR442C	SIR3	W11*
P14	chrXV	441777	SNP/INDEL	nonsynonymous	YOR061W	CKA2	K82*
P14	chrXV	442247	SNP/INDEL	nonsynonymous	YOR061W	CKA2	F238indel
P15	chrV	299655	SNP/INDEL	nonsynonymous	YER070W	RNR1	K236E
P15	chrVII	358707	SNP/INDEL	synonymous	YGL080W	MPC1	K24K
P15	chrXIII	25025	SNP/INDEL	nonsynonymous	YML123C	PHO84	L259P
P15	chrXVI	245969	SNP/INDEL	nonsynonymous	YPL161C	BEM4	I84M
P16	chrV	507356	SNP/INDEL	nonsynonymous	YER164W	CHD1	L655indel
P16	chrVI	166290	SNP/INDEL	nonsynonymous	YFR010W	UBP6	W408*
P16	chrXII	236668	SNP/INDEL	nonsynonymous	YLR045C	STU2	E346K
P17	chrVII	1073612	SNP/INDEL	intergenic	NA	NA	NA
P17	chrXI	165801	SNP/INDEL	nonsynonymous	YKL151C	NNR2	Y44D
P17	chrXIII	25025	SNP/INDEL	nonsynonymous	YML123C	PHO84	L259P
P17	chrXVI	339609	SNP/INDEL	intergenic	NA	NA	NA
P18	chrI	180841	Ty	Upstream	tL(CAA)A	SUP56	
P18	chrIII	127392	Ty	Upstream	YCR007C	None	
P18	chrIII	127392	Ty	Upstream	tN(GUU)C	None	
P18	chrIII	261235	Ty	Inside	YCR084C	TUP1	
P18	chrIV	432295	Ty	Upstream	YDL010W	GRX6	
P18	chrIV	432295	Ty	Downstream	YDL009C	None	
P18	chrIV	432295	Ty	Upstream	YDL012C	None	
P18	chrVII	74889	Ty	Upstream	tV(AAC)G3	None	
P18	chrX	424752	Ty	Upstream	YJL006C	CTK2	
P18	chrX	424752	Ty	Upstream	YJL005W	CYR1	
P18	chrX	424752	Ty	Upstream	tL(UAA)J	SUP51	
P18	chrXI	308428	Ty	Downstream	YKL069W	None	
P18	chrXI	308428	Ty	Upstream	tV(AAC)K1	None	
P18	chrXI	308428	Ty	Upstream	YKL068W-A	None	
P18	chrXII	1020964	SNP/INDEL	nonsynonymous	YLR442C	SIR3	E430*

P18	chrXV	441564	SNP/INDEL	nonsynonymous	YOR061W	CKA2	K11*
P18	chrXVI	743920	Ty	Upstream	YPR109W	GLD1	
P18	chrXVI	743920	Ty	Upstream	tT(UGU)P	None	
P18	chrXVI	743920	Ty	Upstream	YPR108W-A	None	
P18	chrXVI	743920	Ty	Downstream	YPR108W	RPN7	
P19	chrI	180941	Ty	Upstream	tL(CAA)A	SUP56	
P19	chrI	203221	Ty	Upstream	YAR050W	FLO1	
P19	chrI	203299	Ty	Upstream	YAR050W	FLO1	
P19	chrII	794199	SNP/INDEL	nonsynonymous	YBR295W	PCA1	E451K
P19	chrV	300207	SNP/INDEL	nonsynonymous	YER070W	RNR1	G420R
P19	chrXIII	25025	SNP/INDEL	nonsynonymous	YML123C	PHO84	L259P
P2	chrIV	1029648	SNP/INDEL	synonymous	YDR283C	GCN2	T134T
P2	chrV	507968	SNP/INDEL	nonsynonymous	YER164W	CHD1	E859indel
P2	chrVII	583100	SNP/INDEL	nonsynonymous	YGR044C	RME1	K265E
P2	chrXIII	25025	SNP/INDEL	nonsynonymous	YML123C	PHO84	L259P
P20	chrI	203249	Ty	Upstream	YAR050W	FLO1	
P20	chrM	74424	SNP/INDEL	nonsynonymous	Q0250	COX2	E223K
P20	chrM	74424	SNP/INDEL	5'-upstream	Q0255	Q0255	NA
P20	chrV	506319	SNP/INDEL	nonsynonymous	YER164W	CHD1	K310E
P20	chrV	506391	SNP/INDEL	nonsynonymous	YER164W	CHD1	Q334indel
P20	chrXIII	25025	SNP/INDEL	nonsynonymous	YML123C	PHO84	L259P
P20	chrXVI	747035	Ty	Upstream	YPR111W	DBF20	
P20	chrXVI	747035	Ty	Upstream	YPR110C	RPC40	
P21	chrVII	583069	SNP/INDEL	nonsynonymous	YGR044C	RME1	R275K
P21	chrXIII	25025	SNP/INDEL	nonsynonymous	YML123C	PHO84	L259P
P22	chrV	547112	SNP/INDEL	nonsynonymous	YER178W	PDA1	D99A
P22	chrX	54928	SNP/INDEL	nonsynonymous	YJL201W	ECM25	T184P
P22	chrXII	604531	SNP/INDEL	5'-upstream	YLR230W	YLR230W	NA
P22	chrXII	920148	SNP/INDEL	synonymous	YLR399C	BDF1	L483L
P22	chrXVI	819266	Ty	Downstream	YPR144C	NOC4	
P22	chrXVI	819266	Ty	Upstream	tI(AAU)P1	None	
P22	chrXVI	819266	Ty	Downstream	YPR143W	RRP15	
P23	chrI	180942	Ty	Upstream	tL(CAA)A	SUP56	
P23	chrVII	583193	SNP/INDEL	nonsynonymous	YGR044C	RME1	H234Y
P23	chrXI	159727	SNP/INDEL	nonsynonymous	YKL155C	RSM22	S539T
P23	chrXIV	60690	SNP/INDEL	nonsynonymous	YNL304W	YPT11	Q132K
P23	chrXIV	62724	SNP/INDEL	intron	YNL302C	NA	NA
P23	chrXV	441753	SNP/INDEL	nonsynonymous	YOR061W	CKA2	Q74*
P24	chrI	40819	SNP/INDEL	nonsynonymous	YAL056W	GPB2	D521Y

P24	chrII	548433	SNP/INDEL	nonsynonymous	YBR154C	RPB5	G193C
P24	chrX	233745	Ty	Downstream	YJL101C	GSH1	
P24	chrX	233745	Ty	Inside	YJL102W	MEF2	
P24	chrX	233745	Ty	Upstream	tR(ACG)J	None	
P24	chrXI	308604	Ty	Downstream	YKL069W	None	
P24	chrXI	308604	Ty	Upstream	tV(AAC)K1	None	
P24	chrXI	308604	Ty	Upstream	YKL068W-A	None	
P24	chrXIII	25025	SNP/INDEL	nonsynonymous	YML123C	PHO84	L259P
P24	chrXIV	492017	SNP/INDEL	synonymous	YNL071W	LAT1	S165S
P24	chrXV	1012026	SNP/INDEL	synonymous	YOR359W	VTS1	L280L
P25	chrI	203250	Ty	Upstream	YAR050W	FLO1	
P25	chrIV	564826	SNP/INDEL	nonsynonymous	YDR055W	PST1	G434S
P25	chrXIV	345147	SNP/INDEL	nonsynonymous	YNL154C	YCK2	H44Y
P25	chrXIV	757318	SNP/INDEL	synonymous	YNR067C	DSE4	V594V
P25	chrXV	442216	SNP/INDEL	nonsynonymous	YOR061W	CKA2	S228*
P26	chrI	203250	Ty	Upstream	YAR050W	FLO1	
P26	chrIV	378422	SNP/INDEL	nonsynonymous	YDL042C	SIR2	Y8*
P26	chrIV	378422	SNP/INDEL	synonymous	YDL041W	YDL041W	A107A
P26	chrV	299397	SNP/INDEL	nonsynonymous	YER070W	RNR1	T150P
P26	chrV	300466	SNP/INDEL	nonsynonymous	YER070W	RNR1	A506D
P26	chrXIII	25025	SNP/INDEL	nonsynonymous	YML123C	PHO84	L259P
P27	chrI	203249	Ty	Upstream	YAR050W	FLO1	
P27	chrX	367104	SNP/INDEL	synonymous	YJL041W	NSP1	G401G
P27	chrXI	87500	SNP/INDEL	nonsynonymous	YKL188C	PXA2	N429indel
P27	chrXIII	25025	SNP/INDEL	nonsynonymous	YML123C	PHO84	L259P
P27	chrXV	658660	SNP/INDEL	5'-upstream	YOR174W	MED4	NA
P27	chrXV	1060708	SNP/INDEL	synonymous	YOR383C	FIT3	H116H
P28	chrI	203120	Ty	Upstream	YAR050W	FLO1	
P28	chrIV	556537	SNP/INDEL	5'-upstream	YDR050C	TPI1	NA
P28	chrX	339908	SNP/INDEL	nonsynonymous	YJL051W	IRC8	D41A
P28	chrXII	604531	SNP/INDEL	5'-upstream	YLR230W	YLR230W	NA
P28	chrXV	71887	SNP/INDEL	synonymous	YOL132W	GAS4	P196P
P28	chrXVI	743920	Ty	Upstream	YPR109W	GLD1	
P28	chrXVI	743920	Ty	Upstream	tT(UGU)P	None	
P28	chrXVI	743920	Ty	Upstream	YPR108W-A	None	
P28	chrXVI	743920	Ty	Downstream	YPR108W	RPN7	
P29	chrVI	36890	SNP/INDEL	nonsynonymous	YFL049W	SWP82	V30L
P29	chrVII	583519	SNP/INDEL	nonsynonymous	YGR044C	RME1	Q125indel

P29	chrXI	641265	SNP/INDEL	nonsynonymous	YKR101W	SIR1	N242indel
P29	chrXIII	25024	SNP/INDEL	nonsynonymous	YML123C	PHO84	L259indel
P29	chrXV	441663	SNP/INDEL	nonsynonymous	YOR061W	CKA2	W44indel
P3	chrIV	255912	SNP/INDEL	synonymous	YDL114W	YDL114W	A103A
P3	chrVII	583105	SNP/INDEL	nonsynonymous	YGR044C	RME1	C263S
P3	chrVII	583303	SNP/INDEL	nonsynonymous	YGR044C	RME1	L197*
P3	chrXII	1022054	SNP/INDEL	nonsynonymous	YLR442C	SIR3	Y66*
P3	chrXIII	25025	SNP/INDEL	nonsynonymous	YML123C	PHO84	L259P
P30	chrV	507507	SNP/INDEL	nonsynonymous	YER164W	CHD1	R706*
P30	chrXIII	25025	SNP/INDEL	nonsynonymous	YML123C	PHO84	L259P
P30	chrXV	387806	SNP/INDEL	nonsynonymous	YOR030W	DFG16	E328*
P32	chrVII	583282	SNP/INDEL	nonsynonymous	YGR044C	RME1	R204T
P32	chrXIII	25025	SNP/INDEL	nonsynonymous	YML123C	PHO84	L259P
P32	chrXIII	136638	SNP/INDEL	nonsynonymous	YML069W	POB3	D380G
P32	chrXIII	702315	SNP/INDEL	nonsynonymous	YMR217W	GUA1	H176N
P4	chrVII	583036	SNP/INDEL	nonsynonymous	YGR044C	RME1	S286*
P4	chrXIII	25025	SNP/INDEL	nonsynonymous	YML123C	PHO84	L259P
P5	chrII	210769	SNP/INDEL	nonsynonymous	YBL008W	HIR1	V373F
P5	chrIV	209881	SNP/INDEL	synonymous	YDL140C	RPO21	V227V
P5	chrV	505587	SNP/INDEL	nonsynonymous	YER164W	CHD1	E66*
P5	chrVI	166068	Ty	Downstream	YFR011C	MIC19	
P5	chrVI	166068	Ty	Inside	YFR010W	UBP6	
P5	chrVII	583892	SNP/INDEL	nonsynonymous	YGR044C	RME1	M1L
P5	chrXIII	25025	SNP/INDEL	nonsynonymous	YML123C	PHO84	L259P
P5	chrXIII	348189	SNP/INDEL	nonsynonymous	YMR038C	CCS1	I24M
P6	chrVII	596693	SNP/INDEL	nonsynonymous	YGR054W	YGR054W	M1V
P6	chrVIII	172918	SNP/INDEL	nonsynonymous	YHR031C	RRM3	S18*
P6	chrXIII	25025	SNP/INDEL	nonsynonymous	YML123C	PHO84	L259P
P6	chrXVI	167009	SNP/INDEL	nonsynonymous	YPL203W	TPK2	G252C
P7	chrII	798080	SNP/INDEL	nonsynonymous	YBR296C	PHO89	S148*
P7	chrV	508903	SNP/INDEL	nonsynonymous	YER164W	CHD1	W1171*
P7	chrVII	368360	SNP/INDEL	intergenic	NA	NA	NA
P7	chrX	642520	SNP/INDEL	nonsynonymous	YJR117W	STE24	A172indel
P7	chrXII	1021104	SNP/INDEL	nonsynonymous	YLR442C	SIR3	S383*
P7	chrXIII	25025	SNP/INDEL	nonsynonymous	YML123C	PHO84	L259P
P7	chrXIII	685203	SNP/INDEL	nonsynonymous	YMR208W	ERG12	I246S
P8	chrI	18651	SNP/INDEL	intergenic	NA	NA	NA
P8	chrIV	920138	SNP/INDEL	nonsynonymous	YDR227W	SIR4	N856K
P8	chrIV	920313	SNP/INDEL	nonsynonymous	YDR227W	SIR4	Q915*

P8	chrXII	1020295	SNP/INDEL	nonsynonymous	YLR442C	SIR3	V653F
P8	chrXIII	25025	SNP/INDEL	nonsynonymous	YML123C	PHO84	L259P
P9	chrXI	641180	SNP/INDEL	nonsynonymous	YKR101W	SIR1	S214*
P9	chrXI	641559	SNP/INDEL	nonsynonymous	YKR101W	SIR1	K340indel
P9	chrXIII	25025	SNP/INDEL	nonsynonymous	YML123C	PHO84	L259P
S1	chrII	405793	Ty	Upstream	tD(GUC)B	None	
S1	chrII	405793	Ty	Upstream	tR(UCU)B	None	
S1	chrII	405793	Ty	Upstream	YBR081C	SPT7	
S1	chrII	405793	Ty	Downstream	YBR082C	UBC4	
S10	chrII	404510	Ty	Inside	YBR081C	SPT7	
S10	chrII	405304	Ty	Upstream	tD(GUC)B	None	
S10	chrII	405304	Ty	Upstream	tR(UCU)B	None	
S10	chrII	405304	Ty	Upstream	YBR081C	SPT7	
S10	chrIV	410260	Ty	Upstream	YDL024C	DIA3	
S10	chrIV	410260	Ty	Upstream	tA(AGC)D	None	
S10	chrIV	410260	Ty	Upstream	YDL022C-A	None	
S10	chrXV	282057	Ty	Downstream	YOL021C	DIS3	
S10	chrXV	282057	Ty	Upstream	tG(GCC)O2	SUF17	
S10	chrXV	282057	Ty	Upstream	YOL022C	TSR4	
S11	chrIII	50702	SNP/INDEL	5'-upstream	YCL041C	YCL041C	NA
S11	chrIII	50702	SNP/INDEL	nonsynonymous	YCL042W	YCL042W	L40R
S11	chrM	53653	SNP/INDEL	intergenic	NA	NA	NA
S11	chrVII	1078634	SNP/INDEL	intergenic	NA	NA	NA
S11	chrXIII	796148	SNP/INDEL	nonsynonymous	YMR264W	CUE1	E115A
S11	chrXIV	93981	SNP/INDEL	nonsynonymous	YNL287W	SEC21	Q663L
S12	chrII	404322	Ty	Inside	YBR081C	SPT7	
S12	chrIV	569431	Ty	Downstream	tD(GUC)D	None	
S12	chrIV	569431	Ty	Downstream	tR(UCU)D	None	
S12	chrIV	569431	Ty	Upstream	YDR058C	TGL2	
S12	chrIV	569431	Ty	Inside	YDR059C	UBC5	
S12	chrM	20438	SNP/INDEL	intron	Q0070	NA	NA
S12	chrM	20438	SNP/INDEL	intron	Q0065	NA	NA
S12	chrM	20438	SNP/INDEL	intron	Q0045	NA	NA
S12	chrVII	378345	SNP/INDEL	nonsynonymous	YGL066W	SGF73	S246*
S12	chrVII	378764	SNP/INDEL	nonsynonymous	YGL066W	SGF73	K386*
S12	chrX	468950	SNP/INDEL	nonsynonymous	YJR021C	REC107	N184Y
S12	chrXI	660868	Ty	Upstream	YKR106W	GEX2	
S12	chrXI	660868	Ty	Upstream	YKR105C	VBA5	
S12	chrXV	465407	SNP/INDEL	nonsynonymous	YOR073W	SGO1	E213K

S13	chrII	789984	SNP/INDEL	nonsynonymous	YBR294W	SUL1	N250K
S13	chrIV	568676	Ty	Upstream	tD(GUC)D	None	
S13	chrIV	568676	Ty	Upstream	tR(UCU)D	None	
S13	chrIV	568676	Ty	Inside	YDR058C	TGL2	
S13	chrIV	568676	Ty	Downstream	YDR059C	UBC5	
S13	chrXVI	498632	SNP/INDEL	nonsynonymous	YPL028W	ERG10	D179E
S14	chrII	405319	Ty	Upstream	tD(GUC)B	None	
S14	chrII	405319	Ty	Upstream	tR(UCU)B	None	
S14	chrII	405319	Ty	Upstream	YBR081C	SPT7	
S14	chrIV	1259639	Ty	Upstream	YDR393W	SHE9	
S14	chrIV	1259639	Ty	Inside	YDR392W	SPT3	
S14	chrVII	378409	SNP/INDEL	nonsynonymous	YGL066W	SGF73	Y267*
S15	chrII	404265	Ty	Inside	YBR081C	SPT7	
S15	chrIX	370139	Ty	Upstream	YIR007W	EGH1	
S15	chrIX	370139	Ty	Upstream	tE(UUC)I	None	
S15	chrIX	370139	Ty	Upstream	YIR006C	PAN1	
S15	chrXI	578478	Ty	Upstream	YKR074W	AIM29	
S15	chrXI	578478	Ty	Inside	YKR073C	None	
S15	chrXI	578478	Ty	Upstream	tK(UUU)K	None	
S15	chrXI	578478	Ty	Upstream	YKR072C	SIS2	
S15	chrXI	578649	Ty	Upstream	YKR074W	AIM29	
S15	chrXI	578649	Ty	Upstream	YKR073C	None	
S15	chrXI	578649	Ty	Upstream	tK(UUU)K	None	
S15	chrXI	578649	Ty	Upstream	YKR072C	SIS2	
S15	chrXII	502430	Ty	Upstream	YLR172C	DPH5	
S15	chrXII	502430	Ty	Inside	YLR173W	None	
S16	chrI	174563	SNP/INDEL	synonymous	YAR019C	CDC15	G191G
S16	chrIV	384473	SNP/INDEL	intergenic	NA	NA	NA
S16	chrIV	1257258	Ty	Downstream	YDR391C	None	
S16	chrIV	1257258	Ty	Upstream	tG(CCC)D	SUF3	
S16	chrIV	1257258	Ty	Upstream	YDR390C	UBA2	
S16	chrVII	378764	SNP/INDEL	nonsynonymous	YGL066W	SGF73	K386*
S17	chrII	405404	Ty	Upstream	tD(GUC)B	None	
S17	chrII	405404	Ty	Upstream	tR(UCU)B	None	
S17	chrII	405404	Ty	Upstream	YBR081C	SPT7	
S17	chrII	790023	SNP/INDEL	nonsynonymous	YBR294W	SUL1	N263K
S17	chrIV	489131	Ty	Upstream	YDR022C	ATG31	
S17	chrIV	489131	Ty	Upstream	tV(UAC)D	None	
S17	chrIV	489131	Ty	Upstream	YDR023W	SES1	

S17	chrIV	1259639	Ty	Upstream	YDR393W	SHE9	
S17	chrIV	1259639	Ty	Inside	YDR392W	SPT3	
S17	chrV	142064	SNP/INDEL	nonsynonymous	YEL007W	MIT1	S58L
S17	chrVII	377746	SNP/INDEL	nonsynonymous	YGL066W	SGF73	Y46*
S17	chrVII	377966	Ty	Downstream	YGL067W	NPY1	
S17	chrVII	377966	Ty	Inside	YGL066W	SGF73	
S17	chrVII	378115	SNP/INDEL	nonsynonymous	YGL066W	SGF73	Y169*
S17	chrXI	46934	Ty	Upstream	YKL208W	CBT1	
S17	chrXI	46934	Ty	Upstream	YKL209C	STE6	
S17	chrXI	46934	Ty	Upstream	tT(CGU)K	TRT2	
S17	chrXIV	748413	SNP/INDEL	nonsynonymous	YNR063W	YNR063W	V491L
S18	chrIII	210593	Ty	Downstream	YCR047C	BUD23	
S18	chrIII	210593	Ty	Upstream	YCR046C	IMG1	
S18	chrIII	210593	Ty	Upstream	YCR045C	RRT12	
S18	chrIII	235114	SNP/INDEL	nonsynonymous	YCR067C	SED4	D403E
S18	chrIV	1259639	Ty	Upstream	YDR393W	SHE9	
S18	chrIV	1259639	Ty	Inside	YDR392W	SPT3	
S18	chrVII	378437	SNP/INDEL	nonsynonymous	YGL066W	SGF73	E277*
S18	chrVII	378757	SNP/INDEL	nonsynonymous	YGL066W	SGF73	Y383*
S18	chrVII	379348	SNP/INDEL	nonsynonymous	YGL066W	SGF73	S580indel
S18	chrXIV	136117	Ty	Inside	YNL270C	ALP1	
S18	chrXIV	136117	Ty	Upstream	YNL271C	BN11	
S18	chrXV	111155	Ty	Downstream	YOL108C	INO4	
S18	chrXV	111155	Ty	Upstream	YOL107W	None	
S18	chrXV	111155	Ty	Upstream	tG(UCC)O	SUF1	
S18	chrXV	111155	Ty	Downstream	YOL109W	ZEO1	
S19	chrI	41522	SNP/INDEL	nonsynonymous	YAL056W	GPB2	C755F
S19	chrII	126166	SNP/INDEL	intergenic	NA	NA	NA
S19	chrII	789984	SNP/INDEL	nonsynonymous	YBR294W	SUL1	N250K
S19	chrII	799657	Ty	Upstream	YBR297W	MAL33	
S19	chrII	799657	Ty	Downstream	YBR296C-A	None	
S19	chrV	508238	SNP/INDEL	nonsynonymous	YER164W	CHD1	Q949indel
S19	chrVI	66592	SNP/INDEL	nonsynonymous	YFL034W	MIL1	D372E
S19	chrVII	544796	Ty	Downstream	YGR029W	ERV1	
S19	chrVII	544796	Ty	Upstream	tD(GUC)G2	None	
S19	chrVII	544796	Ty	Downstream	YGR030C	POP6	
S19	chrVII	544796	Ty	Upstream	snR46	SNR46	
S19	chrX	424854	Ty	Upstream	YJL006C	CTK2	
S19	chrX	424854	Ty	Upstream	YJL005W	CYR1	

S19	chrX	424854	Ty	Upstream	tL(UAA)J	SUP51	
S19	chrX	709758	Ty	Upstream	YJR150C	DAN1	
S19	chrXI	578803	Ty	Upstream	YKR074W	AIM29	
S19	chrXI	578803	Ty	Upstream	YKR073C	None	
S19	chrXI	578803	Ty	Upstream	tK(UUU)K	None	
S19	chrXI	578803	Ty	Upstream	YKR072C	SIS2	
S19	chrXII	20727	Ty	Downstream	YLL060C	GTT2	
S19	chrXVI	819353	Ty	Downstream	YPR144C	NOC4	
S19	chrXVI	819353	Ty	Upstream	tI(AAU)P1	None	
S19	chrXVI	819353	Ty	Downstream	YPR143W	RRP15	
S2	chrII	332445	Ty	Downstream	YBR047W	FMP23	
S2	chrII	332445	Ty	Upstream	YBR048W	RPS11B	
S2	chrII	332445	Ty	Upstream	YBR046C	ZTA1	
S2	chrII	405301	Ty	Upstream	tD(GUC)B	None	
S2	chrII	405301	Ty	Upstream	tR(UCU)B	None	
S2	chrII	405301	Ty	Upstream	YBR081C	SPT7	
S2	chrII	789984	SNP/INDEL	nonsynonymous	YBR294W	SUL1	N250K
S2	chrII	790021	SNP/INDEL	nonsynonymous	YBR294W	SUL1	N263H
S2	chrIV	384473	SNP/INDEL	intergenic	NA	NA	NA
S2	chrVI	252115	Ty	Upstream	YFR051C	RET2	
S2	chrVI	252115	Ty	Upstream	YFR052W	RPN12	
S2	chrVII	378402	Ty	Inside	YGL066W	SGF73	
S2	chrVII	857792	Ty	Upstream	tL(CAA)G3	None	
S2	chrVII	857792	Ty	Upstream	YGR181W	TIM13	
S2	chrVII	879487	SNP/INDEL	intergenic	NA	NA	NA
S2	chrXI	578803	Ty	Upstream	YKR074W	AIM29	
S2	chrXI	578803	Ty	Upstream	YKR073C	None	
S2	chrXI	578803	Ty	Upstream	tK(UUU)K	None	
S2	chrXI	578803	Ty	Upstream	YKR072C	SIS2	
S2	chrXII	550702	SNP/INDEL	nonsynonymous	YLR203C	MSS51	M420T
S2	chrXII	550702	SNP/INDEL	5'-upstream	YLR202C	YLR202C	NA
S20	chrII	790023	SNP/INDEL	nonsynonymous	YBR294W	SUL1	N263K
S20	chrIV	1259644	Ty	Upstream	YDR393W	SHE9	
S20	chrIV	1259644	Ty	Inside	YDR392W	SPT3	
S20	chrIX	22492	Ty	Downstream	YIL169C	CSS1	
S20	chrIX	435789	SNP/INDEL	synonymous	YIR042C	YIR042C	A65A
S20	chrVII	378248	SNP/INDEL	nonsynonymous	YGL066W	SGF73	K214*
S20	chrVII	378449	Ty	Inside	YGL066W	SGF73	
S20	chrXV	28246	Ty	Downstream	YOL155C	HPF1	

S21	chrII	790021	SNP/INDEL	nonsynonymous	YBR294W	SUL1	N263H
S21	chrIII	84581	SNP/INDEL	intergenic	NA	NA	NA
S21	chrV	86340	Ty	Downstream	YEL034W	HYP2	
S21	chrV	86340	Ty	Upstream	YEL032W	MCM3	
S21	chrV	86340	Ty	Inside	YEL033W	MTC7	
S21	chrV	86340	Ty	Upstream	tS(AGA)E	None	
S21	chrV	86340	Ty	Upstream	YEL035C	UTR5	
S21	chrVII	879487	SNP/INDEL	intergenic	NA	NA	NA
S21	chrXI	578803	Ty	Upstream	YKR074W	AIM29	
S21	chrXI	578803	Ty	Upstream	YKR073C	None	
S21	chrXI	578803	Ty	Upstream	tK(UUU)K	None	
S21	chrXI	578803	Ty	Upstream	YKR072C	SIS2	
S21	chrXII	550702	SNP/INDEL	nonsynonymous	YLR203C	MSS51	M420T
S21	chrXII	550702	SNP/INDEL	5'-upstream	YLR202C	YLR202C	NA
S22	chrIV	1295417	SNP/INDEL	5'-upstream	YDR413C	YDR413C	NA
S22	chrVII	378242	SNP/INDEL	nonsynonymous	YGL066W	SGF73	K212*
S22	chrVII	378368	Ty	Inside	YGL066W	SGF73	
S22	chrXIV	150178	SNP/INDEL	nonsynonymous	YNL262W	POL2	P656Q
S23	chrII	402196	SNP/INDEL	nonsynonymous	YBR081C	SPT7	I1019R
S23	chrII	405319	Ty	Upstream	tD(GUC)B	None	
S23	chrII	405319	Ty	Upstream	tR(UCU)B	None	
S23	chrII	405319	Ty	Upstream	YBR081C	SPT7	
S23	chrII	405546	Ty	Upstream	tD(GUC)B	None	
S23	chrII	405546	Ty	Upstream	tR(UCU)B	None	
S23	chrII	405546	Ty	Upstream	YBR081C	SPT7	
S23	chrII	788467	Ty	Upstream	YBR294W	SUL1	
S23	chrII	788467	Ty	Downstream	YBR293W	VBA2	
S23	chrII	789984	SNP/INDEL	nonsynonymous	YBR294W	SUL1	N250K
S23	chrII	789984	SNP/INDEL	nonsynonymous	YBR294W	SUL1	N250K
S23	chrIII	281102	SNP/INDEL	nonsynonymous	YCR093W	CDC39	T329I
S23	chrIV	569127	Ty	Downstream	tD(GUC)D	None	
S23	chrIV	569127	Ty	Downstream	tR(UCU)D	None	
S23	chrIV	569127	Ty	Upstream	YDR058C	TGL2	
S23	chrIV	569127	Ty	Downstream	YDR059C	UBC5	
S23	chrIV	592545	Ty	Inside	YDR073W	SNF11	
S23	chrVI	5529	SNP/INDEL	ARS	ARS600	NA	NA
S23	chrVI	5529	SNP/INDEL	telomere	TEL06L	NA	NA
S23	chrVI	229099	SNP/INDEL	nonsynonymous	YFR037C	RSC8	P30S
S23	chrVII	378389	Ty	Inside	YGL066W	SGF73	

S23	chrVII	962310	Ty	Upstream	YGR235C	MIC26	
S23	chrVII	962310	Ty	Downstream	YGR237C	None	
S23	chrVII	962310	Ty	Downstream	YGR236C	SPG1	
S23	chrVIII	188938	Ty	Inside	YHR040W	BCD1	
S23	chrVIII	188938	Ty	Downstream	YHR041C	SRB2	
S23	chrVIII	266602	Ty	Inside	YHR080C	LAM4	
S23	chrVIII	266602	Ty	Upstream	YHR081W	LRP1	
S23	chrXI	108243	SNP/INDEL	nonsynonymous	YKL181W	PRS1	I310V
S23	chrXI	650135	Ty	Downstream	YKR102W	FLO10	
S23	chrXII	279503	SNP/INDEL	nonsynonymous	YLR072W	LAM6	M214I
S23	chrXII	485327	Ty	Downstream	YLR160C	ASP3-4	
S23	chrXII	485327	Ty	Upstream	YLR159W	None	
S23	chrXII	485327	Ty	Downstream	YLR159C-A	None	
S23	chrXII	485327	Ty	Upstream	RDN5-5	RDN5-5	
S23	chrXIII	481621	SNP/INDEL	intergenic	NA	NA	NA
S23	chrXV	586898	SNP/INDEL	5'-upstream	YOR140W	SFL1	NA
S23	chrXVI	299161	SNP/INDEL	nonsynonymous	YPL134C	ODC1	T115indel
S23	chrXVI	819322	Ty	Downstream	YPR144C	NOC4	
S23	chrXVI	819322	Ty	Upstream	tI(AAU)P1	None	
S23	chrXVI	819322	Ty	Downstream	YPR143W	RRP15	
S24	chrII	790021	SNP/INDEL	nonsynonymous	YBR294W	SUL1	N263H
S24	chrIX	292408	SNP/INDEL	5'-upstream	YIL032C	YIL032C	NA
S24	chrX	617485	Ty	Upstream	YJR100C	AIM25	
S24	chrX	617485	Ty	Upstream	tI(UAG)J	None	
S24	chrX	617485	Ty	Upstream	YJR101W	RSM26	
S24	chrXII	32066	SNP/INDEL	intergenic	NA	NA	NA
S24	chrXVI	70489	SNP/INDEL	nonsynonymous	YPL254W	HF11	Y335*
S25	chrII	789984	SNP/INDEL	nonsynonymous	YBR294W	SUL1	N250K
S25	chrXVI	186734	SNP/INDEL	nonsynonymous	YPL190C	NAB3	R331K
S25	chrXVI	494094	SNP/INDEL	synonymous	YPL030W	TRM44	K184K
S26	chrI	180861	Ty	Upstream	tI(CAA)A	SUP56	
S26	chrII	405369	Ty	Upstream	tD(GUC)B	None	
S26	chrII	405369	Ty	Upstream	tR(UCU)B	None	
S26	chrII	405369	Ty	Upstream	YBR081C	SPT7	
S26	chrII	574062	SNP/INDEL	synonymous	YBR169C	SSE2	K645K
S26	chrII	789984	SNP/INDEL	nonsynonymous	YBR294W	SUL1	N250K
S26	chrII	790023	SNP/INDEL	nonsynonymous	YBR294W	SUL1	N263K
S26	chrIV	541535	SNP/INDEL	intergenic	NA	NA	NA
S26	chrIV	1259709	SNP/INDEL	5'-upstream	YDR393W	SHE9	NA

S26	chrIV	1259709	SNP/INDEL	nonsynonymous	YDR392W	SPT3	*338Y
S26	chrVII	754777	Ty	Inside	YGR131W	FHN1	
S26	chrVII	754777	Ty	Upstream	YGR130C	None	
S26	chrVII	754777	Ty	Downstream	YGR132C	PHB1	
S26	chrX	524198	Ty	Downstream	YJR047C	ANB1	
S26	chrX	524198	Ty	Upstream	tS(AGA)J	None	
S26	chrX	524198	Ty	Downstream	YJR046W	TAH11	
S26	chrXVI	69359	SNP/INDEL	5'-upstream	YPL254W	HF11	NA
S27	chrII	790023	SNP/INDEL	nonsynonymous	YBR294W	SUL1	N263K
S27	chrVII	863792	Ty	Inside	YGR184C	UBR1	
S27	chrXII	499056	SNP/INDEL	nonsynonymous	YLR167W	RPS31	P37R
S28	chrI	203274	Ty	Upstream	YAR050W	FLO1	
S28	chrM	7649	SNP/INDEL	rRNA	15S_rRNA	NA	NA
S28	chrXI	578649	Ty	Upstream	YKR074W	AIM29	
S28	chrXI	578649	Ty	Upstream	YKR073C	None	
S28	chrXI	578649	Ty	Upstream	tK(UUU)K	None	
S28	chrXI	578649	Ty	Upstream	YKR072C	SIS2	
S28	chrXIV	331839	SNP/INDEL	splice-site	YNL162W	NA	NA
S29	chrII	789984	SNP/INDEL	nonsynonymous	YBR294W	SUL1	N250K
S29	chrII	790023	SNP/INDEL	nonsynonymous	YBR294W	SUL1	N263K
S29	chrIV	410069	Ty	Upstream	YDL024C	DIA3	
S29	chrIV	410069	Ty	Upstream	tA(AGC)D	None	
S29	chrIV	410069	Ty	Upstream	YDL022C-A	None	
S29	chrXIII	437834	SNP/INDEL	nonsynonymous	YMR085W	YMR085W	I115K
S29	chrXIV	45788	SNP/INDEL	synonymous	YNL313C	EMW1	I745I
S3	chrII	403980	Ty	Inside	YBR081C	SPT7	
S3	chrII	789984	SNP/INDEL	nonsynonymous	YBR294W	SUL1	N250indel
S3	chrIX	183668	Ty	Upstream	YIL096C	BMT5	
S3	chrIX	183668	Ty	Upstream	tI(AAU)I1	None	
S3	chrIX	183668	Ty	Upstream	YIL095W	PRK1	
S3	chrVII	195260	SNP/INDEL	nonsynonymous	YGL163C	RAD54	L382V
S3	chrVII	378446	Ty	Inside	YGL066W	SGF73	
S3	chrVII	583184	SNP/INDEL	nonsynonymous	YGR044C	RME1	E237*
S3	chrVIII	315940	SNP/INDEL	nonsynonymous	YHR101C	BIG1	L10R
S3	chrXII	666548	SNP/INDEL	nonsynonymous	YLR260W	LCB5	L235F
S3	chrXIII	736078	SNP/INDEL	nonsynonymous	YMR231W	PEP5	R845K
S3	chrXVI	631634	Ty	Downstream	YPR030W	CSR2	
S3	chrXVI	631634	Ty	Inside	YPR031W	NTO1	
S30	chrIX	174942	Ty	Upstream	YIL102C	None	

S30	chrIX	174942	Ty	Upstream	tT(AGU)I1	None	
S30	chrIX	174942	Ty	Downstream	YIL101C	XBP1	
S30	chrIX	363142	SNP/INDEL	5'-upstream	YIR004W	DJP1	NA
S30	chrVII	378334	SNP/INDEL	nonsynonymous	YGL066W	SGF73	Y242*
S30	chrVII	378488	SNP/INDEL	nonsynonymous	YGL066W	SGF73	E294*
S30	chrXV	757730	SNP/INDEL	5'-upstream	YOR221C	MCT1	NA
S31	chrII	39328	SNP/INDEL	nonsynonymous	YBL098W	BNA4	L62M
S31	chrII	405404	Ty	Upstream	tD(GUC)B	None	
S31	chrII	405404	Ty	Upstream	tR(UCU)B	None	
S31	chrII	405404	Ty	Upstream	YBR081C	SPT7	
S31	chrII	789984	SNP/INDEL	nonsynonymous	YBR294W	SUL1	N250K
S31	chrII	789984	SNP/INDEL	nonsynonymous	YBR294W	SUL1	N250K
S31	chrIV	590497	SNP/INDEL	nonsynonymous	YDR072C	IPT1	G283V
S31	chrVII	74255	Ty	Downstream	YGL226W	MTC3	
S31	chrVII	74255	Ty	Upstream	tV(AAC)G3	None	
S31	chrX	524284	Ty	Downstream	YJR047C	ANB1	
S31	chrX	524284	Ty	Upstream	tS(AGA)J	None	
S31	chrX	524284	Ty	Downstream	YJR046W	TAH11	
S31	chrXI	308327	Ty	Downstream	YKL069W	None	
S31	chrXI	308327	Ty	Upstream	tV(AAC)K1	None	
S31	chrXI	308327	Ty	Upstream	YKL068W-A	None	
S31	chrXII	666548	SNP/INDEL	nonsynonymous	YLR260W	LCB5	L235F
S31	chrXIV	531723	SNP/INDEL	5'-upstream	YNL052W	COX5a	NA
S31	chrXVI	62472	SNP/INDEL	intergenic	NA	NA	NA
S31	chrXVI	433530	SNP/INDEL	nonsynonymous	YPL061W	ALD6	Q315*
S31	chrXVI	744097	Ty	Upstream	YPR109W	GLD1	
S31	chrXVI	744097	Ty	Upstream	tT(UGU)P	None	
S31	chrXVI	744097	Ty	Upstream	YPR108W-A	None	
S31	chrXVI	744097	Ty	Downstream	YPR108W	RPN7	
S4	chrV	517729	SNP/INDEL	intergenic	NA	NA	NA
S5	chrVII	378501	SNP/INDEL	nonsynonymous	YGL066W	SGF73	L298indel
S5	chrX	286288	SNP/INDEL	nonsynonymous	YJL080C	SCP160	D980A
S5	chrXIII	202796	SNP/INDEL	synonymous	YML038C	YMD8	S436S
S6	chrII	405489	SNP/INDEL	intergenic	NA	NA	NA
S6	chrII	789984	SNP/INDEL	nonsynonymous	YBR294W	SUL1	N250K
S7	chrVII	378368	SNP/INDEL	nonsynonymous	YGL066W	SGF73	M254indel
S7	chrVIII	192224	SNP/INDEL	nonsynonymous	YHR042W	NCP1	S561*
S7	chrXVI	728341	SNP/INDEL	nonsynonymous	YPR097W	YPR097W	A983D

S8	chrII	404438	Ty	Inside	YBR081C	SPT7	
S8	chrII	404688	Ty	Inside	YBR081C	SPT7	
S8	chrII	767936	Ty	Upstream	YBR281C	DUG2	
S8	chrII	767936	Ty	Upstream	YBR282W	MRPL27	
S8	chrII	797486	Ty	Downstream	YBR295W	PCA1	
S8	chrII	797486	Ty	Inside	YBR296C	PHO89	
S8	chrIII	6401	SNP/INDEL	intergenic	NA	NA	NA
S8	chrIV	1509994	Ty	Upstream	YDR538W	PAD1	
S8	chrIV	1509994	Ty	Downstream	YDR536W	STL1	
S8	chrVII	378650	SNP/INDEL	nonsynonymous	YGL066W	SGF73	G348*
S8	chrXI	578867	Ty	Upstream	YKR074W	AIM29	
S8	chrXI	578867	Ty	Upstream	YKR073C	None	
S8	chrXI	578867	Ty	Downstream	YKR075C	None	
S8	chrXI	578867	Ty	Upstream	tK(UUU)K	None	
S8	chrXI	578867	Ty	Upstream	YKR072C	SIS2	
S8	chrXIV	427209	SNP/INDEL	intergenic	NA	NA	NA
S8	chrXIV	696260	SNP/INDEL	nonsynonymous	YNR038W	DBP6	N222K
S8	chrXV	115639	SNP/INDEL	nonsynonymous	YOL105C	WSC3	S57C
S9	chrVII	378437	SNP/INDEL	nonsynonymous	YGL066W	SGF73	E277*
S9	chrXIII	454261	SNP/INDEL	nonsynonymous	YMR093W	UTP15	V83I

APPENDIX B: Supplementary materials for Chapter 3

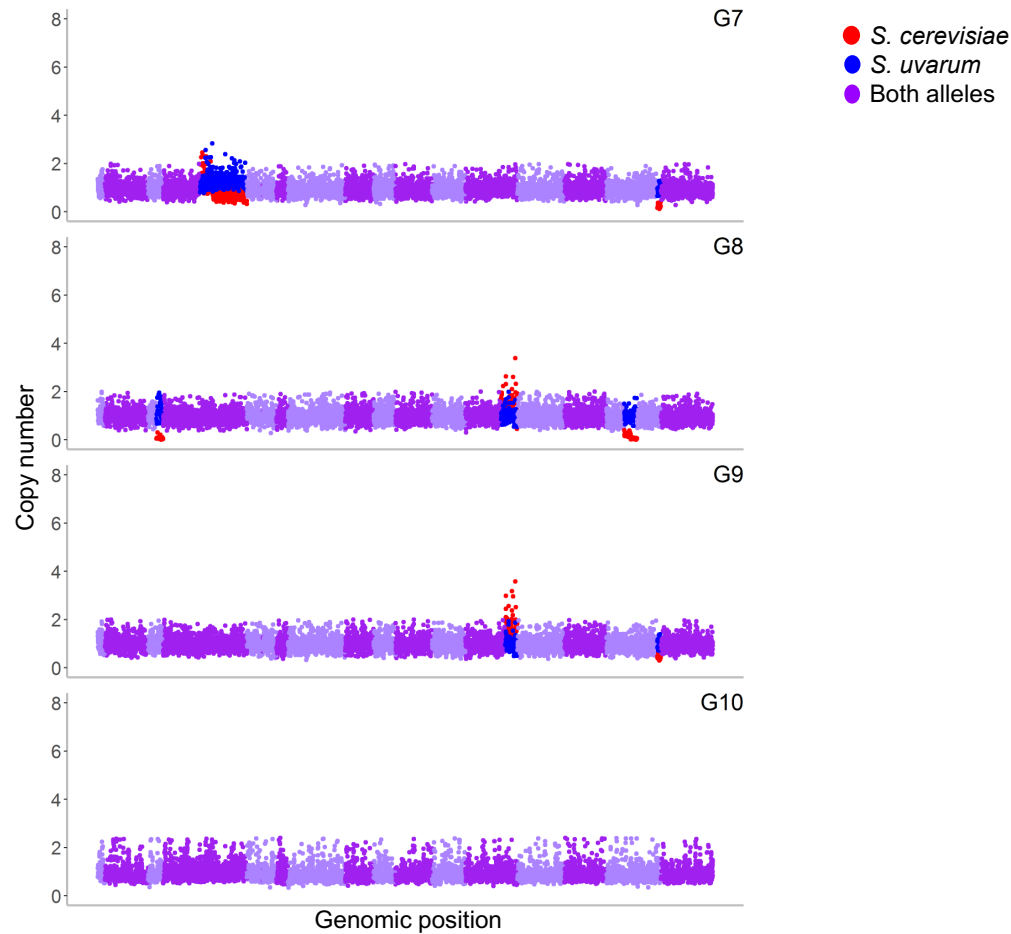


Figure B.1. Copy number plots of cold-evolved hybrids populations.

Genome wide copy number is plotted for evolved hybrid populations at 15°C. Nutrient limitation is indicated in the upper right corner (G=glucose, S=sulfate, P=phosphate), numbers indicate independent populations. Purple denotes a region where both alleles are present at a single copy (alternating purple indicates different chromosomes from chrI - chrXVI), blue denotes a *S. uvarum* change in copy number, red denotes a *S. cerevisiae* change in copy number. Note, copy number was derived from population sequencing read depth at homologous ORFs.

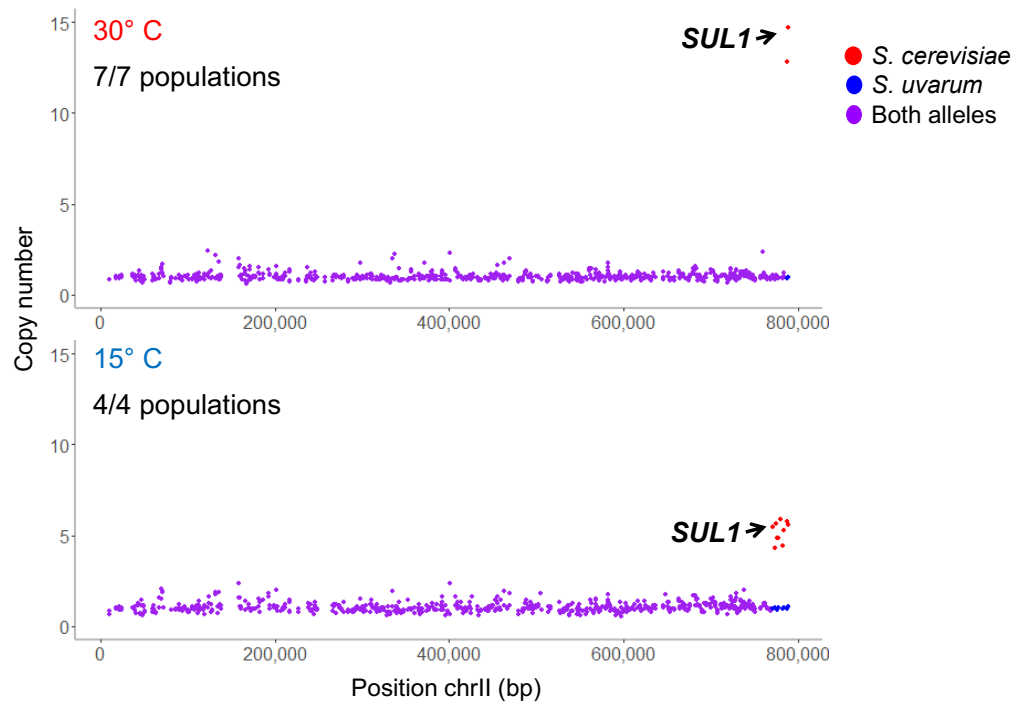


Figure B.2. Amplification of *S. cerevisiae* *SUL1* in hybrids evolved at 15°C and 30°C.

Copy number is plotted across chrII in a representative hybrid clone evolved in sulfate limitation at 30°C and a population evolved in sulfate limitation at 15°C. Copy number was derived from sequencing read depth at homologous ORFs. A region containing the *S. cerevisiae* allele of the high affinity sulfate transporter *SUL1* is amplified in 7/7 populations evolved at 30°C and 4/4 populations evolved at 15°C, suggesting that the locus is not temperature sensitive, and instead that *S. cerevisiae* allele is more fit at both temperatures.

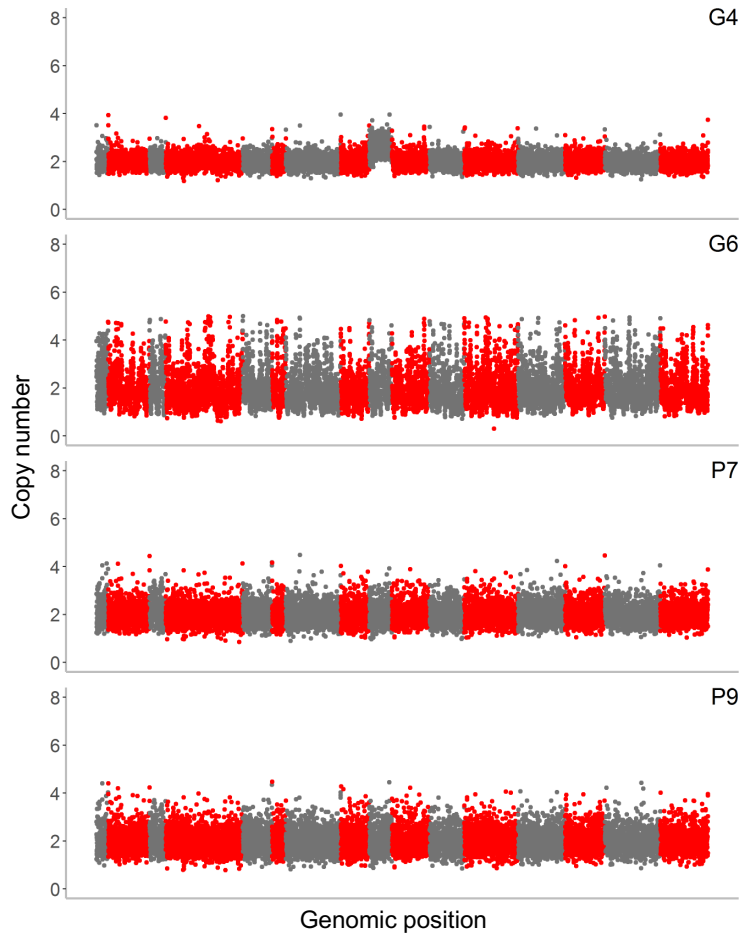


Figure B.3. Copy number plots of cold-evolved *S. cerevisiae* diploid populations.

Copy number is plotted across the genome for *S. cerevisiae* evolved populations. Alternating grey and red indicate different chromosomes (from chrI – chrXVI). Copy number was derived from average population sequencing read depth in 1000 bp intervals. Nutrient limitation is indicated in the upper right corner (G=glucose, S=sulfate, P=phosphate), numbers indicate independent populations.

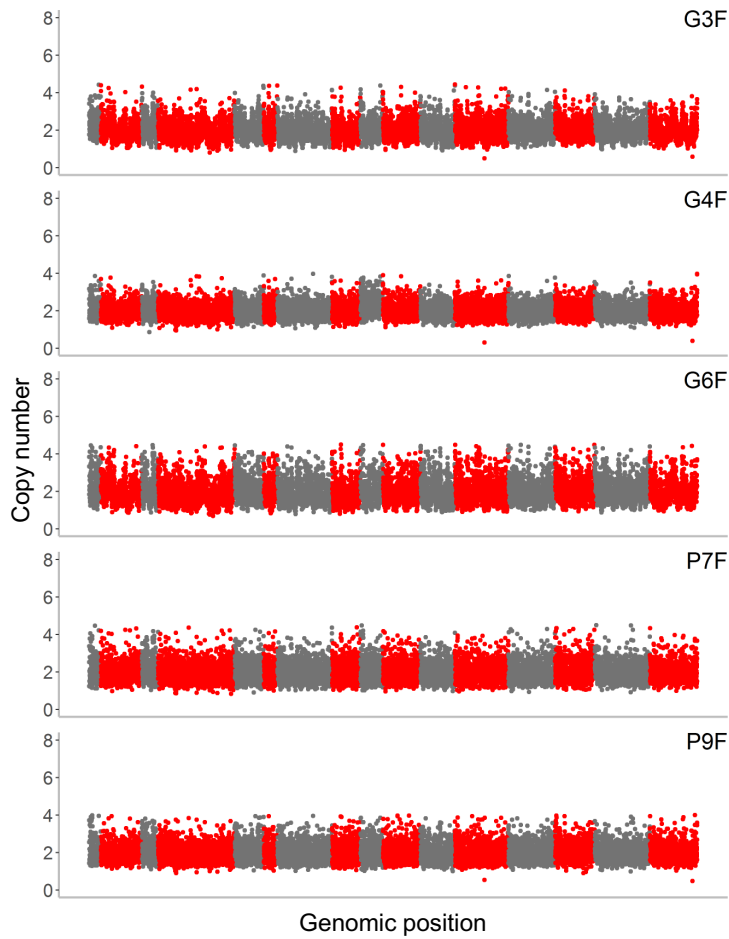


Figure B.4. Copy number plots of cold-evolved, flocculent *S. cerevisiae* diploid populations.

Copy number is plotted across the genome for *S. cerevisiae* evolved, flocculent populations that were isolated separately from populations dispersed in the culture. Alternating grey and red indicate different chromosomes (from chrI – chrXVI). Copy number was derived from average population sequencing read depth in 1000 bp intervals. Nutrient limitation is indicated in the upper right corner (G=glucose, S=sulfate, P=phosphate), numbers indicate independent populations.

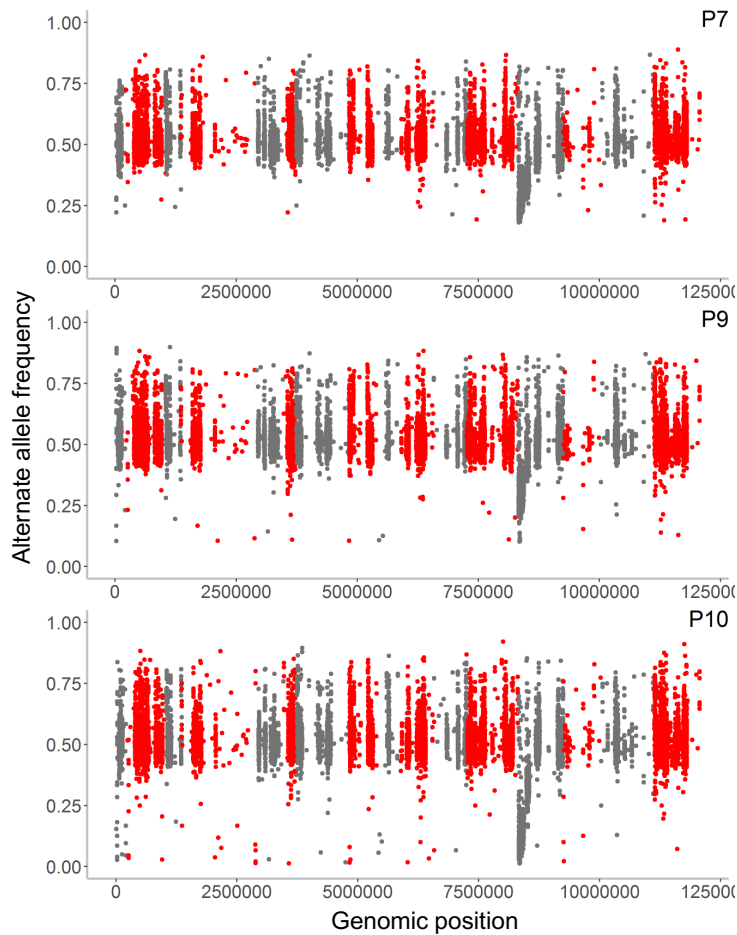


Figure B.5. Loss of heterozygosity plots of cold-evolved *S. cerevisiae* diploid populations.

Alternate allele (e.g., non-reference allele) frequency is plotted across the genome for *S. cerevisiae* evolved populations. The unique pattern of heterozygosity is produced by a strain history of crossing FL100 to S288C to produce GF167, which was crossed to S288C to produce the diploid strain used here. This produced regions of heterozygosity and regions of homozygosity (regions that appear blank because no alternate allele is called). This also allows the detection of loss of heterozygosity (LOH), where regions that were heterozygous become homozygous for the reference or non-reference allele. Alternating grey and red indicate different chromosomes (from chrI – chrXVI). Nutrient limitation is indicated in the upper right corner (G=glucose, S=sulfate, P=phosphate), numbers indicate independent populations. Note that LOH events are not at fixation in the population, so these events are instead indicated by allele frequencies approaching zero or one.

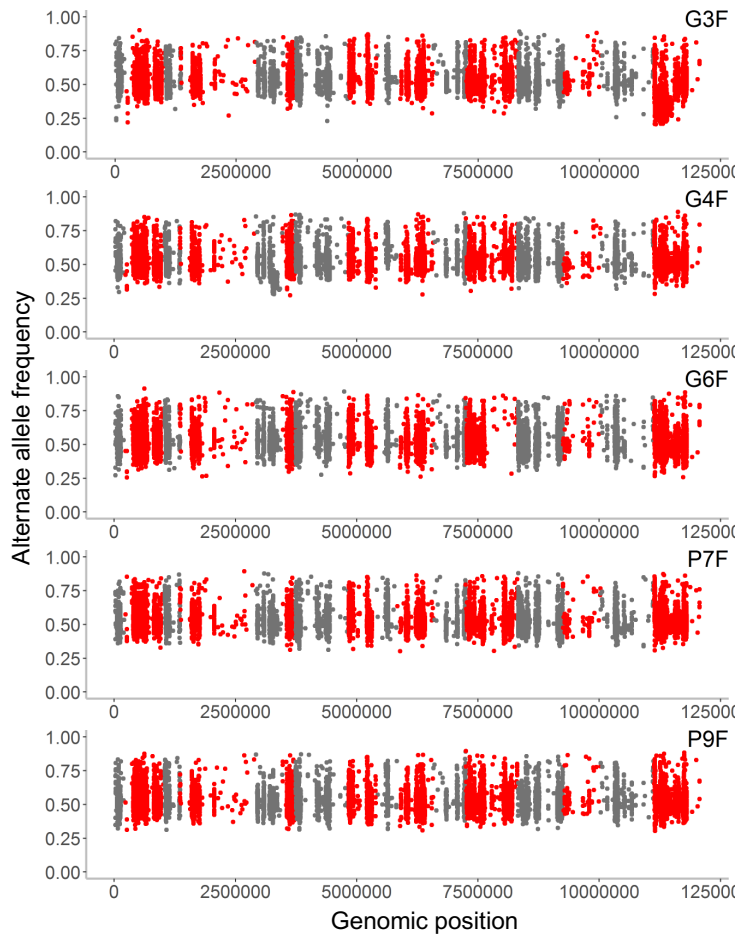


Figure B.6. Loss of heterozygosity plots of cold-evolved, flocculent *S. cerevisiae* diploid populations. Alternate allele (e.g., non-reference allele) frequency is plotted across the genome for *S. cerevisiae* evolved, flocculent populations that were isolated separately from populations dispersed in the culture. The unique pattern of heterozygosity is produced by a strain history of crossing FL100 to S288C to produce GF167, which was crossed to S288C to produce the diploid strain used here. This produced regions of heterozygosity and regions of homozygosity (regions that appear blank because no alternate allele is called). This also allows the detection of loss of heterozygosity (LOH), where regions that were heterozygous become homozygous for the reference or non-reference allele. Alternating grey and red indicate different chromosomes (from chrI – chrXVI). Nutrient limitation is indicated in the upper right corner (G=glucose, S=sulfate, P=phosphate), numbers indicate independent populations. Note that LOH events are not at fixation in the population, so these events are instead indicated by allele frequencies approaching zero or one.

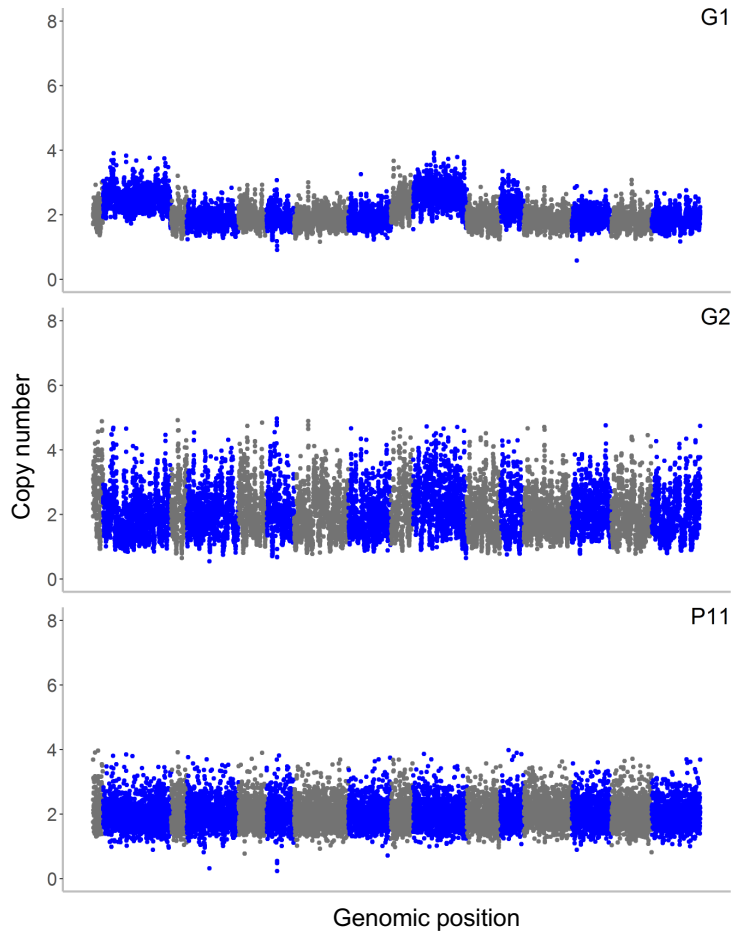


Figure B.7. Copy number plots of cold-evolved *S. uvarum* diploid populations.

Copy number is plotted across the genome for *S. uvarum* evolved populations. Alternating grey and blue indicate different chromosomes (from chrI – chrXVI). Copy number was derived from average population sequencing read depth in 1000 bp intervals. Nutrient limitation is indicated in the upper right corner (G=glucose, S=sulfate, P=phosphate), numbers indicate independent populations.

<i>S.cerevisiae</i>	1	MSSV	NKDT	THVA	ERSL	HEHL	TEGG	NAF	HNHL	NDFAH	IEDPL	ERRR	LALES	IDDE	EGFG	W																																											
<i>S.uvarum</i>	1	MSSV	AKDN	THVA	ERSL	HEHL	TEGG	NAF	HNHL	NDFAH	IEDPL	ERRR	LALES	IDDE	EGFG	W																																											
<i>S.cerevisiae</i>	61	QQVK	TISI	AGVG	FLTDS	YDIF	AINL	GIIM	MSYV	YWHG	SMP	GF	SQT	LLK	VST	SVGT	VIGQ	F																																									
<i>S.uvarum</i>	61	QQVK	TISI	AGVG	FLTDS	YDIF	AINL	GIIM	MSYV	YWHG	DMP	AS	SQT	LLK	VST	SVGT	VIGQ	V																																									
<i>S.cerevisiae</i>	121	GFGT	LADIV	GRK	LIYG	ELI	IMIV	CTIL	QTTVA	HSPAIN	FVAV	LTFF	YRIV	MGI	GIGG	DYP																																											
<i>S.uvarum</i>	121	GFGT	LADIV	GRK	LIYG	ELI	IMIV	CTIL	QTTVA	HSPAIN	FVAV	LTFF	YRIV	MGI	GIGG	DYP																																											
<i>S.cerevisiae</i>	181	LSSI	ITSE	FATTK	WRGAI	MGA	VFA	NQAW	GQIS	GGI	IALI	LVA	AYK	GN	LN	YANS	GAEC	DAR																																									
<i>S.uvarum</i>	181	LSSI	ITSE	FATTK	WRGAI	MGA	VFA	NQAW	GQIS	GGI	IALI	LVA	AYK	GN	LN	YANS	GAEC	DAR																																									
<i>S.cerevisiae</i>	241	CQK	ACDQ	MWR	VLI	GLG	TVL	GLA	CLY	FRL	TIP	ES	PRY	Q	LDV	NA	EL	LA	AAA	Q	E	D	G	E	K	K	I	H																															
<i>S.uvarum</i>	241	CQK	ACDQ	MWR	VLI	GLG	TVL	GLA	CLY	FRL	TIP	ES	PRY	Q	LDV	NA	EL	LR	-	VE	K	K	E	Q	E	A	E	K	K	L	Y																												
<i>S.cerevisiae</i>	301	DTSD	EDMA	ING	LERAS	TAVES	LDN	HPP	KAS	FKD	FCR	HFG	QW	KY	GK	ILL	GT	AG	SW	F	LD	V	A																																				
<i>S.uvarum</i>	300	GTSD	EDMA	HGL	ERAP	TAVES	LDN	HPP	KAS	FKD	FCR	HFG	QW	KY	GK	ILL	GT	AG	SW	F	LD	V	A																																				
<i>S.cerevisiae</i>	361	FYGL	SLNSA	VIL	QTI	G	YAG	S	KNV	YK	KLYD	AV	GN	LIL	CAG	SL	PG	Y	W	SV	F	T	V	D	I	I	G	R	K	P																													
<i>S.uvarum</i>	360	FYGL	SLNSA	VIL	QTI	G	YAG	S	KNV	YK	KLYD	AV	GN	LIL	CAG	SL	PG	Y	W	SV	F	T	V	D	I	I	G	R	K	P																													
<i>S.cerevisiae</i>	421	IQL	AGFI	I	L	T	A	L	F	C	V	I	G	F	A	Y	H	K	I	G	D	H	G	L	L	A	L	Y	V	I	C	Q	F	F	Q	N	F	G	P	N	T	T	F	I	V	P	G	E	C	F	P	T	R	Y	R				
<i>S.uvarum</i>	420	IQL	AGFI	I	L	T	I	L	F	C	V	I	G	F	A	Y	H	K	I	G	D	H	G	L	L	A	L	Y	V	I	C	Q	F	F	Q	N	F	G	P	N	T	T	F	I	V	P	G	E	C	F	P	T	R	Y	R				
<i>S.cerevisiae</i>	481	STA	H	G	I	S	A	A	S	G	K	L	G	A	I	I	A	Q	T	A	L	G	T	L	I	D	H	N	C	A	R	D	G	K	P	T	N	C	W	L	P	H	V	M	E	I	F	A	L	F	M	L	L	G	I	F	T	T	L
<i>S.uvarum</i>	480	STA	H	G	I	S	A	A	S	G	K	L	G	A	I	I	A	Q	T	A	L	G	T	L	I	D	H	N	C	A	R	D	G	K	A	T	N	C	W	L	P	H	V	M	E	I	F	A	L	F	M	L	L	G	I	F	T	T	L
<i>S.cerevisiae</i>	541	LIP	E	T	K	R	K	T	L	E	E	I	N	E	L	Y	H	D	E	I	D	P	A	T	L	N	E	R	N	K	N	N	D	E	S	S	P	S	Q	L	Q	H	E	A															
<i>S.uvarum</i>	540	LIP	E	T	K	R	K	T	L	E	E	I	N	E	K	Y	H	D	E	I	D	P	G	T	L	N	E	R	N	K	M	N	D	E	S	S	P	S	Q	L	Q	H	--																

Figure B.8. Protein alignment of *PHO84*

S. cerevisiae and *S. uvarum* alleles of *PHO84* were aligned using Clustal Omega. Black indicates shared identity, white indicates a radical substitution, and grey indicates a conservative substitution.

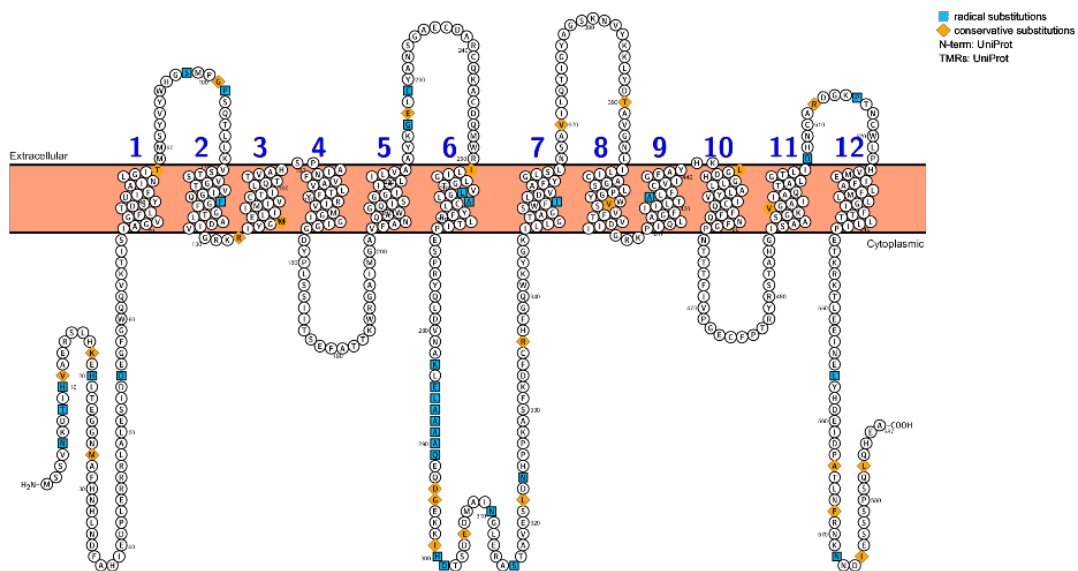


Figure B.9. Predicted protein structure of *PHO84*

A 2D depiction of the structure of *PHO84* was created by using UniProt protein accession P25297 (*S. cerevisiae PHO84*) with the program Protter (Omasits et al., 2014). Radical (blue square) and conservative (orange diamond) substitutions between *S. cerevisiae* and *S. uvarum* amino acids were annotated using a protein alignment (**Figure S8**).

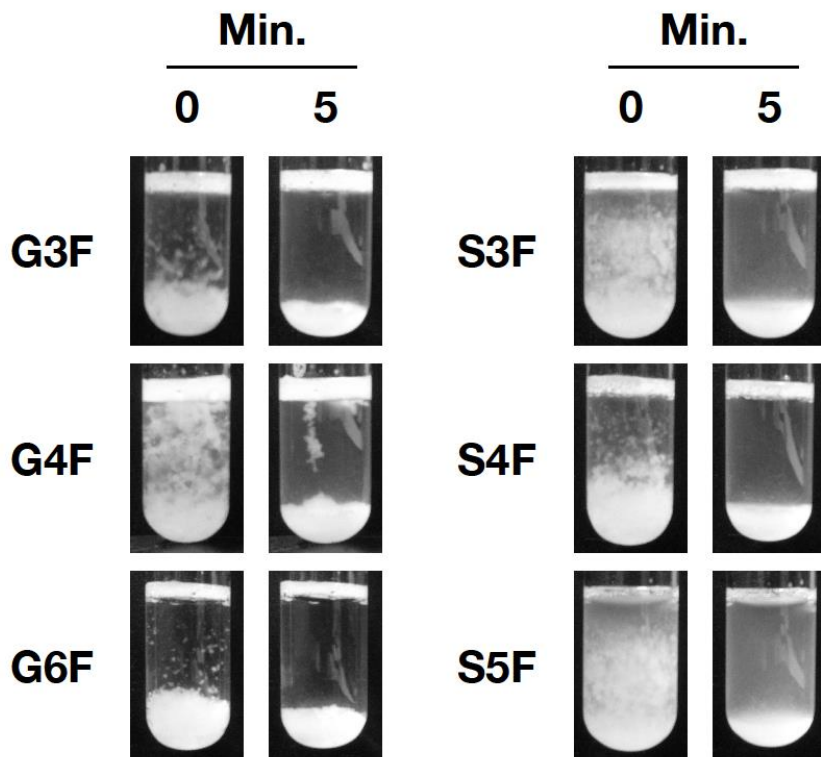


Figure B.10. Flocculation assay of several flocculent clones isolated from *S. cerevisiae* cold-evolved populations.

Overnight cultures were resuspended by vortexing for three seconds. Flocculent clones were photographed immediately after vortexing and then again after 5 minutes.

Table B.1. Mutations in cold-evolved *S. cerevisiae* diploid populations.

Population	Location	Gene(s)	Mutation
P7	chrIV:1323639	<i>BNA7</i>	coding-nonsynonymous : I201L
	chrVII:469931	<i>PDR1</i>	coding-nonsynonymous : I790F
	chrXVI:166971	<i>SGE1</i>	5' upstream
	chrXVI:933898	<i>YPR197C</i>	coding-nonsynonymous: *188Y
	chrXIII:1-221882	Includes <i>PHO84</i>	LOH, multiple tract lengths, loss of S288C allele
P7F	chrIV:1323639	<i>BNA7</i>	coding-nonsynonymous: I201L
	chrXVI:933898	<i>YPR197C</i>	coding-nonsynonymous: *188Y
P8F	chrIV:1323639	<i>BNA7</i>	coding-nonsynonymous: I201L
	chrXVI:167064	<i>TPK2</i>	coding-nonsynonymous: P270R
	chrXVI:933898	<i>YPR197C</i>	coding-nonsynonymous: *188Y
	chrXIII:1-86512	Includes <i>PHO84</i>	LOH: loss of S288C allele
P9	chrXIII: 1-221882	Includes <i>PHO84</i>	LOH, multiple tract lengths, loss of S288C allele
P9F	chrXIII: 1-76194	Includes <i>PHO84</i>	LOH: loss of S288C allele
P10	chrXIII: 1-221882	Includes <i>PHO84</i>	LOH, multiple tract lengths, loss of S288C allele
G3F	chrIV: 971450	<i>RKM4</i>	coding-nonsynonymous: E9Q
	chrIV: 1214351	<i>YPR1</i>	coding-nonsynonymous: T150P
	chrXVI: 166845	<i>TPK2</i>	coding-nonsynonymous: E197A
	chrXVI:24965-376139		LOH: loss of S288C
G4	chrXVI: 166595	<i>TPK2</i>	coding-nonsynonymous: H114N
	chrIX: 1- 439888		CNV: whole chromosome amplification of S288C
	chrV: 374386-576874		LOH: loss of S288C
G4F	chrIV: 857504	<i>RAV2</i>	coding-nonsynonymous: F150L
	chrV: 374386-576874		LOH: loss of S288C
	chrIX: 1- 439888		CNV: whole chromosome amplification of S288C
	chrXIII: 742394	<i>RNA1</i>	coding-nonsynonymous: N114N
	chrXVI: 166595	<i>TPK2</i>	coding-nonsynonymous: H114N
G6	chrII:211737	<i>HIR1</i>	coding-nonsynonymous: G695indel
	chrVI: 71469	<i>RIM15</i>	coding-nonsynonymous: P987S
	chrVII: 624765	<i>YGR067C</i>	coding-nonsynonymous: Y8N
	chrXII:1-388272		LOH: loss of GRF167 allele
	chrXII:537901-1078177		LOH: loss of S288C allele
	chrXII:202237	<i>RPL15A</i>	coding-synonymous: S118S
	chrXV:587229	<i>YOR139C</i>	coding-synonymous: H38H
	chrXV:587229	<i>SFL1</i>	coding-nonsynonymous: W83*
	chrM:27782	<i>ATP8</i>	coding-synonymous: Y39Y
	G6F	chrVI: 71469	<i>RIM15</i>

Table B.2. Mutations in cold-evolved *S. uvarum* diploid populations.

Population	Location	Gene(s)	Mutation
G1	chrII:1-1289935		CNV: whole chromosome amplification
	chrX: 1-1016005		CNV: whole chromosome amplification
	chrXII: 1-445542		CNV: whole chromosome amplification
S2	<i>S. uvarum</i> chrXII: 111565	<i>CYRI</i>	coding-nonsynonymous: R1343C

CNV: copy number variant. No mutations were detected in P11, P12, G2, S1.

Table B.3. Comparison of single nucleotide variants called in 15°C and 30°C experimental evolution.

		Number of SNPs and InDels					
		Hybrid			Parental species		
		<i>S. cer</i>	<i>S. uva</i>	Total	<i>S. cer</i>	<i>S. uva</i>	Total
15°C	Populations	12	7	19	19	1	20
	Floc. Clones	1	1	2	34	0	34
30°C	Clones	16	14	40	7	12	19

Table B.4. Strain list.

Strain	Identifier	Genotype	Species	Notes	Strain background
YMD139		<i>lys2Δ0/LYS2 ura3-167/URA3 MATa/MATα</i>	cer	Ancestor of <i>S. cerevisiae</i> evolved diploids (high Ty)	GRF167 x S288C
YMD140		<i>lys2Δ0/LYS2 ura3-167/URA3 MATa/MATα</i>	cer	Ancestor of <i>S. cerevisiae</i> evolved diploids	GRF167 x S288C
YMD129		<i>HOA::kanMX/HOA::kanMX lys2-1/ LYS2 ura3-167/URA3 MATa/MATα</i>	hybrid	Ancestor of evolved hybrids	GRF167 x CBS7001
YMD130		<i>HOA::kanMX/HOA::kanMX lys2-1/ LYS2 ura3-167/URA3 MATa/MATα</i> (high Ty)	hybrid	Ancestor of evolved hybrids (high Ty)	GRF167 x CBS7001
YMD366		<i>HOA::kanMX /HOA::kanMX lys2-1/ LYS2 ura3Δ::cloNAT/URA3 MATa/MATα</i>	uva	Ancestor of <i>S. uvarum</i> evolved diploids	CBS7001
	G1		uva	Glucose limitation, 15°C	YMD366
	G2		uva	Glucose limitation, 15°C	YMD366
	G3F		cer	Glucose limitation, 15°C	YMD139
	G4		cer	Glucose limitation, 15°C	YMD139
	G4F		cer	Glucose limitation, 15°C	YMD139
	G6		cer	Glucose limitation, 15°C	YMD140
	G6F		cer	Glucose limitation, 15°C	YMD140
	G7		hybrid	Glucose limitation, 15°C	YMD130
YMD3928	G7 c1		hybrid	Glucose limitation, 15°C	YMD130
YMD3929	G7 c2		hybrid	Glucose limitation, 15°C	YMD130
	G8		hybrid	Glucose limitation, 15°C	YMD130
YMD3930	G8 c1		hybrid	Glucose limitation, 15°C	YMD130
YMD3931	G8 c2		hybrid	Glucose limitation, 15°C	YMD130
	G9		hybrid	Glucose limitation, 15°C	YMD129
YMD3932	G9 c1		hybrid	Glucose limitation, 15°C	YMD129
YMD3933	G9 c2		hybrid	Glucose limitation, 15°C	YMD129
	G10		hybrid	Glucose limitation, 15°C	YMD129

Table B.5. Competitive fitness of evolved hybrid strains.

Population Identifier	Original evolution conditions	Competitive Fitness at 15°C (+/- 95% C.I.)	Competitive Fitness at 30°C (+/- 95% C.I.)
G7-15°	Glucose limitation, 15°C	C1: -0.66 C2: 6.37 (+/-50.27)	C1: 1.86 C2: 6.63 (+/-17.66)
G8-15°	Glucose limitation, 15°C	C1: 2.65 (+/-10.79) C2: 14.83 (+/-46.16)	C2: 2.07 (+/-49.67)
G9-15°	Glucose limitation, 15°C	C1: 6.40 (+/-3.55) C2: 11.76	C1: 10.10 (+/-35.96) C2: -2.45 (+/-21.37)
G10-15°	Glucose limitation, 15°C	C1: 5.14 (+/-0.36)	C1: 13.06 (+/-58.47)
S7-15°	Sulfate limitation, 15°C	C1: 7.43 (+/-3.47) C2: 28.52 (+/-18.04)	C1: 23.66 C2: 30.12 (+/-129.57)
S8-15°	Sulfate limitation, 15°C	C1: 18.55 (+/-46.41) C2: 30.85 (+/-15.04)	C1: 39.38 (+/-15.94) C2: 37.47 (+/-9.72)
S9-15°	Sulfate limitation, 15°C	C1: 7.40 (+/-55.15)	C1: 12.54 (+/-47.03)
S10-15°	Sulfate limitation, 15°C	C1: 12.26 (+/-16.05)	C1: 41.01 (+/-51.94)
P1-15°	Phosphate limitation, 15°C	C1: 7.38 (+/-1.52) C2: 10.01 (+/-1.96)	C1: -4.81 (+/-5.14) C2: 0.40 (+/-10.07)
P2-15°	Phosphate limitation, 15°C	C1: -1.83 (+/-5.08) C2: -1.93(+/-1.16)	C1: -3.82 (+/-8.73) C2: 9.34 (+/-9.70)
P3-15°	Phosphate limitation, 15°C	C1: 8.34 (+/-3.67) C2: 5.13 (+/-2.76)	C1: -7.59 (+/-6.58) C2: 0.76 (+/-29.25)
P4-15°	Phosphate limitation, 15°C	C1: 0.07 (+/-3.18) C2: -3.50 (+/-44.24)	C1: 14.87 (+/-28.11) C2: -0.58 (+/-32.39)
P5-15°	Phosphate limitation, 15°C	C1: 16.46 (+/-11.85) C2: 10.23 (+/-15.04)	C1: 10.48 (+/-14.72)
P6-15°	Phosphate limitation, 15°C	C1: 10.09 (+/-7.72) C2: 6.90 (+/-10.01)	C1: 10.49 (+/-18.45)
P1-30°	Phosphate limitation, 30°C	21.01	29.18 (+/-17.42)

Table B.6. Filters used in variant calling.

Samtools Filter Parameters

Type	Shorthand	Value
Mapping quality	MQ	>30
Quality score	QUAL	>50
Read depth	DP	>40
Alternate read count	DP4[2]+DP4[3]	>4
Forward read balance	(DP4[0]+DP4[2])/DP	>0.01
Reverse read balance	(DP4[1]+DP4[3])/DP	>0.01

Freebayes Filter Parameters

Type	Shorthand	Value
Mapping quality of observed alternate alleles	MQM	>30
Mapping quality of observed reference alleles	MQMR	>30
Quality score	QUAL	>20
Read depth	DP	>40
Forward strand alternate read count	SAF	>2
Reverse strand alternate read count	SAR	>2
Forward read balance	SRF + SAF / DP	>0.01
Reverse read balance	SRR + SAR / DP	>0.01

LoFreq Filter Parameters

Type	Shorthand	Value
Quality score	QUAL	>20
Read depth	DP	>20
Forward strand alternate read count	DP4[2]	>2
Reverse strand alternate read count	DP4[3]	>2
Forward read balance	(DP4[0]+DP4[2])/DP	>0.01
Reverse read balance	(DP4[1]+DP4[3])/DP	>0.01

APPENDIX C: Supplementary materials for Chapter 4

C.1. *Relationship and ancestry of the American brewing strains*

The history of the American brewing strains as told by brewers originates from just a handful of breweries. The Chico yeasts are specifically thought to originate from a ‘house-strain’ of the Sierra Nevada Brewing Company’s isolate of BRY-96, which is sold by the Siebel Institute. BRY-96 itself is thought to originate from P. Ballantine and Sons Brewing Company, which started in 1840 in Newark, New Jersey. The strain has since been distributed to a large number of breweries and yeast propagation companies. To provide a fuller picture of the genetic history of the American brewing yeasts, we collected not just the strains used by our brewery partners but also new clone samples of American brewing strains that are available for purchase and not believed to have been previously sequenced. In all, we sequenced 13 American brewing strains, and reanalyzed an additional 17 strains that had previously been sequenced using short-read sequencing (**Table C.3**). Wanting to confirm the relationships between our study cohort, we applied phylogenetic inference on the strains. From their whole-genome sequence, we built a maximum likelihood tree based on the variation between these strains. However, as mentioned earlier, because there has been extensive mitotic recombination in these yeasts, we suspected that phylogenetic inference could be influenced by large blocks of shared, ancestral variation being lost. To avoid this issue, we filtered the American brewery strains variant calls by the most diverged American strain, BE051, to control for the potential loss of shared variation. As well, to encapsulate the polyploid nature of the beer strains, we encoded heterozygous variation in the genome sequences for phylogenetic inference (see methods in **Chapter 4** for more details).

Matching with oral history, we found from our constructed phylogeny that Wyeast 1056 (Postdoc Brewing Co.), Imperial A07 (Postdoc Brewing Co.), White Labs WLP001 (Drake’s

Brewing Co.) and Escarpment's Cali Ale (Red Circle Brewing Co.), and other Chico yeasts are all closely related and form two large clades (**Figure C.1**). As well, we found that the WLP001 and Wyeast 1056 clades are likely derived from BRY-96 (Elysian Brewing Co.), as there is only an 11 SNP difference between a reconstructed common ancestor of the two Chico strains and an isolate of what is thought to be the original BRY-96 (kindly donated by Lallemand Inc.). Additionally, from a sequenced isolate of a strain from P. Ballantine and Sons Brewing Company that was deposited in a strain repository in 1972 (NRRL Y-7408), we found that this strain groups outside of the rest of the American brewing strains, indicating that it is indeed a diverged American brewing strain. However, because large segments of variation are lost from NRRL Y-7408 that exist in the internal American brewing strains, we suspect that this particular Ballantine isolate is not the literal genetic ancestor. However, this does not conclusively rule out Ballantine Brewing as the source of BRY-96 as the NRRL Y-7408 could have been isolated before or after the sample leading to BRY-96, making the observed pattern.

C.2. Records on recipe and fermentation performance of repitching experiments

As is common with most breweries, the same recipe was not used for each beer pitch, resulting in a potentially changing environment for the yeasts. Although these experiments are less controlled than traditional laboratory evolution experiments, they provide a more realistic capture of the brewing environment. For the Postdoc Brewing Co. experiments, the order of different styles that the yeast went through is available in **Table C.2**. As well, for the Elysian samples, data collected at the brewery about the fermentation performance of each beer are available in **Table C.3**.

C.3. De novo single nucleotide polymorphisms, insertions, and deletions

Using multiple computational tools, we called *de novo* mutations that occurred during each repitching time course. Within the first replicate of the Postdoc Brewing Co. populations we did not find any *de novo* SNP or InDel that occurred during the course of the repitching experiment and reached a detectable frequency (estimated detection limit of ~2% of alternate reads). Using sequencing of clones isolated from the first time point to filter the variant calls from the populations, we found 11 mutations that were shared by all of the Postdoc Brewing Co. time points and had occurred in the population before entering the brewery based on the sequences from the clone isolates, the population from the second Postdoc Brewing Co. replicate, and the Imperial A07 clone isolate. Calculating the change in frequency of these mutations over the time course, we found that the only mutation that changed by more than a 1% increase in the population was a synonymous mutation in *PTC6* (which increased from 25.2% to 44.4% in the population, **Table C.4**). While it is known that synonymous mutations can impact traits, it's more likely that this is a passenger mutation, particularly since the mutation affects only one allele in a pentaploid region of the genome. We additionally observed a number of private SNPs and InDels within clones from both the first and last time points, with an average of 11.9 mutations per clone and a total of 177 unique mutations (**Table C.5**).

Expanding our analysis to the samples from the other collaborations, we found a total of 106 mutations, with an overall average of 15.1 mutations observed in each population (**Table C.5**). Looking for evidence of adaptive evolution through convergence of mutations, we found that between experiments, there were 5 genes wherein multiple mutations were observed in the coding sequence between experiments (**Table C.6**). We note that mutations in *UBP1*, which encodes a ubiquitin protease, were previously identified in experimental evolution of a lager strain (Gibson et al., 2018), and mutations in *TFBI*, a nucleotide excision repair factor and subunit of TFIIH,

were found in strains that had survived for two years in a sealed beer bottle (Aouizerat et al., 2019). However, in neither of these cases were phenotypic consequence proven. Further experiments recreating these mutations in clean genetic backgrounds will be necessary to determine their impact.

C.4. *Soft sweep chromosome V CNV further indicates adaptive benefit*

Wanting to determine whether the potential benefit of the aneuploidy was due to an increase in copy number of a particular haplotype or a restoration of a euploid copy number for dosage balance, we investigated whether one particular copy of chromosome V was recurrently amplified between populations. Our expectation is that gaining a chromosome copy will change the allele frequency of heterozygous variants by a change in the proportion of haplotypes. Through investigation of the direction that variants change allele frequency, we can determine which chromosome is amplified (See **Figure 4.1** for allele frequency plot description). Therefore, we investigated whether the allelic ratio between haplotypes had changed by plotting the allele frequency of variants on chromosome V for the two Postdoc Brewing Co. and Drake's Brewing Co. experiments. However, upon plotting the allele frequency from the first and last time points we found very little to no change had occurred despite the chromosome copy number change (**Figure C.2**).

From a clone isolated from the final population of the Postdoc Brewing Co., replicate 1 experiment that had an extra copy of chromosome V, we found that, in a clonal sample, as expected, the allele frequency does change and shows three large chromosomal regions with different allele frequency patterns. The clone helped show that the starting strain has three haplotypes on the left arm, two in the middle in a 2:1 ratio and is homozygous on the right arm.

Given these patterns, we expect that depending on which chromosome was amplified, the allele frequency will shift according to the number of haplotypes (Left: 0.33/0.66 to 0.25/0.50/0.75; Center: 0.33/0.66 to 0.25/0.75 or 0.50; Right: No change, summarized on the right of **Figure C.2**). However, because the allele frequency pattern did not change in a significant manner, we instead concluded that there are likely multiple mutation events, each of which amplified a different chromosome V haplotype. These independent mutations have occurred in separate lineages that have risen in frequency with similar kinetics. Therefore, we conclude that the increase in copy number of chromosome V occurred multiple times in both Postdoc Brewing Co. replicates, indicating a haplotype independent fitness benefit.

The experiment(s) at Elysian Brewing Co. utilized BRY-96, which already contained 4 copies of chromosome V and did not show any additional evidence of whole chromosome CNV. It is likely that the ancestral state of chromosome V is euploid based on the phylogenetic relationship between the American brewing strains (**Figure C.1**).

C.5. *Additional mitotic recombination events in the beer brewing strains*

We additionally observed chromosomes XII and XV experiencing convergent mitotic recombination events in 6 and 4 of the other populations respectively (**Figure C.5**). After noting the mitotic recombination on chromosome XII in the other populations, we noticed that the first Postdoc Brewing Co. replicate likely had a similar event nearly fix in the population before it entered the brewery as one of the starting clones, Postdoc Brewing Co., timepoint 1 clone 1, did not have the allele frequency change. Using the clone that did not have the allele frequency change, we looked for any variation that experienced a LOH as a result of the mitotic recombination as this is the most likely source of an adaptive benefit for a mitotic recombination. However, through

computational and manual inspection, we determined that no variation was lost as a result of the chromosome XII mitotic recombination (though other explanations are possible as well, such as allele copy number changes). Notably, the right arm of chromosome XII has been observed to have the highest amount of homozygosity among natural and industrial strains of yeast, potentially due to the presence of the rDNA locus on chromosome XII (Peter et al., 2018).

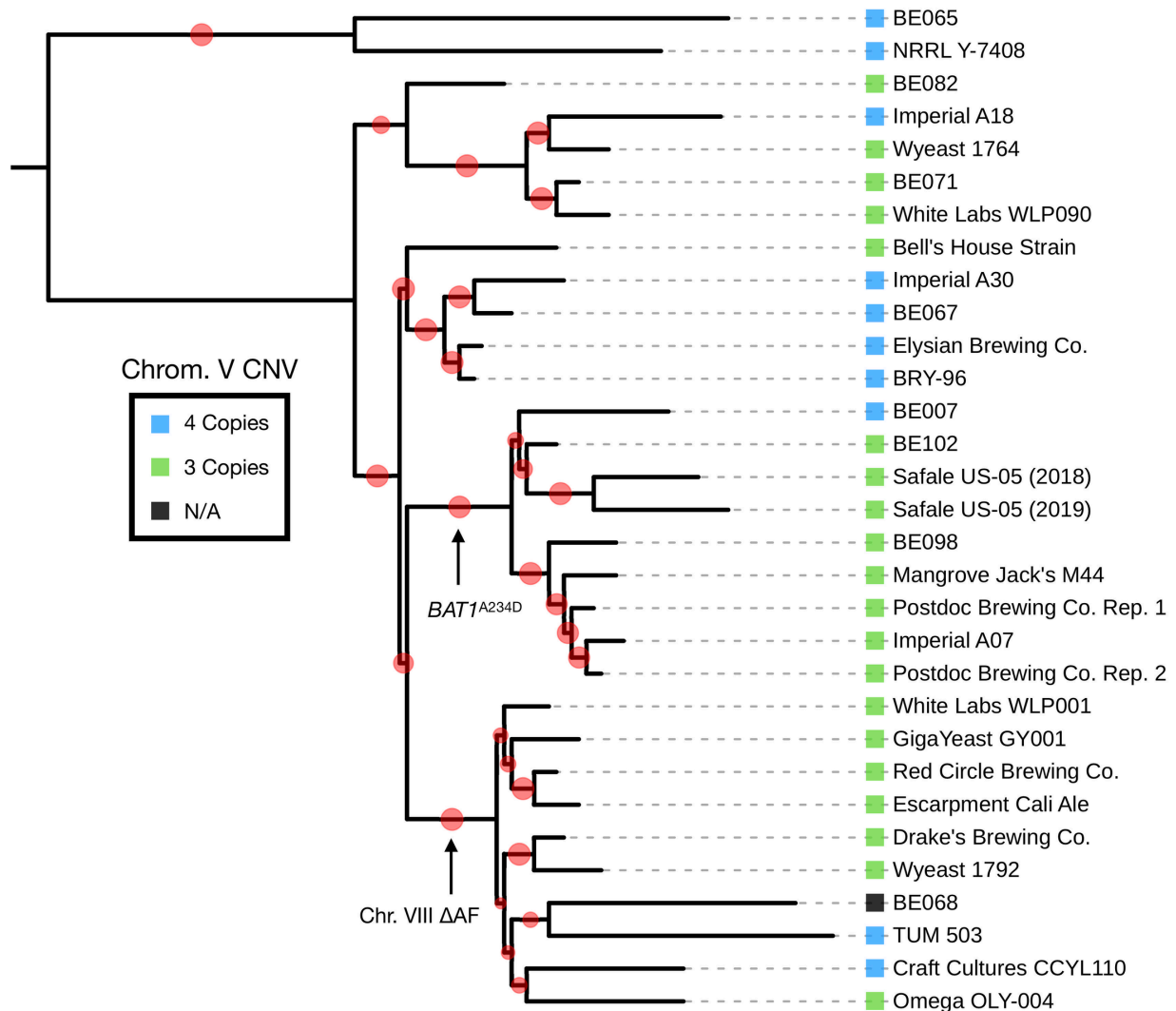


Figure C.1. A maximum-likelihood phylogeny of the American brewing strains reveals several large clades. Specifically, two Chico yeast groups, and their presumed genetic ancestor, BRY-96 were found to group with other commercially available strains. The branch support bootstrap values are displayed in red on the adjoining branch, with smaller values corresponding to less support.



Figure C.2 Allele frequency of the Postdoc Brewing Co. replicate 1 population and a clone isolated from that population showing the number and pattern of haplotypes on chromosome V. The lack of a shift in allele frequency indicates that in the population, multiple lineages likely independently had different haplotypes amplified. The probability of any given haplotype being amplified is displayed on the right.

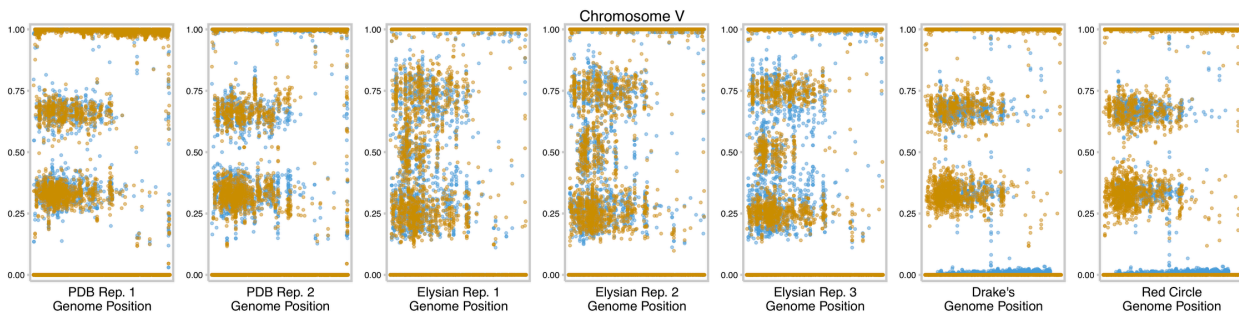


Figure C.3. Allele frequency of chromosome V for every brewery population. The first timepoint is colored in blue and the final timepoint in orange.

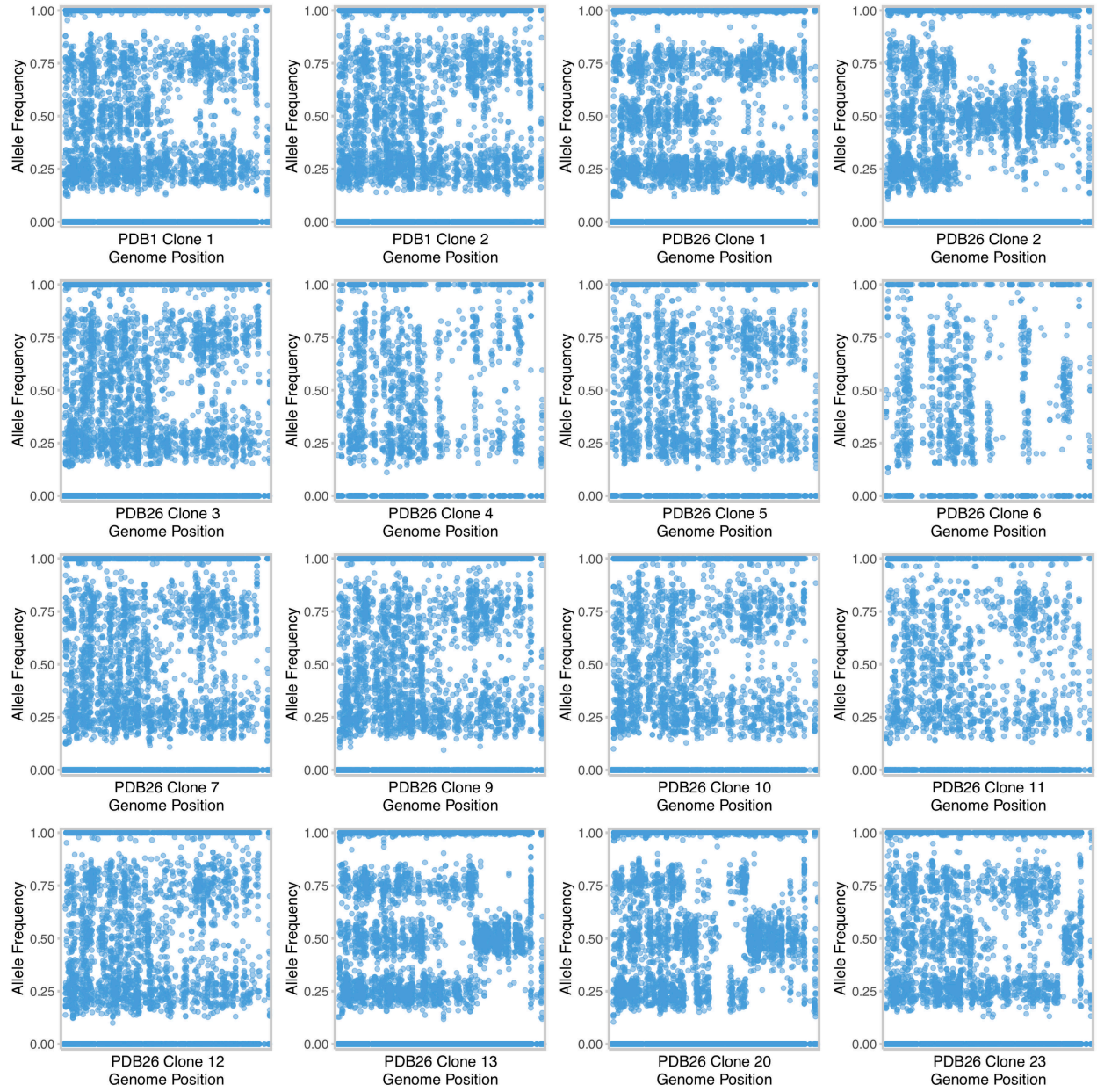


Figure C.4. Allele frequency of chromosome VIII for clones isolated from the first Postdoc Brewing Co. replicate.

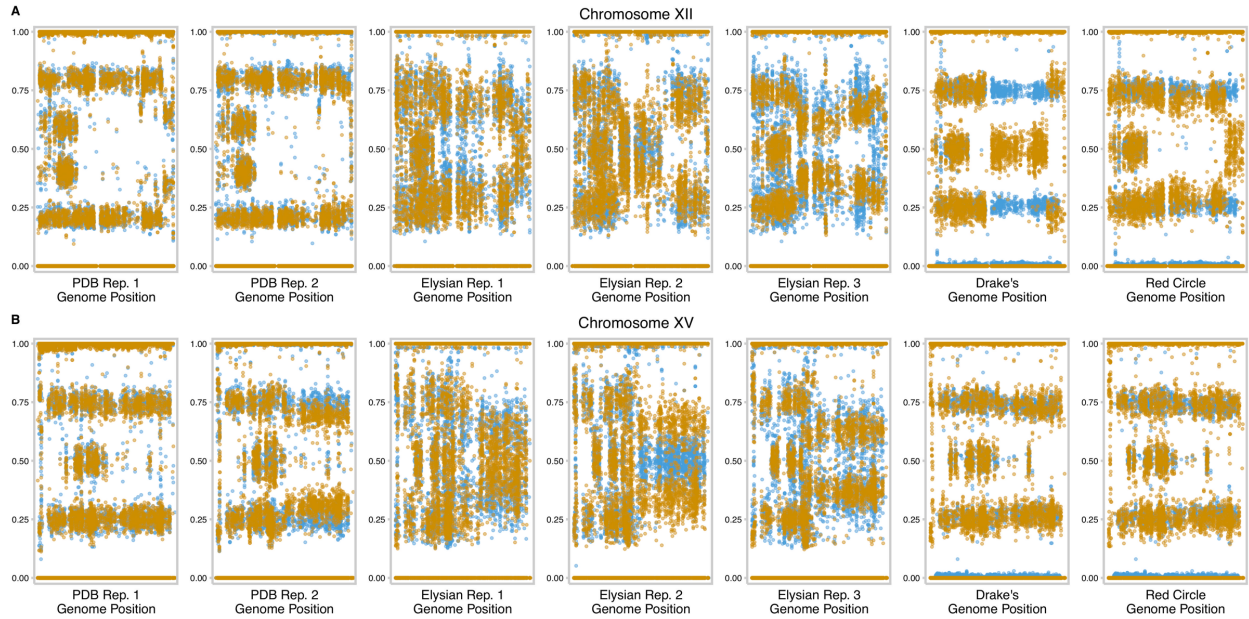


Figure C.5. Allele frequency of chromosome XII and XV for every brewery population. The first timepoint is colored in blue and the final timepoint in orange.

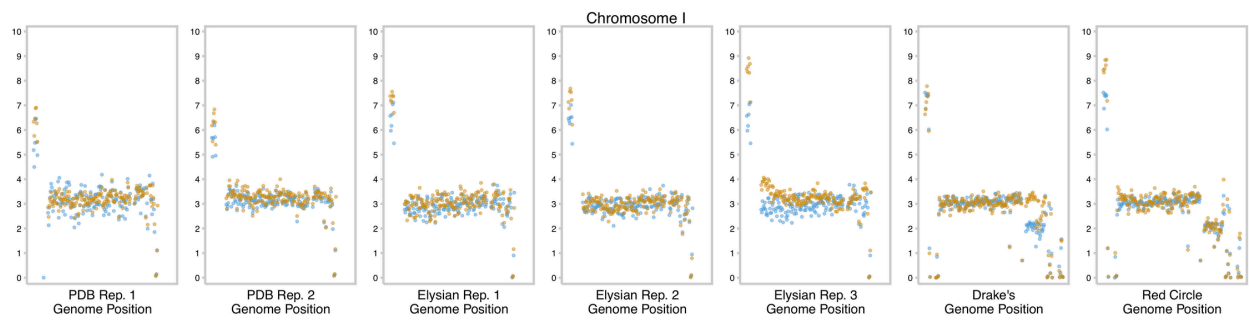


Figure C.6. Copy number of chromosome I for every brewery population showing an increase at the left terminal end for every population that experienced a mitotic recombination event. Each dot represents a 1000-bp sliding window, normalized by the average genome copy number. The first timepoint is colored in blue while the final timepoint is in orange.

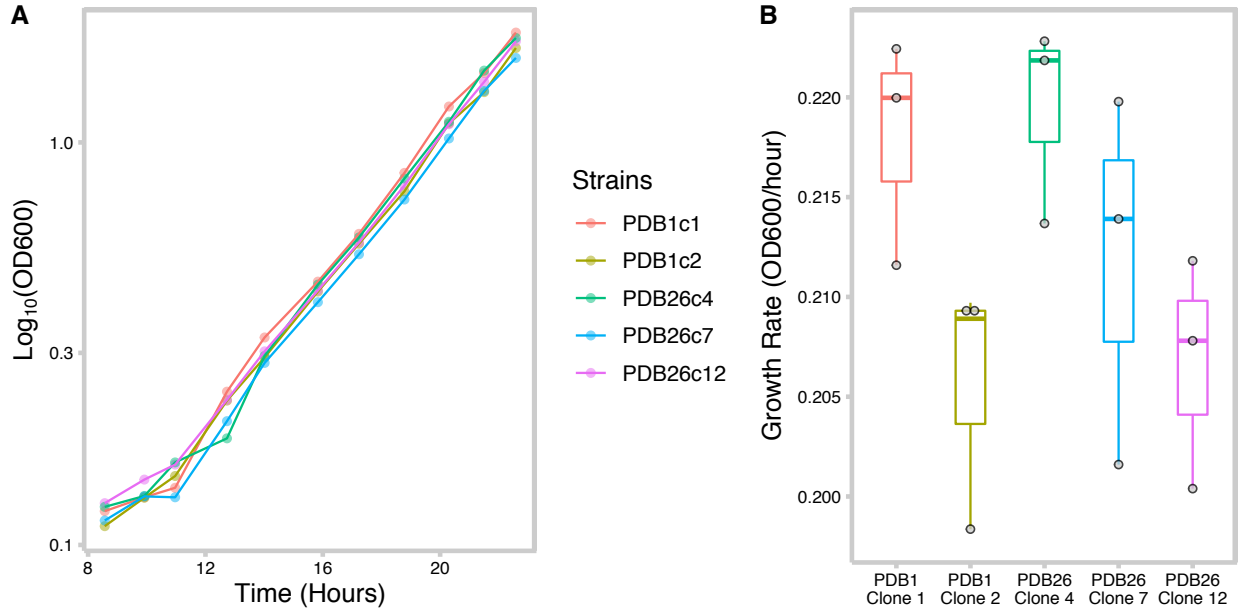


Figure C.7. Growth rate measurements of brewery isolates from the first Postdoc Brewing replicate indicating no change in growth patterns. Each strain was grown in triplicate from a single colony and cultured aerobically in wort medium at room temperature. The growth rate (shown in panel B) was calculated from the data presented in panel A using the GrowthRates package in the R programming language.

Table C.1. Record of repitching populations from Postdoc Brewing Co.

Sample number	PopulationID	Replicate	Beer Style	Repitch #
PD01	PDB1	1	None	0
PD05		1	Pale Ale	1
PD03		1	Porter	2
PD11		1	Pale Ale	3
PD07		1	IPA	4
PD06		1	Blonde	5
PD09	PDB6	1	Scottish	6
PD12		1	Porter	7
PD13		1	Amber	8
PD14		1	IIPA	9
PD15		1	Porter	10
PD17		1	Pale	11
PD19		1	Scottish	12
PD20		1	Scottish	13
PD22		1	Blonde	14
PD24	PDB15	1	Pale	15
PD26		1	Amber	16
PD27		1	Scottish	17
PD30		1	Pale	18
PD34	PDB19	1	Alpha	19
PD35		1	Pale	20

PD39		1	Alpha	21
PD40		1	Blonde	22
PD42		1	IPA	23
N/A		1	N/A	24
PD45		1	IPA	25
PD48	PDB26	1	Pale	26
PD68	PDB1_Rep_2	2	Pale	1
PD70		2	IPA	2
PD75		2	Scottish	3
PD74		2	IPA	4
PD71		2	Pale	5
PD76		2	Blonde	6
PD78		2	Stout	7
PD82		2	IPA	8
PD83		2	Pale	9
PD84		2	IPA	10
PD88		2	Blonde	11
PD91		2	IPA	12
PD92		2	Scottish	13
PD96		2	Blonde	14
PD98		2	IPA	15
N/A		2	Pale	16
PD104		2	IPA	17
PD107		2	IPA	18
PD110		2	Blonde	19
PD112		2	IPA	20
PD116		2	Blonde	21
PD121		2	Gose	22
PD120		2	Porter	23
PD125		2	IPA	24
PD129		2	Pale	25
PD131		2	IPA	26
PD137		2	IPA	27
PD138		2	Stout	28
PD140	PDB29_Rep_2	2	Blonde	29

Table C.2. Record of repitching populations from Elysian Brewing Co.

Repitch #	PopulationID	Replate	Original Gravity	Final Gravity (AE)	RDF
1	E01	1	13.64	3.09	64.14
2		1	19	4.03	66.05
3		1	19.9	5.05	62.89
4		1	18.95	3.87	66.68
5		1	12.63	2.81	64.37
6		1	13.64	2.85	65.54

7		1	18.97	3.83	66.86
8		1	20	4.95	63.28
8		1	14.59	2.98	66.42
10		1	18.28	3.614	80.23
11		1	14.88	3.1	65.78
12		1	14.82	3.28	64.75
13		1	13.47	3.1	63.89
14		1	14.1	2.75	N/A
15	E03	1	13.47	2.95	64.72
1		2	18.51	3.65	67.161
2		2	14.28	2.77	66.839
3		2	19.88	4.815	63.796
4		2	13.55	3.09	64.037
5		2	18.23	3.7	66.7
6		2	18.29	3.434	67.881
7		2	15.38	3.08	66.481
8		2	14.92	3.29	64.83
9		2	14.82	3.05	65.968
10		2	15.46	3.04	66.759
11		2	15.36	3.17	66.001
12		2	15.38	3.08	66.506
13		2	18.31	3.267	68.624
14		2	14.85	3.18	65.287
15	E08	2	15.41	3.06	66.6
16		2	18.47	3.176	69.15
17	E09	2	N/A	N/A	N/A
1	E05	3	15.37	3	66.619
2		3	13.33	3.032	64.039
3		3	15.26	3.39	65.264
4		3	15.28	3.12	66.177
5		3	15.38	3.09	66.419
6		3	14.42	2.9	2.901
7		3	15.38	3	66.419
8		3	15.34	2.963	67.054
9		3	14.85	2.9	66.841
10		3	18.08	3.28	68.357
11		3	18.93	3.63	67.663
12		3	18.32	3.13	69.233
13		3	18.42	3.28	68.675
14	E10	3	18.88	3.833	66.759

Table C.3. Record of samples used in Figure C.1

StrainID	StrainID	StrainName	FromStudy
ERX1380630	ERS1082766	SafAle US-05 (2018)	Peter

SRR10047107	SRS5328257	Wyeast1792	Langdon
SRR10047299	SRS5328195	SafAle US-05 (2019)	Langdon
SRR2968036	SRS1184859	WLP001	Borneman
SRR5678596	SRS2280390	BE007	Gallone
SRR5688154	SRS2280340	BE051	Gallone
SRR5688182	SRS2280392	BE065	Gallone
SRR5688186	SRS2280394	BE067	Gallone
SRR5688188	SRS2280395	BE068	Gallone
SRR5688194	SRS2280383	BE071	Gallone
SRR5688216	SRS2280445	BE082	Gallone
SRR5688248	SRS2280428	BE098	Gallone
SRR5688256	SRS2280404	BE102	Gallone
SRR7406282	SRR7406282	Escarpment Cali Ale	Preiss
SRR8172945	SRS4029082	Wyeast 1764	Fay
ERR1352858	ERS1108626	TUM 503	Goncalves
ERX1380252	ERS1082772	WLP090	Peter
YMD3211	YMD3211	GY001	Large
YMD3965	YMD3965	OYL004	Large
YMD3971	YMD3971	MangroveJack M44	Large
YMD3975	YMD3975	CCYL110	Large
YMD3977	YMD3977	Bell's House Strain	Large
YMD3978	YMD3978	Siebel BRY-96	Large
YMD3980	YMD3980	Drake's Breiwnng Co.	Large
YMD3984	YMD3984	Imperial A18	Large
YMD3985	YMD3985	Imperial A30	Large
YMD3986	YMD3986	Imperial A07	Large
E01	E01	Elysian Brewing Co.	Large
PDB1	PDB1	Postdoc Brewing Rep. 1	Large
PDB68	PDB68	Postdoc Brewing Rep. 2	Large

Table C.4. The frequencies of recurrent mutation during Postdoc Brewing replicate 1

Chr	Pos	Mutation	Gene	Gen. 0	Gen. 6	Gen. 15	Gen. 19	Gen. 26	Change	Change Ploidy 4
chrII	564578	5'-upstream	YBR162C	0.06	0.02	0.06	0.09	0.05	-0.01	-0.03
chrIII	248944	5'-upstream	YCR075C	0.02	0.02	0.01	0.00	0.01	0.00	-0.02
chrIII	254131	synonymous	YCR079W	0.05	0.06	0.05	0.06	0.09	0.04	0.15
chrXIV	213174	nonsynonymous	YNL233W	0.07	0.10	0.10	0.09	0.07	-0.01	-0.02
chrXIV	49495	nonsynonymous	YNL311C	0.06	0.03	0.07	0.06	0.06	0.00	-0.01
chrXVI	44064	nonsynonymous	YPL264C	0.02	0.02	0.02	0.00	0.03	0.00	0.00
chrIV	821800	nonsynonymous	YDR180W	0.03	0.04	0.11	0.06	0.03	0.00	0.01

chrIX	225225	nonsynonymous	YIL073C	0.08	0.06	0.05	0.07	0.08	0.00	-0.01
chrVII	405858	nonsynonymous	YGL050W	0.05	0.07	0.09	0.10	0.05	0.00	0.01
chrXI	245205	nonsynonymous	YKL104C	0.09	0.08	0.07	0.04	0.08	-0.01	-0.05
chrXV	720452	nonsynonymous	YOR199W	0.10	0.04	0.07	0.07	0.08	-0.01	-0.05

Table C.5. Mutations in populations and clones

Sample	Chr	Pos	Mutation Type	Formal	Gene	Effect	AF
Elysian03	chrIV	467441	nonsynonymous	YDR011W	SNQ2	T508N	0.12
Elysian03	chrIV	1181396	intergenic	NA	NA	NA	0.08
Elysian03	chrVII	216509	nonsynonymous	YGL153W	PEX14	M79I	0.12
Elysian03	chrXII	884019	nonsynonymous	YLR382C	NAM2	A245T	0.11
Elysian03	chrXII	905505	synonymous	YLR392C	ART10	N267N	0.18
Elysian03	chrXIII	224450	nonsynonymous	YML025C	YML6	A273S	0.16
Elysian03	chrXV	130923	nonsynonymous	YOL100W	PKH2	G563S	0.19
Elysian03	chrXV	429612	synonymous	YOR055W	YOR055W	G45G	0.23
Elysian03	chrXV	432347	synonymous	YOR057W	SGT1	G54G	0.22
Elysian03	chrXV	914680	nonsynonymous	YOR320C	GNT1	S139P	0.16
Elysian05	chrV	257694	nonsynonymous	YER052C	HOM3	I89F	0.09
Elysian07	chrXV	366694	nonsynonymous	YOR018W	ROD1	F776I	0.06
Elysian08	chrVI	87991	synonymous	YFL024C	EPL1	Q785Q	0.34
Elysian08	chrVI	88000	synonymous	YFL024C	EPL1	Q782Q	0.29
Elysian08	chrXII	851986	synonymous	YLR362W	STE11	L707L	0.05
Elysian08	chrXII	853078	nonsynonymous	YLR363C	NMD4	S25L	0.06
Elysian08	chrXII	905987	nonsynonymous	YLR392C	ART10	P107S	0.05
Elysian08	chrXIII	114453	nonsynonymous	YML076C	WAR1	S299A	0.04
Elysian08	chrXIV	494616	intron	YNL069C	RPL16B	NA	0.06
Elysian08	chrXV	712945	nonsynonymous	YOR195W	SLK19	S27*	0.07
Elysian08	chrXV	774369	intergenic	NA	NA	NA	0.08
Elysian08	chrXVI	725156	5'-upstream	YPR096C		NA	0.05
Elysian09	chrI	40062	nonsynonymous	YAL056W	GPB2	I268M	0.14
Elysian09	chrIII	198188	synonymous	YCR038C	BUD5	S454S	0.11
Elysian09	chrIII	218916	synonymous	YCR054C	CTR86	L384L	0.08
Elysian09	chrIV	188256	nonsynonymous	YDL148C	NOP14	Y777*	0.10
Elysian09	chrIV	308486	intron	YDL082W	RPL13A	NA	0.02
Elysian09	chrVII	981698	nonsynonymous	YGR245C	SDA1	P124R	0.03
Elysian09	chrVIII	35723	synonymous	YHL033C	RPL8A	T101T	0.04
Elysian09	chrX	288072	synonymous	YJL080C	SCP160	S385S	0.09
Elysian09	chrX	645314	nonsynonymous	YJR119C	JHD2	P393S	0.12
Elysian09	chrXII	585083	nonsynonymous	YLR223C	IFH1	E136D	0.25

Elysian09	chrXII	605041	intergenic	NA	NA	NA	0.12
Elysian09	chrXIV	413954	nonsynonymous	YNL112W	DBP2	H106D	0.07
Elysian09	chrXIV	698423	nonsynonymous	YNR039C	ZRG17	T337P	0.09
Elysian09	chrXV	425669	nonsynonymous	YOR051C	ETT1	S139N	0.13
Elysian09	chrXV	618740	intergenic	NA	NA	NA	0.16
Elysian09	chrXVI	165834	intergenic	NA	NA	NA	0.14
Elysian09	chrXVI	725156	5'-upstream	YPR096C	YPR096C	NA	0.14
Elysian10	chrIV	188256	nonsynonymous	YDL148C	NOP14	Y777*	0.13
Elysian10	chrIV	1085392	nonsynonymous	YDR311W	TFB1	R110W	0.11
Elysian10	chrIV	1283152	nonsynonymous	YDR406W	PDR15	A1315S	0.09
Elysian10	chrXI	228939	nonsynonymous	YKL110C	KTI12	*314C	0.09
Elysian10	chrXVI	245905	nonsynonymous	YPL161C	BEM4	D106N	0.09
Elysian10	chrXVI	691609	nonsynonymous	YPR072W	NOT5	R501S	0.12
PDB29	chrIV	244970	nonsynonymous	YDL122W	UBP1	D807Y	0.10
PDB29	chrIV	494647	intergenic	NA	NA	NA	0.12
PDB29	chrIV	1474219	nonsynonymous	YDR515W	SLF1	S264L	0.05
PDB29	chrVI	33375	nonsynonymous	YFL050C	ALR2	R825K	0.10
PDB29	chrVII	89292	nonsynonymous	YGL215W	CLG1	H438D	0.07
PDB29	chrXI	245205	nonsynonymous	YKL104C	GFA1	G57R	0.12
PDB29	chrXV	435107	synonymous	YOR058C	ASE1	C413C	0.06
PDB1_c1	chrII	98224	nonsynonymous	YBL066C	SEF1	C631S	0.23
PDB1_c1	chrII	564578	5'-upstream	YBR162C	TOS1	NA	0.22
PDB1_c1	chrIII	248944	5'-upstream	YCR075C	ERS1	NA	0.19
PDB1_c1	chrIII	254131	synonymous	YCR079W	PTC6	T429T	0.28
PDB1_c1	chrIV	64205	nonsynonymous	YDL220C	CDC13	M272L	0.25
PDB1_c1	chrX	282133	nonsynonymous	YJL082W	IML2	V317F	0.29
PDB1_c1	chrXI	543364	nonsynonymous	YKR054C	DYN1	S1521*	0.19
PDB1_c1	chrXIV	213174	nonsynonymous	YNL233W	BNI4	T418R	0.29
PDB1_c1	chrXV	352514	nonsynonymous	YOR011W	AUS1	D946H	0.19
PDB1_c1	chrXV	856724	nonsynonymous	YOR290C	SNF2	I1179V	0.27
PDB1_c2	chrI	53429	nonsynonymous	YAL048C	GEM1	I454N	0.27
PDB1_c2	chrII	727811	nonsynonymous	YBR256C	RIB5	V98F	0.23
PDB1_c2	chrIV	203874	nonsynonymous	YDL141W	BPL1	A279D	0.31
PDB1_c2	chrIV	761910	nonsynonymous	YDR150W	NUM1	F2095L	0.25
PDB1_c2	chrX	145224	nonsynonymous	YJL145W	SFH5	I22T	0.37
PDB1_c2	chrXIV	496764	nonsynonymous	YNL068C	FKH2	S509*	0.17
PDB1_c2	chrXV	434322	nonsynonymous	YOR058C	ASE1	T675K	0.25
PDB26_c1	chrI	67559	5'-upstream	YAL040C	CLN3	NA	0.27
PDB26_c1	chrIV	1000470	nonsynonymous	YDR266C	HEL2	N518indel	0.39

PDB26_c1	chrIX	77309	5'-upstream	YIL145C	PAN6	NA	0.28
PDB26_c1	chrIX	255387	synonymous	YIL053W	GPP1	I91I	0.19
PDB26_c1	chrVI	79652	nonsynonymous	YFL028C	CAF16	L188V	0.25
PDB26_c1	chrVII	314838	nonsynonymous	YGL099W	LSG1	Q70E	0.26
PDB26_c1	chrVII	864096	nonsynonymous	YGR184C	UBR1	S553F	0.18
PDB26_c1	chrVII	886856	nonsynonymous	YGR194C	XKS1	F340L	0.19
PDB26_c1	chrVIII	20627	nonsynonymous	YHL040C	ARN1	I115M	0.33
PDB26_c1	chrXII	825795	nonsynonymous	YLR347C	KAP95	D207Y	0.23
PDB26_c1	chrXII	849220	5'-upstream	YLR361C	DCR2	NA	0.14
PDB26_c1	chrXII	1003779	nonsynonymous	YLR432W	IMD3	D408G	0.16
PDB26_c1	chrXIII	780759	nonsynonymous	YMR257C	PET111	E425*	0.27
PDB26_c1	chrXIII	879965	nonsynonymous	YMR305C	SCW10	Q90*	0.23
PDB26_c1	chrXIV	49495	nonsynonymous	YNL311C	SKP2	D732N	0.27
PDB26_c1	chrXIV	237707	5'-upstream	YNL219C	ALG9	NA	0.35
PDB26_c1	chrXV	286970	nonsynonymous	YOL020W	TAT2	G267R	0.30
PDB26_c1	chrXV	755822	nonsynonymous	YOR220W	RCN2	K165N	0.22
PDB26_c1	chrXV	795069	nonsynonymous	YOR245C	DGA1	W88C	0.18
PDB26_c1	chrXVI	551574	synonymous	YPL004C	LSP1	T28T	0.27
PDB26_c10	chrII	732024	nonsynonymous	YBR259W	YBR259W	N546K	0.24
PDB26_c10	chrIV	235004	synonymous	YDL127W	PCL2	T26T	0.24
PDB26_c10	chrIV	1172535	nonsynonymous	YDR349C	YPS7	S548T	0.25
PDB26_c10	chrX	531862	5'-upstream	YJR052W	RAD7	NA	0.34
PDB26_c10	chrXII	638535	nonsynonymous	YLR249W	YEF3	L586M	0.21
PDB26_c10	chrXIII	317369	nonsynonymous	YMR021C	MAC1	Y350*	0.38
PDB26_c11	chrIV	951223	nonsynonymous	YDR244W	PEX5	I221L	0.35
PDB26_c11	chrX	324069	synonymous	YJL060W	BNA3	V228V	0.32
PDB26_c11	chrXV	717837	nonsynonymous	YOR197W	MCA1	I251S	0.33
PDB26_c11	chrXVI	760998	nonsynonymous	YPR117W	YPR117W	W325*	0.20
PDB26_c12	chrII	11619	nonsynonymous	YBL106C	SRO77	P754Q	0.24
PDB26_c12	chrII	467376	nonsynonymous	YBR114W	RAD16	S43R	0.21
PDB26_c12	chrIV	724752	nonsynonymous	YDR135C	YCF1	V934L	0.34
PDB26_c12	chrIX	46046	5'-upstream	YIL158W	AIM20	NA	0.35
PDB26_c12	chrVIII	349166	nonsynonymous	YHR119W	SET1	R1042C	0.25
PDB26_c12	chrXVI	682496	nonsynonymous	YPR067W	ISA2	Q93E	0.29
PDB26_c13	chrII	75251	5'-upstream	YBL079W	NUP170	NA	0.32
PDB26_c13	chrII	110874	nonsynonymous	YBL059W	IAI11	A94E	0.30
PDB26_c13	chrIV	118481	synonymous	YDL191W	RPL35A	I109I	0.25
PDB26_c13	chrIV	1122367	synonymous	YDR326C	YSP2	H853H	0.25
PDB26_c13	chrVII	356350	nonsynonymous	YGL082W	YGL082W	S175Y	0.34

PDB26_c13	chrVII	955174	nonsynonymous	YGR233C	PHO81	Q1013*	0.24
PDB26_c13	chrVII	1044637	nonsynonymous	YGR276C	RNH70	V282F	0.26
PDB26_c13	chrVIII	262535	nonsynonymous	YHR079C-A	SAE3	Q7*	0.26
PDB26_c13	chrXI	258801	nonsynonymous	YKL097C	YKL097C	G38V	0.25
PDB26_c13	chrXIII	745338	nonsynonymous	YMR237W	BCH1	M530I	0.24
PDB26_c13	chrXIV	533617	nonsynonymous	YNL051W	COG5	Y320C	0.22
PDB26_c13	chrXVI	44064	nonsynonymous	YPL264C	YPL264C	R94L	0.28
PDB26_c2	chrIV	1364129	nonsynonymous	YDR452W	PPN1	V418F	0.15
PDB26_c2	chrIX	352879	nonsynonymous	YIL002C	INP51	V185I	0.25
PDB26_c2	chrX	94713	5'-upstream	YJL176C	SWI3	NA	0.31
PDB26_c2	chrXI	220553	nonsynonymous	YKL117W	SBA1	P77H	0.37
PDB26_c2	chrXII	164201	5'-upstream	YLR007W	NSE1	NA	0.15
PDB26_c2	chrXIV	49495	nonsynonymous	YNL311C	SKP2	D732N	0.15
PDB26_c2	chrXIV	312957	synonymous	YNL172W	APC1	D774D	0.33
PDB26_c2	chrXIV	675076	nonsynonymous	YNR027W	BUD17	G52W	0.20
PDB26_c2	chrXVI	385553	nonsynonymous	YPL086C	ELP3	L298F	0.23
PDB26_c2	chrXVI	593148	5'-upstream	YPR016C	TIF6	NA	0.27
PDB26_c20	chrIV	821800	nonsynonymous	YDR180W	SCC2	T169N	0.27
PDB26_c20	chrIX	225225	nonsynonymous	YIL073C	SPO22	T214P	0.21
PDB26_c20	chrIX	374261	nonsynonymous	YIR008C	PRI1	E16Q	0.18
PDB26_c20	chrV	342706	5'-upstream	YER092W	IES5	NA	0.30
PDB26_c20	chrV	532099	nonsynonymous	YER172C	BRR2	F1308C	0.29
PDB26_c20	chrVI	239646	nonsynonymous	YFR043C	IRC6	C61S	0.29
PDB26_c20	chrVII	405858	nonsynonymous	YGL050W	TYW3	K28T	0.26
PDB26_c20	chrVII	630259	nonsynonymous	YGR070W	ROM1	R818S	0.29
PDB26_c20	chrVII	1054961	nonsynonymous	YGR281W	YOR1	G713A	0.26
PDB26_c20	chrVIII	235322	nonsynonymous	YHR070W	TRM5	E148K	0.20
PDB26_c20	chrVIII	363826	nonsynonymous	YHR129C	ARP1	P110S	0.30
PDB26_c20	chrX	279131	synonymous	YJL083W	TAX4	T97T	0.20
PDB26_c20	chrX	396004	nonsynonymous	YJL024C	APS3	T171K	0.21
PDB26_c20	chrX	623929	nonsynonymous	YJR105W	ADO1	G117R	0.24
PDB26_c20	chrXI	245205	nonsynonymous	YKL104C	GFA1	G57R	0.30
PDB26_c20	chrXII	190495	nonsynonymous	YLR024C	UBR2	I929M	0.17
PDB26_c20	chrXIII	83919	nonsynonymous	YML093W	UTP14	R277L	0.33
PDB26_c20	chrXIII	99098	nonsynonymous	YML085C	TUB1	V63I	0.25
PDB26_c20	chrXIII	429073	nonsynonymous	YMR080C	NAM7	E185D	0.29
PDB26_c20	chrXIII	568040	nonsynonymous	YMR154C	RIM13	L48W	0.28
PDB26_c20	chrXIV	59722	nonsynonymous	YNL305C	BXI1	D24Y	0.25
PDB26_c20	chrXV	456356	nonsynonymous	YOR070C	GYP1	M489V	0.23

PDB26_c20	chrXV	523696	nonsynonymous	YOR108W	LEU9	V224I	0.22
PDB26_c20	chrXV	720452	nonsynonymous	YOR199W	YOR199W	V91A	0.24
PDB26_c20	chrXV	1029795	synonymous	YOR370C	MRS6	G400G	0.22
PDB26_c20	chrXVI	651211	nonsynonymous	YPR042C	PUF2	D818Y	0.23
PDB26_c23	chrII	733737	nonsynonymous	YBR260C	RGD1	N301K	0.13
PDB26_c23	chrIII	264061	nonsynonymous	YCR087W	YCR087W	E29G	0.24
PDB26_c23	chrIV	207174	nonsynonymous	YDL140C	RPO21	Q1130*	0.24
PDB26_c23	chrVII	189450	nonsynonymous	YGL167C	PMR1	A340E	0.34
PDB26_c23	chrVII	649699	nonsynonymous	YGR086C	PIL1	Q307E	0.24
PDB26_c23	chrVIII	158621	nonsynonymous	YHR024C	MAS2	R191I	0.22
PDB26_c23	chrVIII	275899	nonsynonymous	YHR084W	STE12	N576Y	0.22
PDB26_c23	chrXI	535206	nonsynonymous	YKR053C	YSR3	G26S	0.30
PDB26_c23	chrXII	376567	nonsynonymous	YLR114C	AVL9	N224K	0.16
PDB26_c23	chrXIII	550042	nonsynonymous	YMR141C	YMR141C	M1I	0.32
PDB26_c23	chrXIII	680775	nonsynonymous	YMR207C	HFA1	W930C	0.31
PDB26_c23	chrXIV	311284	nonsynonymous	YNL172W	APC1	Y217D	0.30
PDB26_c23	chrXV	406206	nonsynonymous	YOR039W	CKB2	Q147E	0.24
PDB26_c23	chrXVI	323095	nonsynonymous	YPL120W	VPS30	R342I	0.18
PDB26_c23	chrXVI	709061	nonsynonymous	YPR085C	ASA1	N256K	0.18
PDB26_c3	chrII	601957	nonsynonymous	YBR186W	PCH2	T469P	0.30
PDB26_c3	chrIII	51960	nonsynonymous	YCL040W	GLK1	H375Y	0.22
PDB26_c3	chrIII	254131	synonymous	YCR079W	PTC6	T429T	0.21
PDB26_c3	chrIV	844924	5'-upstream	YDR192C	NUP42	NA	0.23
PDB26_c3	chrIV	996794	synonymous	YDR264C	AKR1	K510K	0.29
PDB26_c3	chrIX	250375	nonsynonymous	YIL056W	VHR1	S129T	0.21
PDB26_c3	chrX	316905	synonymous	YJL062W-A	COA3	D61D	0.18
PDB26_c3	chrXI	217299	5'-upstream	YKL120W	OAC1	NA	0.22
PDB26_c3	chrXII	909121	nonsynonymous	YLR394W	CST9	L391*	0.18
PDB26_c3	chrXIII	68591	nonsynonymous	YML102W	CAC2	Q100K	0.27
PDB26_c3	chrXIII	289233	synonymous	YMR011W	HXT2	S385S	0.31
PDB26_c3	chrXIII	772786	5'-upstream	YMR251W	GTO3	NA	0.24
PDB26_c3	chrXV	558049	synonymous	YOR124C	UBP2	V198V	0.18
PDB26_c3	chrXVI	750415	nonsynonymous	YPR112C	MRD1	V502A	0.23
PDB26_c4	chrI	127842	synonymous	YAL015C	NTG1	P87P	0.41
PDB26_c4	chrIV	1352006	nonsynonymous	YDR444W	YDR444W	E573Q	0.47
PDB26_c4	chrVII	1061037	nonsynonymous	YGR284C	ERV29	T185I	0.15
PDB26_c4	chrXV	473169	nonsynonymous	YOR078W	BUD21	E149Q	0.23
PDB26_c4	chrXV	917896	nonsynonymous	YOR321W	PMT3	L623M	0.24
PDB26_c4	chrXVI	44064	nonsynonymous	YPL264C	YPL264C	R94L	0.21

PDB26_c5	chrII	51751	synonymous	YBL088C	TEL1	R2544R	0.32
PDB26_c5	chrIII	283326	nonsynonymous	YCR093W	CDC39	D1070E	0.28
PDB26_c5	chrIV	1078532	5'-upstream	YDR308C	SRB7	NA	0.26
PDB26_c5	chrIV	1412625	nonsynonymous	YDR477W	SNF1	I85F	0.36
PDB26_c5	chrVII	247324	nonsynonymous	YGL139W	FLC3	F537V	0.22
PDB26_c5	chrVIII	340697	nonsynonymous	YHR115C	DMA1	R221S	0.30
PDB26_c5	chrXIII	70299	synonymous	YML100W-A	YML100W-A	A54A	0.28
PDB26_c5	chrXIII	179990	nonsynonymous	YML047W-A	YML047W-A	L33S	0.17
PDB26_c5	chrXIII	215474	nonsynonymous	YML031W	NDC1	D429G	0.39
PDB26_c5	chrXIII	714380	nonsynonymous	YMR221C	FMP42	V356I	0.52
PDB26_c5	chrXIV	36496	nonsynonymous	YNL321W	VNX1	A601S	0.23
PDB26_c5	chrXIV	210795	nonsynonymous	YNL234W	YNL234W	C188Y	0.30
PDB26_c5	chrXV	519791	nonsynonymous	YOR106W	VAM3	Q224P	0.36
PDB26_c6	chrIII	63483	nonsynonymous	YCL032W	STE50	A15S	0.23
PDB26_c6	chrIII	222621	nonsynonymous	YCR057C	PWP2	Q203L	0.14
PDB26_c6	chrIII	254131	synonymous	YCR079W	PTC6	T429T	0.18
PDB26_c6	chrIV	869318	nonsynonymous	YDR208W	MSS4	T365indel	0.36
PDB26_c6	chrIV	1331303	nonsynonymous	YDR434W	GPI17	V23I	0.22
PDB26_c6	chrIX	186813	nonsynonymous	YIL094C	LYS12	A274S	0.40
PDB26_c6	chrXIV	409296	nonsynonymous	YNL116W	DMA2	V319E	0.30
PDB26_c6	chrXVI	35552	nonsynonymous	YPL268W	PLC1	C106F	0.29
PDB26_c7	chrIII	282527	nonsynonymous	YCR093W	CDC39	K804M	0.20
PDB26_c7	chrV	48657	synonymous	YEL055C	POL5	T961T	0.50
PDB26_c7	chrVI	65806	synonymous	YFL034W	MIL1	L110L	0.37
PDB26_c7	chrVII	394293	nonsynonymous	YGL058W	RAD6	A103V	0.32
PDB26_c7	chrX	688516	nonsynonymous	YJR138W	IML1	S1317C	0.19
PDB26_c7	chrXII	830036	nonsynonymous	YLR351C	NIT3	Y110S	0.22
PDB26_c7	chrXIV	372616	synonymous	YNL134C	YNL134C	A322A	0.35
PDB26_c7	chrXVI	40896	5'-upstream	YPL265W	DIP5	NA	0.36
PDB26_c9	chrII	313193	nonsynonymous	YBR038W	CHS2	L432F	0.30
PDB26_c9	chrII	734561	nonsynonymous	YBR260C	RGD1	A27P	0.32
PDB26_c9	chrIII	202922	nonsynonymous	YCR042C	TAF2	R826C	0.29
PDB26_c9	chrIV	117655	5'-upstream	YDL191W	RPL35A	NA	0.38
PDB26_c9	chrIV	821800	nonsynonymous	YDR180W	SCC2	T169N	0.31
PDB26_c9	chrVIII	160686	5'-upstream	YHR026W	VMA16	NA	0.20
PDB26_c9	chrXI	245205	nonsynonymous	YKL104C	GFA1	G57R	0.28
PDB26_c9	chrXI	409327	nonsynonymous	YKL015W	PUT3	K262E	0.23
PDB26_c9	chrXI	525109	5'-upstream	YKR046C	PLN1	NA	0.28
PDB26_c9	chrXIII	166863	nonsynonymous	YML054C	CYB2	N149T	0.22

PDB26_c9	chrXIII	334605	5'-upstream	YMR031W-A	YMR031W-A	NA	0.32
PDB26_c9	chrXIV	49495	nonsynonymous	YNL311C	SKP2	D732N	0.24
PDB26_c9	chrXIV	441876	synonymous	YNL097C	PHO23	A161A	0.17
PDB26_c9	chrXV	793712	synonymous	YOR244W	ESA1	L394L	0.19
PDB26_c9	chrXV	924654	synonymous	YOR325W	YOR325W	N26N	0.17
PDB26_c9	chrXVI	144176	nonsynonymous	YPL216W	YPL216W	F119C	0.19
PDB26_c9	chrXVI	203589	nonsynonymous	YPL181W	CTI6	V57I	0.19
PDB26_c9	chrXVI	327275	nonsynonymous	YPL118W	MRP51	N216K	0.17
Drakes	chrII	294593	synonymous	YBR028C	YPK3	T470T	0.06
Drakes	chrIII	46605	nonsynonymous	YCL045C	EMC1	A101S	0.39
Drakes	chrIV	487600	nonsynonymous	YDR021W	FAL1	T266I	0.10
Drakes	chrIV	617377	intergenic	NA	NA	NA	0.20
Drakes	chrIV	1085083	nonsynonymous	YDR311W	TFB1	A7S	0.08
Drakes	chrIV	1170220	intergenic	NA	NA	NA	0.07
Drakes	chrIX	314661	nonsynonymous	YIL020C	HIS6	Q54E	0.06
Drakes	chrV	61847	intergenic	NA	NA	NA	0.12
Drakes	chrVI	121682	nonsynonymous	YFL008W	SMC1	I752V	0.04
Drakes	chrVII	678677	5'-upstream	YGR097W	ASK10	NA	0.23
Drakes	chrVII	794400	intergenic	NA	NA	NA	0.06
Drakes	chrVII	940773	nonsynonymous	YGR222W	PET54	S284F	0.08
Drakes	chrVII	972129	nonsynonymous	YGR240C	PFK1	M536L	0.21
Drakes	chrVIII	10799	intergenic	NA	NA	NA	0.24
Drakes	chrX	703550	intergenic	NA	NA	NA	0.28
Drakes	chrXI	300060	nonsynonymous	YKL072W	STB6	S160L	0.27
Drakes	chrXI	321083	nonsynonymous	YKL063C	YKL063C	Q146K	0.14
Drakes	chrXI	345312	synonymous	YKL050C	YKL050C	S103S	0.24
Drakes	chrXII	786005	nonsynonymous	YLR328W	NMA1	A365T	0.09
Drakes	chrXIII	85826	intergenic	NA	NA	NA	0.08
Drakes	chrXIII	214844	nonsynonymous	YML031W	NDC1	D219G	0.08
Drakes	chrXIII	899139	synonymous	YMR312W	ELP6	I245I	0.29
Drakes	chrXIV	144390	nonsynonymous	YNL265C	IST1	E263K	0.08
Drakes	chrXIV	443294	intergenic	NA	NA	NA	0.23
Drakes	chrXIV	547163	nonsynonymous	YNL042W-B	YNL042W-B	C17*	0.08
Drakes	chrXV	684910	nonsynonymous	YOR187W	TUF1	T294I	0.06
Drakes	chrXVI	201159	nonsynonymous	YPL183C	RTT10	S460C	0.27
Drakes	chrXVI	277975	intergenic	NA	NA	NA	0.06
Drakes	chrXVI	901544	nonsynonymous	YPR183W	DPM1	H264Y	0.26
RedCircle	chrII	352461	nonsynonymous	YBR057C	MUM2	T278N	0.21
RedCircle	chrII	450592	nonsynonymous	YBR104W	YMC2	A309V	0.26

RedCircle	chrII	514630	nonsynonymous	YBR138C	YBR138C	T236K	0.03
RedCircle	chrIV	197030	nonsynonymous	YDL145C	COP1	H383Y	0.30
RedCircle	chrIV	244223	nonsynonymous	YDL122W	UBP1	E558*	0.04
RedCircle	chrIV	305798	nonsynonymous	YDL084W	SUB2	V188I	0.25
RedCircle	chrIV	961135	synonymous	YDR251W	PAM1	N174N	0.26
RedCircle	chrIV	1161967	intergenic	NA	NA	NA	0.42
RedCircle	chrV	271300	5'-upstream	YER057C	HMF1	NA	0.05
RedCircle	chrV	295459	nonsynonymous	YER069W	ARG5,6	K17I	0.04
RedCircle	chrVII	56179	intergenic	NA	NA	NA	0.36
RedCircle	chrVII	259900	nonsynonymous	YGL133W	ITC1	R732G	0.38
RedCircle	chrXII	236845	nonsynonymous	YLR045C	STU2	Q287K	0.20
RedCircle	chrXVI	212366	nonsynonymous	YPL178W	CBC2	G70V	0.26
RedCircle	chrXVI	786381	synonymous	YPR123C	YPR123C	V65V	0.04

Table C.6. Recurrent mutations across all brewery evolution experiments

Sample	Chr	Pos	Ref	Alt	Mutation Type	Gene	Gene	Effect	Final AF
PDB29 Rep. 2	chrIV	244970	G	T	nonsynonymous	YDL122W	UBP1	D807Y	0.103
Red Circle Brewing	chrIV	244223	G	T	nonsynonymous	YDL122W	UBP1	E558Stop	0.04
Elysian09	chrIV	188256	G	C	nonsynonymous	YDL148C	NOP14	Y777Stop	0.101
Elysian10	chrIV	188256	G	C	nonsynonymous	YDL148C	NOP14	Y777Stop	0.129
Elysian10	chrIV	1085392	C	T	nonsynonymous	YDR311W	TFB1	R110W	0.108
Drake's Brewing Co.	chrIV	1085083	G	T	nonsynonymous	YDR311W	TFB1	A7S	0.077
PDB26 Rep. 1	chrXI	245205	C	G	nonsynonymous	YKL104C	GFA1	G57R	0.077
PDB29 Rep. 2	chrXI	245205	C	G	nonsynonymous	YKL104C	GFA1	G57R	0.117
Elysian03	chrXII	905505	G	A	synonymous	YLR392C	ART10	N267N	0.176
Elysian08	chrXII	905987	G	A	nonsynonymous	YLR392C	ART10	P107S	0.049

Table C.7. Results of a sensory panel sampling beer produced by clones isolated from the Postdoc Brewing Replicate 1 populations

	Esters	Phenols	Alcohol	Sweetness	Phenols	Harshness	Warmth	Acidity	Hops	Bitterness	Malt
p-value	0.003	0.1413	0.6405	0.0003	0.1413	0.5821	0.4401	0.8831	0.0048	0.5594	0.0056
PDB26 c6	2.18	1.03	1.4	2.27	1.03	2.16	2.34	0.83	3.02	3.47	2.86
Ancestor	1.82	1.19	1.36	1.76	1.19	2.2	1.72	0.91	2.63	3.29	2.52
PDB26 c1	1.76	0.83	1.29	1.76	0.83	1.95	1.63	0.8	2.8	3.36	2.6

Table C.8. Filters used in variant calling.

Samtools Filter Parameters

Type	Shorthand	Value
Mapping quality	MQ	>30
Quality score	QUAL	>50
Read depth	DP	>40
Alternate read count	DP4[2]+DP4[3]	>4
Forward read balance	(DP4[0]+DP4[2])/DP	>0.01
Reverse read balance	(DP4[1]+DP4[3])/DP	>0.01

Freebayes Filter Parameters

Type	Shorthand	Value
Mapping quality of observed alternate alleles	MQM	>30
Mapping quality of observed reference alleles	MQMR	>30
Quality score	QUAL	>20
Read depth	DP	>40
Forward strand alternate read count	SAF	>2
Reverse strand alternate read count	SAR	>2
Forward read balance	SRF + SAF / DP	>0.01
Reverse read balance	SRR + SAR / DP	>0.01

LoFreq Filter Parameters

Type	Shorthand	Value
Quality score	QUAL	>20
Read depth	DP	>20
Forward strand alternate read count	DP4[2]	>2
Reverse strand alternate read count	DP4[3]	>2
Forward read balance	(DP4[0]+DP4[2])/DP	>0.01
Reverse read balance	(DP4[1]+DP4[3])/DP	>0.01

VITA

Christopher Large was born in Redbank, New Jersey and raised in Woodinville, Washington. He attended the University of Puget Sound and received a Bachelor of Science degree in Molecular and Cellular Biology. While an undergraduate at the University of Puget Sound, he conducted research in the laboratory of Professor Leslie Saucedo, investigating the seemingly contradictory role of the human tumor suppressor, *Phosphatase of Regenerating Liver-3* in *Drosophila melanogaster*. In the summer before his senior year, he interned with Dr. Harmit Malik, studying the functional divergence of a potentially rapid evolving transcriptional regulator of histones, *Abnormal Oocyte*, between *D. melanogaster* and *D. simulans*. After graduating the University of Puget Sound he worked as a research technician in the laboratory of Professor Nitin Phadnis, investigating the molecular and cellular causes of a speciation event between two subspecies of *D. pseudoobscura*. Afterwards, Christopher entered the Molecular and Cellular Biology PhD program the University of Washington and joined the laboratory of Professor Maitreya Dunham in the Department of Genome Sciences. While in the Dunahm lab, he has contributed to scientific research through collaborations with research groups across five continents. Christopher has presented his research at numerous international scientific conferences and has been involved in efforts within the department to increase diversity, equity, and inclusion. Outside of the laboratory, Christopher has contributed to his graduate training on beer yeast genetics through the production and consumption of yeast products with friends and family.

PUBLICATIONS

Large C. R. L., Hanson N. A., Tsouris A., Saada O. A., Koonthongkaew J., Toyokawa Y., Schmidlin T., Moreno-Habel D. A., McConnellogue H., Preiss R., Takagi H., Schacherer J., Dunham M. J. (2020) Genomic stability and adaptation of beer brewing yeasts during serial repitching in the brewery. bioRxiv doi: <https://doi.org/10.1101/2020.06.26.166157>

Koonthongkaew J., Toyokawa Y., Ohashi M., Large C. R. L., Dunham M. J., Takagi H. Effect of the Ala234Asp replacement in mitochondrial branched-chain amino acid aminotransferase on the production of BCAAs and fusel alcohols in yeast. 2020. *Applied Microbiology and Biotechnology*: doi:[10.1007/s00253-020-10800-y](https://doi.org/10.1007/s00253-020-10800-y)

Heil, C. S. S., Large, C. R. L., Patterson, K., Hickey, A. S., Yeh, C. C., Dunham, M. J., Temperature preference can bias parental genome retention during hybrid evolution. 2019. *PLOS Genetics*: vol. 15 no. 9, doi:[10.1371/journal.pgen.1008383](https://doi.org/10.1371/journal.pgen.1008383)

Sanchez, J. C., Ollodart, A., Large, C. R. L., Clough, C., Alvino, G. M., Tsuchiya, M., Crane, M., Kwan, E. X., Kaeberlein, M., Dunham, M. J., M. K. Raghuraman and Brewer, B. J., Phenotypic and genotypic consequences of CRISPR/Cas9 editing of the replication origins in the rDNA of *Saccharomyces cerevisiae*. 2019. *Genetics*: vol. 212 no. 3, doi:[10.1534/genetics.119.302351](https://doi.org/10.1534/genetics.119.302351)